

THE KINETICS OF THE REACTION OF
CARBON WITH CARBON DIOXIDE

by

Pao-chen Wu

Submitted in Partial Fulfillment of the Requirements
for the Degree of
DOCTOR OF SCIENCE
from the
MASSACHUSETTS INSTITUTE OF TECHNOLOGY
December 20, 1949

Signature of Author: _____
Pao-chen Wu

Signature of Thesis Supervisor: _____
Hoyl C. Hottel

Signature of Head of Department: _____
Walter G. Whitman

MASSACHUSETTS INSTITUTE OF TECHNOLOGY

Cambridge 39, Massachusetts

December 20, 1949.

Mr. Joseph S. Newell
Secretary of the Faculty
Massachusetts Institute of Technology
Cambridge 39, Massachusetts

Dear Sir:

The thesis entitled " The Kinetics of the
Reaction of Carbon with Carbon Dioxide " is hereby
submitted in partial fulfillment of the requirements
for the degree of Doctor of Science in Chemical
Engineering.

Respectfully,

Pao-chen Wu

ACKNOWLEDGMENTS

The author is greatly indebted to Prof. H. C. Hottel, under whose direction this investigation was carried out, for his kind advice and many valuable suggestions which made the completion of this work possible.

He wishes to express his appreciation to Prof. G.C. Williams for his inspiring criticism, constant interest and encouragement, which helped greatly in the course of this investigation.

He wishes to thank Mr. W. E. Lower, who helped enormously in the construction of the equipment, gave unstintingly his time in the solution of day-to-day problems, and performed part of the experimental work.

Acknowledgments are also due to Mr. L. F. Blanc, who helped to build the equipment, and Mr. R. W. Shade, who assisted in the experimental work.

The author is very grateful to the Bituminous Coal Research, Inc., which financed the coal combustion research project at M.I.T., of which this present work forms a part.

TABLE OF CONTENTS

	<u>Page</u>
I. SUMMARY - - - - -	1
II. INTRODUCTION - - - - -	8
A. Object - - - - -	8
B. Review of Previous Work - - - - -	9
C. Scope of the Present Work - - - - -	18
III. CONSTRUCTION OF EQUIPMENT - - - - -	19
IV. PROCEDURE - - - - -	40
V. RESULTS - - - - -	43
A. Presentation of Data - - - - -	43
1. Experiments using New England coke particles of 50-60 mesh - - - - -	43
2. Experiments using New England coke particles of different sizes, reacting with different times of reaction - - - - -	48
3. Experiments using National electrode carbon particles of 50-60 mesh - - - - -	53
B. Discussion of Validity of Data and of Corrections Applied thereto - - - - -	63
1. Experiments using New England coke particles of 50-60 mesh - - - - -	63
2. Experiments using New England coke particles of different sizes, reacting with different times of reaction - - - - -	67
3. Experiments using National electrode carbon particles of 50-60 mesh - - - - -	68
VI. DISCUSSION AND INTERPRETATION OF RESULTS - - - - -	72
A. Experiments Using National Electrode Carbon Particles of 50-60 Mesh - - - - -	73
B. Experiments Using New England Coke Particles of Different Sizes, Reacting with Different Times of Reaction - - - - -	100
C. Experiments Using New England Coke Particles of 50-60 Mesh - - - - -	110
D. Comparison of the Results of the Present Work on Coke with those Obtained in a Fluidized Bed by McBride - - - - -	120

	<u>Page</u>
E. Comparison of the Reactivity of Coke with that of Electrode Carbon - - - - -	130
VII. CONCLUSIONS - - - - -	134
VIII. RECOMMENDATIONS - - - - -	137
APPENDIX - - - - -	139
A. Details on Construction of Equipment - - - - -	140
1. Furnace - - - - -	140
2. Nichrome screen pan and sample pan supporter - - - - -	145
3. Flexure tube and yoke arrangement - - - - -	145
4. Cylindrical furnace container - - - - -	147
5. Calcium chloride drying tower - - - - -	151
6. Oxygen removal apparatus - - - - -	151
7. Temperature controller - - - - -	152
8. Cooling coil - - - - -	152
9. Cenco Megavac vacuum pump - - - - -	153
B. Description and Calibration of Measuring Devices - - - - -	154
1. Rotameter - - - - -	154
2. McLeod gauge - - - - -	154
3. Potentiometer - - - - -	154
4. Wet test gas meter - - - - -	154
5. Ammeters - - - - -	156
6. Micro oxygen analyzer - - - - -	156
7. Thermocouples - - - - -	156
8. Balance - - - - -	158
C. Details on Materials Used - - - - -	159
1. Carbon - - - - -	159
2. Carbon dioxide - - - - -	160
3. Carbon monoxide - - - - -	160
4. Nitrogen - - - - -	160
5. Cupric oxide - - - - -	161
6. Calcium chloride - - - - -	161
7. Drierite - - - - -	161
8. Bricks and cement - - - - -	161
9. Chromel-A ribbon - - - - -	161
10. Nichrome screen and nickel screen - - - - -	162
11. Alundum rods - - - - -	162
12. Heating wires - - - - -	162
13. Thermocouple wires - - - - -	162
14. Insulation for oxygen removal apparatus - - - - -	162
15. Cenco-Sealstix vacuum cement - - - - -	163

	<u>Page</u>
D. Data Sheets - - - - -	164
E. Calculations for Experiments Using Electrode Carbon Particles of 50-60 Mesh - - - - -	180
1. Sample calculations - - - - -	180
2. Integration of instantaneous specific reaction rate equation - - - - -	182
3. Calculation of (m/R_0) values - - - - -	184
4. Effective surface area ratio calculations - - - - -	186
5. Testing the validity of equation (11) -	187
F. Calculations for Experiments Using Coke Particles of Different Sizes - - - - -	188
1. Sample calculations - - - - -	188
2. Calculation of R_1 values - - - - -	189
3. List of values of R_0 , $R_1(\text{max.})$ and $R_{av.}$ at $F = 0.1$ - - - - -	191
4. Calculation of the density and the specific reaction rate based on superficial surface area at $F=0$ - - - - -	192
G. Calculation for Experiments Using Coke Particles of 50-60 Mesh - - - - -	194
1. Sample calculations - - - - -	194
2. Correction of gas composition of CO_2 - CO runs for CO generated - - - - -	195
3. Correction of $R_{av.}$ for CO_2 - N_2 runs due to CO generation - - - - -	198
4. Integration of the Langmuir equation -	199
5. Calculation of the fraction of CO_2 decomposed in a fluidized bed - - - - -	201
H. Equilibrium of the Carbon-Carbon Dioxide Reaction - - - - -	206
I. Discussion of Errors - - - - -	208
1. Oxygen effect - - - - -	208
2. Reaction between gases or carbon and nichrome screen - - - - -	208
3. The effect of volatile combustible matter present in carbon - - - - -	209
4. The effect of gas composition - - - - -	210
5. The effect of oxygen and moisture adsorbed on the surface of carbon - - - - -	211
6. The effect of change in particle size of the carbon due to reaction - - - - -	211
7. The temperature control of the furnace -	212
8. The weighing - - - - -	212
9. Sample losses due to jerking of the pan	212

	<u>Page</u>
10. Particles blown off the sample supporter - - - - -	213
11. Particles fallen through the screen - -	214
12. Brick particles falling on the sample supporter - - - - -	214
13. Preparation and analysis of gas mixtures	215
J. Derivation of Rate Equation for Reaction of Carbon with Carbon Dioxide - - - - -	216
1. Langmuir-Hinshelwood derivation - - - -	216
2. Derivation of Semechkova and Frank-Kamenetzky - - - - -	219
3. Modified Semechkova and Frank-Kamenetzky Derivation - - - - -	222
K. Nomenclature - - - - -	223
L. Literature Cited - - - - -	225
M. Biographical Note - - - - -	229

TABLE OF GRAPHS, ILLUSTRATIONS AND PHOTOGRAPHS

	<u>Page</u>
Figure 1. Front View of Equipment - - - - -	20
Figure 2. Back View of Equipment - - - - -	21
Figure 3. Sketch of Equipment - - - - -	23
Figure 4. Nichrome Sample Pan Supporter and Double Pans - - - - -	28
Figure 5. Nichrome Sample Pan Supporter for the Double Pans - - - - -	29
Figure 6. Nichrome Sample Pan Supporter and Sample Pan (1) - - - - -	31
Figure 7. Nichrome Sample Pan Supporter and Sample Pan (2) - - - - -	32
Figure 8. Nichrome Sample Pan Supporter for the Single Sample Pans - - - - -	33
Figure 9. Coke Particles before and after the Reaction - - - - -	34
Figure 10. F_{N_2} vs. θ - Pure N_2 Runs (Coke) - - - -	45
Figure 11. $R_{av.}$ vs. P_{CO_2} for CO_2-N_2 Runs (Coke) -	46
Figure 12. $R_{av.}$ vs. P_{CO} for CO_2-CO Runs (-Coke) - -	47
Figure 13. $R_{av.}$ vs. $1/V$ - Pure CO_2 Runs (Coke) - -	49
Figure 14. F vs. D (Coke) - - - - -	51
Figure 15. $(1-F)$ vs. θ (-Coke) - - - - -	52
Figure 16. $R_{av.}$ vs. θ (Coke) - - - - -	54
Figure 17. $R_{av.}$ vs. D (Coke) - - - - -	55
Figure 18. Weight per Particle vs. D^3 (Coke) - - -	56
Figure 19. Photographs of Coke Particles - - - - -	57
Figure 20. Photomicrograph of 50-60 mesh Coke Particles - - - - -	58
Figure 21. $R_{av.}$ vs. P_{CO_2} for CO_2-N_2 Runs (Electrode Carbon) - - - - -	60

	<u>Page</u>
Figure 22. $R_{av.}$ vs. P_{CO} for CO_2 -CO Runs (Electrode Carbon) - - - - -	61
Figure 23. $R_{av.}$ vs. $1/V$ - Pure CO_2 Runs (Electrode Carbon) - - - - -	62
Figure 24. F vs. θ (Electrode Carbon) - - - - -	64
Figure 25. $(1+14F)/(1-F)$ vs. θ (Electrode Carbon) -	80
Figure 26. A/A_0 vs. F (Electrode Carbon) - - - - -	81
Figure 27. Test of Results } $T = 1600^\circ F$ - -	86
Figure 28. by Langmuir Equation } $T = 1700^\circ F$ - -	87
Figure 29. CO_2 - N_2 Runs } $T = 1800^\circ F$ - -	88
Figure 30. (Electrode Carbon) } $T = 1900^\circ F$ - -	89
Figure 31. Test of Results } $T = 1600^\circ F$ - -	91
Figure 32. by Langmuir Equation } $T = 1700^\circ F$ - -	92
Figure 33. CO_2 -CO Runs } $T = 1800^\circ F$ - -	93
Figure 34. (Electrode Carbon) } $T = 1900^\circ F$ - -	94
Figure 35. Langmuir Equation Constants (Electrode Carbon) - - - - -	96
Figure 36. Test of Correlation (Electrode Carbon) -	99
Figure 37. R_1 vs. F (Coke) - - - - -	101
Figure 38. R_1 vs. D (Coke) - - - - -	103
Figure 39. Density of Coke Particles - - - - -	104
Figure 40. Reaction Rate based on Superficial Surface Area at $F=0$ vs. the Diameter of Particle (Coke) - - - - -	106
Figure 41. Actual R_1 and Ash-free R_1 vs. F - - - - -	108
Figure 42. Ash Retardation Factor vs. F - - - - -	108
Figure 43. Test of Results by Langmuir Equation - - - (Coke)	111
Figure 44. $R_{av.}$ vs. P_{CO_2} for CO_2 - N_2 Runs (Coke) - -	114

	<u>Page</u>
Figure 45. R_{av} . vs. PCO for CO_2 - CO Runs (Coke) - - -	115
Figure 46. Test of Results by Langmuir Equation (Final Plot for Coke) - - - - -	116
Figure 47. Langmuir Equation Constants (Coke) - - -	117
Figure 48. Test of Correlation (Coke) - - - - -	119
Figure 49. McBride's Langmuir Equation Constants - - -	122
Figure 50. Plot of $f_{exp't.}$ vs. $f_{calc.}$ (McBride's Constants) - - - - -	123
Figure 51. Plot of $f_{exp't.}$ vs. $f_{calc.}$ (Wu's Constants) - - - - -	124
Figure 52. Fraction CO_2 Decomposed vs. Amount of Carbon in a Fluidized Bed - - - - -	128
Figure 53. Comparison of Specific Reaction Rates Calculated by means of Rate Constants Evaluated by McBride and by Wu - - - - -	129
Figure 54. Comparison of Specific Reaction Rates Calculated for Coke and for Electrode Carbon - - - - -	131
Figure A1. Cross Section of Furnace - - - - -	141
Figure A2. Photographs of Steel Box - - - - -	142
Figure A3. Flowrator Calibration - - - - -	155
Figure A4. Photograph of Oxygen Analyzer - - - - -	157
Figure A5. Equilibrium Constant - - - - -	207

TABLES

	<u>Page</u>
Table 1. Langmuir Equation Constants (Electrode Carbon) - - - - -	95
Table 2. Values of E and K_0 (Electrode Carbon) - -	97
Table 3. Approximate Langmuir Equation Constants (Coke) - - - - -	-112
Table 4. Langmuir Equation Constants (Coke) - - -	-113
Table 5. Values of E and K_0 (Coke) - - - - -	-118
Table 6. Smoothed Langmuir Equation Constants - - -	-132
Table 7. Langmuir Equation Constants from Different Authors - - - - -	133
Table A1. List of Gas Mixtures - - - - -	-165
Table A2. N_2 Blank Runs (Coke) - - - - -	-166
Table A3. CO_2-N_2 Runs (Coke) - - - - -	-167
Table A4. CO_2-CO Runs (Coke) - - - - -	-168
Table A5. Influence of Gas Flow Rate on Reaction Rate (Coke) - - - - -	169
Table A6. N_2 Blank Runs (Coke) - - - - -	170
Table A7. Influence of D on R (Coke) - - - - -	171
Table A8. Weight per Coke Particle - - - - -	174
Table A9. Coking Run and N_2 Blank Runs - - - - -	175
Table A10. CO_2-N_2 Runs (Electrode Carbon) - - - - -	176
Table A11. CO_2-CO Runs (Electrode Carbon) - - - - -	177
Table A12. Influence of Gas Flow Rate on Reaction Rate	178
Table A13. Influence of Reaction Time on Reaction Rate	179
Table A14. Calculation of (m/R_0) - - - - -	185

	<u>Page</u>
Table A15. Effective Surface Area Ratios (Electrode Carbon) - - - - -	186
Table A16. Calculation of F and θ (Electrode Carbon)-	187
Table A17. Values of R_1 (Coke) - - - - -	190
Table A18. Values of R_0 , $R_1(\text{max.})$ and $R_{av.}$ at $F = 0.1$ (Coke) - - - - -	191
Table A19. The density of Coke and the Reaction Rate based on Superficial Surface Area - - - - -	193
Table A20. Fraction of Carbon Dioxide Decomposed in a Fluidized Bed - - - - -	202
Table A21. Equilibrium Mixture Composition of CO_2 , CO and Carbon System - - - - -	206

I. SUMMARY

The object of this work was to study the kinetics of the reaction of carbon with carbon dioxide. Two types of carbon were used, electrode carbon and coke. Among the reaction variables, the effects of temperature, pressure, gas composition and velocity and particle size were investigated. The reacting system consisted of a single layer of particles, evenly distributed on an inert metal screen, with the reacting gas passing through the bed under well controlled conditions of temperature, gas velocity and gas composition. The reaction rates were obtained from the fractional decrease in weight of carbon during reaction and the time of reaction.

An electrode carbon was used as one reacting carbon because its negligible content of ash and V.C.M. made a clear visualization of the reaction picture possible. The temperatures investigated ranged from 1600 to 1900°F.; the particle size of the electrode carbon was 50-60 mesh. Both $\text{CO}_2\text{-N}_2$ and $\text{CO}_2\text{-CO}$ gas mixtures were used as the reacting gases. The reaction pressure was kept substantially at one atmosphere.

From the results obtained, it was possible to express the instantaneous specific reaction rate R_1 (mass rate of carbon reaction per unit mass of carbon sample) as a linear

function of the mass fraction of carbon reacted F :

$$R_1 = mF + R_0 = R_0 \left(\frac{m}{R_0} F + 1 \right)$$

in which m and R_0 are constants, the rate of change of R_1 with respect to F , and the instantaneous specific reaction rate at $F = 0$, respectively. It was found that the dimensionless ratio $\frac{m}{R_0}$, called the surface activation factor, was independent of temperature and gas composition, and could be represented by a constant of magnitude 14.

The initial specific reaction rate R_0 could be correlated by a Langmuir type reaction-rate equation including surface adsorption, of the form:

$$R_0 = \frac{K_1 P_{CO_2}}{1 + K_2 P_{CO} + K_3 P_{CO_2}}$$

in which the K 's are the rate constants, and P 's are the partial pressures of the respective gases.

The constants were evaluated for each temperature investigated, and fell on straight lines when plotted on semi-logarithmic coordinates vs. the reciprocal of the absolute temperature.

This investigation brings out the interesting point that the effective surface area increases in the course of reaction and that the carbon surface is characteristic of the fraction of carbon reacted. Because of the fact that ash is practically absent, no ash retarding effect exists.

Experiments were also performed using New England coke particles from the same lot used by Graham and McBride, who

studied the reaction kinetics in a fluidized system. It was the object, when planning the experiments, to compare the results using the single layer bed technique with those obtained in a fluidized system. The coke contained 9.5% ash and about 2% V.C.M. The reaction rates are expressed on ash- and V.C.M.-free bases.

Two groups of experiments using coke were performed:

(1) Experiments using coke particles of different sizes, reacting with pure carbon dioxide at 1800°F. with different times of reaction.

(2) Experiments using coke particles of 50-60 mesh reacting at different temperatures with different gas compositions.

Results obtained using different sizes of coke particles at 1800°F. and 1 atm. showed that the reaction rate is influenced by both particle size and time of reaction.

The specific reaction rate based on unit weight of carbon was shown to be lower for larger particles. However, when the specific reaction rate is based on unit superficial surface area, the effect of particle size is not as pronounced. These results indicate that the reaction rate is somewhat proportional to the superficial surface area of the particles.

The instantaneous specific reaction rates evaluated from the corrected data show that, during the course of the reaction, the rate increases steadily, reaches a maximum, and then declines. There is a pronounced trend for the maximum to

occur at larger values of the fractional decrease in weight of carbon as smaller particles are used. This can be explained as being due to the presence in the coke of ash, which amounts to 9.5%. With large particles, only a small fraction of carbon reacted is required to form a substantial layer of ash on the surface, while for small particles, a large fractional reaction is required. This layer of ash makes the carbon less accessible to the reacting gas.

The steady increase in the instantaneous specific reaction rate in the early stage of reaction indicates that more effective surface area was created. If there were no ash present, this increase would presumably continue during the whole course of reaction, as shown in the case of electrode carbon. However, the resistant layer of ash formed during the reaction tends to retard the reaction, so that only a fraction of the ash-free rate can be achieved. The maximum occurs as a net result of these competing factors. An empirical equation, which represents this scheme of mechanism, is shown below:

$$R_1 = R_0 \left(1 + \frac{10 (2 + \log_{10} D)}{R_0} F \right) e^{-5.5DF^{1.85}}$$

in which D is the initial diameter of the particle in mm.

The experiments using coke particles of 50-60 mesh were performed according to the same scheme as the experiments using electrode carbon, except that no study was made of the effect of fractional completion of reaction on rate.

In most of the runs (made before those on electrode carbon) F lay in the range 0.05 to 0.1. In the correlation using a Langmuir type reaction-rate equation which includes effects of adsorption, the average specific reaction rates R_{av} , calculated from the corrected data were considered to be equal to R_0 . This assumption was permissible in view of the results of the investigation of coke with different times of reaction at 1800°F., which showed that the variation in reaction rate for variation in F over the above range was not sufficient to negate the Langmuir equation.

The experiments using coke particles of 50-60 mesh were performed at temperatures ranging from 1500 to 1900°F. Both CO_2-N_2 and CO_2-CO gas mixtures were used as the reacting gases. The reaction pressure was kept substantially at one atmosphere. The results were also correlated by the Langmuir equation. The constants were evaluated for each temperature investigated, and for each constant, could be shown to fall on a straight line when plotted on semi-logarithmic coordinates vs. the reciprocal of the absolute temperature.

The rate constants for coke have been compared with those evaluated by McBride who had used the fluidized bed technique on the same coke. McBride correlated his results by means of the same Langmuir equation in its integrated form assuming the gas flow in the bed to be piston-like. The constants from these two sources differ to a great extent,

especially the values of K_2 . The great retarding effect of CO found in the present work was underestimated by McBride. This was due to the nature of the fluidized bed process, from which only the overall effects, and not the path of the reaction could be obtained.

The rate constants evaluated from the present work were used to correlate the experimental results of McBride. Fair approximations were obtained at low temperatures, while at high temperatures the calculated fractional decomposition of CO_2 was always higher than the experimental values, indicating low effectiveness of the fluidized bed under conditions when the conversion of CO_2 is high, and consequently the gas flow pattern cannot be treated as piston-like.

Furthermore, it was shown that the point reaction rates calculated from these two sets of constants also differ greatly. This indicates strongly that although McBride's constants may be used with fair success to interpret the overall results in a fluidized bed, yet they fail to represent the point data. Consequently, these shortcomings exclude the fluidized bed technique as a laboratory tool for elucidation of the reaction mechanism.

This investigation was carried out under atmospheric pressure. In order to extend the scope of the experiments, it is recommended that for the continuation of this work, pressure equipment be designed, in which sample weighing can be performed continuously so that the change in reaction rate

in the course of reaction can be accurately recorded.
Photomicrographs and surface area measurements of the
carbon particles used are suggested as helpful techniques
in further investigations.

II. INTRODUCTION

A. Object

Since the end of last century, the reactions of carbon with oxygen, steam and carbon dioxide have been studied extensively. The impetus came in part from the interest in gas producers. During recent years, the expansion of the fuel gas industry and the development of the Fischer-Tropsch process have produced new efforts in the search for more reliable data on the reaction rates of oxidation of carbon in various forms under different conditions in oxidizing gas streams. At M.I.T. a project was recently initiated to study the reaction mechanism using the fluidized bed technique. The work done so far comprises the following:

- (1) Gasification of coke and anthracite by carbon dioxide and steam, by Graham (1).
- (2) A study of the retarding effect of carbon monoxide on the carbon-carbon dioxide reaction, by McBride (2).
- (3) Gasification of coke by carbon dioxide at high pressures, by Goring (3).
- (4) A study of carbon-oxygen reactions at low temperatures, by Paxton (4).

The fluidized-bed technique provides a uniform bed temperature and large exposed reaction surface. However, due to the nature of the process it is possible only to compare the overall results of experiments with an integrated form of the reaction process postulated.

As a general principle, such a procedure is open to the objection that the process of integration can often hide the true mechanism, particularly where the mechanism postulated involves a considerable number of constants. To overcome this shortcoming, the present work was initiated to study what goes on in a reaction bed consisting of a single layer of carbon particles. This method makes it possible to approach point reaction conditions and thereby obtain true local reaction rates.

In view of its significance and relative simplicity in comparison with the rest of the carbon gasification reactions, the carbon-carbon dioxide reaction was chosen as the reaction to be investigated in the present work, parallel to the study made by McBride in a fluidized bed. It was further decided for purposes of comparison, to start with coke of the same lot used by McBride, despite the obvious complications introduced by ash and V.C.M. in any fundamental study of mechanism.

B. Review of Previous Work

Three experimental methods, the fixed bed, the single particle, and the fluidized bed have been used up to the

present to obtain an insight into the kinetics and mechanism of the reaction between carbon and carbon dioxide, and heterogeneous reactions in general.

Of these methods, the fixed bed was used almost exclusively until quite recently by most investigators. Credit for the application of the fluidized-bed technique is due mainly to the development of oil cracking processes. Operations in a fluidized bed are characterized by easily controllable isothermal conditions.

An extensive literature survey on the results obtained in fixed-bed experiments was given by Guerin (5). A survey by Wu (6) gave the results of experiments applying to fixed-bed as well as fluidized-bed techniques.

As early as 1861, Henri Sainte-Claire Deville (7) performed experiments on the reduction of carbon dioxide to carbon monoxide by means of solid carbon. However, the first quantitative studies, on the equilibrium of the above-mentioned reaction, were made by Boudouard (8) in 1898, who investigated the reduction of carbon dioxide by carbon in the forms of wood charcoal, coke, etc., in the presence of metal oxides acting as catalysts. Even though the purpose of his investigation was mainly the equilibrium conditions of the reaction, he also made the statement:

"The reaction rate is the greater, the higher the temperature, and depends on the type and particle size of the carbon used".

Following Boudouard, numerous workers have used different fixed-bed techniques. These investigations can be classified and presented as follows:

(1). Evaluation of the Reaction Rate from the Change in Volume of the Reacting Gas

"
Kassler (9), Pire (10), Muller and Jandl (11), Hoehn (12) and Hollings and Siderfin (13) are among the investigators who used the volume measuring technique to determine the amount of CO₂ reacted. In all these experiments, the object was to determine the reactivity of different kinds of carbon in order to get information on their behavior in a blast furnace. Because of the continuous change in gas composition in passing through the bed and a lack of knowledge of the flow pattern, from the point of view of studying the reaction mechanism, these results are of little value.

(2). Evaluation of the Reaction Rate from the Change in Pressure in the System

Rhead and Wheeler (14) and Wheeler and Stopes (15) used a circulation system, and from the increase in pressure the amount of CO formed was calculated. The authors, in interpreting their results assumed that the reaction was of first order with respect to CO₂ and neglected the reverse reaction. This enabled them to obtain an expression by means of which the results of their experiments could be calculated. It is clear today that the complex reaction

mechanism of carbon with carbon dioxide cannot be represented by a simple relation which does not even take cognizance of the retarding effect of CO, later proved to be very significant.

(3). Evaluation of the Reaction Rate from the Change in Weight of the Sample

Oshima and Fukuda (16) designed a continuous-weighing equipment which consisted essentially of a spring balance to which the sample being held in the reaction zone was attached. In this way, the weight of the sample could be recorded continuously in the course of reaction. Different kinds of coke powders and charcoals were used as samples. The object of this work was primarily to investigate the effect of ash on the reactivity of carbon.

There are two reasons why the results reported cannot be considered as representing the true reaction rate. In the first place, the V.C.M. liberated during the reaction was included in the measured weight loss, and therefore the results obtained are not dependable. In the second place, the perfusion effect must have played an important role in the reaction, as the sample was piled up in the sample supporter, resulting in non-uniform reaction conditions.

More definite information was obtained by Tu, Davis and Hottel (17), and Parker and Hottel (18). They

held a simply shaped carbon sample in the reaction stream and obtained the reaction rate from the loss in weight of the sample in the course of reaction. Most of their work, however, was limited to the study of carbon-oxygen reactions. The relative importance of diffusional and chemical processes at various temperatures was quantitatively studied. For the carbon-carbon dioxide reaction Dubin, using the apparatus of Tu and spherical electrode carbon and brush-carbon samples, found that between 1100°C. and 1350°C. the chemical reaction rate is the more important factor.

(4). Evaluation of the Reaction Rate from the Change in Composition of the Reacting Gas

Clement, Adams and Haskins (19) used a reaction tube filled with granular charcoal or coke samples, and passed CO₂ through the tube under controlled reaction conditions. The product gas was analyzed, and rate equations were derived on the basis of the assumptions that the forward reaction was of the first order and the reverse reaction was of the second order which would be true for homogeneous reactions of this type. For a heterogeneous reaction, such assumptions are usually unsound. In this particular case, the later-found retarding effect of CO should be considered in correlating the results. However, as no information was available for the flow pattern of gas in such a fixed-bed system, the results as such could

hardly tell anything about the reaction mechanism.

Cobb et al. (20), (21), (22), (23) used a similar reaction system and studied many special cokes with different ash constituents. The object of these studies was to devise a method by means of which the reactivity of coke to carbon dioxide could be determined. A great deal of experimental work was done in this direction, which may be of value in appropriate practical applications. The correlations developed were also based on the general concept used in dealing with homogeneous reactions. For the same reasons mentioned above, these results help very little in the elucidation of the reaction mechanism.

Drakeley (24) used a similar technique to investigate the reactivity of various carbonized coals and correlated the results by means of the expression used by Clement, Adams and Haskins. The reactivity of coke was found to be influenced by the temperature of carbonization.

Mayers (25) found that when the reacting gas was passed over a constant exposed area of carbon sample, the reaction rate depended on the thickness of the sample. He called this the "perfusion effect" which existed not only in the case of granular carbon samples but also in the case of monolithic carbon samples. Due to the intrinsic complexities of this effect, a successful theoretical approach is still lacking.

Many other investigators performed experiments using beds or columns of carbon and obtaining the reaction rates by analysis of the product gas. Among them are Perrott and Fieldner (26), Fischer, Breuer and Broche (27), Arend and Wagner (28), Bodmer (29), Rieffel (30), Gevers-Orban (31), and Cassan (32). But the most important contributions are those of Semechkova and Frank-Kamenetzky (33) and Hinshelwood et al. (34), (35), (36).

In contrast to the common fixed-bed methods, Semechkova and Frank-Kamenetzky performed their experiments using a static system, which eliminated many unknown variables inherent to a flow system. They postulated a general reaction mechanism which involved the surface adsorption of gases which, in principle, is in accordance with Langmuir's adsorption theory.

Following this work, Hinshelwood studied the reaction using both flow and static methods. In the flow equipment, the reacting gases were passed through a long vertical silica tube filled with coconut charcoal particles. The fraction of CO_2 reacting rarely exceeded 0.1 so that the volume of the reacting gas could be assumed to be constant. Also in this work a Langmuir form of adsorption equation was used to correlate the results. Each of the constants occurring in this equation was found to vary exponentially with temperature. The static experiments were performed to investigate the adsorption of gases on the

carbon surface in the course of the reaction, and thus to illustrate in a very direct way the general nature of the mechanism. From these experiments the retarding effect of CO was clearly shown to be due to the adsorption of the gas on the reaction sites.

Whereas all the above-mentioned experiments were performed at substantially atmospheric pressure, Langmuir (37), Meyer (38), (39), Sihvonen (40) and Eucken (41) investigated the reaction of a glowing carbon filament with CO₂ at extremely low pressures under which conditions the carbon dioxide molecules could strike the filament of carbon only once in the course of the reaction. Langmuir suspected already as early as 1915 that when CO₂ struck the carbon surface, one molecule of CO would be formed and one atom of oxygen would be attached to the carbon surface, which could be desorbed only very slowly to form another CO molecule. Meyer concluded that at low pressures the reaction was of zero order below 2600°K. but stated that the presence of minute amounts of impurities on the carbon surface might change the reaction order to anything between zero and first order, as had been repeatedly reported. However, the results obtained in these low-pressure experiments are of very little value in clarifying the reaction mechanism under atmospheric conditions, which are of utmost practical value, simply because in the present state of knowledge about the reaction direct extrapolation from low pressure regions to atmospheric conditions is impossible.

(5). Evaluation of the Reaction Rate from the Change in Dimensions of the Sample

Mungen (42), Mullery (43), and Smith (44) used successively the same technique in studying the reaction rates of small carbon rods with a stream of CO_2 at high velocities. The carbon rods were heated by means of an electric current passed through the rod. The reaction rate was obtained by measuring the decrease in diameter of the rod during reaction. Although this technique possessed the advantage of identifying reaction rate with a well-defined superficial surface, an offsetting disadvantage was the lack of knowledge of the extent to which the interior of the specimen contributed to the reaction.

Investigations using the fluidized technique were recently performed by Graham, McBride and Göring. They too used Langmuir-type adsorption equations in correlating their data. Although the application of the fluidized-bed technique may result in information which can sometimes be applied directly to industrial plants, and also can clarify some fundamentally important points, the method suffers from the inability to obtain more than an average rate in a system in which the gas composition varies considerably and in an unknown manner from inlet to outlet.

In conclusion, the previous investigations, numerous as they are, offer rather limited information on the mechanism of the carbon-carbon dioxide reaction. The

techniques which have been applied are not adequate to evaluate the specific effect of any single variable which influences the point reaction rate.

C. Scope of the Present Work

It was the original object to investigate the reaction rates under various specific reaction conditions using coke particles from the same lot used by McBride, and by comparing the results obtained, determine the performance of the fluidized bed.

Because of the presence of ash and V.C.M. in the coke, it was later realized that, in order to get a more clear visualization of the reaction mechanism, some other kind of carbon should also be investigated. The National electrode carbon used by Mungen, Mullery and Smith was employed. This carbon contains 0.4% ash and negligible V.C.M., and is suitable for the study of reaction kinetics. However, the results using coke were considered of more immediate practical importance.

The experiments were carried out at one atmosphere using temperatures ranging from 1500°F. to 1900°F. Both $\text{CO}_2\text{-N}_2$ and $\text{CO}_2\text{-CO}$ gas mixtures were employed. The effects of gas velocity, particle size and reactivity of carbon as influenced by the time of reaction were studied under well-controlled point-reaction conditions.

III. CONSTRUCTION OF EQUIPMENT

To obtain the data required for the evaluation of specific point reaction rates of carbon particles with carbon dioxide, the design of the equipment had to embody the following features:

(1) The equipment should be so constructed that a single carbon particle could react with the reacting gas without the interference of other particles or foreign materials.

(2) It should be possible to determine accurately the weight of the sample before and after reaction.

(3) In the reaction zone, it should be possible to control the temperature, pressure and gas flow rate accurately.

(4) The gas composition should be known and completely free from oxygen.

(5) It should be possible to control the time of reaction.

It was with these points in mind that the equipment was designed and constructed. Photographs of the complete equipment are shown in Figures 1 and 2.

Essentially, the equipment consisted of a magnetic moving device by means of which a screen pan, on which a single layer of carbon particles is evenly distributed, could

Figure 1

Front View of Equipment

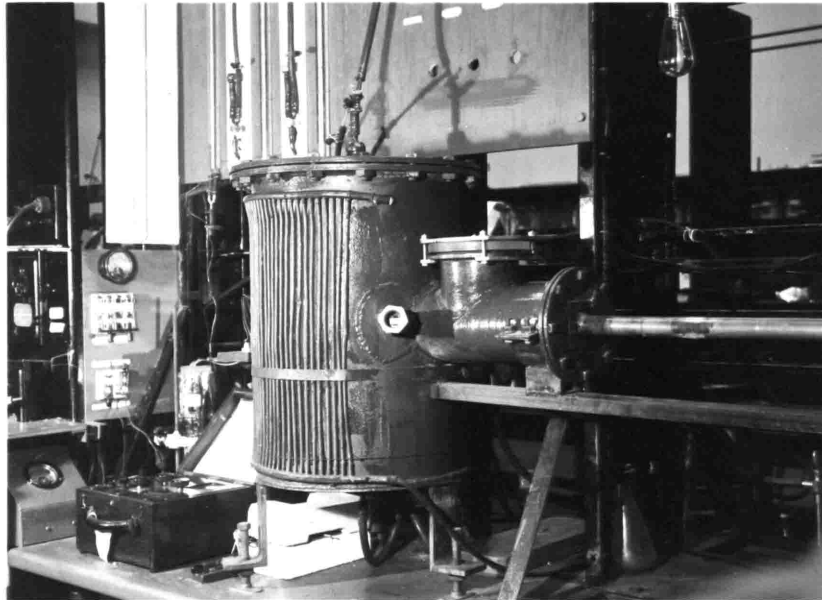
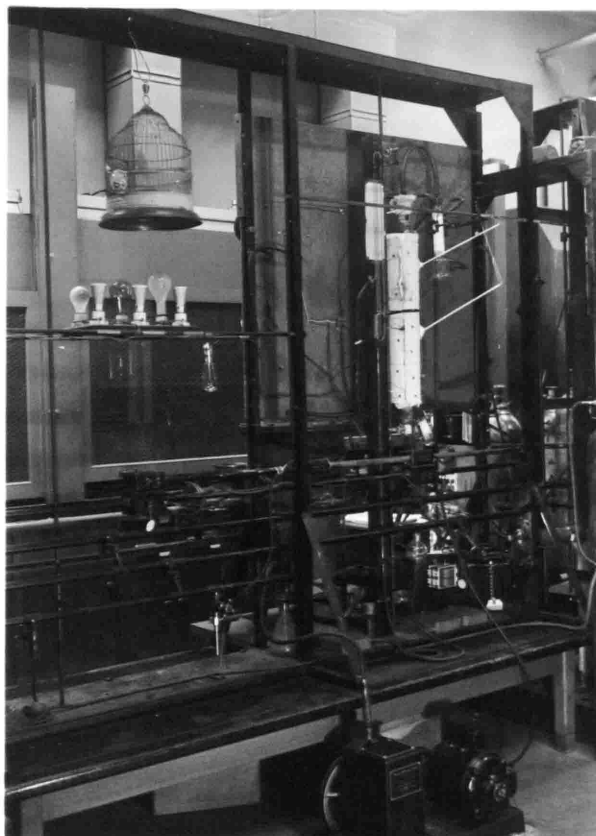


Figure 2

Back View of Equipment



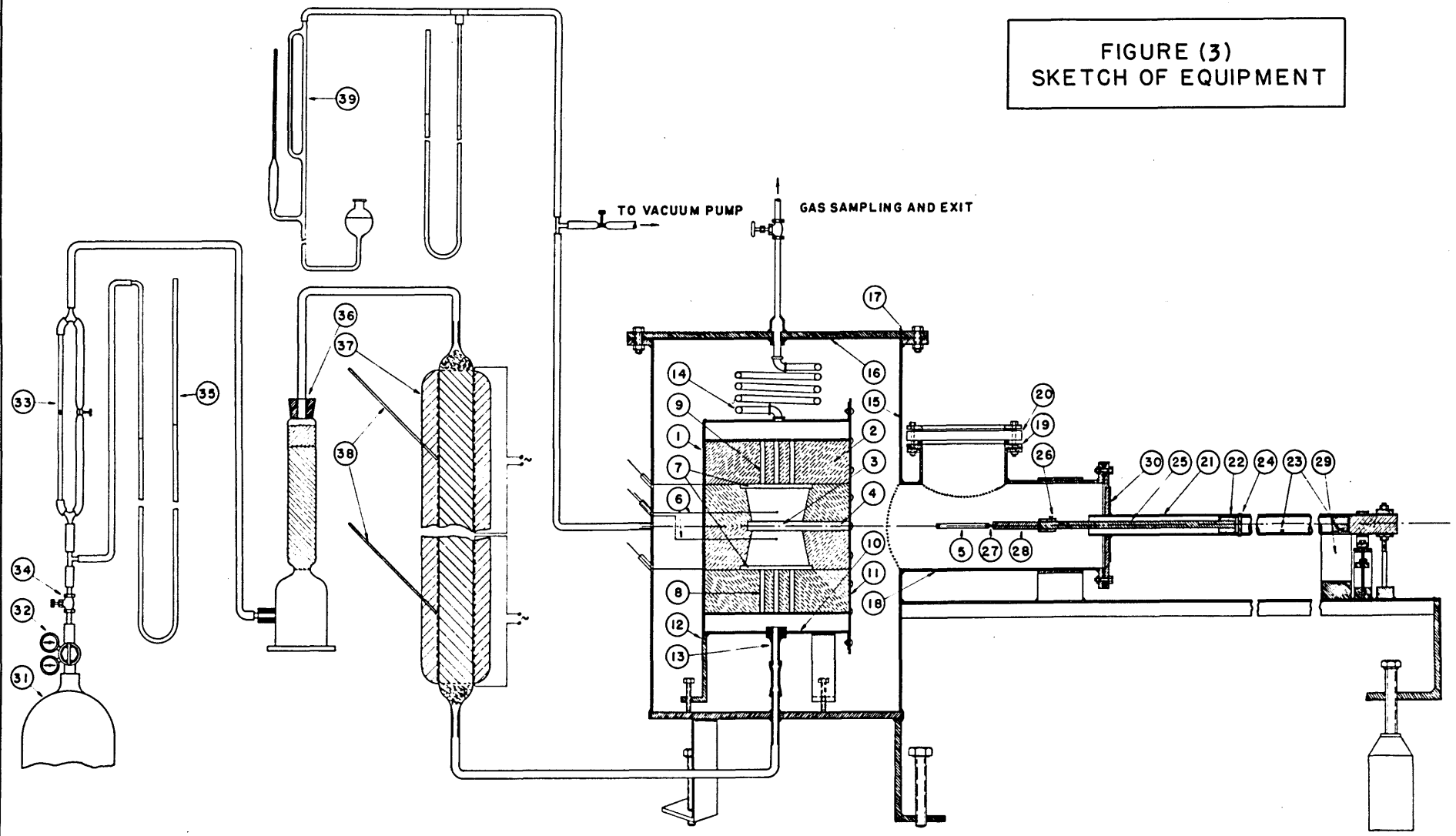
be moved into and out of the furnace from outside the system. To eliminate traces of oxygen present in the system, both evacuation and flushing procedures were used.

The following description refers to Figure 3 which is a complete drawing of the equipment:

The furnace (1) was constructed by fitting together eight blocks of Kl6 B & W insulating firebrick (2). These bricks were carved out to form a combustion chamber (3), an entrance (4) for the sample pan supporter (5), entrance ports for two thermocouples (6), positions for two heating coils (7) and entrance (8) and exit ports (9) for the entering and leaving gas streams. After the bricks were cut to fit together snugly, they were completely coated with a high-temperature brick coating mortar and after drying in air, baked for two hours at 1800°F. This treatment produced a smooth and hard surface over the bricks, and reduced the tendency for particles to dislodge from the surface.

The brick furnace was fitted into a steel box (10) constructed of sheet steel welded at the seams. The front cover (11) of this steel box was bolted to the rest of the unit and was provided with an opening of the proper size to admit the sample pan supporter. The steel box could be elevated or lowered into proper position by three adjustable legs (12). The gas entrance connection (13) was located at the bottom, and the outlet (14) at the top.

FIGURE (3)
SKETCH OF EQUIPMENT



In order to eliminate the effect of reaction with oxygen the apparatus had to be constructed airtight so that it could be freed from air by evacuation and then filled and flushed with the gas mixture used for reaction. This was achieved by use of a cylindrical steel shell (15) with butt-welded seams and a removable top cover (16), which could be bolted to the top flange with a rubber gasket (17) forming an airtight junction. A connecting side arm (18) with a machined horizontal flange surface (19) was welded onto the cylindrical wall. Upon this surface a 7 inch diameter x 1/2 inch thick Lucite plastic disc (20) could be clamped down, with a rubber gasket in between. This Lucite disc served as an observation area to view the nichrome screen pan and its contents when moving it in and out of the combustion chamber, to be sure that the moving procedures were performed smoothly and that the carbon particles were not subjected to any jerking motion. This flange opening was also used for putting the nichrome screen pan on and removing it from the alundum rods.

To prevent any air leakage through stuffing boxes on moving rods, a long brass flexure tube (21) closed at one end was constructed, enclosing the pan moving mechanism. Inside this tube a cylindrical steel block (22) rolled easily on two small wheels (23), and was kept in a vertical position by a slot and key arrangement (24). To this cylindrical steel block was attached a long steel rod (25), at the

25

end of which was a yoke (26) into which the two alundum supporting rods (27) were cemented. To reduce the heat loss through the entrance of the pan in the furnace bricks, a piece of brick (28) was made to fit between the alundum rods and attached to the yoke, thus filling the slot opening once the nichrome pan was in the furnace. The motion of the cylindrical steel block and hence of the nichrome pan was controlled externally by means of a powerful horseshoe magnet (29) which made inserting the pan into and withdrawing it from the reaction area possible without imparting any jerking motion to the pan. The angle of attachment of the flexure tube to the reaction chamber side-arm could be modified slightly by moving the closed end of the tube. This tilting procedure was used as a final adjustment to obtain an absolutely unhampered motion of the nichrome pan, and was made possible by a thin brass diaphragm (30) soldered to the flexure tube and the end of the side arm.

In the combustion chamber two chromel-alumel thermocouples were located, one above and one below the nichrome screen pan. The temperature was determined by readings from a Brown semi-precision potentiometer accurate to 0.02 millivolt.

The furnace was heated using electric heating coils made from Kanthal ribbon. The ribbon was formed into flat grids by bending it around steel pegs set in a wooden frame. To remove its elasticity after bending, the unit was then

transferred to a muffle furnace, heat treated at 1800°F., and cooled slowly to room temperature. This treatment made the ribbon very brittle and necessitated extreme care in fitting it into place. The current of 9-15 amperes required for the heating coils was obtained from the 115-volt A.C. power line by means of a Variac, type 100-Q.

In the runs using coke particles of 50-60 mesh, the difference between the temperature above and below the nichrome screen pan amounted to about 40°F. In all the later runs using coke particles of different sizes and electrode carbon particles of 50-60 mesh, alundum rods were placed between the ribbons of the heating coils. The more homogeneous heating surface so created resulted in temperatures above and below the pan which differed at most by 10°F. The reaction temperature was taken as the average of these two readings. Another advantage of inserting the alundum rods was that the tendency of the Kanthal ribbon to stretch and buckle after many heating periods was somewhat controlled by the rods, which prevented the ribbons from touching each other, hence eliminating possible short circuits.

The desired reaction temperature was maintained constant within 1°F., by a temperature regulator designed and described by Port (45) and Egbert (46). The general principle of the temperature regulator is outlined here: The movement of the pointer of a galvanometer, connected to the lower furnace thermocouple exposes or covers a slot in

the scale under the pointer. Beneath this slot is an R.C.A. Radiotron 922, which is excited by a beam of light from a projector bulb. Exposing or covering the slot thus affects the Radiotron which operates a relay which opens or closes a shunt on a resistance in the furnace heating-coil circuit, resulting in an increase or decrease of 1 ampere of current through the heating coil. The variac is so adjusted that when the shunt is opened the temperature attained in the reaction zone is slightly below the required reaction temperature, and when the shunt is closed it is slightly above the required reaction temperature.

After the temperature regulator was properly adjusted for each run, it needed very little further attention. It operated smoothly and dependably throughout the course of the experiments.

In the progress of the experiments, three different modifications of the sample screen pan were used. For all the runs using coke particles of 50-60 mesh reacting with different gas mixtures at the standard gas flow rate, the double-pan setup shown in Figure (4) was employed. Two semi-circular pans, each carrying about 0.15 gms. of samples, were fitted into the sample pan supporter shown in Figure 5. Pan No. 1 (as indicated in Figure (4)), which was located farther from the slot opening, indicated a temperature very close to the average of the temperatures indicated by the two thermocouples. Pan No. 2, which was located near the

Figure 4

Nichrome Sample Pan Supporter
and Double Pans

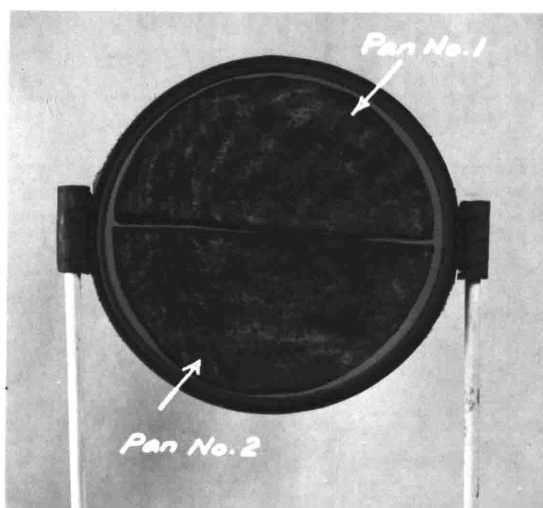
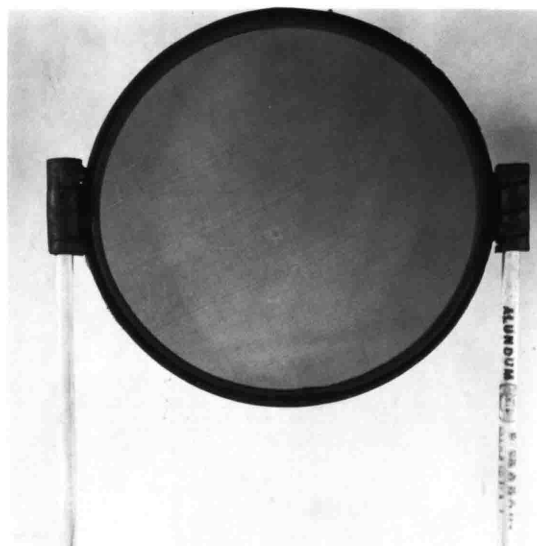


Figure 5

Nichrome Sample Pan Supporter
for the Double Pans



entrance opening of the furnace, was found to be 10°F. lower in temperature than the average of the two thermocouple readings. Usually the data from Pan No. 2 served as a check on the data from Pan No. 1, generally giving a lower reaction rate consistent with the temperature decrement.

This consistency caused abandonment of the double pan in the later runs; single pans as shown in Figures [6] and [7] were used. The runs using coke of 50-60 mesh particle size reacting at different gas flow rates were made using the setup shown in Figure 6, the sample pan supporter being shown in Figure 8. In this setup, a circular piece of screen was bent all around the circumference perpendicular to the plane of the screen, thus forming a pan of approximately 0.5 cm. in depth and 5 cm. in diameter. A hole was cut in the sample pan supporter, about 0.5 cm. smaller in diameter than the pan. This arrangement had the advantage of having only one layer of screen, which caused less by-passing of gases than when using two layers of screen. The holes in the screen served as reference points. Pictures, as shown in Figure [9], were taken before and after reaction to find out whether any particles were lost or displaced in the handling of the sample pan or in the course of the reaction when the gas velocities were relatively high.

In all later runs using coke particles of different sizes and electrode carbon particles of 50-60 mesh, a

Figure 6

Nichrome Sample Pan Supporter
and Sample Pan (1)

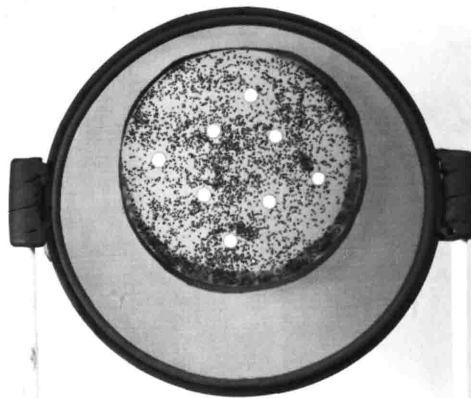


Figure 7

Nichrome Sample Pan Supporter
and Sample Pan (2)

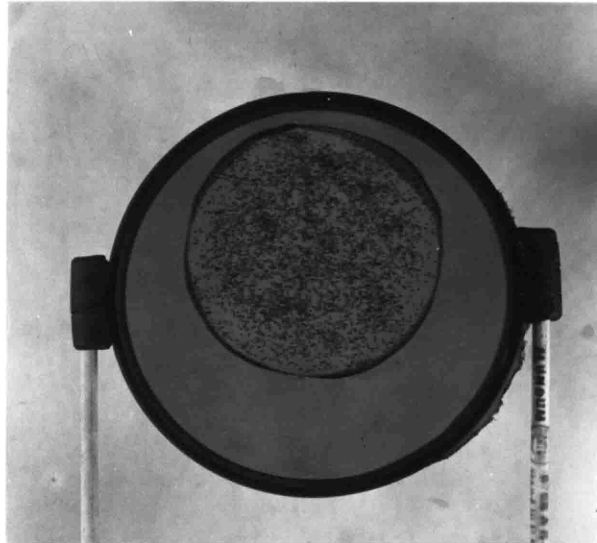


Figure 8

Nichrome Sample Pan Supporter
for the Single Sample Pans

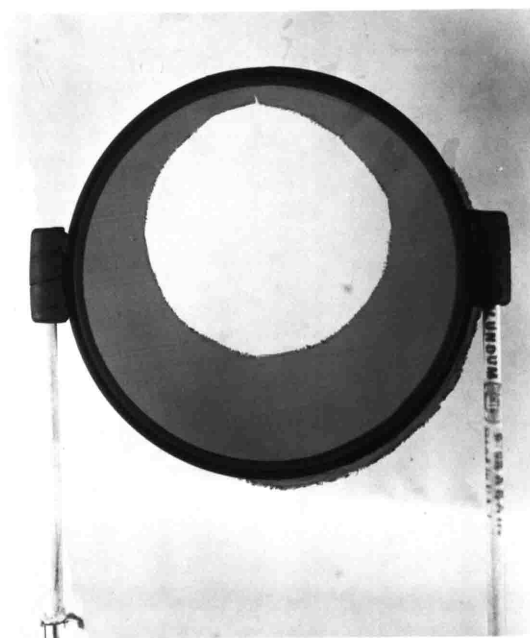
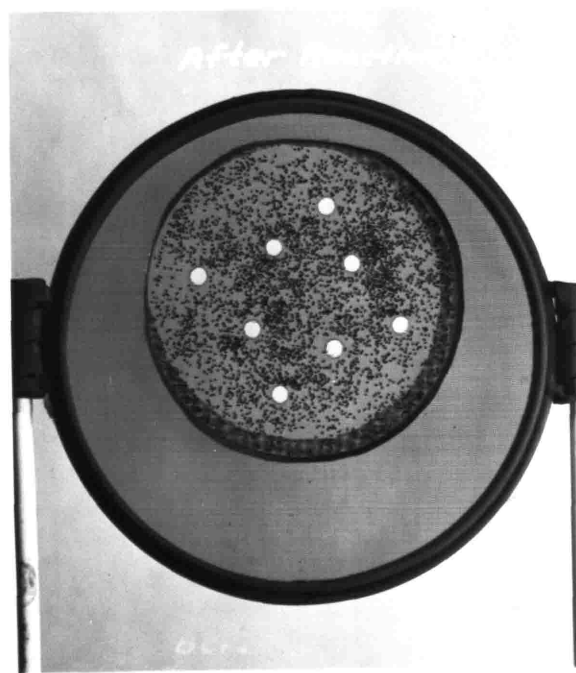
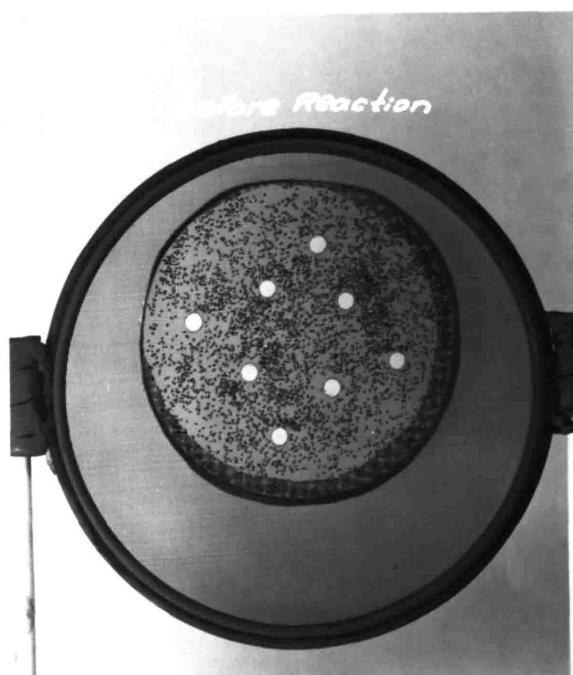


Figure 9

Smoke Particles before and
after the Reaction



one-pan setup as shown in Figure 7 was used. The pan, like the former one, carrying about 0.1 grams of coke, was situated off-center in relation to the entrance opening of the furnace, so that the temperature of the sample was close to the average of the two thermocouple readings.

In most of the runs, 100 mesh nichrome screen was chosen as the supporting screen for the carbon particles. Preliminary tests had shown that nichrome screen was inert with respect to reaction with carbon, carbon monoxide or carbon dioxide, between temperatures of 1500 to 2000°F., once a protective layer had been formed on the screen. This protective layer, giving a dull green color to the originally bright and shiny screen, was formed during the first two or three runs, and added about 0.2% to the weight of the screen. After this protective coating was established, the weight remained practically constant in further exposure to the reaction atmosphere. It was found to be advisable to replace the pans with new ones after about 30 runs, as the screen then showed some sagging and buckling.

The sample pan supporter shown in Figure 8, constructed of 100 mesh nichrome screen, was circular in shape with a diameter of 7.8 cm. Around the periphery it was braced with two chromel-A rings to keep it rigid. Welded on the outer ring were two "slip-on" fixtures, into which the ends of two alundum rods were inserted. These alundum rods were used to hold the sample pan supporter in a horizontal position while it was being moved into the combustion chamber,

while the reaction proceeded, and while it was being withdrawn after reaction.

This system, as described here, made it possible to hold a single layer of coke particles in the reaction chamber, and to allow the reacting gas to pass up through the horizontal screen. In this way the particles were completely bathed in fresh reacting gas at all times.

The system was equipped with a Cenco Megavac vacuum pump, which made it possible to remove practically all the oxygen in the system. The vacuum was measured by means of a McLeod gage (39).

The gas mixtures used were made up prior to starting a run. The gas components required for a particular mixture were taken from the conventional compressed gas cylinders, and were mixed in a pressure cylinder (31) reserved for this purpose. The cylinder was then put into a hot water bath and heated overnight to insure complete mixing. The composition of the gas mixture was determined a few times during a series of runs by means of an Orsat gas analysis apparatus. The gas, whether a mixture or a pure gas, flowed through a standard diaphragm pressure regulator (32), thence through a rotameter (33) provided with a bypass, in a stream regulated by means of a 1/8 inch needle valve (34). The pressure between diaphragm regulator and rotameter was measured by means of a U-shaped, mercury-filled pressure gage (35). From the rotameter the

gas flowed to a 4.5 cm. diameter x 30 cm. high glass drying tower (36) filled with calcium chloride, on top of which some Drierite had been put to act as an indicator. From the drying tower the gas flowed to the oxygen removal apparatus (37) constructed of an 80 cm. length of 5 cm. diameter heavy-walled Pyrex tube provided with 1.5 cm. diameter x 9 cm. long Pyrex connections at each end for slipping on rubber tubing. The Pyrex tube was filled with 0.5 mm. diameter x 5 mm. long activated copper rods. The oxygen removal apparatus was heated to a temperature of about 450°C. by means of two electric heating coils wound around its outside. At this temperature the trace of oxygen present in the gas stream was rapidly removed by reaction with the copper. To check the temperature of the oxygen removal apparatus, two thermometers (38) were placed on the outside of the tube, respectively 1/4 and 3/4 of the height of the tube from the gas inlet. The outside of the tube and thermometers were insulated by means of 1" magnesia pipe insulation. The electric current required for the heating coils of the oxygen removal apparatus was obtained from the 115-volt A.C. power line by means of two variacs, type 200-C.

The gas entered the furnace through a 1/4" steel pipe brazed into the bottom of the steel shell and protruding 3" on both sides of the shell. A piece of rubber tubing

connected the pipe extending inside the shell with the entrance port in the bottom of the steel box. From this entrance port the gas flowed through twenty-five $3/16$ " holes in the bottom layer of the bricks, past the lower heating unit, and into the combustion chamber. The product gases resulting from the reaction passed through the upper heating unit and left the furnace through another set of $3/16$ " holes in the uppermost layer of bricks. The exit gases passed out of the unit through a semi-flexible spiral steel tube, designed to allow slight variations in the height of the steel box caused by adjusting the three legs.

All connections outside the furnace were made by means of heavy-walled rubber tubing. Rubber-glass joints were tightened by means of steel wire and sealed with Glyptal. The pressure in the equipment, which was maintained at 780 mm. Hg. during all runs, was regulated by means of a valve in the gas outlet pipe from the furnace. Generally the gas was led from this outlet directly into the hood. For the velocity runs a wet test gas meter was installed at the outlet of the equipment because of the limited capacity of the rotameter, and the latter was bypassed. The pressure in the equipment was then controlled by means of a valve at the outlet of the wet test gas meter.

The oxygen content of the gases used was periodically checked by means of a micro oxygen analyzer constructed by

R. J. Kallal (47), according to methods described by Uhrig, Roberts and Levin (48) and Powell and Joy (49). The oxygen content was always found to be below 50 parts per million, so that it can be assumed that the effect of oxygen was nearly completely eliminated.

IV. PROCEDURE

To obtain experimental data under controlled reaction conditions for the evaluation of specific point reaction rates, the procedure followed in this investigation consisted in passing the reacting gas consisting of either pure carbon dioxide, carbon dioxide with nitrogen, or carbon dioxide with carbon monoxide through a single-layer fixed bed of carbon particles, at a specified temperature for a fixed length of time.

To start a run, the furnace was brought up to the required reaction temperature, and the oxygen removal apparatus filled with activated copper rods was heated to 450°C. The sample pan was weighed before and after a uniform layer of carbon had been scattered on the screen. The pan was next put on the sample pan supporter, which in turn was placed on the alundum rods through the charging opening of the equipment. The charging opening was then closed with a plastic cover, which when tightened was vacuum proof. The complete system was thereupon evacuated by means of a Cenco-Megavac vacuum pump for 12 to 20 minutes, after which period the pressure in the system, measured by means of a McLeod gauge, was 1.2 to 0.9 mm. Hg. The system was then filled with the reacting gas in approximately four minutes. The time of this fill-

43

ing operation was kept at a minimum in order to reduce the amount of oxygen leaking into the system to a minimum. The furnace temperature and the flow rate of the gas stream were then adjusted to proper values; the time required was usually 10-15 minutes. When the proper reaction conditions were obtained, the pan containing the carbon layer was inserted into the combustion chamber, using the magnetic moving device. The sample was allowed to react with the reacting gas for a fixed length of time.

During the reaction period, the furnace temperature was automatically maintained at the required reaction temperature by means of a temperature regulator. The flow rate was kept at the required value by means of a 1/8 inch needle valve after the diaphragm-pressure regulator on the compressed gas cylinder. At the end of the reaction period the nichrome pan with its contents was withdrawn from the combustion chamber; the reacting gas stream was discontinued, and the pan allowed to cool to slightly above room temperature. After the pan had cooled, the plastic cover was removed from the charging opening, and the pan was taken off the alundum supporting rods. The pan with the sample and the empty pan were weighed again to determine the change in weight during the reaction period.

From the decrease in weight of the carbon and the time of reaction, the specific reaction rate for each run was determined.

The evacuation time applied in the runs using coke was 12 minutes, resulting in a pressure in the system of 1.2 mm. Hg. In the later runs while electrode carbon was used, the evacuation time was 20 minutes, resulting in a pressure in the system of 0.9 mm. Hg.

The coke was initially heated in an oven at 110°C. for 24 hours to remove the moisture. To correct for the weight loss due to volatile matter, blank runs were made in pure nitrogen with dried coke for the same time and at the same temperature as the reaction runs.

Two methods were used to prepare coke particles of different sizes. For the small particles (8 - 100 mesh), crushing and sieving procedures were used, resulting in particles of rather irregular shapes. The eleven large particles (2.5 to 9.2 mm. in diameter), however, were shaped by hand, resulting in particles of more or less spherical form.

The electrode carbon particles of 50-60 mesh were also made by crushing and sieving procedures. The particles appeared to be denser and less porous than the coke particles.

During the experiments, the oxygen removal apparatus and the calcium chloride tube were always kept active by re-activation and refilling procedures.

V. RESULTS

A. Presentation of Data

For the symbols used in this section, see Appendix. In the descriptions, the following terms are generally applied:

- N₂ blank runs -- Runs made with pure nitrogen.
- CO₂-N₂ runs -- Runs made with CO₂ and CO₂-N₂ mixtures.
- CO₂-CO runs -- Runs made with CO₂ and CO₂-CO mixtures.
- Velocity runs -- Runs made at various gas flow rates, using pure CO₂ as the reacting gas.
- Time runs -- Runs made with different times of reaction for a certain gas composition.

A list of the gas mixtures used and their compositions is given in Table A1.

An explanation of the run numbers, assigned to the runs listed in the data sheets, is given at the top of each Table. A consistent system to number all the runs was adopted.

The experimental results obtained can be classified into the following three groups, according to the order in which they were performed:

1. Experiments using New England coke particles of 50-60 mesh.

In all the experiments the total pressure was kept at 780 mm. Hg. The gas flow rate, except in the

velocity runs, was maintained at 15 cc. per second (measured at 85°F. and 1 atm.). The initial particle size of coke was 50-60 mesh.

(a) N₂ blank runs: The results are listed in Table A2, and fractional decrease in weight of the sample, F_{N_2} , calculated from the data on an ash-free basis, is plotted versus θ at different temperatures in Figure 10 which serves as a correction chart for V.C.M. liberated during the reaction runs.

(b) CO₂-N₂ runs: Five temperatures (1500, 1600, 1700, 1800 and 1900°F.) were investigated. The time of reaction was assigned to each run so as to give approximately $F_{CO_2} = 0.1$. The results are shown in Table A3. In Figure 11 the values of the average specific reaction rate R_{av} are plotted vs. the partial pressure of CO₂ on semi-logarithmic coordinates. For each pair of curves at a certain temperature, the upper one shows R_{av} calculated on an ash-free basis, and the lower one shows that calculated on an ash-free basis, after being corrected for V.C.M. based on the N₂ blank runs.

(c) CO₂-CO runs: The temperatures investigated were the same as in the CO₂-N₂ runs. The results are shown in Table A4. In Figure 12

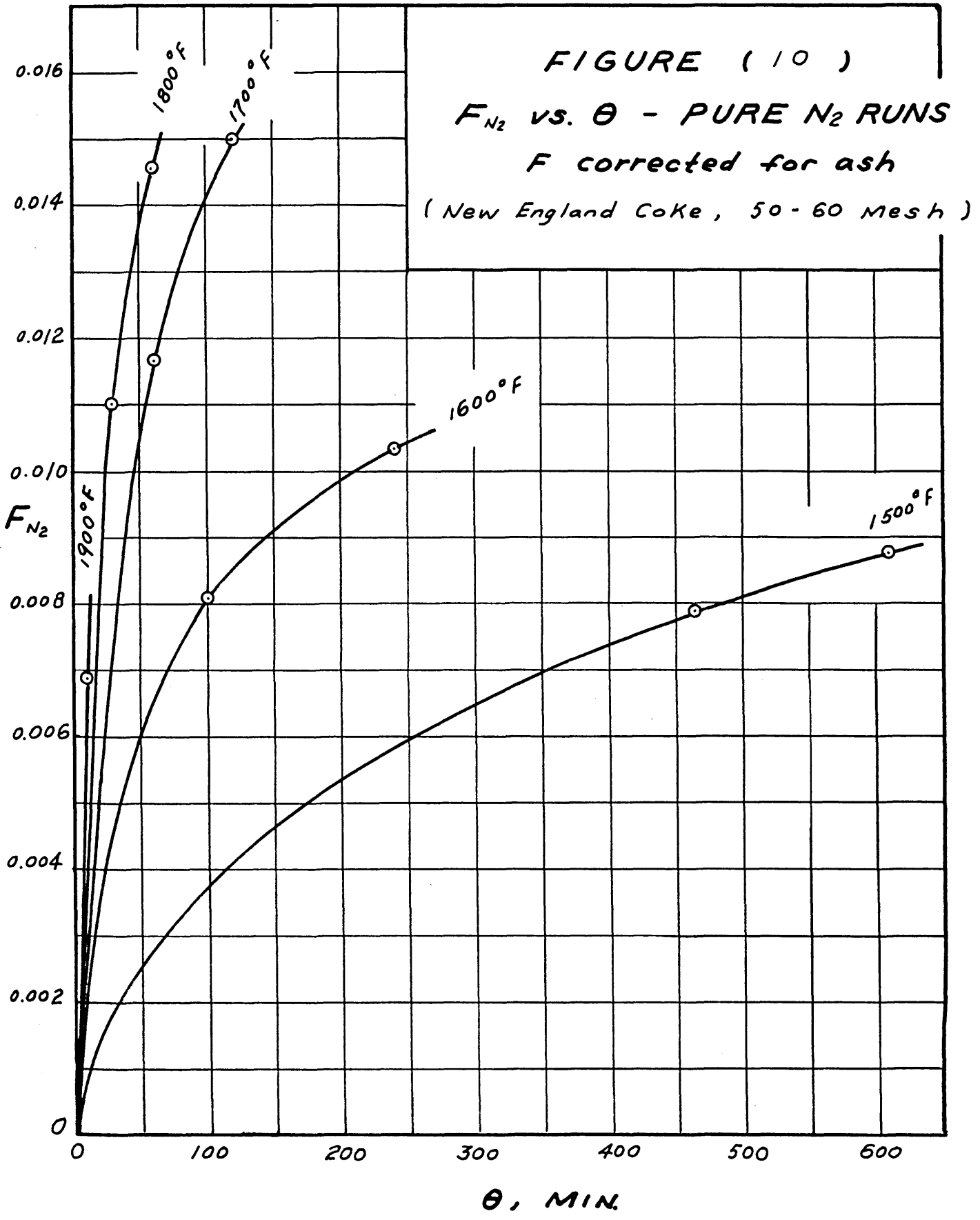


FIGURE (11) R_{AV} vs. P_{CO_2} FOR CO_2-N_2 RUNS

(New England Coke, 50-60 Mesh)

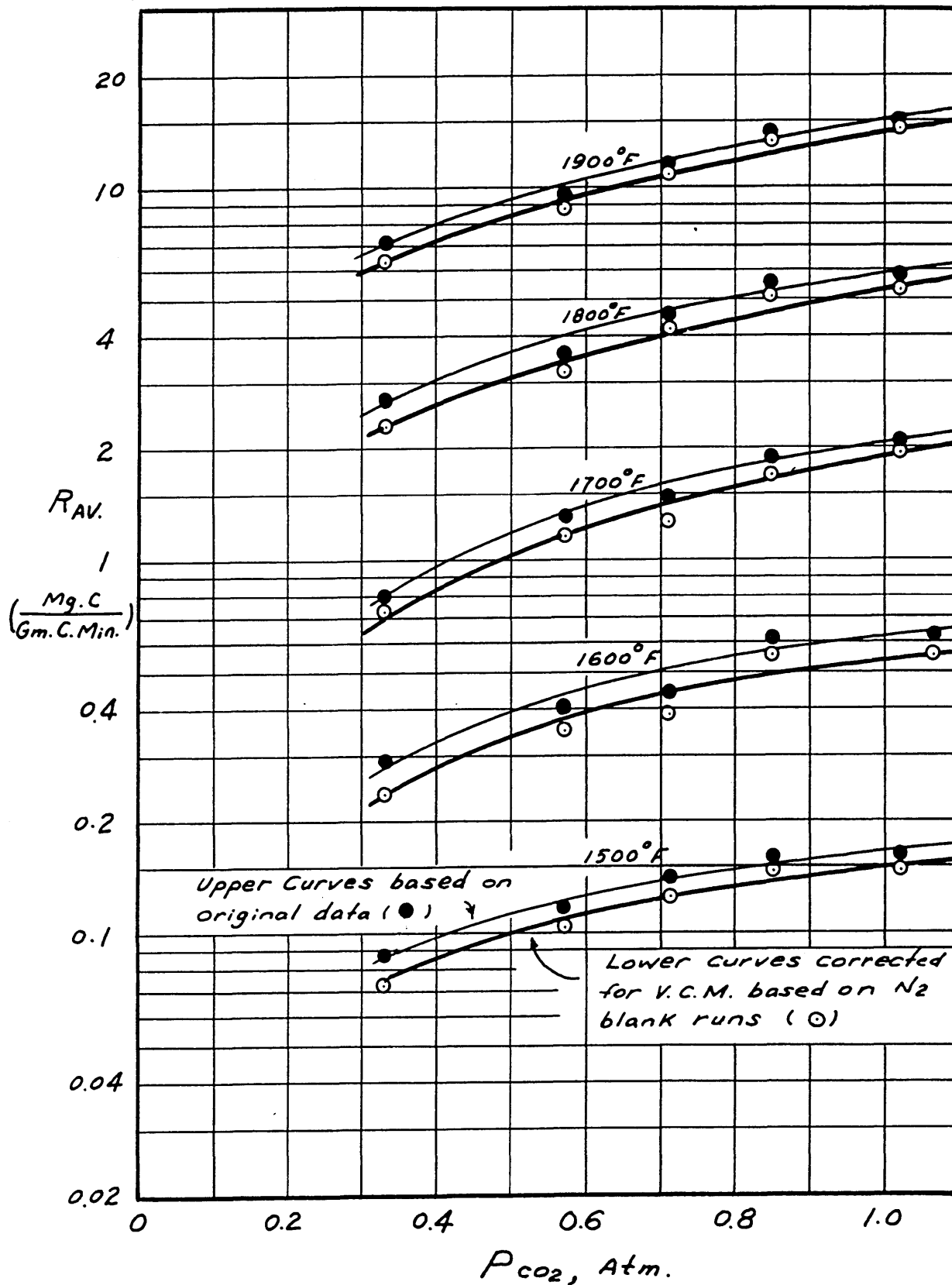
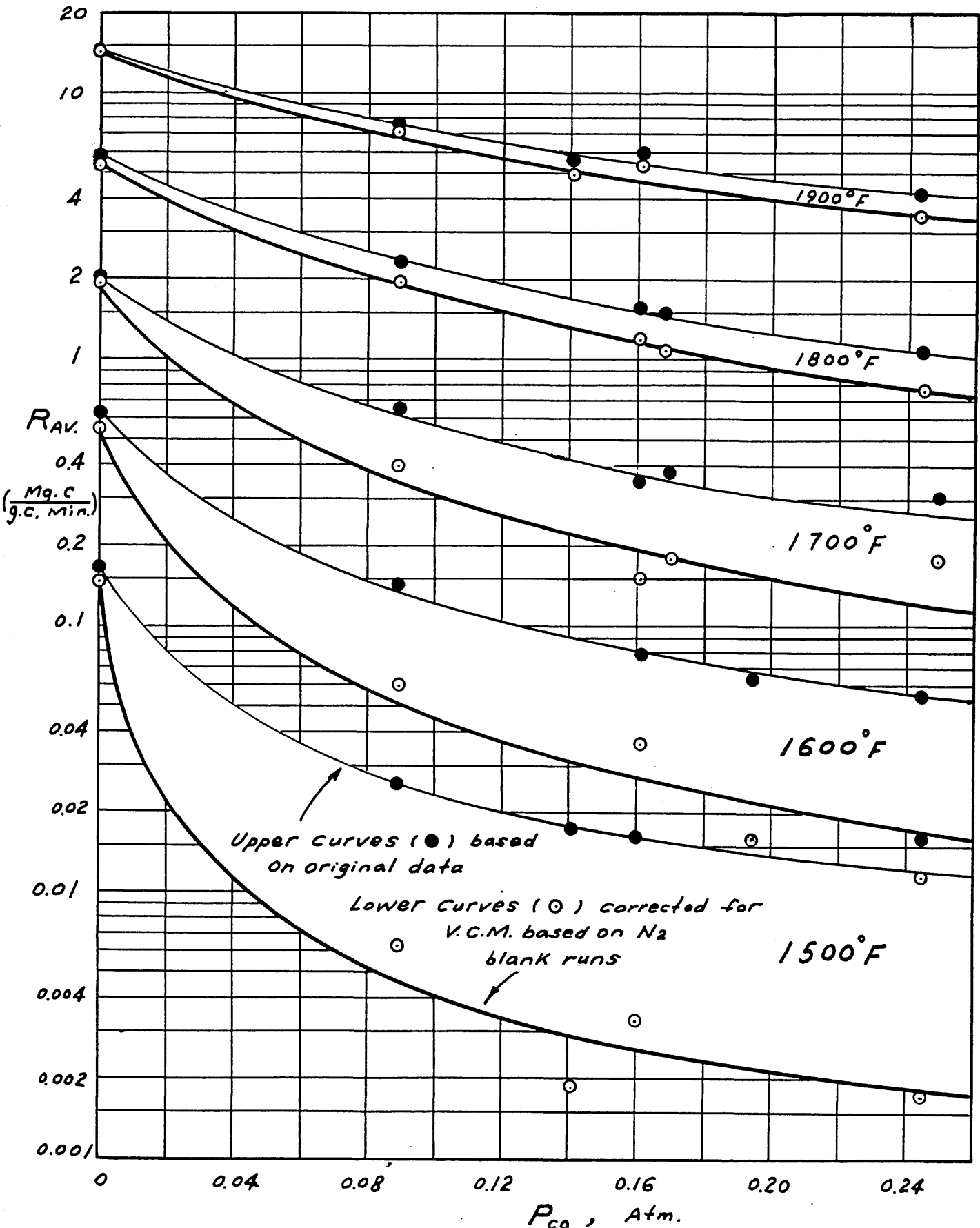


FIGURE (12) R_{AV} vs. P_{CO} FOR CO_2-CO RUNS
 (New England Coke, 50-60 Mesh)



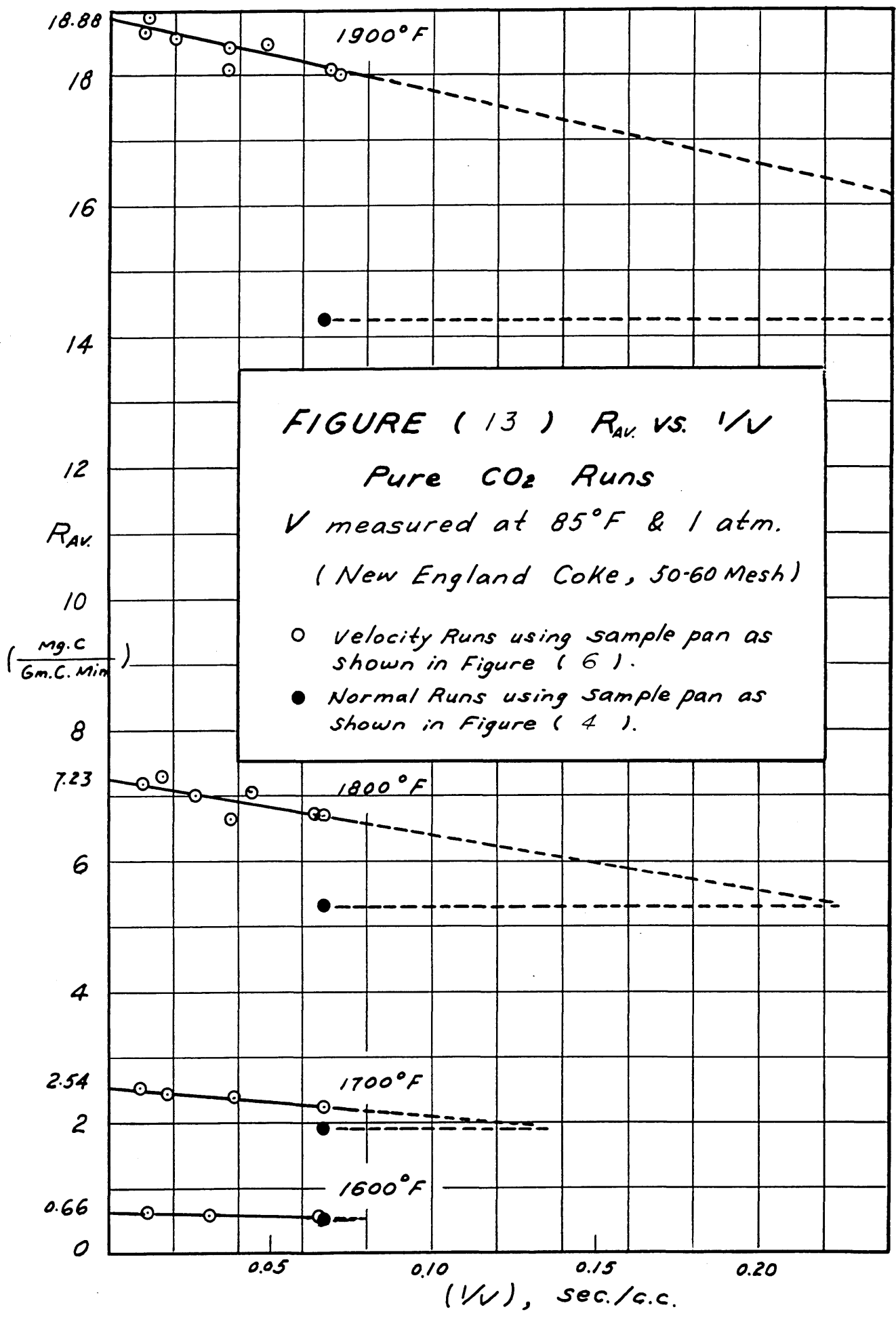
the values of R_{av} are plotted versus the partial pressure of CO on semi-logarithmic coordinates. For each pair of curves at a certain temperature, the upper one shows R_{av} calculated on an ash-free basis, and the lower one shows that calculated on an ash-free basis, after being corrected for V.C.M. based on the N_2 blank runs.

(d) Velocity runs: The temperatures investigated were the same as in the CO_2-N_2 runs. The results are shown in Table A5. The values of R_{av} calculated on an ash-free basis after being corrected for V.C.M., are plotted versus the reciprocal of the gas flow rate $1/V$ on linear coordinates in Figure 13.

2. Experiments using New England coke particles of different sizes, reacting with pure carbon dioxide at 1800°F. with different times of reaction.

In all the experiments the total pressure was kept at 780 mm. Hg. The temperature used was 1800°F. The gas flow rate was maintained at 15 cc. per second (measured at 85°F. and 1 atm.).

(a) N_2 blank runs: The results are listed in Table A6. The values of F_{N_2} , calculated from the data, are plotted versus the time θ . A cross plot of F_{N_2} vs. the initial diameter of the



particle D is shown in Figure 14, which serves as a correction chart for V.C.M. liberated during the reaction runs.

(b) Time runs: Reaction runs were made with samples of particle sizes between 8-100 mesh. Six different particle sizes were used, namely, 8-12, 16-20, 30-40, 50-60, 70-80, and 80-100 mesh. Each sample weighed about 0.1 grams. Generally, five runs were made with each size, at different reaction times of 10, 20, 30, 50 and 90 minutes. In a separate test run, 50-60 mesh particles were subjected to three consecutive reaction periods of 30 minutes each. The results were consistent with those mentioned above and the data hence are not presented.

Reaction runs were also made with samples of particle sizes between 2.5 and 9.2 mm. in diameter. Eleven separate particles were used. Each particle was subjected to three consecutive reaction periods of 30 minutes each. Two series of runs of this kind were made, one including seven particles (D1-D7), and the other four particles (D8-D11).

The data of all runs and correction factors for V.C.M. are listed in Table A7. The values of (1-F) are plotted versus θ in Figure 15,

0.03

0.02

F

0.01

0

FIGURE (14)

F vs. D

T 1800° F

P 1.026 atm.

Pure N₂ Blank Runs
(New England coke)

F vs. θ

.03

F .02

.01

0

90

60

30

0

θ , MIN.

80-100 Mesh

50-60 Mesh

8-12 Mesh

D₁₀

D₈

D₆

D₄

D₂

90 Min.

60 Min.

50 Min.

40 Min.

30 Min.

20 Min.

10 Min.

16-20

30-40

50-60

70-80

80-100 Mesh

0.2

0.4

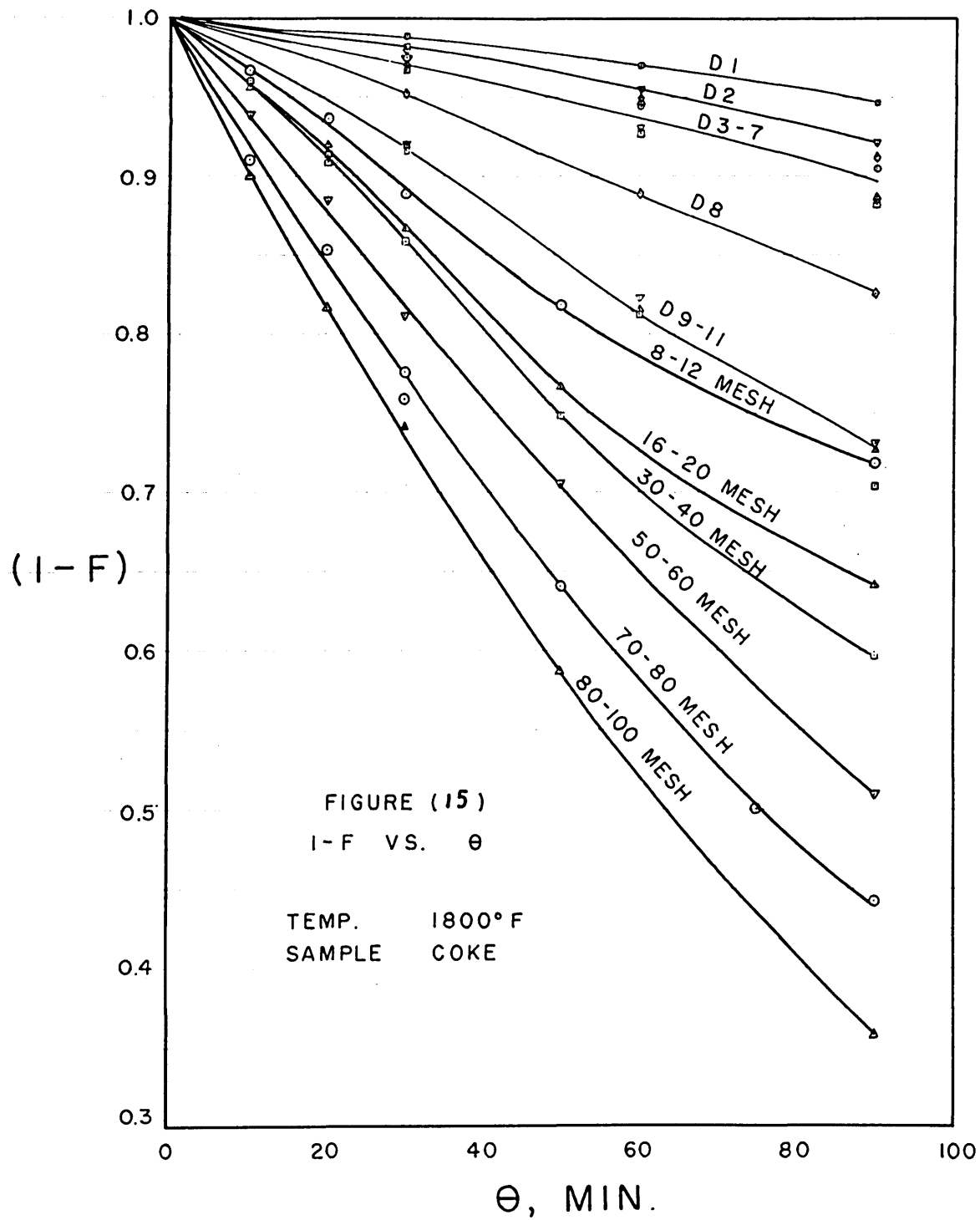
1.0

2.0

4.0

10

D, mm.



wherein F is the fractional decrease in weight of the carbon sample on an ash-free basis, after being corrected for V.C.M. based on the N_2 blank runs. The values of R_{av} , calculated from the corrected data are plotted vs. θ in Figure 16 with constant F lines drawn on the same graph.

The values of R_{av} at $F = 0.1$ are plotted vs. D , the initial particle diameter, in Figure 17. For comparison, the data of Blanc (50), who performed preliminary runs using this equipment, are plotted in the same figure.

(c) The average weight of a single particle of different sizes was determined and the results are shown in Table A8. The average weight per particle is plotted vs. D^3 on logarithmic coordinates, in Figure 18.

Photographs of the particles D1-D7 before and after reaction of 90 minutes are shown in Figure 19. Figure 20 shows a photograph of coke particles of 50-60 mesh scattered on the 100 mesh screen, magnified 12.5 times in diameter.

3. Experiments using National electrode carbon particles of 50-60 mesh.

In all the experiments, the total pressure was kept at 780 mm. Hg. The gas flow rate was maintained at 15 cc. per second (measured at 85°F. and 1 atm.). The initial

FIGURE (16) R_{AV} vs. θ

T 1800°F P 1.026 atm.

Pure CO₂ Runs (New England Coke)

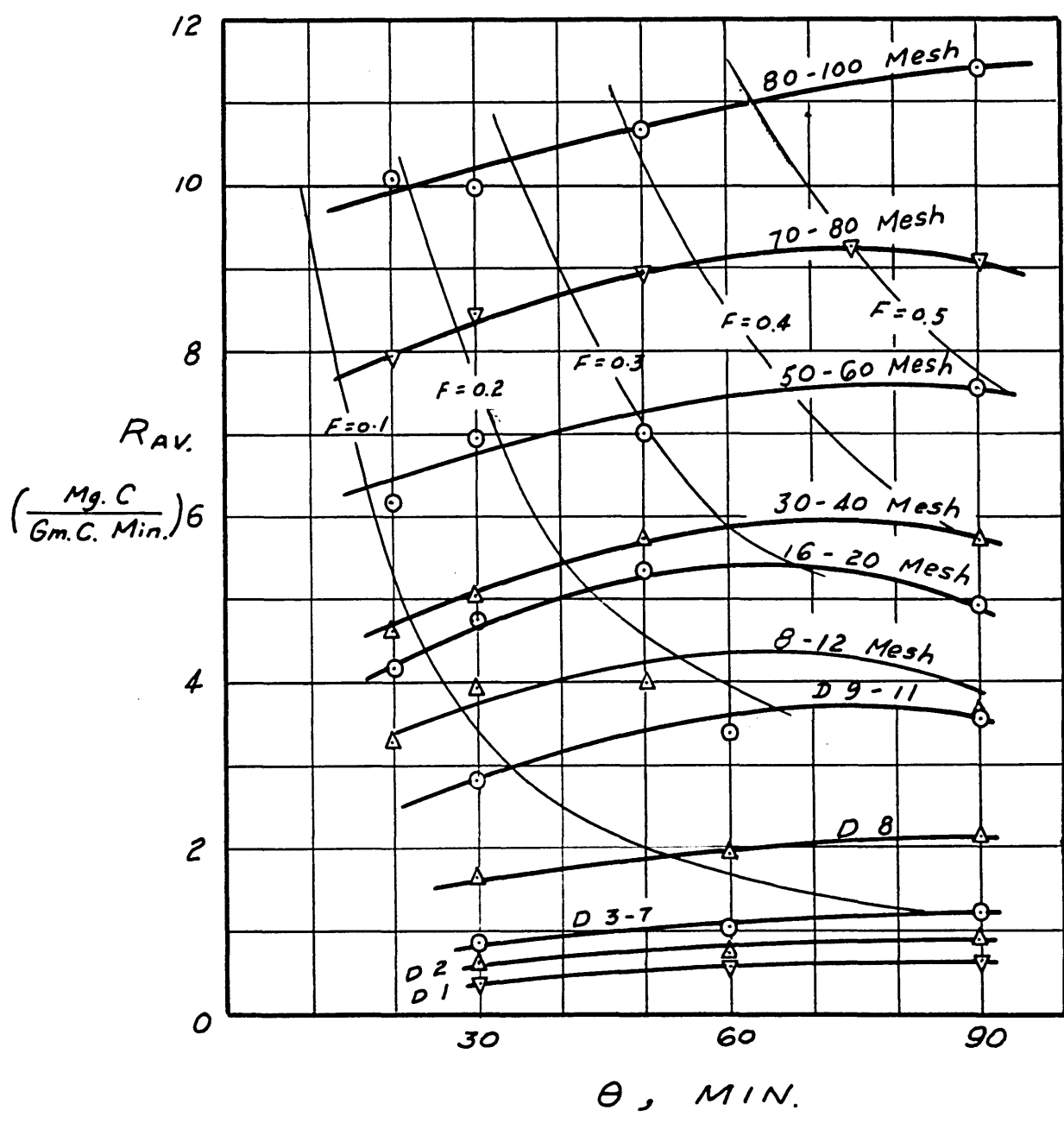


FIGURE (17) R_{av} vs. D

(New England Coke Particles)

PURE CO₂ RUNS

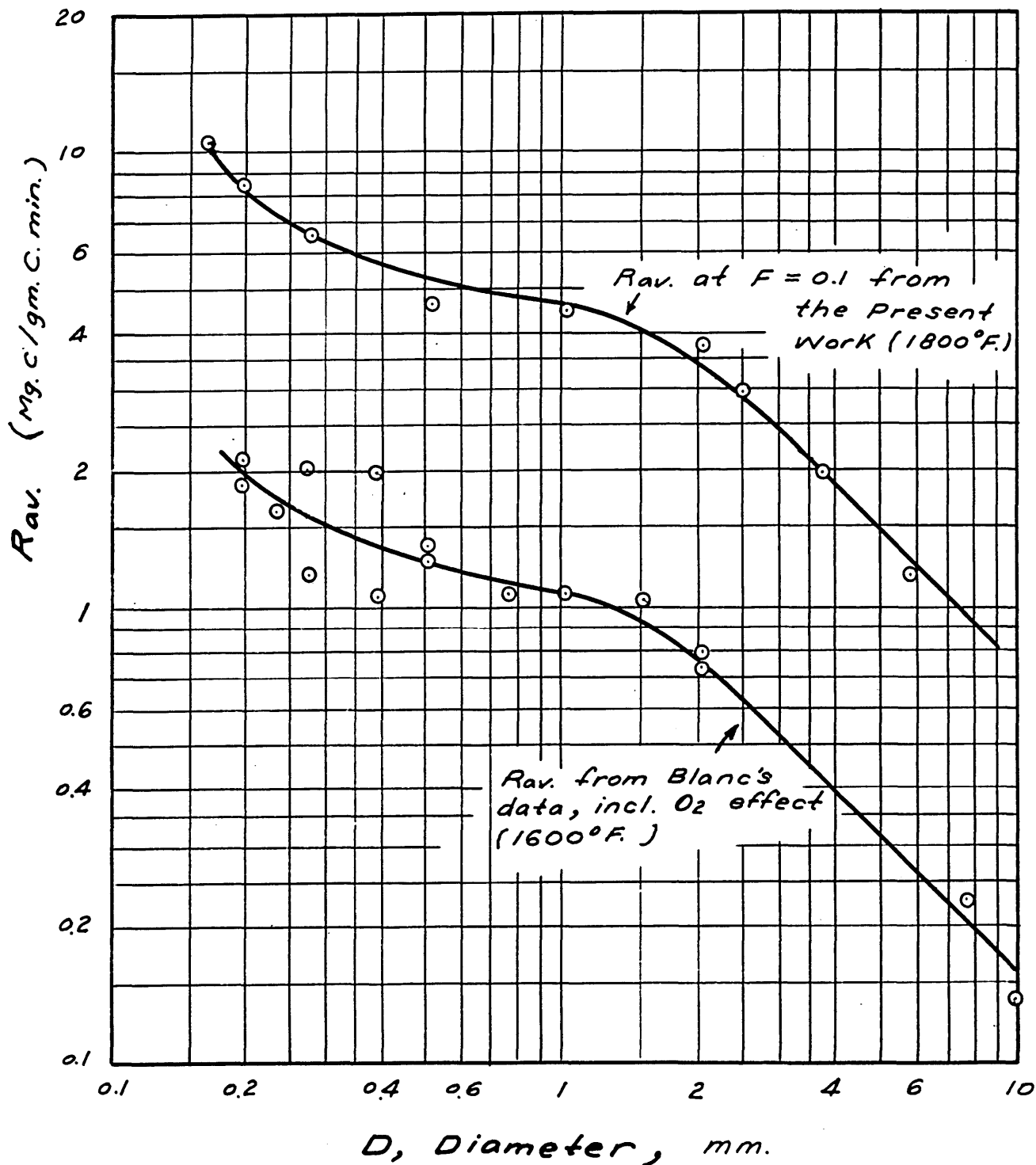


FIGURE (18)
 WEIGHT PER PARTICLE vs. D^3
 (New England Coke Particles)

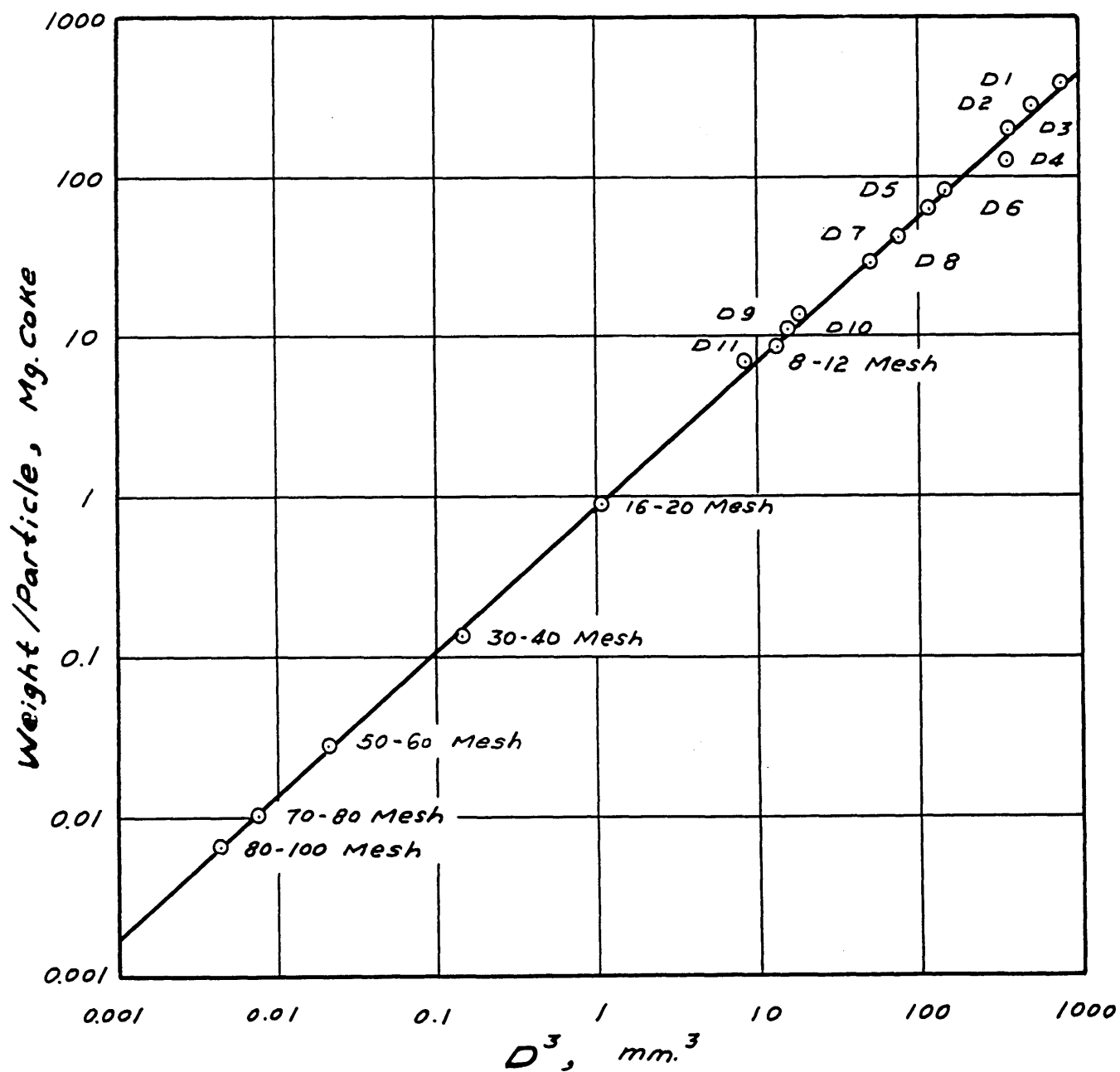


Figure 19

Photographs of Coke Particles

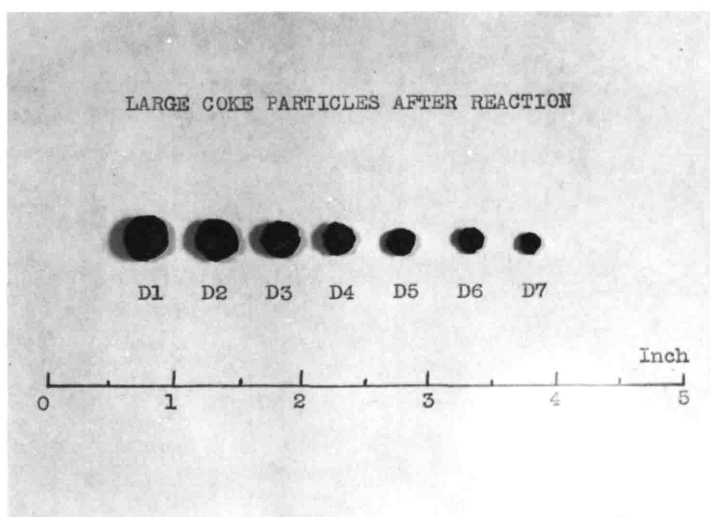
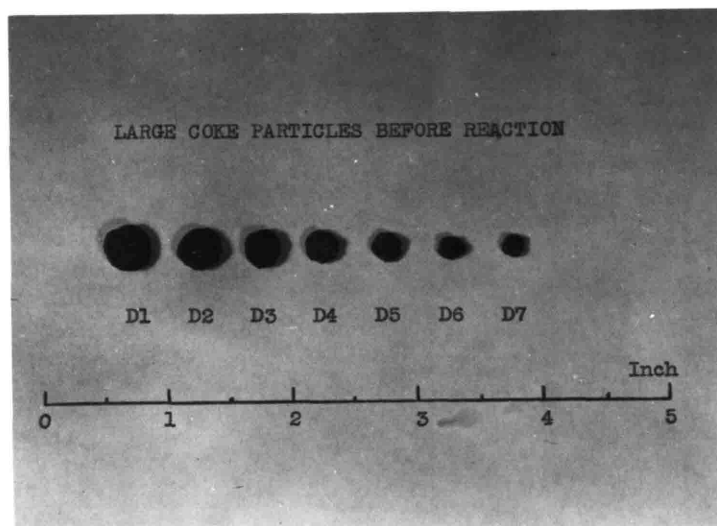
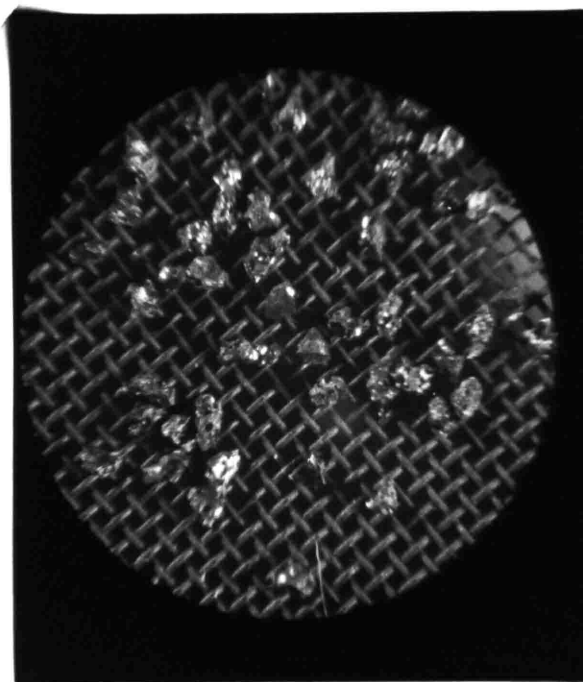


Figure 20

Photomicrograph of 50-60 mesh
Coke Particles



particle size of the electrode carbon was 50-60 mesh.

(a) N₂ blank runs: The results of N₂ blank runs as well as coking runs are listed in Table A9.

(b) CO₂-N₂ runs: Four temperatures (1600, 1700, 1800 and 1900°F.) were investigated. The time of reaction was so chosen for each temperature as to give approximately $F = 0.1$ in pure CO₂. The results are shown in Table A10. The values of $R_{av.}$ calculated from the results are plotted vs. P_{CO_2} on semi-logarithmic coordinates in Figure 21.

(c) CO₂-CO runs: The temperatures investigated and the time of reaction for each temperature were the same as in the CO₂-N₂ runs. The results are shown in Table A11. The values of $R_{av.}$ calculated from the results are plotted vs. P_{CO} on semi-logarithmic coordinates in Figure 22.

(d) Velocity runs: The temperatures investigated and the time of reaction for each temperature were the same as in CO₂-N₂ runs. The results are shown in Table A12. The values of $R_{av.}$ calculated from the results are plotted vs. the reciprocal of the gas flow rate $1/V$ on linear coordinates in Figure 23.

(e) Time runs: Several gas compositions were used, CO₂, CO₂-N₂ as well as CO₂-CO mixtures. The temperatures investigated were the same as for the CO₂-N₂ runs. The results are listed in Table A13,

FIGURE (21)
 $R_{AV.}$ VS. P_{CO_2} FOR CO_2-N_2 RUNS

(National Electrode Carbon, 50-60 Mesh)

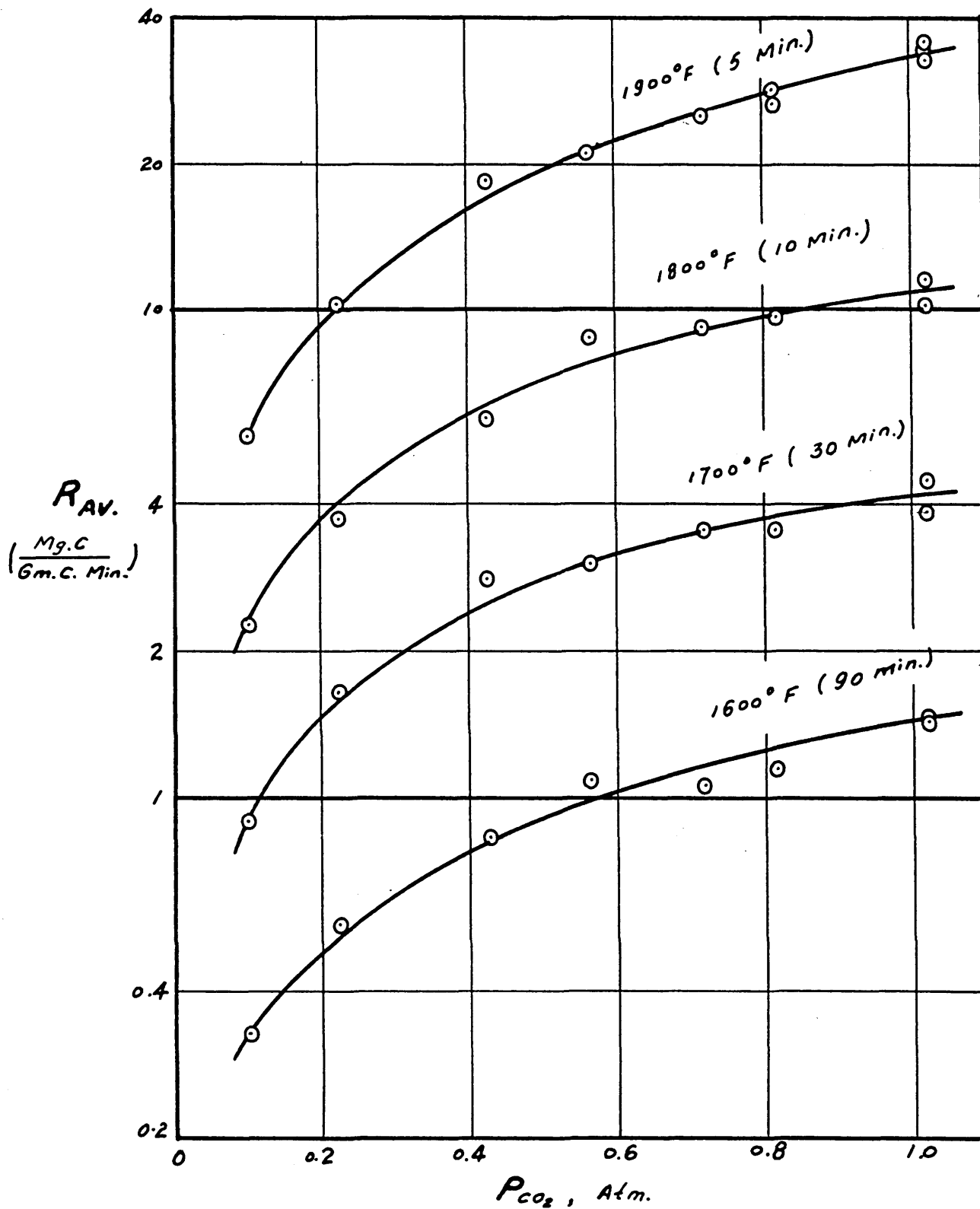
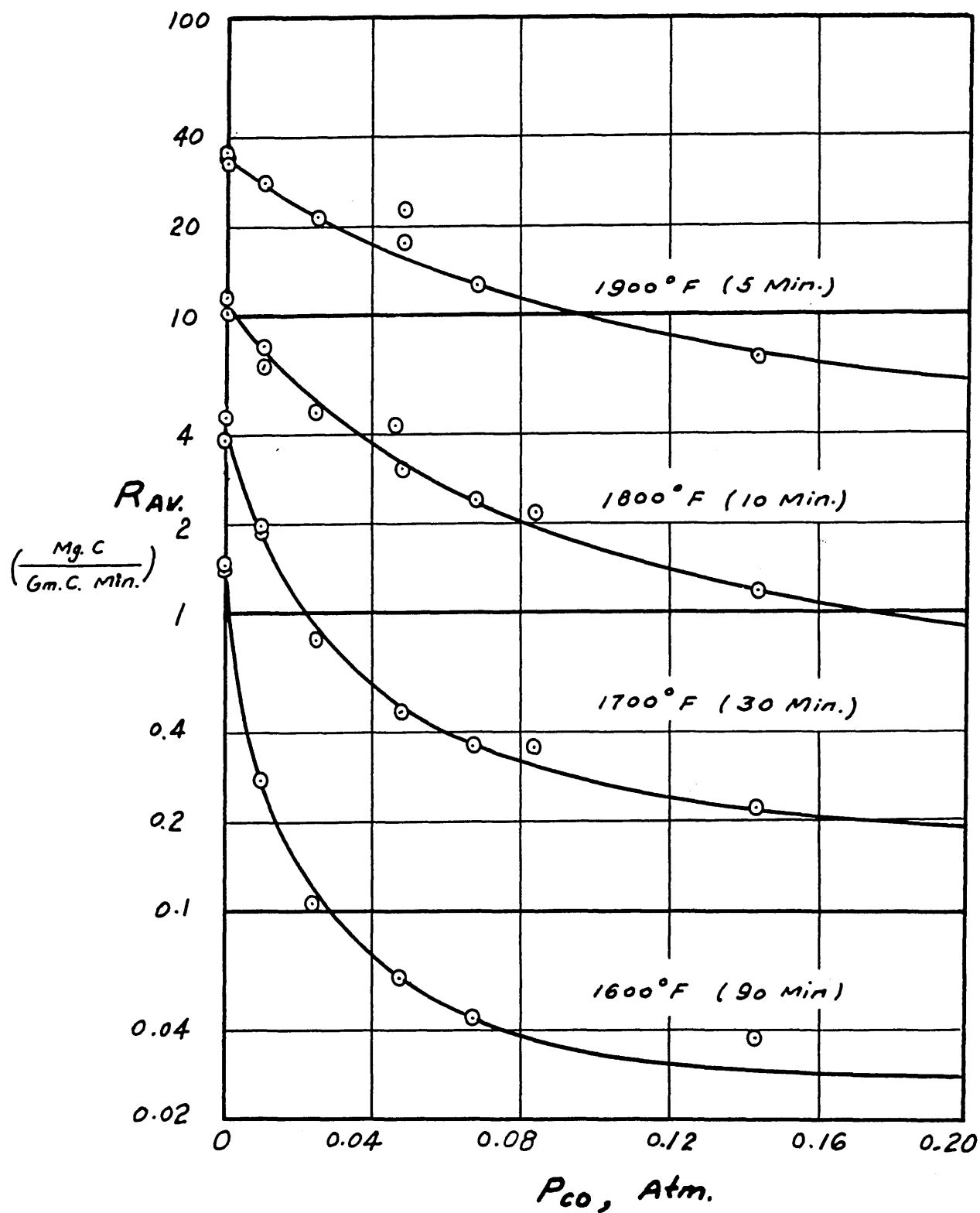
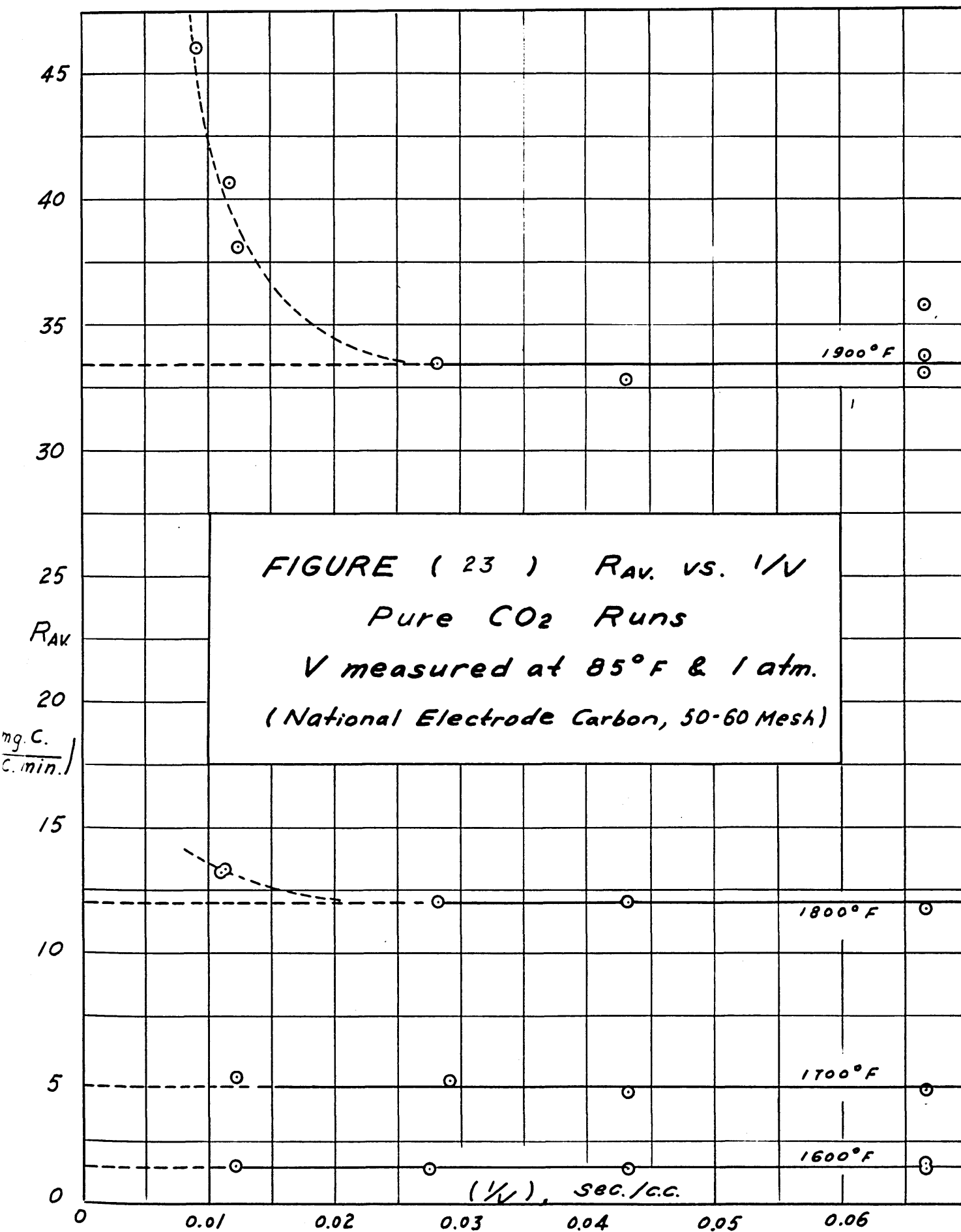


FIGURE (22)

 R_{AV} VS. P_{CO} FOR CO_2 - CO RUNS

(National Electrode Carbon, 50-60 Mesh)





and a plot was made showing the values of F vs. θ , as in Figure 24.

B. Discussion of Validity of Data and of Corrections Applied Thereto

1. Experiments using New England coke particles of 50-60 mesh

For all the data obtained using coke, two corrections were applied to the raw data before correlations were made. These corrections were necessary because of the presence of ash and V.C.M. in the coke.

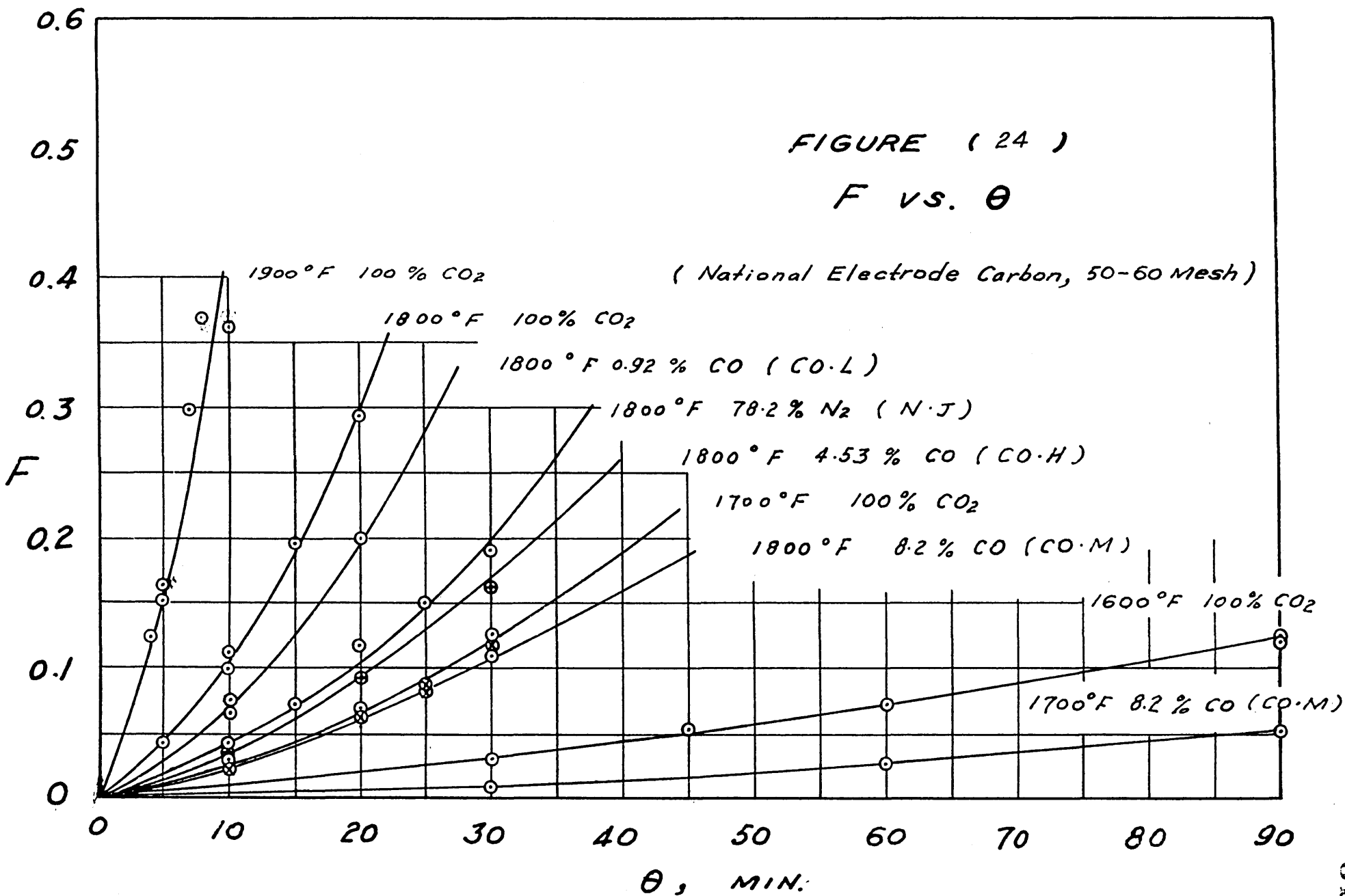
To correct the data recorded during the runs to an ash-free basis, the weight of the original coke sample was multiplied by a factor 0.905.

The weight decrease during the reaction period was due to the combined effect of the carbon-carbon dioxide reaction and to the liberation of some of the V.C.M. in the coke. Therefore, to find the weight change caused by the reaction alone, the weight of the V.C.M. liberated was subtracted from the total weight loss. The amount of V.C.M. that came out during the reaction period was calculated based on the amount of V.C.M. removed in an atmosphere of pure nitrogen. It was assumed that the same amount was liberated in both carbon dioxide (or any gas mixtures used) and nitrogen at the same temperature and pressure in an equal time interval.

Even though this method of correcting for V.C.M. is not completely satisfactory, it seems a rather reasonable

FIGURE (24)

F vs. θ



one, because of the following:

(a) It is not possible to remove all V.C.M. by heating the coke for a short time in either nitrogen or in vacuum, whereas heating the coke too long may result in a radical change in structure.

(b) The adsorption of oxygen on the coke surface is important. The weighing and handling of the coke must take place in air. Hence, even with coke which contains no V.C.M. at all, reaction of adsorbed oxygen with the coke during the reaction period cannot be avoided.

This correction is small for high reaction rates, corresponding to high temperatures, but is relatively large at low temperatures, especially when the reacting gas contains a high percentage of CO. Accordingly, the accuracy of the data becomes poorer for reaction rates obtained under these conditions.

From Figures 11 and 12, it can be seen that CO has a great retarding effect on the reaction rate while N₂ has little effect.

When the sample pan supporter is in position for a run, it does not completely block the gas passageway from lower to upper plenum chamber. In consequence, part of the gas flows through the screen, and part around it. The effective concentration of CO in the reaction atmosphere is thus certainly higher than its concentration in the

entering stream, and also probably higher than the average CO concentration of the inlet and exit gases. The increase from inlet to exit was calculated to be from 0 to 3%.

From the effect of temperature on the reaction rate, it is clear that the carbon-carbon dioxide reaction is controlled by chemical and not by diffusional processes. If the effective CO concentration is kept constant, the reaction rate should be independent of the gas velocity. However, an increase in gas velocity will minimize the difference between the effective CO concentration in the combustion area and its concentration in the reacting gas. Figure 13 shows the reaction rates obtained with pure CO₂ entering the system, plotted vs. the reciprocal of the entering gas velocity. Upon extrapolation to infinite gas velocity, the reaction rates should approach those corresponding to the reaction with pure CO₂. All these runs were made with the pan as shown in Figure 6.

Figure 13 shows in addition the results (solid black points) obtained with the pan arrangement of Figure 4, in which two layers of screen were used. Since that arrangement increased the resistance to flow through the sample, more of the gas was by-passed around the edge of the screen, with a resulting lower reaction rate due to higher CO concentration around the particles. In all later runs (including the runs using coke particles of different sizes at 1800°F. and runs using electrode carbon particles of 50-60 mesh), the results were obtained with the pan arrangement of

Figure 7, in which one layer of screen was used. This arrangement caused less by-passing of gas, and consequently the lowering in reaction rate due to higher CO concentration around the particles is not as pronounced.

The accuracy of the weighing procedure is about 0.0001 gm. When considering the runs made at low temperatures with a high percentage of CO in the gas, 0.0001 gm. may represent considerable error. This causes the results calculated from the data of these runs to be inaccurate. When plotting the calculated results of these runs, the possible spread in these values due to a change in the determined amount reacted of ± 0.0001 gm. was indicated by a vertical line in the appropriate plots.

2. Experiments using New England coke particles of different sizes, reacting with pure carbon dioxide at 1800°F. with different times of reaction

Corrections for ash and V.C.M. in the coke were applied to the raw data before any plots were made.

In extreme cases, the weight loss due to V.C.M. amounted to as much as 35% of the total weight loss, but usually the value was below 5%.

The $(1-F)$ versus θ curves (Figure 15) show that for the range in which F is small, the curves are concave downward, representing an increasing reaction rate with progressing reaction, while for the range in which F is large, the curves are concave upward, representing a decreasing reaction rate with further reaction. A plot of

average specific reaction rate, $R_{av.}$, vs. Θ with constant F lines, as shown in Figure 16, indicates that the reaction rate increases, reaches a maximum and then decreases. However, the percentage variations are small.

The curve of $R_{av.}$ vs. D (Figure 17) can be divided into three distinct parts. The first part, for a particle diameter larger than 1 mm., has a slope of minus one. The second part, the section including intermediate size particles, is a transitional zone, with slopes varying between zero and minus one. The third part, for particle diameter less than 0.3 mm., again reverts to a slope of minus one.

The original particle diameter was used in plotting, because it was found that the diameter decrease was very small. Therefore, errors introduced by a change in diameter are negligible.

In the plot of weight per particle vs. D^3 (Figure 18) the slope is less than one, which means that the small particles have greater bulk densities than the large ones.

3. Experiments using National electrode carbon particles of 50-60 mesh

The electrode carbon particles were coked at 1800°F. in vacuum for 2 hours before being used. When examining the results of the nitrogen blank runs, listed in Table A9, it can be concluded that the elimination of

V.C.M. from the carbon particles in the coking procedure was very effective. When it is assumed that in the nitrogen blank runs the same amount of V.C.M. was removed as in the normal reaction runs, applying the same time of reaction and reaction temperature, then no correction for V.C.M. liberated during these normal runs seems to be justified. The reason for this decision is that the difference in weight before and after reaction is of the same magnitude as the accuracy of the weighing procedure, namely 0.0001 gm. It should be pointed out that a difference in weight of 0.0001 gm., whether it be due to the weighing procedure or V.C.M., causes an error of 1% in those cases where the amount of carbon reacted is about 0.01 gm. ($F = 0.1$). However, when considering the runs made at 1600 and 1700°F., with a high percentage of CO, then 0.0001 gm. may represent an error of 10-25%, which is relatively high. When plotting the calculated results of these last runs, the possible spread in these values due to a change in the determined amount reacted of ± 0.0001 gm., was indicated by a vertical line in the appropriate plots.

The results of the velocity runs justify rather definite conclusions. As Figure 23 shows, at reaction temperatures of 1600 and 1700°F., variation in gas velocity has no detectable effect on the reaction rate. At reaction temperatures of 1800 and 1900°F., the reaction rate stays nearly constant until a velocity of about 35 cc./sec. is reached. At higher velocities, a sudden increase in reaction

rate apparently occurs. However, the definite lack of influence of velocity on the reaction rate shown at lower velocities and temperatures, combined with the absence of "jumps" in the results on coke (see Figure 13) performed under very similar conditions, seem to justify the conclusion that at 1800 and 1900°F., the reaction rate can also be considered to be constant over the whole range. The fact that the loss in weight during reaction suddenly increases as higher velocities and temperatures are used must very probably be attributed to sloughing off of minute carbon particles at those velocities, and not to an increased reaction rate.

A justification for this assumption is found when examination of the carbon particles reacted at lower temperatures only showed an "eaten-up" surface, whereas the carbon reacted at 1800 and especially at 1900°F. showed many loosely held minute particles. These were apparently formed during the faster and more intensive reaction and could rather easily be detached from the surface by high gas velocities. That these particles indeed were rather loosely attached to the surface was found when transferring the reacted particles to sample bottles. The paper funnel used for this transportation procedure was covered with a fine graphite-like dust when handling particles reacted at low temperatures. Even though these qualitative proofs may not be completely convincing, still they may be

considered to supply enough evidence that the "jumps" in loss of weight must be attributed to "sloughing off", and not to an increased reaction rate. It was upon these considerations that it was decided not to apply any correction for the apparent influence of gas velocity upon the reaction rate.

VI. DISCUSSION AND INTERPRETATION OF RESULTS

(For Nomenclature used, see Appendix)

The various reaction rate terms used in this investigation are defined as follows:

(1) The instantaneous specific reaction rate R_1 is defined as the rate of decrease in weight of carbon based on unit weight of carbon at $F = F$:

$$R_1 \equiv \frac{-dW}{W d\theta} \equiv \frac{-d \ln W}{d\theta} \equiv \frac{-d \ln (1-F)}{d\theta} \quad (1)$$

(2) The initial specific reaction rate R_0 is defined as the rate of decrease in weight of carbon based on unit weight of carbon at $F = 0$:

$$R_0 \equiv -\left(\frac{dW}{W d\theta}\right)_{F=0} \equiv -\left(\frac{d \ln (1-F)}{d\theta}\right)_{F=0} \equiv \left(\frac{dF}{d\theta}\right)_{F=0} \quad (2)$$

(3) The average specific reaction rate $R_{av.}$ is defined as the time mean of the instantaneous specific reaction rate R_1 from $F = 0$ to $F = F$:

$$R_{av.} \equiv \frac{\int_0^\theta R_1 d\theta}{\theta} \equiv \frac{\int_0^\theta \frac{-dW}{W d\theta} d\theta}{\theta} \equiv \frac{\int_{W_0}^W -\frac{dW}{W}}{\theta} \equiv \frac{-\ln (1-F)}{\theta} \quad (3)$$

When F is small, $R_{av.}$ can be approximated by using the arithmetic mean of the initial and final weights of the carbon sample, which can be written as:

$$R_{av.} = \frac{\Delta W}{W_{av.} \Theta} = \frac{F}{(1 - \frac{1}{2^F}) \Theta} \quad (4)$$

In the correlation of results, it is desirable first to consider the experimental results using electrode carbon particles of 50-60 mesh, in view of the fact that they contained negligible amounts of ash and V.C.M. and, consequently, complications due to their presence are not existing. The results using coke particles will be presented subsequently.

A. Experiments using National electrode carbon particles of 50-60 mesh

In view of equations (1) and (3), if R_1 is a constant independent of F and Θ , then $R_{av.} = R_1 = \text{constant}$. However, from Figure 24 for the series of runs made with varying reaction time, the F vs. Θ curves indicate that R_1 and, consequently, $R_{av.}$ vary. Both increase with increasing F and Θ , and much faster than would be due solely to the increase in superficial surface area. Therefore, in addition to the variables temperature, pressure and gas composition, there is another independent variable, F , which influences the reaction rate. As the regular runs with $\text{CO}_2\text{-N}_2$ and $\text{CO}_2\text{-CO}$ mixtures were made at a specified time of reaction for each temperature, the average reaction rates thus calculated over that reaction time would mean very little if the F and Θ relation under each set of

specific conditions were not known.

Microscopic observations of the carbon particles before reaction showed that they were solid and dense, with a more or less even surface of a dark gray color. However, after reaction, the particles looked porous and "eaten up", many small capillaries having formed; and the color had turned black. The particle size, however, had not been reduced appreciably, even when a fraction as high as 0.3 or 0.4 had reacted. In view of these observations, the physical picture of the reaction process visualized was that in the course of the reaction the structure of the carbon was so changed that more reactive surface was created, and hence more active centers were available throughout the particles to be attacked by the gas. It is this continuously increasing surface that is responsible for the increase in instantaneous specific reaction rate.

Granting this to be the right picture, then the simplest relation to exist between F and R_1 would be a linear one, which can be expressed as:

$$R_1 \equiv \frac{-dW}{W d\theta} \equiv \frac{-d \ln(1-F)}{d\theta} = mF + R_0 \quad (5)$$

in which R_0 is the instantaneous specific reaction rate at $F = 0$, and m is the rate of increase of R_1 with respect to F .

Dividing both sides by R_0 ,

$$\frac{R_1}{R_0} = \frac{m}{R_0} F + 1 \quad (5a)$$

Before testing the validity of this equation, it is interesting to investigate the meaning of the ratio $\frac{m}{R_0}$. The reaction rate per carbon particle, theoretically speaking, should be proportional to its effective surface area at any moment. The initial reaction rate will be,

$$-\left(\frac{dW}{d\theta}\right)_{F=0} = C_0 A_0 \quad (6)$$

whereas the rate at any time θ will be,

$$-\left(\frac{dW}{d\theta}\right)_{F=F} = C A \quad (7)$$

The terms A_0 and A are called the effective surface areas, the effectiveness of any element of area depending on its position in the particle. Even if the surface area could be measured properly (different surface measurement methods usually give different areas, the magnitude of those values being doubtful) and be used to correlate the reaction rates, then the areas of the capillaries, due to the perfusion effect, would be less effective than areas on the exposed surface. The effective surface area is thus a fictitious value. We could assume the proportionality constants C_0 and C to be equal, and make all adjustments by means of A .

From equations (6) and (7) we can derive:

$$R_0 = \left(\frac{-1}{W_0} \right) \cdot \left(\frac{dW}{d\theta} \right)_{F=0} = \left(\frac{1}{W_0} \right) C_0 A_0 \quad (8)$$

$$R_1 = \left(\frac{-1}{W} \right) \cdot \left(\frac{dW}{d\theta} \right)_{F=F} = \left(\frac{1}{W} \right) C A \quad (9)$$

Division of (9) by (8) and acceptance of (5a) results in

$$\frac{R_1}{R_0} = \left(\frac{W_0}{W} \right) \cdot \left(\frac{A}{A_0} \right) = \frac{1}{1-F} \left(\frac{A}{A_0} \right) = 1 + \left(\frac{m}{R_0} \right) \cdot F \quad (10)$$

or

$$\frac{A}{A_0} = (1 - F) \cdot \left(1 + \left(\frac{m}{R_0} \right) F \right) \quad (10a)$$

This means that if under different conditions, the effective area ratio $\left(\frac{A}{A_0} \right)$ is the same for a certain F , then not the reaction conditions but the fraction of carbon reacted is the factor which characterizes the carbon structure, and consequently $\left(\frac{m}{R_0} \right)$ will be a universal constant independent of the reaction conditions. It should be pointed out that this conclusion depends, inter alia, on the assumption that R_1 is a linear function of F as expressed by equation (5).

The results will now be examined to see whether they support the above picture.

When equation (5) is integrated, (see Appendix), the following expression is obtained:

$$\Theta = \frac{1}{R_0 \left(\frac{m}{R_0} + 1 \right)} \ln \frac{1 + \left(\frac{m}{R_0} \right) \cdot F}{1 - F} \quad (11)$$

When $\frac{1 + \left(\frac{m}{R_0} \right) \cdot F}{1 - F}$ is plotted vs. Θ on semi-logarithmic coordinates, a straight line through $\Theta = 0$ at $\frac{1 + \left(\frac{m}{R_0} \right) \cdot F}{1 - F} = 1$ should be obtained if proper values of (m/R_0) are used. $\left(\frac{m}{R_0} \right)$ was evaluated by substituting two sets of experimental values for F and Θ of the same series into equation (11) and taking the ratio of the two expressions so obtained. The results look as follows:

$$\frac{\Theta_1}{\Theta_2} = \frac{\ln \left(1 + \frac{m}{R_0} F_1 \right) - \ln (1 - F_1)}{\ln \left(1 + \frac{m}{R_0} F_2 \right) - \ln (1 - F_2)} \quad (11a)$$

By applying this procedure and solving for $\left(\frac{m}{R_0} \right)$ by trial and error, (see Appendix), values for $\left(\frac{m}{R_0} \right)$ were calculated for each series of time runs.

As the results in Table (A14) show, in the same series of runs varying values of $\left(\frac{m}{R_0} \right)$ were obtained. However, the results of the procedure described are very sensitive to irregularities in the ordinates of the data points used to determine these (m/R_0) values. There is an obvious spread in the points used for calculating (m/R_0) , (see Figure 24), and consequently some variation in (m/R_0) may be expected. With the exception of the CO.M time runs made at 1700°F., the values of (m/R_0) found for all runs are seen to fall between 11 and 18.5. An explanation for the fact that the (m/R_0) values calculated for the CO.M-17.50 time runs (made at

1700°F., gas composition 91.34% CO₂-8.2% CO - 0.46% N₂), fall far outside the range of 11 to 18.5 is that the accuracy obtained in these runs is very low, due to the small percentage of carbon reacted. It can be seen from Table A13 that at 90 min. reaction time, which is three times the normal reaction time at 1700°F., only 5.27% reaction was obtained. At the normal reaction time of 30 min., only 1.07% of the carbon had reacted. If it be assumed that due to some irregularity in the handling or weighing procedure, the decrease in weight of the sample should have been 1.2 mg. instead of 1.1 mg. as now found, then a value for (m/R_0) of 32 would have been found, instead of 56 as now calculated. This shows clearly the sensitivity of the procedure in this range. It was for this reason that the result of the CO.M-17.50 runs was not included in the following correlation.

Considering that the influence of the (m/R_0) ratio is very much reduced by multiplication with F , (which is generally between 0.1 and 0.15, often even far less and only occasionally higher), a simplification can be obtained by representing all (m/R_0) values by one average value of 14. To check whether this would be allowable, $(m/R_0) = 14$ was substituted in equation (11), and a plot of $\frac{1+14 F}{1-F}$ vs. θ was made on semi-logarithmic coordinates, for each series of runs. Satisfactory straight lines were obtained as shown

in Figure 25. Representation of (m/R_0) by its average value of 14 results in the following expression:

$$\frac{R_1}{R_0} = 1 + \left(\frac{m}{R_0}\right)F = 1 + 14F \quad (5b)$$

This equation indicates that the instantaneous specific reaction rate at the instant when the carbon particle is completely burnt is fifteen times higher than the initial specific reaction rate. Whether this is true or not can never be tested experimentally because this particle would disintegrate and fall through the pan before a fairly high value of F is reached in the course of reaction.

A plot to show how (A/A_0) varies with F by putting $(m/R_0) = 14$ in equation (10a) is given in Figure 26. For numerical values of (A/A_0) calculated as a function of F , see Table A15. The effective area for one particle is seen to reach a maximum at $F = 0.465$, and then drops off to 0 at $F = 1$.

For each run made, the value of R_0 was calculated from equation (11), after substituting $(m/R_0) = 14$, and using F and θ of that specific run. Equation (11) was hence modified to:

$$R_0 = \left(\frac{1}{15\theta}\right) \times \left[\ln(1 + 14F) - \ln(1 - F)\right] \quad (11b)$$

Values thus calculated for R_0 were tabulated in Tables A10, A11 and A13.

It is obvious that the calculated values of R_0 for

FIGURE (25) $\left(\frac{1+14F}{1-F} \right)$ VS. θ

(National Electrode Carbon , 50-60 Mesh)

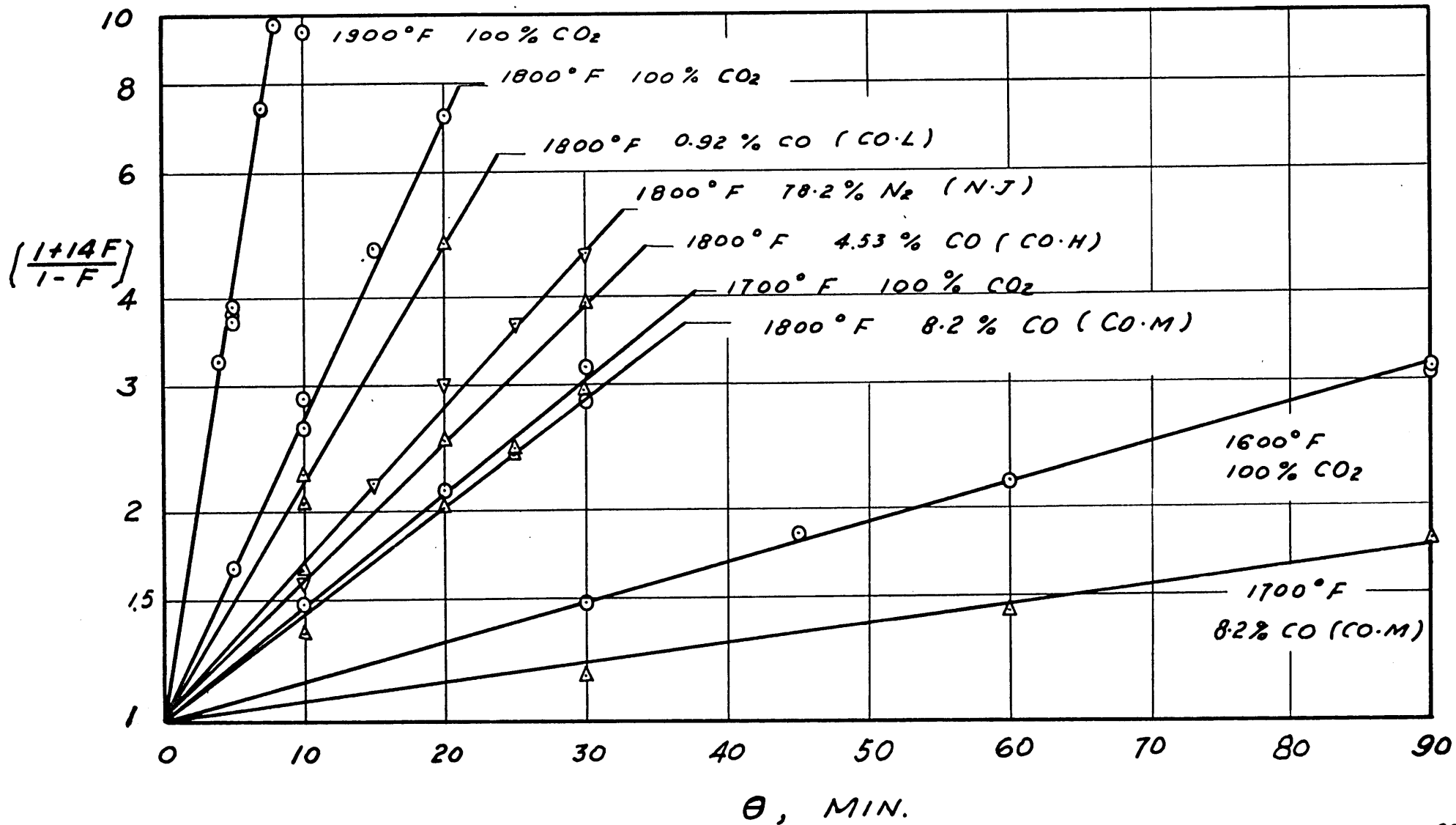
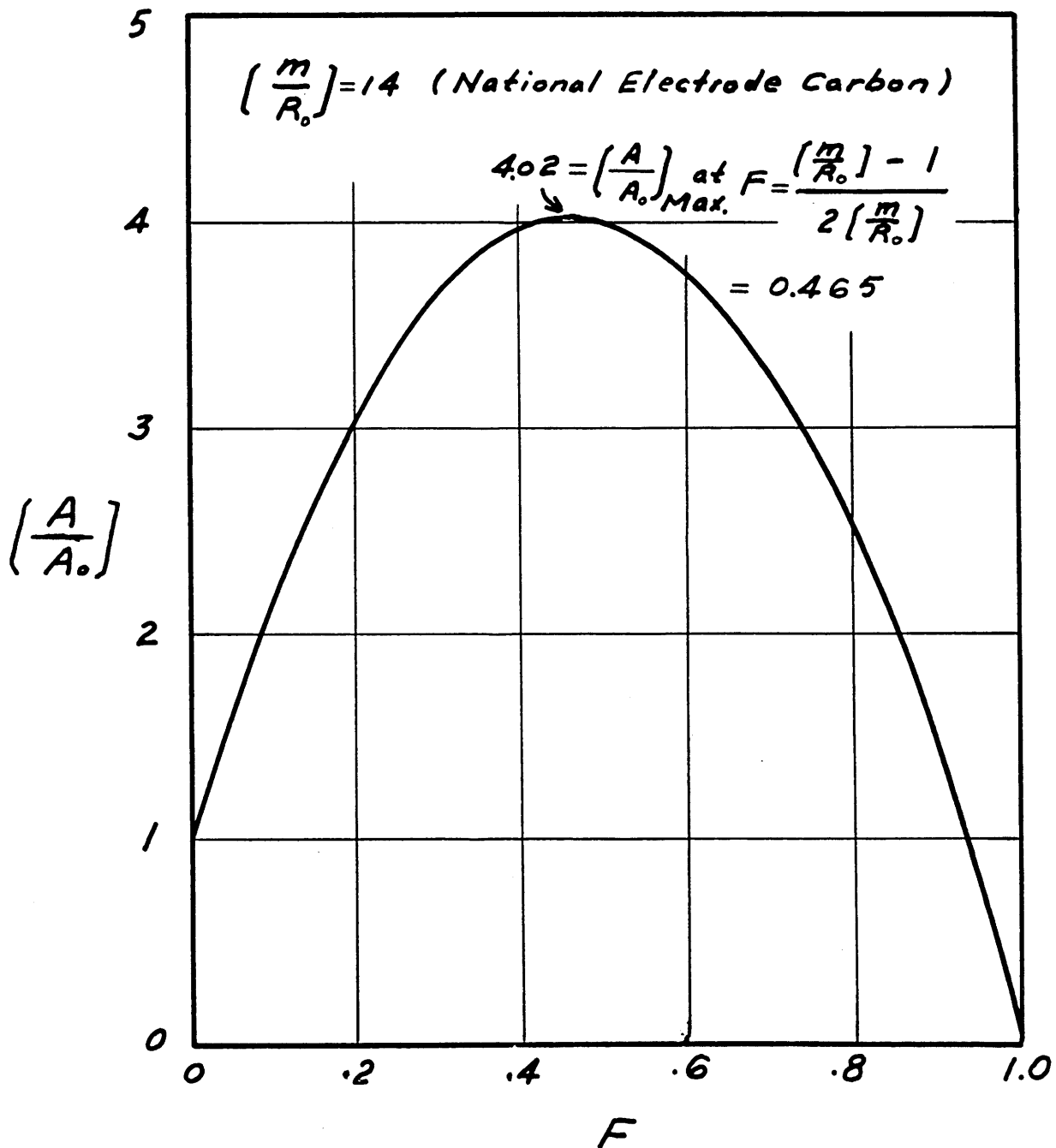


FIGURE (26)

$$\left(\frac{A}{A_0}\right) = (1-F)\left(1 + \frac{m}{R_0}F\right) \quad \text{vs. } F$$



time runs of the same series should be the same. The results obtained indicate that this is the case within reasonable limits. For each series an average R_0 was evaluated, which average values were used to check the experimental F vs. Θ results given in Figure 24. In this plot, the curves drawn were calculated from equation (11b), (see also Table A16), the points shown being data points obtained in the time runs. The fit of the curves to the data is satisfactory.

The next step in the correlation was to obtain an expression for R_0 in terms of the reaction variables, temperature, pressure and gas composition. In this connection the Langmuir adsorption equation, used by Hinshelwood et al, and by McBride in the correlation of their experimental results was adopted. This equation appears in the following form:

$$\text{Rate} = \frac{K_1 P_{\text{CO}_2}}{1 + K_2 P_{\text{CO}} + K_3 P_{\text{CO}_2}} \quad (12)$$

Although the Langmuir adsorption relation has been used extensively in the study of the kinetics of heterogeneous reactions, the validity of the assumptions made in deriving the relation has not been established. The basis of the Langmuir adsorption relation is that if in a heterogeneous reaction any of the products of the reaction are adsorbed strongly enough to occupy an appreciable fraction of the surface, then less surface is left to enter into reaction,

and the reaction rate is consequently decreased. A similar influence may result from the adsorption of the reacting gas. The adsorption of the reacting and product gases are in the Langmuir equation expressed in terms of the partial pressures of those gases, with the aid of constants depending upon temperature, type of reacting surface, etc. The instantaneous specific reaction rate is proportional to the reactant present on the surface, and is in its complete and more detailed form expressed as:

$$R_1 = \frac{-dW}{W d\theta} = K_r \left(\frac{A}{W} \right) \cdot \left(\frac{K_3 P_{CO_2}}{1 + K_2 P_{CO} + K_3 P_{CO_2}} \right) \quad (13)$$

The initial specific reaction rate R_0 can then be expressed as:

$$\begin{aligned} R_0 &= \left(\frac{-dW}{W_0 d\theta} \right)_{F=0} = K_r \left(\frac{A_0}{W_0} \right) \cdot \left(\frac{K_3 P_{CO_2}}{1 + K_2 P_{CO} + K_3 P_{CO_2}} \right) \\ &= \frac{K_1 P_{CO_2}}{1 + K_2 P_{CO} + K_3 P_{CO_2}} \quad (14) \end{aligned}$$

in which:

K_r is the rate of decrease in weight of the carbon per unit effective surface area covered by carbon dioxide, $\frac{A}{W}$ and $\frac{A_0}{W_0}$ are the effective surface area per unit weight of carbon at $F = F$ and $F = 0$, respectively, $\frac{K_3 P_{CO_2}}{1 + K_2 P_{CO} + K_3 P_{CO_2}}$ is the fractional effective surface area covered by carbon dioxide, and K_2 and K_3 are adsorption constants, K_1 being equal to $K_r \left(\frac{A_0}{W_0} \right) K_3$. Referring to equation (10), it can be

seen that R_1 can be expressed as:

$$R_1 = (1 + 14F) \frac{K_1 P_{CO_2}}{1 + K_2 P_{CO} + K_3 P_{CO_2}} \quad (15)$$

The same expression as given in equation (14) can be arrived at by a different reaction mechanism as proposed by Semechkova and Frank-Kamenetzky. According to this mechanism the CO_2 is not adsorbed on the surface, but two consecutive reactions take place on the surface, the adsorbed CO always being in equilibrium with the CO in the gas phase. It is pointed out that even though the final expression arrived at by either mechanism is the same, it must be realized that the meaning of the constants in this equation is different in the two cases.

The development of the mechanisms referred to is given in the Appendix.

The constants K_1 , K_2 and K_3 can be shown to obey an Arrhenius type equation, i.e.,

$$K = K_0 e^{-E/RT} \quad (16)$$

in which K_0 is a basic constant, E an energy value the interpretation of which depends upon the mechanism being adopted, R is the gas-law constant, and T is the reaction temperature in absolute units.

The validity of the proposed Langmuir type equation in this case can be investigated, and the constants involved evaluated by application to the R_0 values obtained in both

CO₂-N₂ and CO₂-CO runs. It is evident that where the surface is completely characterized by F, as shown before, the instantaneous specific reaction rate at any F could be used for this evaluation. However, R₀ was chosen as a reference value for testing the validity of the proposed Langmuir equation. The procedure used was as follows: In the case of the CO₂-N₂ runs, the term K₂ P_{CO} is 0, if the effect of the CO generated during the reaction can be neglected. The equation can hence be reduced and rearranged to:

$$\frac{P_{CO_2}}{R_0} = \frac{K_3}{K_1} P_{CO_2} + \frac{1}{K_1} \quad (17)$$

If the proposed equation fits the data, then for a specific reaction temperature when $\frac{P_{CO_2}}{R_0}$ is plotted vs. P_{CO₂} on linear coordinates a straight line with slope $\frac{K_3}{K_1}$ and intercept $\frac{1}{K_1}$ should result, from which values of K₁ and K₃ can be evaluated. The results obtained are shown in Figures 27, 28, 29, 30.

When the equation is applied to the CO₂-CO runs, rearrangement of the equation to a more convenient form is possible by substituting P_{CO₂} + P_{CO} = π, where π is the total pressure on the reaction system, corrected for a minute amount of nitrogen present. The rearranged equation then becomes

$$\frac{P_{CO_2}}{R_0} = \frac{K_2 - K_3}{K_1} P_{CO} + \frac{1 + K_3 \pi}{K_1} \quad (18)$$

FIGURE (27)
 TEST OF RESULTS BY LANGMUIR EQUATION
 (National Electrode Carbon, 50-60 Mesh)

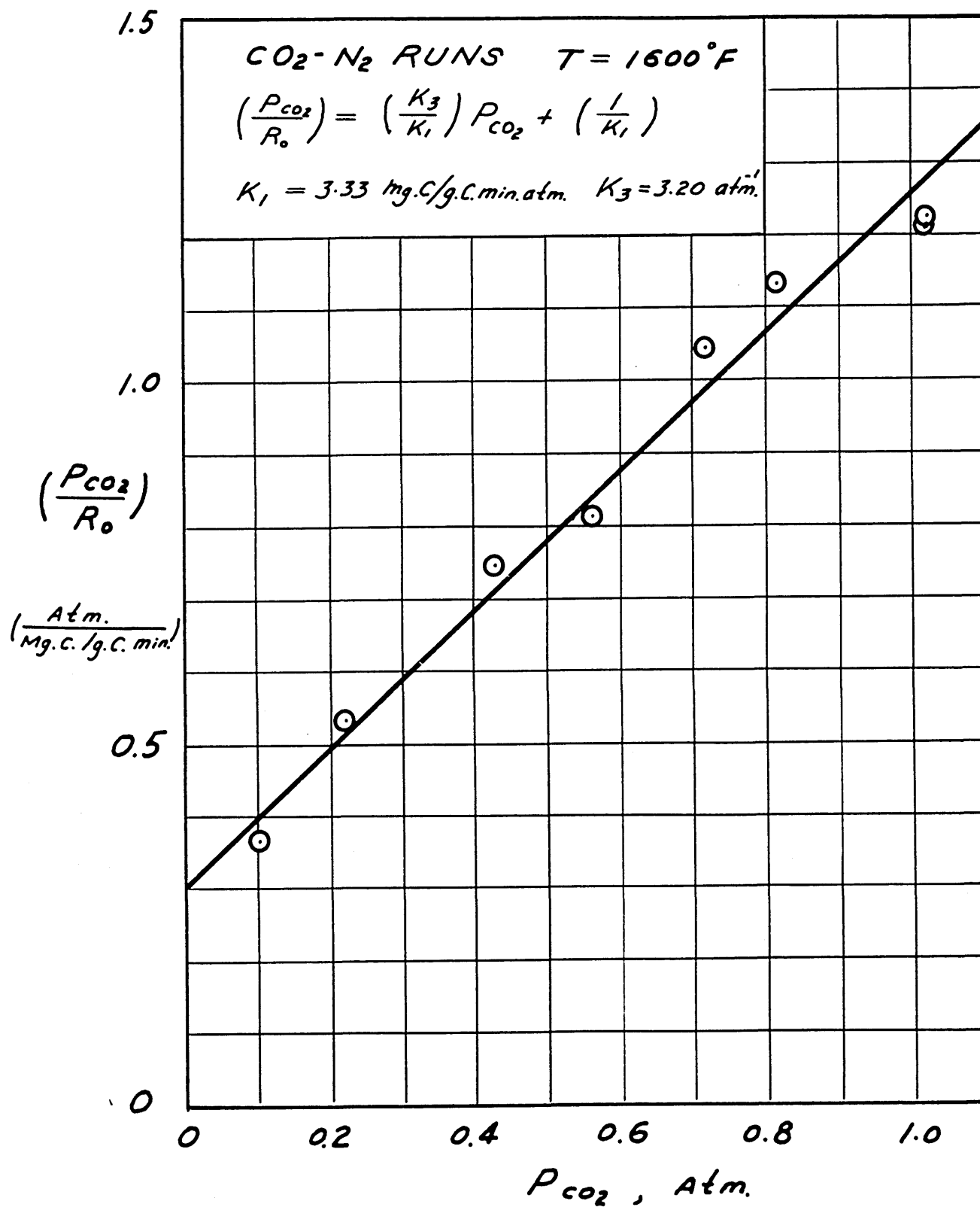


FIGURE (28)
TEST OF RESULTS BY LANGMUIR EQUATION
(National Electrode Carbon, 50-60 Mesh)

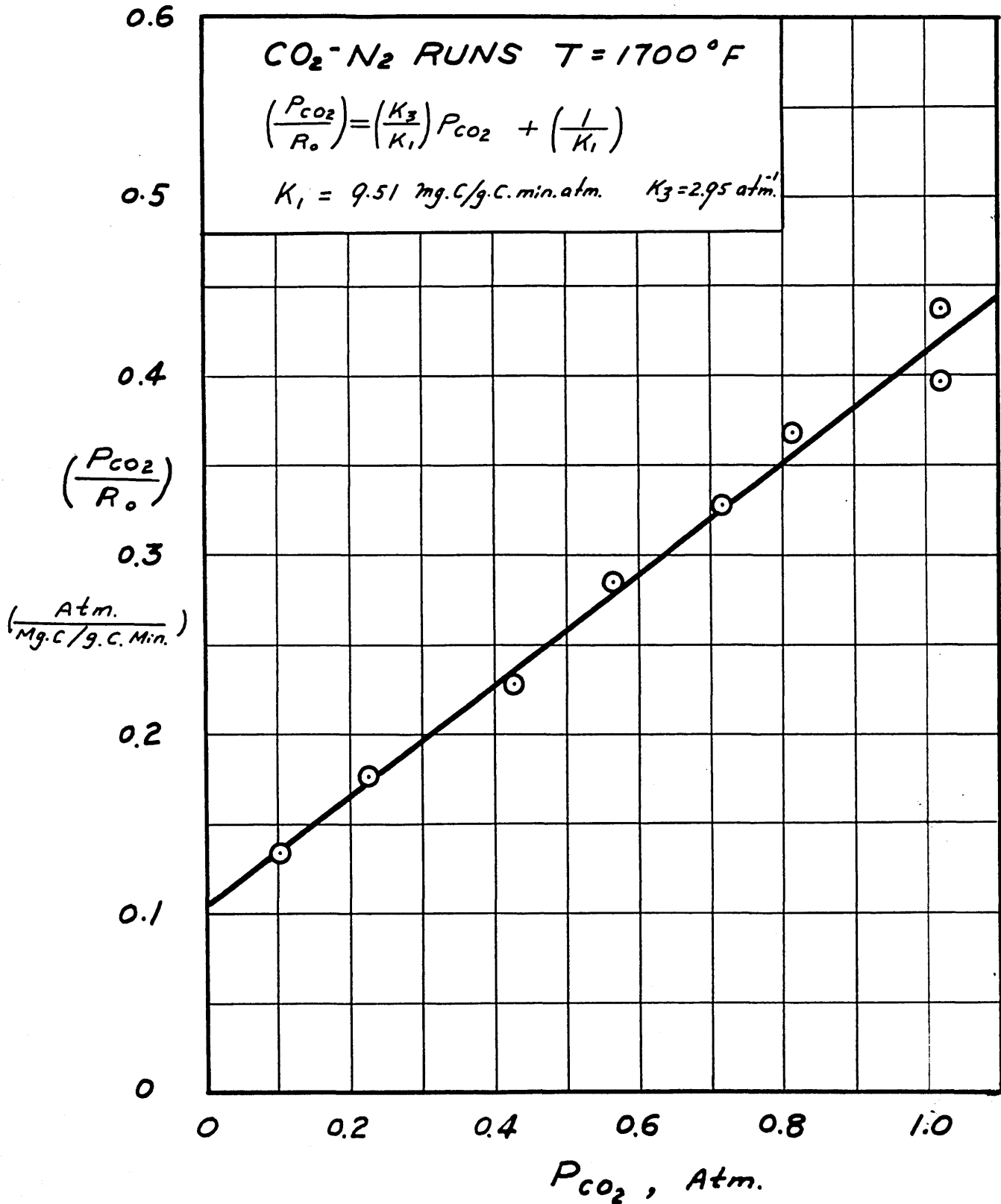


FIGURE (29)
 TEST OF RESULTS BY LANGMUIR EQUATION

(National Electrode Carbon, 50-60 Mesh)

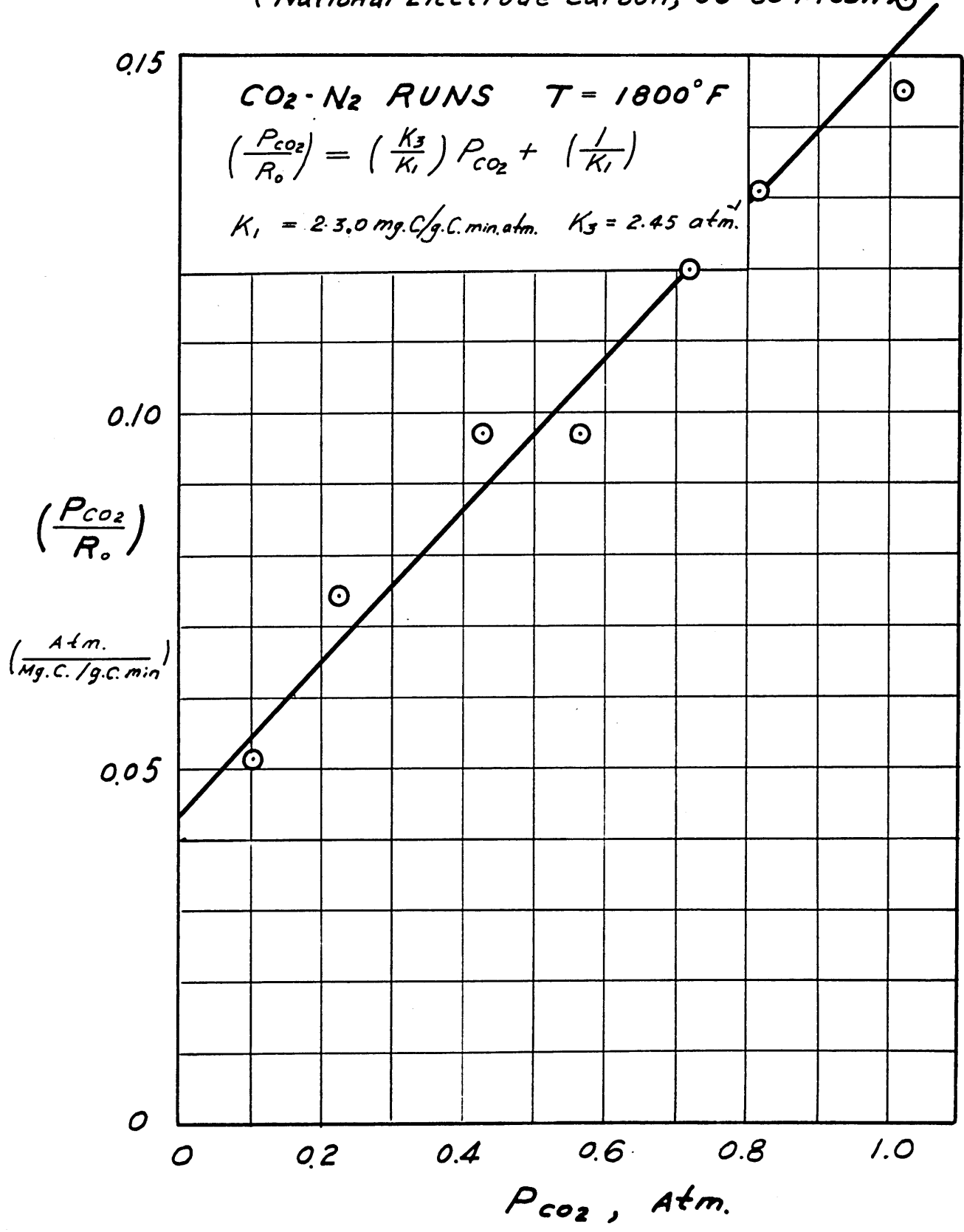
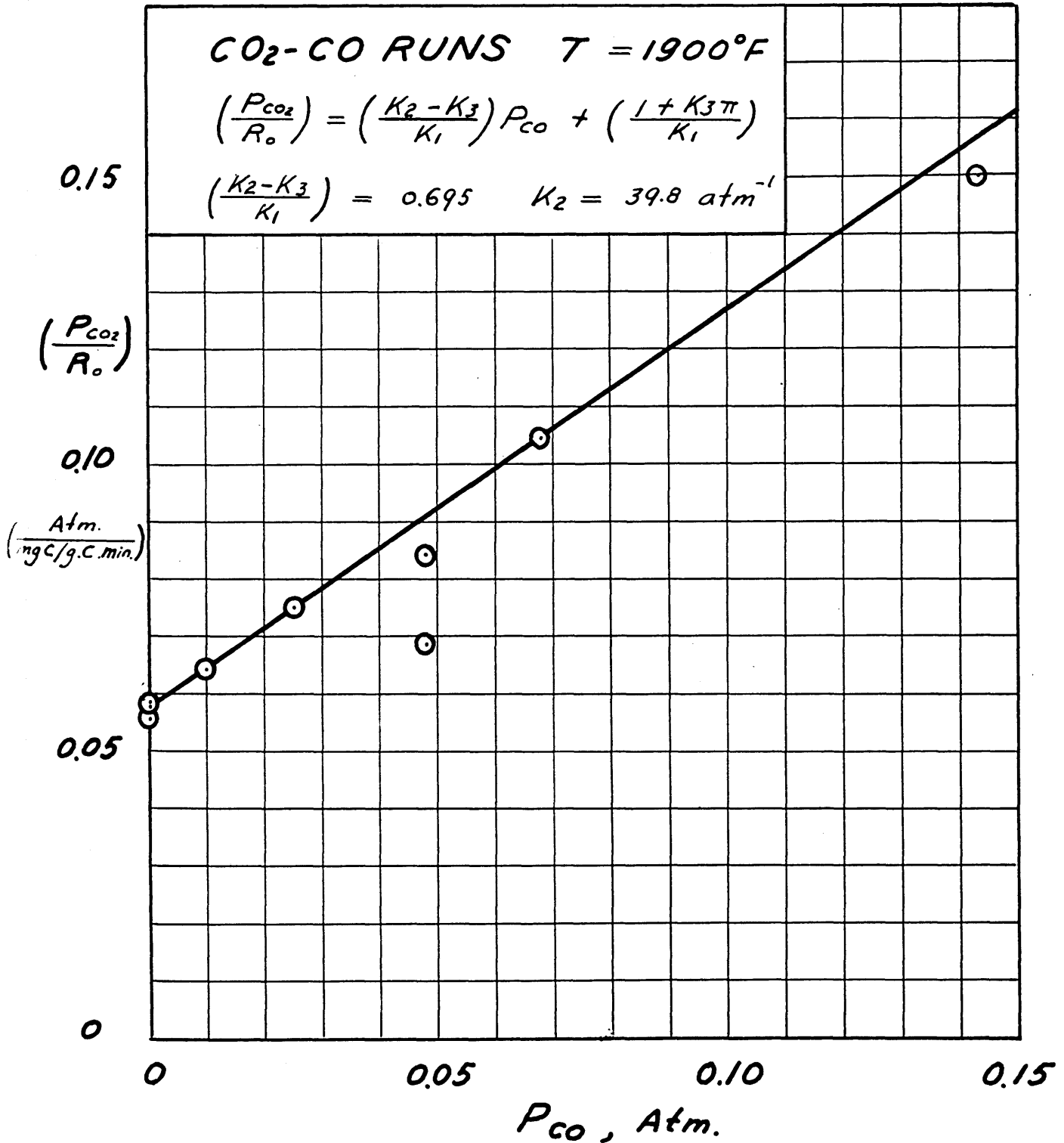


FIGURE (30)
 TEST OF RESULTS BY LANGMUIR EQUATION
 (National Electrode Carbon, 50-60 Mesh)



For a specific reaction temperature when $\frac{P_{CO_2}}{R_0}$ is plotted vs. P_{CO} on linear coordinates, a straight line with slope $\frac{K_2 - K_3}{K_1}$ and intercept $\frac{1 + K_3\pi}{K_1}$ should be obtained. With the aid of the values for K_1 and K_3 calculated from the results of the CO_2-N_2 runs at the same temperature, K_2 can then be evaluated from the slope of this line. Figures 31, 32, 33 and 34 show the results of this procedure.

In drawing the best straight line through the available points, more weight was given to the points calculated from data obtained at low percentages of CO than at high percentages. This was more specifically the case at reaction temperatures of 1600 and 1700°F, (see Figures 31 and 32). The reason for this unequal weighting was that the decrease in weight for high initial CO contents was so small as to cast doubt on the accuracy of the rate determinations. The spread possible in the calculated values due to a change in the observed decrease in weight of the sample of ± 0.0001 gm. is indicated in Figures 31 and 32 by a vertical line through a datum point. The results of this procedure show, however, that much greater "weighing errors" would have to be assumed in order to make the points fit the curve. Errors of this magnitude are out of the question.

When examining Figures 33 and 34, however, we see that also the points calculated from data obtained at reaction temperatures of 1800 and 1900°F. with a high percentage of CO, show the tendency (though far less than at 1600 and 1700°F.)

FIGURE (31)
TEST OF RESULTS BY LANGMUIR EQUATION
(National Electrode Carbon , 50-60 Mesh)

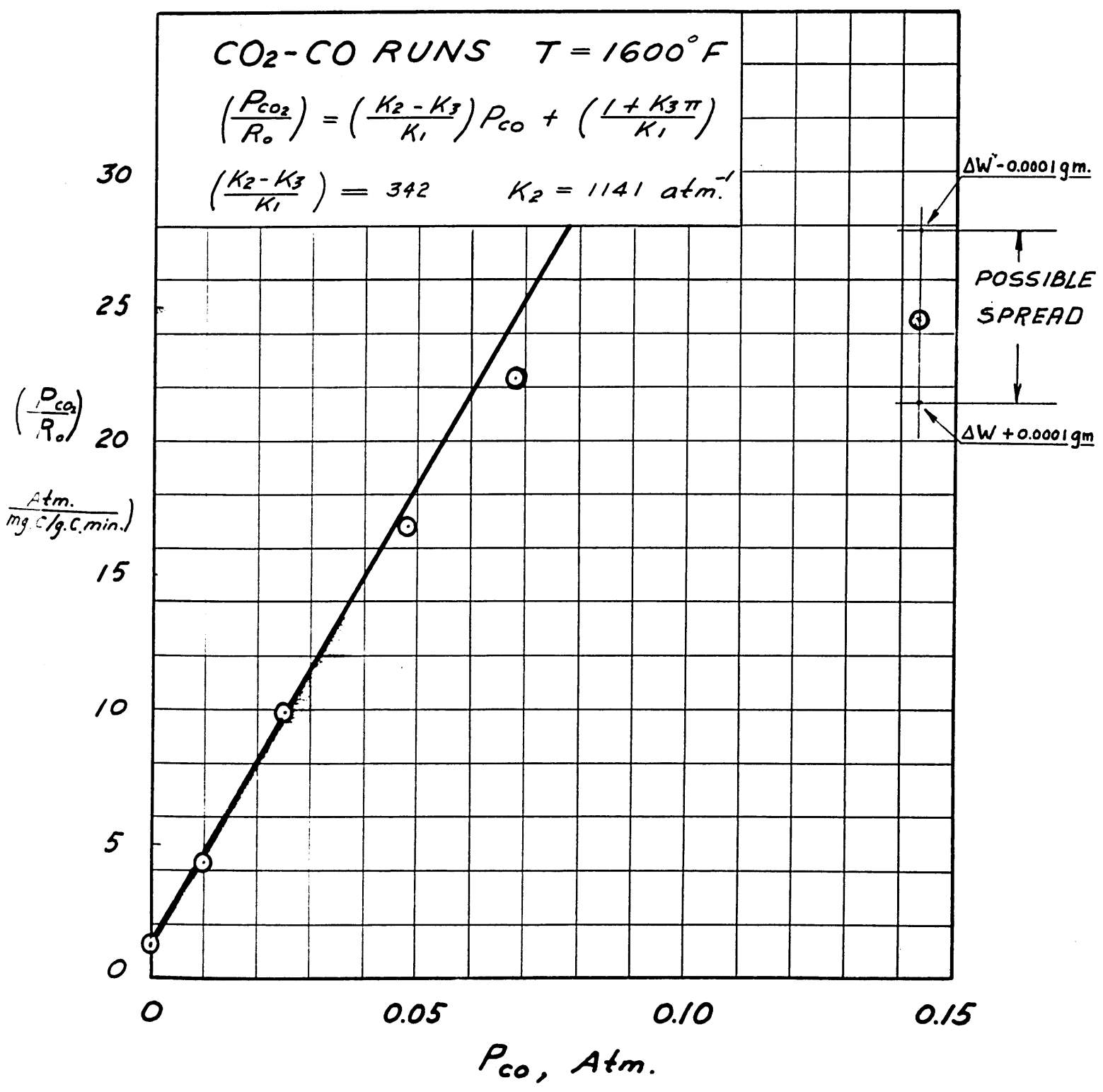


FIGURE (32)
TEST OF RESULTS BY LANGMUIR EQUATION
(National Electrode Carbon, 50-60 Mesh)

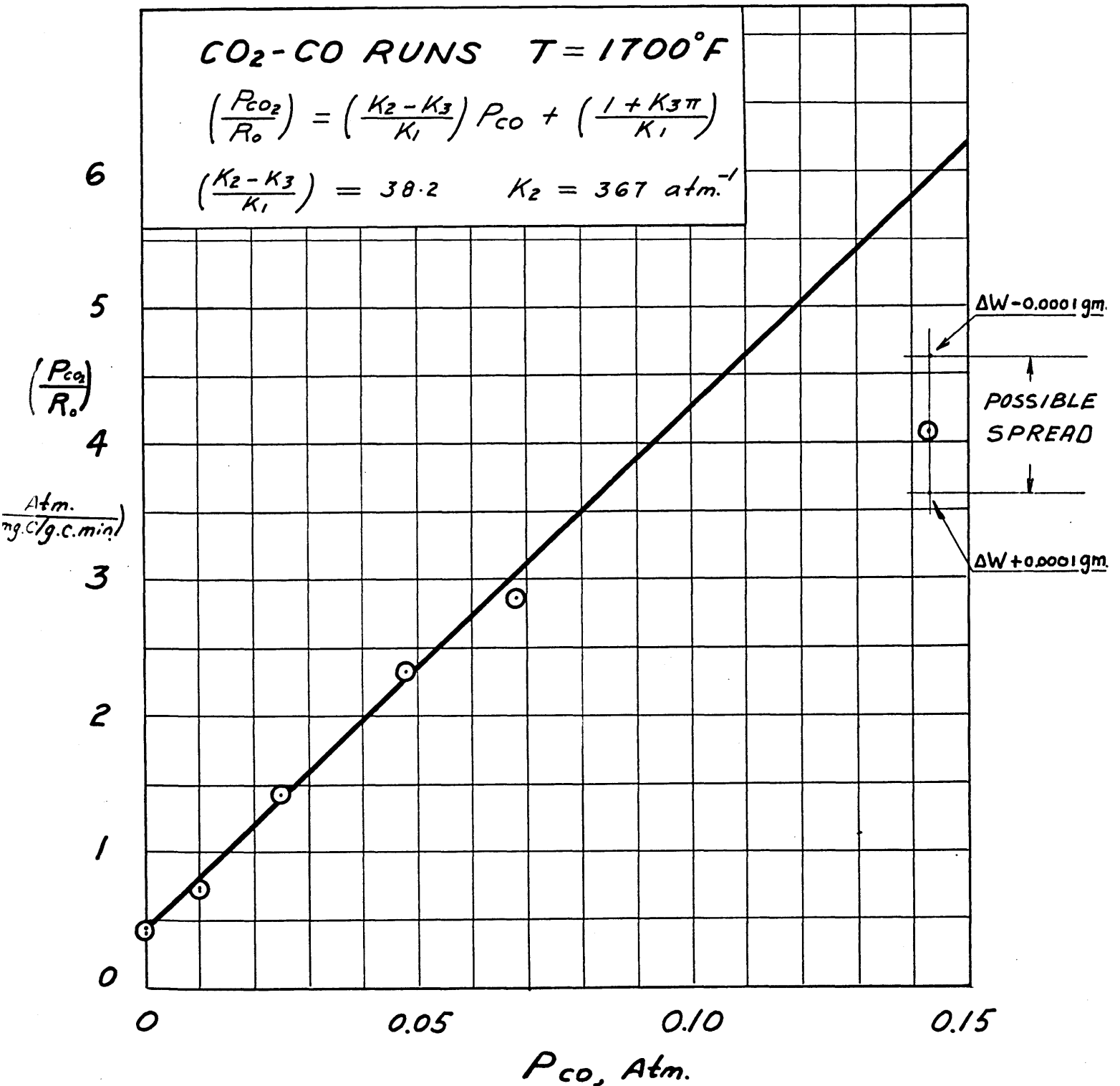


FIGURE (33)
 TEST OF RESULTS BY LANGMUIR EQUATION
 (National Electrode Carbon, 50-60 Mesh)

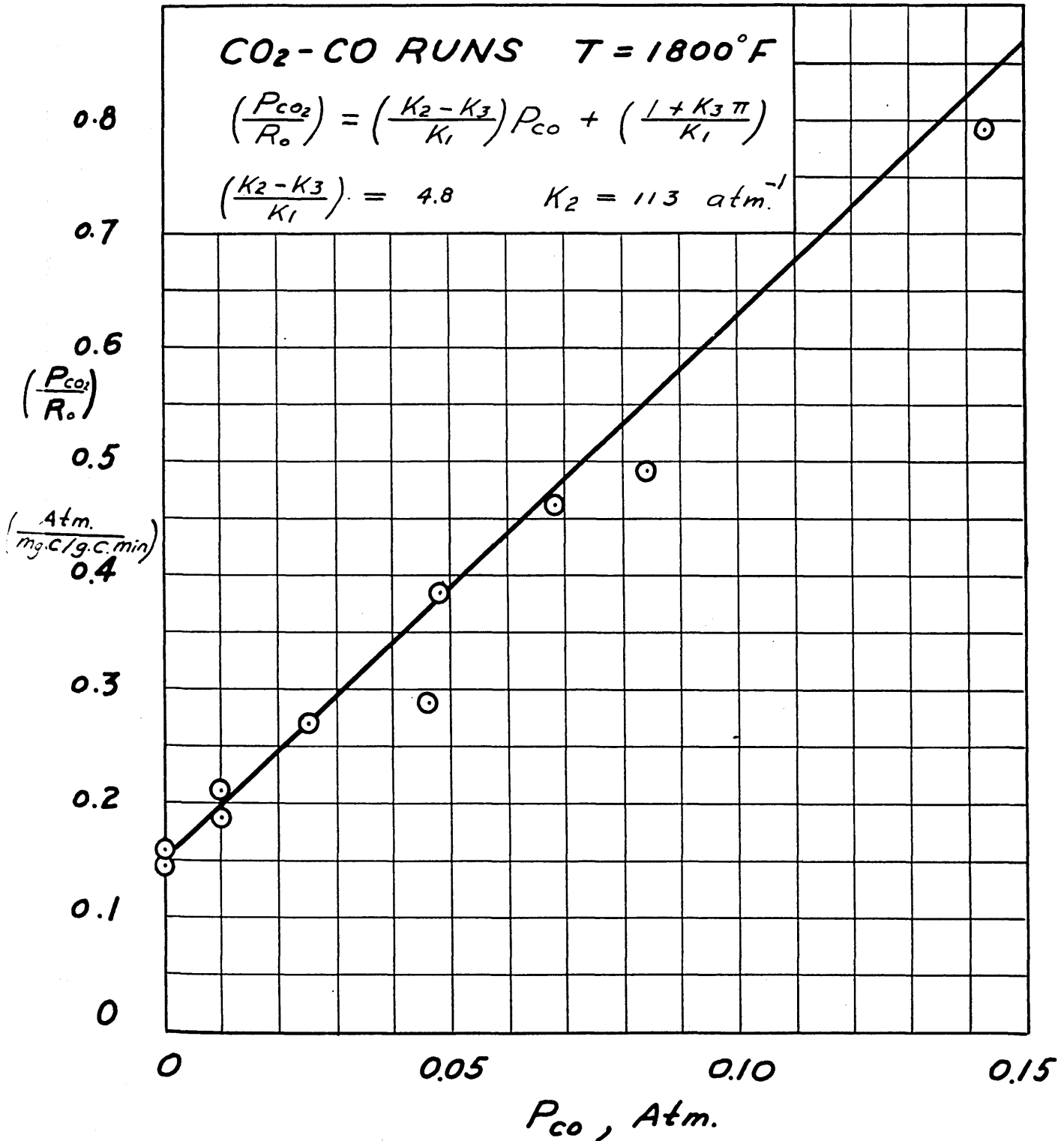
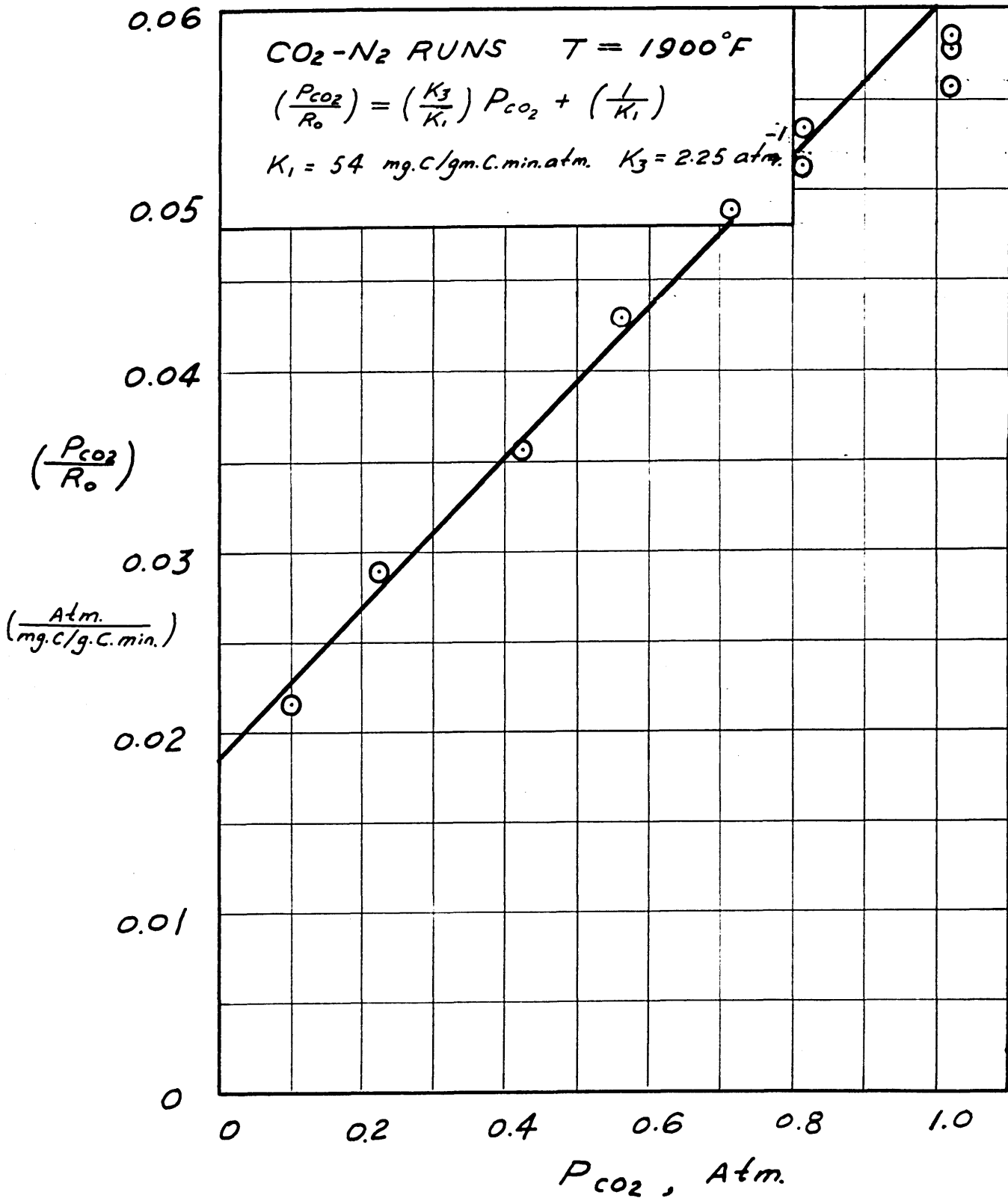


FIGURE (34)
 TEST OF RESULTS BY LANGMUIR EQUATION
 (National Electrode Carbon, 50-60 Mesh)



to be "on the low side" of the straight line drawn. The correct explanation for this behavior seems to be that the Langmuir type equation developed, holds with fair accuracy between 0 and approximately 7% CO, but gives results which may be off by 30% when used between 7 and 14% CO, which was the upper limit of the investigation.

It can hence be said that over the range of temperatures investigated, up to a carbon monoxide partial pressure of about 0.07 atm., R_0 can be represented by a Langmuir type equation of the following form:

$$R_0 = \frac{K_1 P_{CO_2}}{1 + K_2 P_{CO} + K_3 P_{CO_2}} \quad (14)$$

The values of K_1 , K_2 and K_3 were calculated at the reaction temperatures investigated, and are listed in Table 1.

TABLE 1

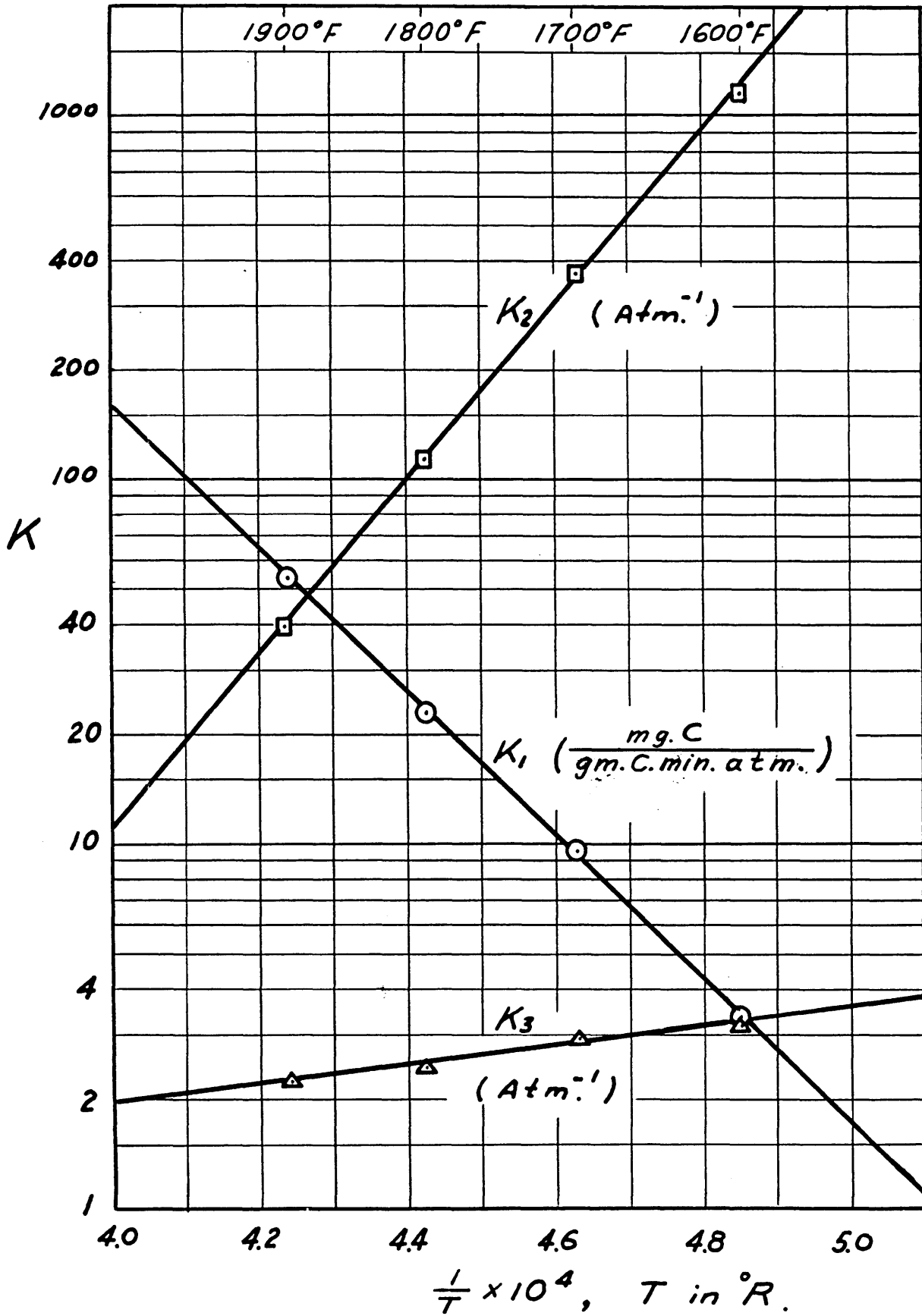
Langmuir Equation Constants

Constants	(Electrode Carbon)			
	Reaction Temperature, °F.			
	<u>1600</u>	<u>1700</u>	<u>1800</u>	<u>1900</u>
K_1 (mg.C./gm.C.min.atm.)	3.33	9.51	23.0	54.0
K_2 (atm. ⁻¹)	1141	367	113	39.8
K_3 (atm. ⁻¹)	3.20	2.95	2.45	2.25

When plotting these values vs. the reciprocal of the absolute temperature on semi-logarithmic coordinates, straight lines were obtained, as required by Equation (16), and shown in Figure 35. The values of K_0 and E were calculated for each

LANGMUIR EQUATION CONSTANTS

(National Electrode Carbon, 50-60 Mesh)



constant from the corresponding straight line, and are listed in Table 2:

TABLE 2
 Values of E and K_o in $K = K_o e^{-E/RT}$
 (Electrode Carbon)

E_1	90,100 (Btu/lb.mole)	K_{10}	1.22×10^{10} (mg.C/gm.C.min.atm.)
E_2	-109,000	"	K_{20} 3.30×10^{-9} (atm. ⁻¹)
E_3	-11,920	"	K_{30} 1.77×10^{-1} (atm. ⁻¹)

It is to be noted that, if the equation describes a rate affected by surface adsorption of CO and CO₂, i.e., if the Langmuir-Hinshelwood derivation, (see Appendix), is substantially correct, then the signs of the three E's are as expected. E_2 and E_3 are associated with adsorption phenomena which should become less important as the temperature rises, whereas E_1 (= $E_r + E_3$) is the primary measure of effect of temperature on reaction rate.

Substitution of the values calculated for K_{10} , K_{20} and K_{30} and E_1 , E_2 and E_3 into equation (15) results in:

$$R_1 = \frac{-d \ln(1-F)}{d \theta} = \frac{(14F+1) \times 1.22 \times 10^{10} \times e^{-90,100/RT}}{1 + 3.3 \times 10^{-9} \times e^{+109,000/RT} + 0.177 \times e^{+11,920/RT}} \quad (15a)$$

This equation makes it possible, within the range of the investigation, to calculate R_1 for 50-60 mesh National electrode carbon particles, knowing the fraction of carbon reacted, F , and the reaction conditions (temperature, pressure

and gas composition).

Combination of equations (3) and (11b) the following expression for $R_{av.}$ is obtained:

$$R_{av.} = \frac{\ln(1-F)}{\left(\frac{1}{15 R_o}\right) \ln\left(\frac{1-F}{1+14F}\right)} \quad (19)$$

which, when substituting the expression developed for R_o , can be modified to:

$$R_{av.} = \frac{15 \ln(1-F)}{\ln\left(\frac{1-F}{1+14F}\right)} \times \frac{1.22 \times 10^{10} \times e^{-90,100/RT}}{1 + 3.3 \times 10^{-9} x e^{+109,000/RT} + 0.177 x e^{+11,920/RT}} \quad (19a)$$

It was by means of this equation that the validity of the correlation developed was tested. Values calculated for $R_{av.}$ from this equation were plotted vs. the values determined from the experimental data, the result of which is shown in Figure 36. With the exception of a few time runs, using a gas mixture containing a high percentage of CO, the correlation obtained can be said to be satisfactory over the 2000-fold range of variation in rate.

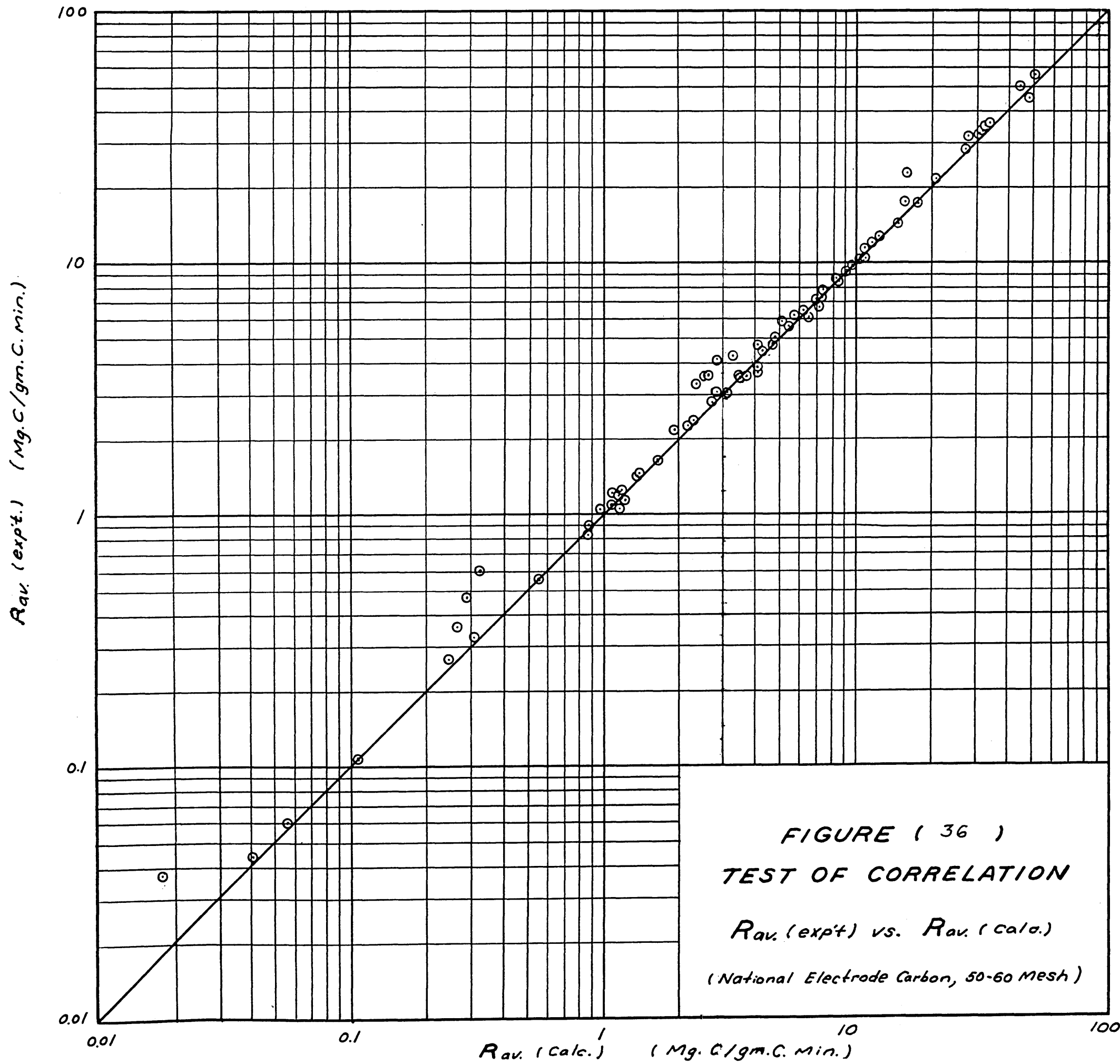


FIGURE (36)
TEST OF CORRELATION
 $R_{av} (exp't.)$ vs. $R_{av} (calc.)$
(National Electrode Carbon, 50-60 Mesh)

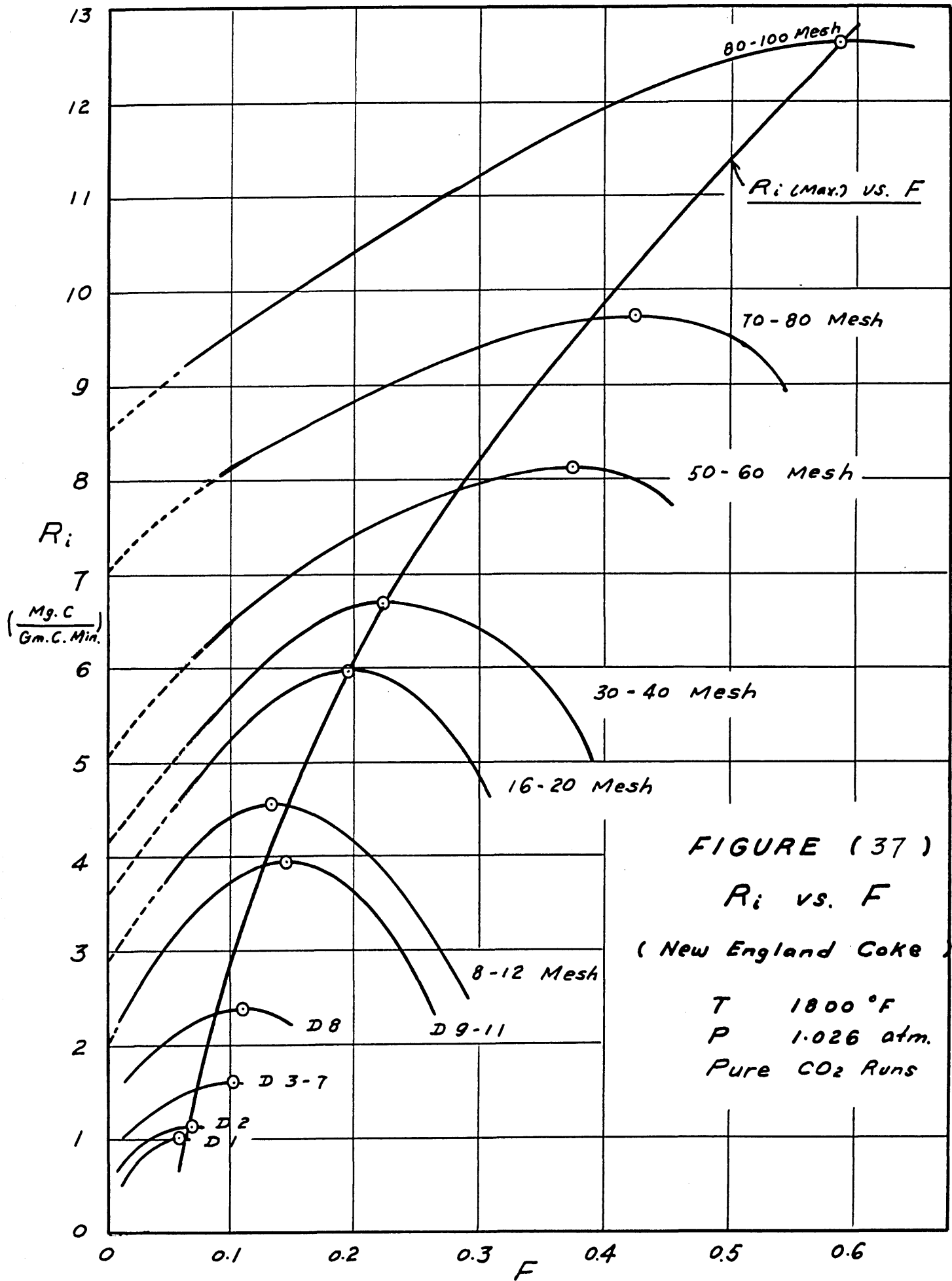
B. Experiments using New England coke particles of different sizes, reacting with pure carbon dioxide at 1800°F. with different times of reaction

From Figure 16 it is clear that the reaction rate is influenced not only by the fractional decrease in weight of carbon, F , but also by the diameter of the coke particle, D . In order to obtain a clear picture of the reaction mechanism, it would be more enlightening to compare the instantaneous specific reaction rates, R_1 , than the average specific reaction rates, $R_{av.}$, shown in Figures 16 and 17.

The method used to evaluate R_1 is different from that used in the case of electrode carbon. For the coke data, R_1 was determined directly as the slope of the $F - \Theta$ curve at a particular point, divided by $(1 - F)$. These values of R_1 are plotted vs. F in Figure 37. The curves are extrapolated to $F = 0$ to obtain the initial value of instantaneous specific reaction rate, R_0 .

For all sizes investigated, R_1 initially increases, reaches a maximum, and then declines with further reaction. There is a pronounced trend for the maximum to occur at larger F values when smaller particles are used. A line showing the values of $R_1(\max.)$ is drawn on the same plot.

The shift of $R_1(\max.)$ to larger values of F when using smaller particles, as shown in Figure 37 can be explained as being due to the presence in the coke of ash, which amounts to 9.5%. In the case of the large particles,



only a relatively small fraction of the weight of the particle has to be reacted to form a substantial layer of ash on the surface. The ash coating then makes the carbon less accessible to the reacting gas, and the reaction rate falls off. However, in the case of the small particles, a large fraction of the weight of the particle must be burned away to produce the substantial ash layer that retards further reaction.

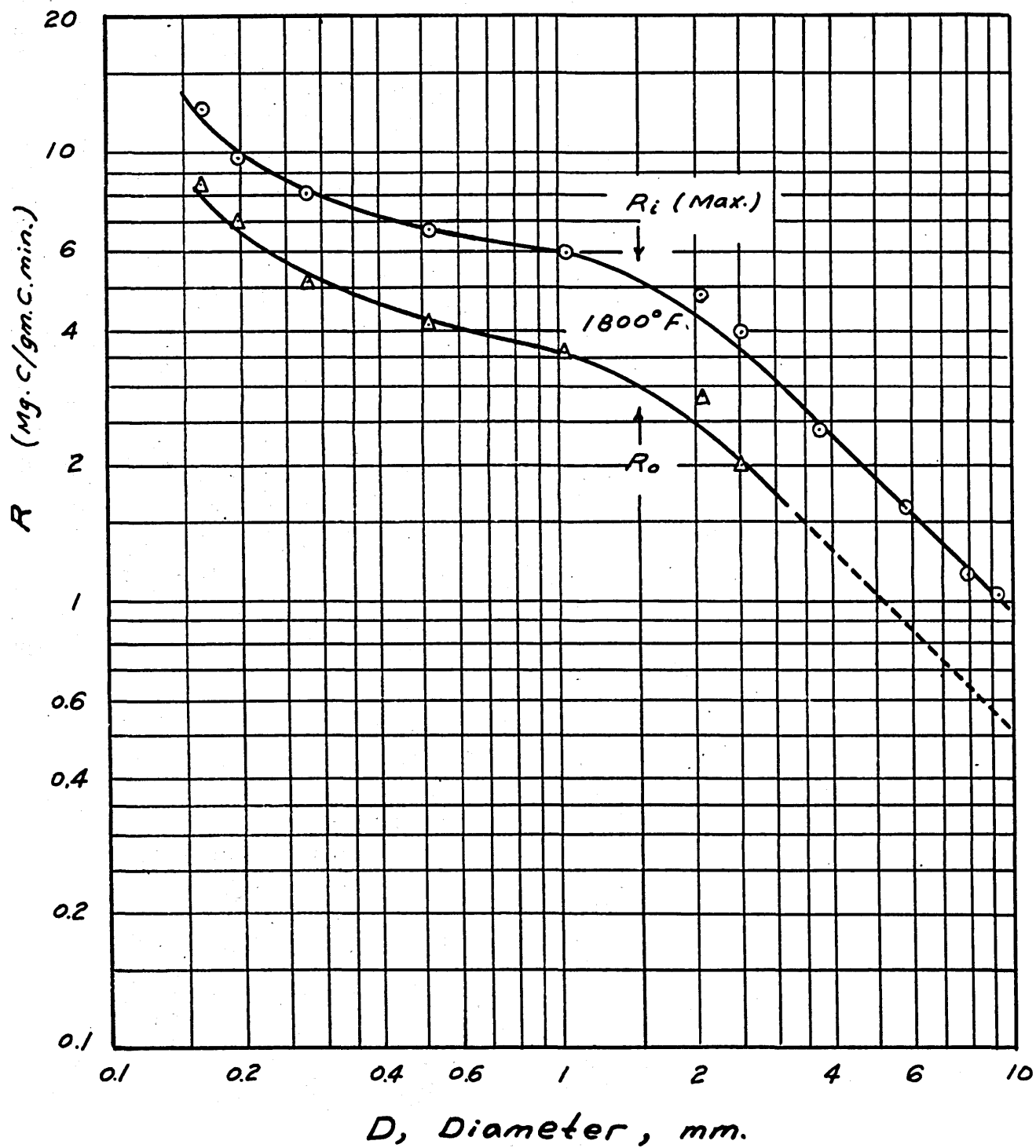
The $R_{1(\max.)}$ and R_0 values taken from each curve are plotted vs. D in Figure 38. These two curves form the limits of the reaction rates investigated. For example, the plot of R_{av} , at $F = 0.1$, vs. D , as given in Figure 17 can be shown to lie between these two curves.

All the R - D curves are of the same shape as the curve of Blanc (the lower curve in Figure 17). The reaction rates reported by Blanc are about 100% higher than they should be because of the interfering effect of minute amounts of oxygen.

To explain the effect of the particle size on the reaction rate, the weight per particle was determined as a function of the particle diameter, as shown in Figure 18. The particle densities were then determined by assuming spheres of diameter equal to the mesh opening; these are shown in Figure 39 as a function of particle diameter. The particle density is seen to increase with decreasing particle diameter. This fact is easily understandable if a large particle is visualized as one that is very porous,

FIGURE (38) R_i vs. D

(New England Coke Particles)

PURE CO_2 RUNS

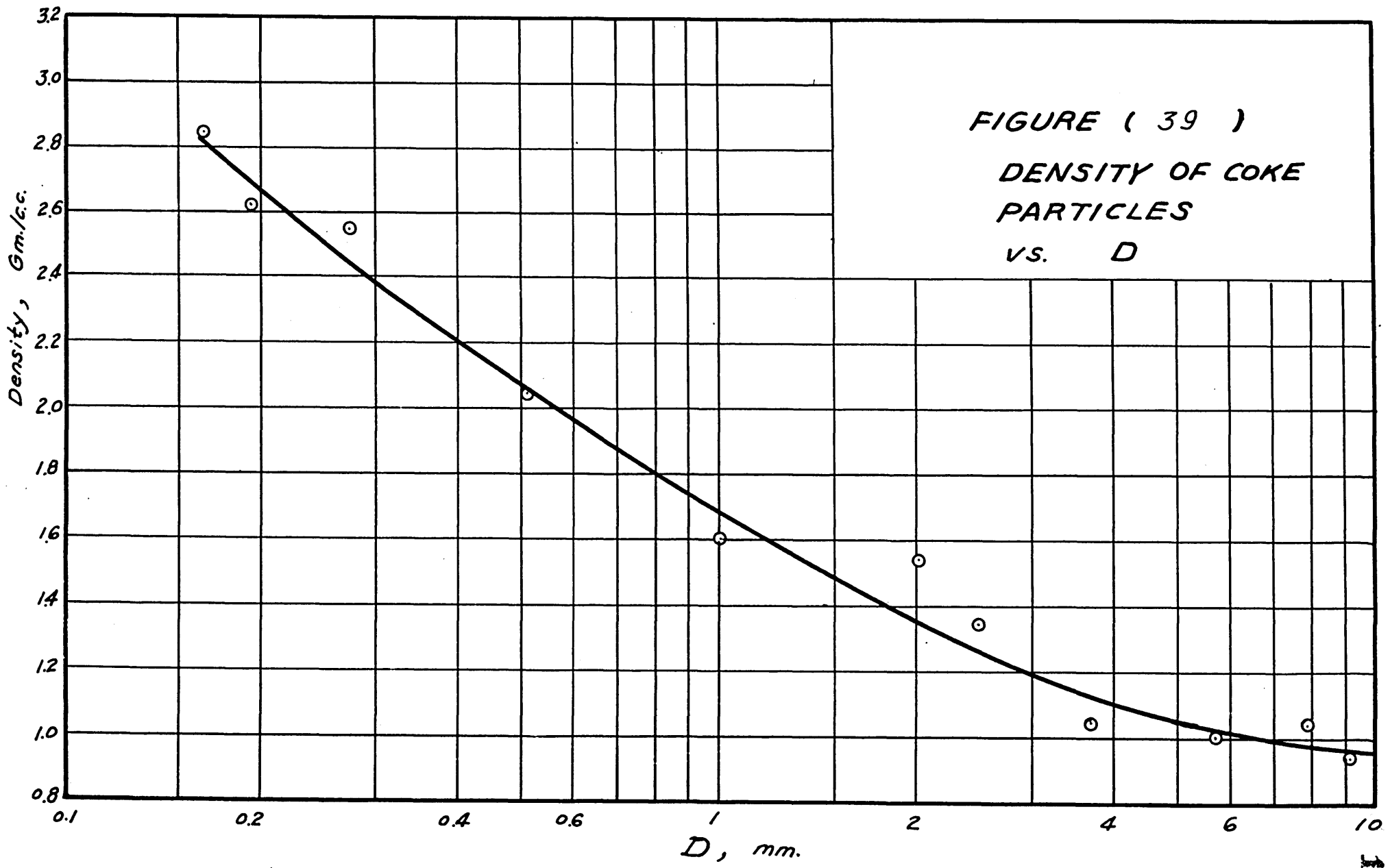


FIGURE (39)
 DENSITY OF COKE
 PARTICLES
 VS. D

having thin tentacle-like sections projecting from the body of the particle. A particle of this description would have a low density. However, crushing such a particle would result in breaking off the projections, and forming small particles that would be more compact. Therefore, the small particles would have a higher density.

To show the effect of porosity on the reaction rate, the reaction rates based on unit superficial area are calculated from R_0 and the density data. The reaction rate based on unit superficial area is equal to:

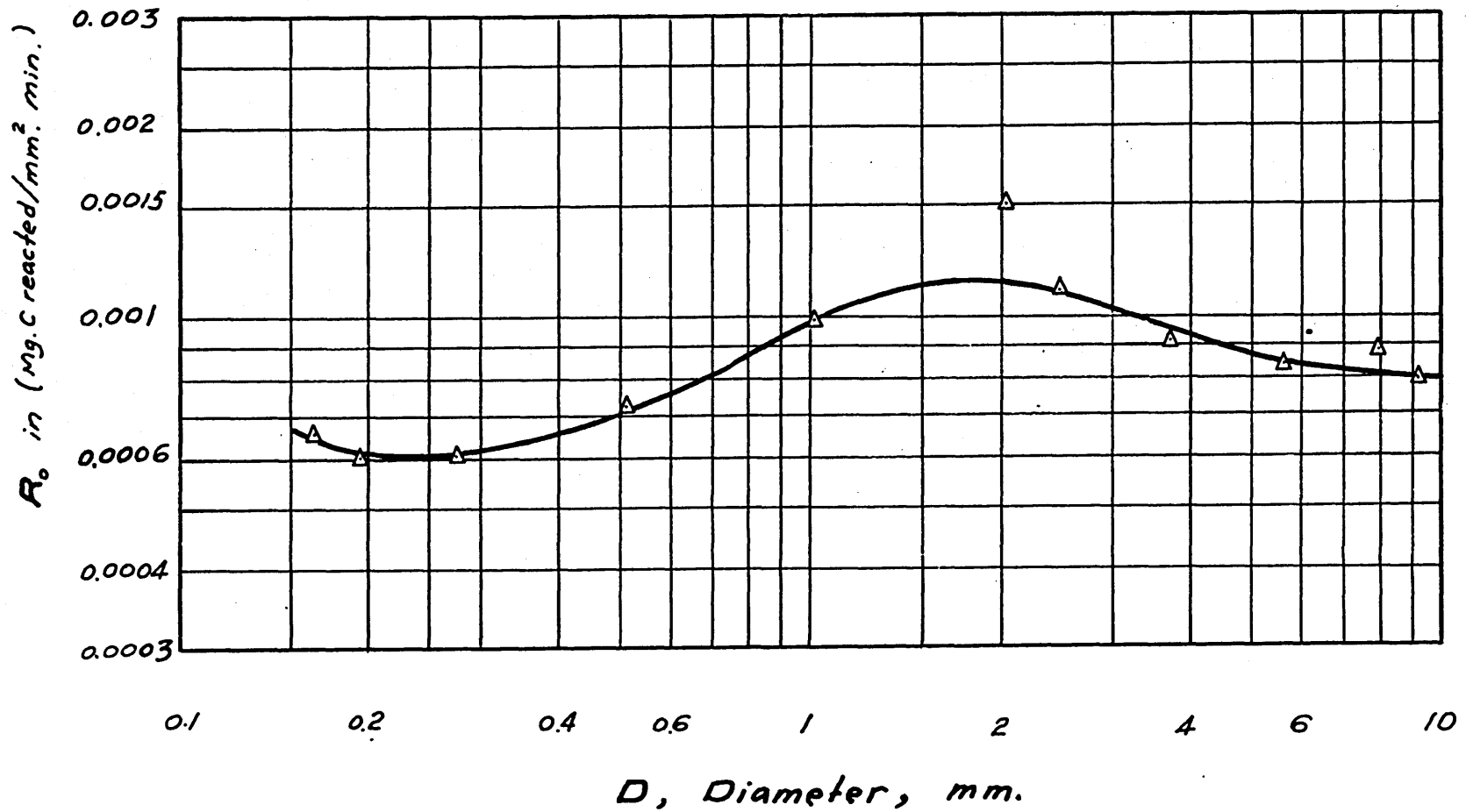
$$\frac{R_0 \times (\text{weight per particle})}{\pi \times D^2} \quad (20)$$

These results are shown in Figure 40. The reaction rate based on the superficial area give less variation with D than those on a weight basis. In spite of the wave shaped curve, for particle diameters larger than 1 mm., the rate can be treated qualitatively as a constant, and for particle diameters less than 0.3 mm., the rate is again a constant, lower in value than the former one. The shift from a higher constant value for the larger particles to a lower constant value for the smaller particles seems to indicate a change in the structure of carbon, from a porous material having a high ratio of effective area to superficial area, to a more dense material in which the superficial area comes nearer measuring the true surface that enters into the reaction.

To explain the shape of the curves shown in Figure 37,

FIGURE (40)

REACTION RATE BASED ON SUPERFICIAL SURFACE AREA
AT $F=0$ VERSUS THE DIAMETER OF PARTICLE
(New England Coke)



it is interesting to refer to the correlation for the results with electrode carbon. As shown by equation (5), the reaction rate is expressible as a linear function of F . The increasing reaction rate was ascribed to an increase in the effective surface area, or the creation of active centers, in the course of the reaction. In view of the fact that one of the important differences between electrode carbon and coke is the ash content (electrode carbon 0.4% and coke 9.5%) it is thought that the reaction at the early stage for coke resembles that of electrode carbon, i.e., a straight line relation would hold for R_1 and F . But, for coke, as the carbon is burned away, the retardation effect of ash would increase, thus tending to reduce the reaction rate. A maximum is reached as a net result of these two competing factors. If there were no ash present in the coke, the linear relation might hold for the whole course of the reaction, but due to the retardation effect of ash only a fraction of the ash-free reaction rate can be achieved. In Figure 41 a fictitious R_1 of the type expected in an ash-free system like electrode carbon is compared with the rate obtained experimentally, as a function of F . In Figure 42 the corresponding ash retardation factor, defined as the ratio of the actual R_1 to the ash-free R_1 , is shown graphically also as a function of F .

Figure 41

Actual R_1 and ash-free R_1
vs. F

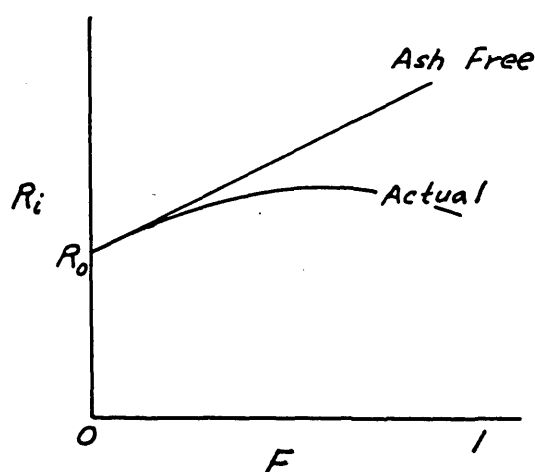


Figure 42

Ash Retardation Factor
vs. F



In order to obtain a relation to represent the above-mentioned mechanism, various empirical formulations were tried. It was first assumed that the effect of surface activation can be expressed by a function similar to that given for electrode carbon, namely:

$$R_1(\text{ash-free}) = R_0 + mF = R_0 \left(1 + \frac{m}{R_0} F\right) \quad (21)$$

in which m is the initial rate of change of R_1 with respect to F .

For electrode carbon particles of 50-60 mesh, the surface activation factor $\frac{m}{R_0}$ had been found to be a constant of magnitude 14. In these experiments using coke of different particle sizes, $\frac{m}{R_0}$ may be expected to vary with D . Empirically it was found that the expression

$$\left(\frac{m}{R_0}\right) = \frac{10 (2 + \log_{10} D)}{R_0} \quad (22)$$

satisfactorily represents the data. (D is in mm.).

Using (22), equation (21) becomes:

$$R_1 \text{ (ash-free)} = R_0 \left(1 + \frac{10 (2 + \log_{10} D) F}{R_0} \right) \quad (21a)$$

The ash retardation factor was found empirically to be expressible in the form:

$$e^{-5.5DF^{1.85}} \quad (23)$$

Combining these two expressions:

$$R_1 = R_0 \left(1 + \frac{10 (2 + \log_{10} D) F}{R_0} \right) e^{-5.5DF^{1.85}} \quad (24)$$

Although this equation gives values for R_1 that are generally within 5% of the R_1 calculated from the data, no claim is made that equation (24) is well established or of the right general form, except within the range over which data are available.

The results of Goring, Oshima and Fukuda, and Duffy and Leinroth (51) in most cases showed an increase in rates during the earlier stage of reaction, and a decrease following the maximum point. A point to be noted is that in all these investigations high ash-content cokes were used. The mechanism as outlined above can well be applied to explain their similar results.

C. Experiments using New England coke particles of 50-60 mesh

The values of $R_{av.}$, calculated from the data corrected for ash and V.C.M., were correlated by the aforementioned Langmuir equation of the following form:

$$R_0 = \frac{K_1 P_{CO_2}}{1 + K_2 P_{CO} + K_3 P_{CO_2}} \quad (12)$$

Theoretically, the values of R_0 should be used in determining the rate constants in this equation. However, in view of the results obtained at 1800°F. using different times of reaction, it can be seen that the values of R_0 and $R_{av.}$ parallel one another, and are close together, especially when F is small. For most of the runs, the values of F lie between 0.05 and 0.1. The use of $R_{av.}$ for R_0 in the determination of rate constants will certainly not negate the Langmuir equation correlation.

Before the true rate constants could be evaluated, approximate values of the constants were first obtained by assuming that the partial pressures of CO and CO₂ in the entering gas were the same as those effective for reaction. Using the technique mentioned in the section on electrode carbon, these approximate constants were evaluated for each of the temperatures investigated. The correlation plots showing $P_{CO_2}/R_{av.}$ as a function of P_{CO_2} and P_{CO} for CO₂-N₂ and CO₂-CO runs, respectively, are shown in Figure 43. The approximate rate constants evaluated are listed in Table 3.

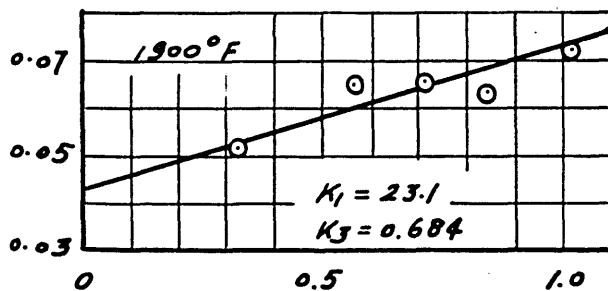
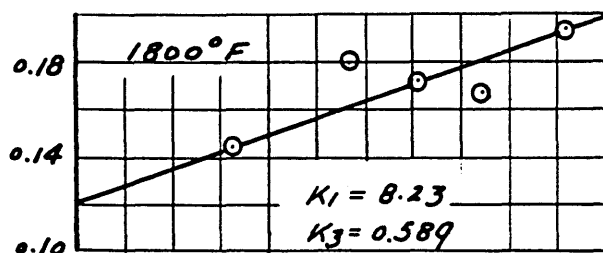
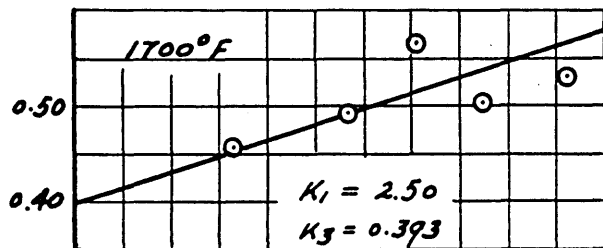
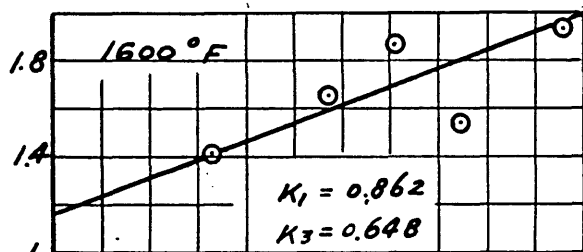
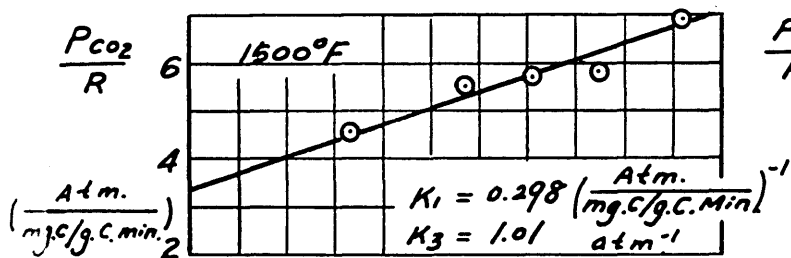
FIGURE (43)

TEST OF RESULTS BY LANGMUIR EQUATION

(New England Coke, 50-60 Mesh, Corrected for V.C.M. based on N₂ Blank Runs)

CO₂-N₂ RUNS

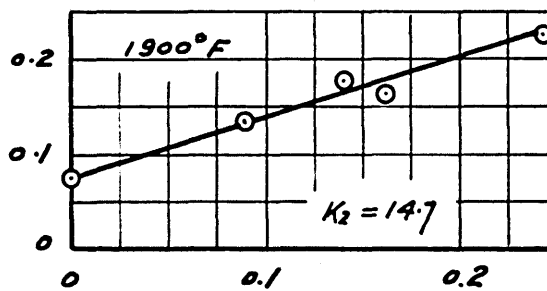
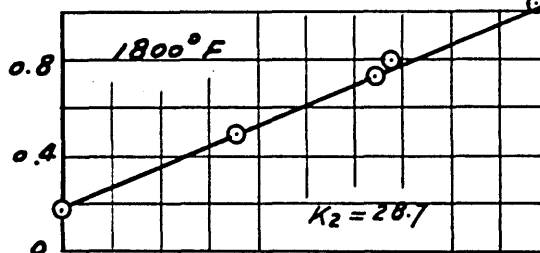
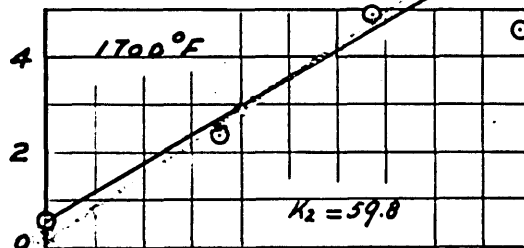
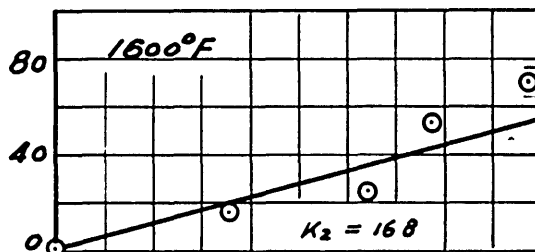
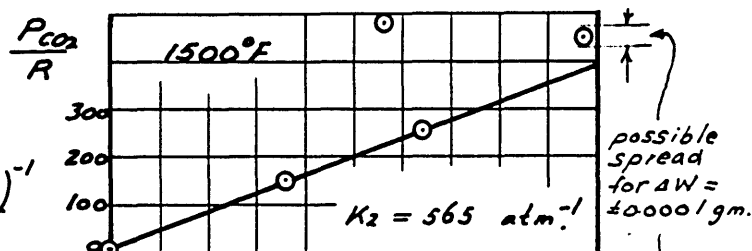
$$\left(\frac{P_{CO_2}}{R}\right) = \left(\frac{K_3}{K_1}\right) P_{CO_2} + \left(\frac{1}{K_1}\right)$$



P_{CO₂}, Atm.

CO₂-CO RUNS

$$\left(\frac{P_{CO_2}}{R}\right) = \left(\frac{K_2 - K_3}{K_1}\right) P_{CO} + \left(\frac{1 + K_3 \pi}{K_1}\right)$$



P_{CO}, Atm.

TABLE 3 - Approximate Langmuir
Equation Constants (Coke)

Constants	Reaction Temperature, °F.				
	<u>1500</u>	<u>1600</u>	<u>1700</u>	<u>1800</u>	<u>1900</u>
K_1 (mg.C./gm.C.min.atm.)	0.298	0.862	2.50	8.23	23.1
K_2 (atm. ⁻¹)	565	168	59.8	28.7	14.7
K_3 (atm. ⁻¹)	1.01	0.648	0.393	0.589	0.684

A correction for gas composition, due to the formation of CO in the reaction area was next attempted. In order to do this, series of runs were made at different gas flow rates using pure CO₂ as inlet gas, and the average specific reaction rates calculated were plotted vs. the reciprocal of the gas flow rate $1/V$ in Figure 13.

The specific reaction rate R_v , obtained by extrapolating the straight lines to $1/V = 0$, was considered as the rate corresponding to 100% CO₂ at the particular temperature. The differences between the values of R_v so obtained and the rates $R_{av.}$ measured for regular pure CO₂ runs are attributed to the retardation by CO generated during reaction when pure CO₂ was used as inlet gas at a finite gas flow rate.

As shown in Figure 13, these differences are fairly large, primarily due to the use of different sample pan setups. In the velocity runs, the single-pan setup as shown in Figure 6 was used, whereas in the regular CO₂-N₂ and CO₂-CO runs, the double-pan setup as shown in Figure 4 was used. It is now believed that the double pan produced so large a pressure drop as to cause a major short-circuiting

of gas flow around the edges.

Using the approximate rate constants and R_v , the effective CO concentrations in the pure CO₂ runs were calculated. Moreover, since the generation of CO from reaction is proportional to the rate of carbon reacted, the effective CO concentration for each of the CO₂-CO runs was calculated, using the effective CO concentrations calculated for the pure CO₂ runs, based on the approximate rate constants. The same principles were used to correct the rates of CO₂-N₂ runs to those corresponding to 0% CO. The corrected rates for the CO₂-N₂ runs are presented in Figure 44, the corrected rates for CO₂-CO runs in Figure 45. (For the methods of calculation, see Appendix G2 and G3).

The final rate constants were evaluated from the data points in Figures 44 and 45. The correlation plots are shown in Figure 46. The constants are listed in Table 4, and plotted vs. $1/T$ in Figure 47.

TABLE 4 - Langmuir Equation Constants (Coke)
(Final)

Constants	Reaction Temperature, °F.				
	<u>1500</u>	<u>1600</u>	<u>1700</u>	<u>1800</u>	<u>1900</u>
K_1 (mg.C./gm.C.min.atm.)	0.313	0.917	3.16	9.44	29.0
K_2 (atm. ⁻¹)	594	178.2	77.8	33.9	19.7
K_3 (atm. ⁻¹)	0.972	0.449	0.256	0.302	0.545

FIGURE (44) R_{AV} vs. P_{CO_2} FOR CO_2-N_2 RUNS

(New England Coke , 50-60 Mesh)

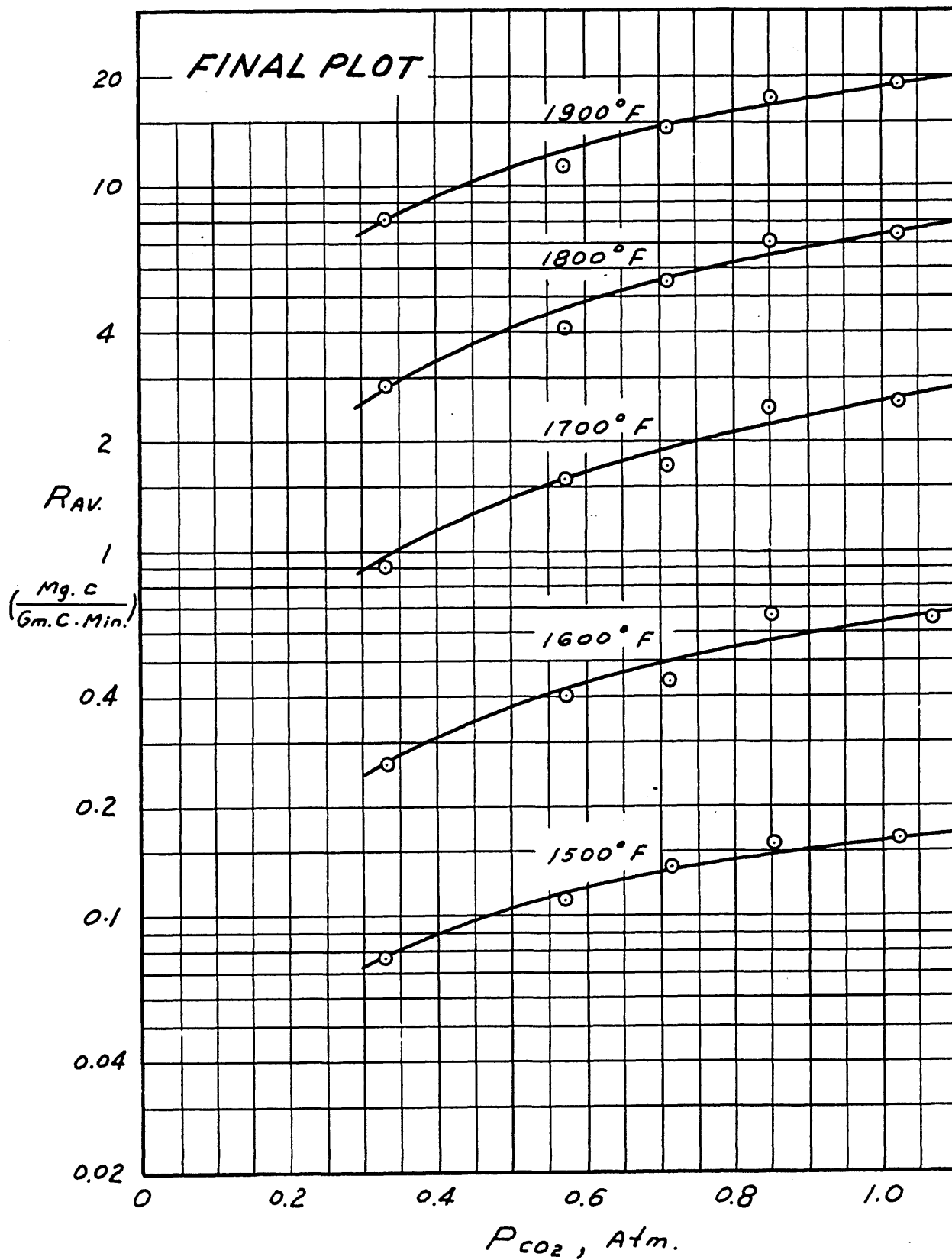


FIGURE (45) R_{AV} VS. P_{CO} FOR CO_2 - CO RUNS
 (New England CoKe , 50-60 Mesh)

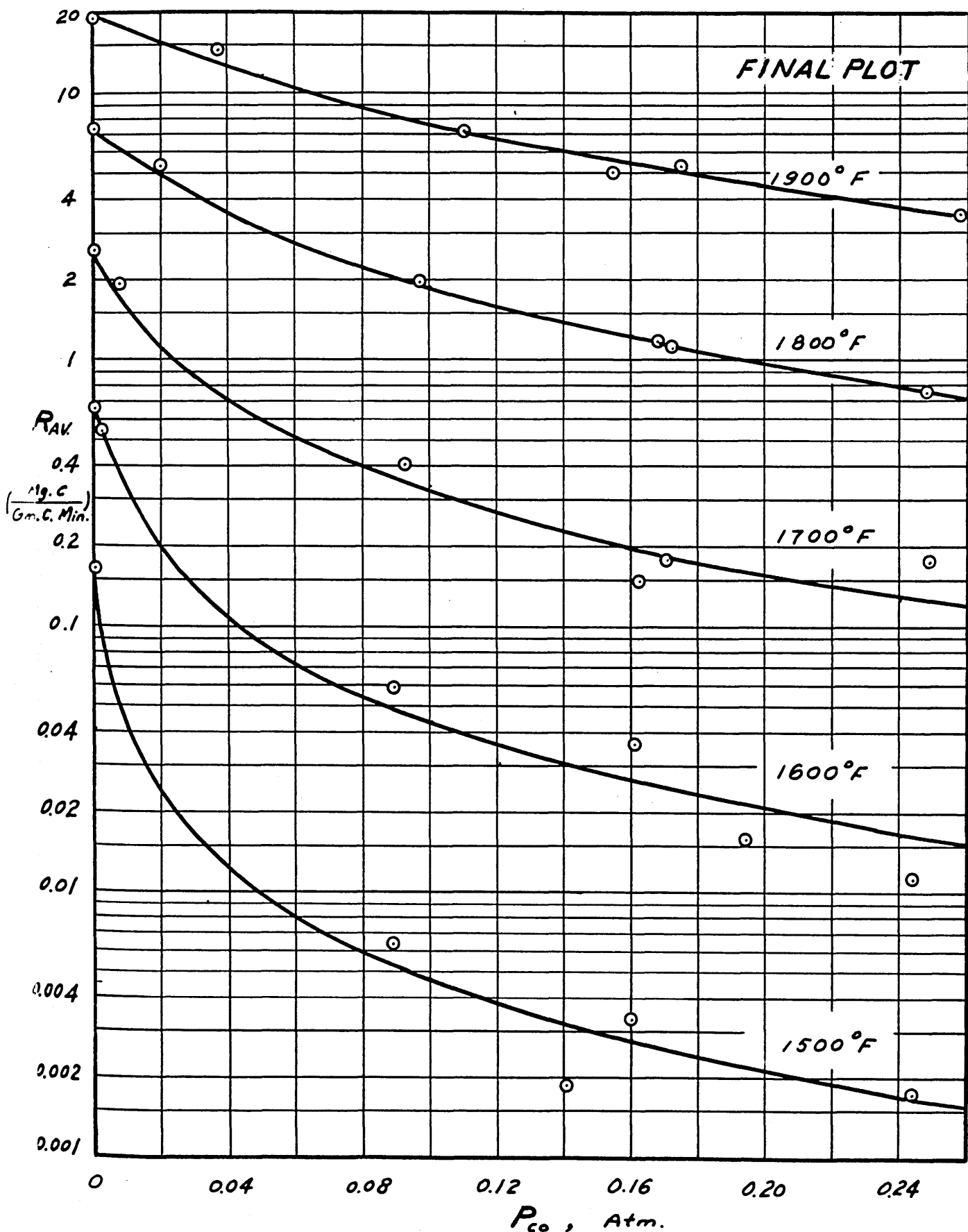


FIGURE (46)

TEST OF RESULTS BY LANGMUIR EQUATION

(Final Plot For New England Coke)
50-60 Mesh

CO₂-N₂ RUNS

CO₂-CO RUNS

$$\left(\frac{P_{CO_2}}{R}\right) = \left(\frac{K_3}{K_1}\right) P_{CO_2} + \left(\frac{1}{K_1}\right)$$

$$\left(\frac{P_{CO_2}}{R}\right) = \left(\frac{K_2 - K_3}{K_1}\right) P_{CO} + \left(\frac{1 + K_3 P}{K_1}\right)$$

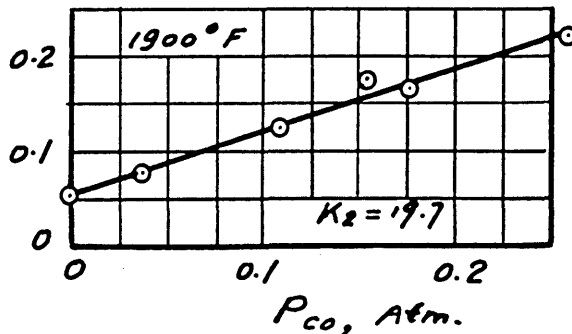
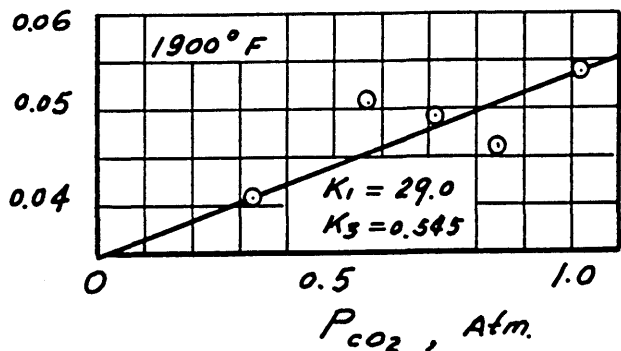
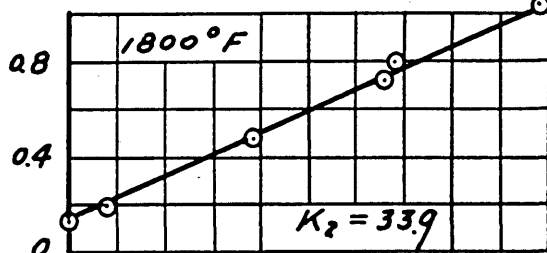
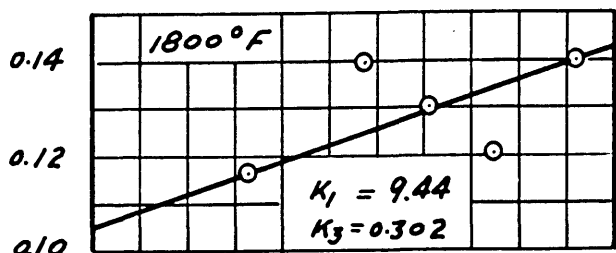
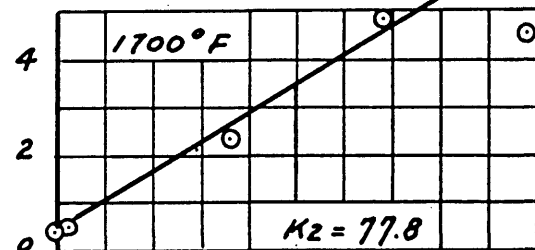
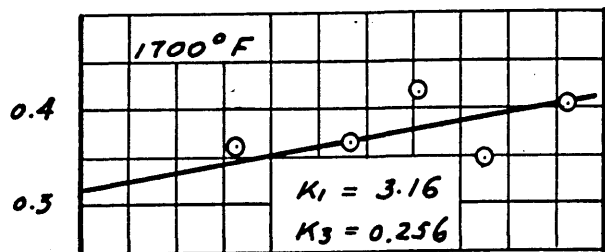
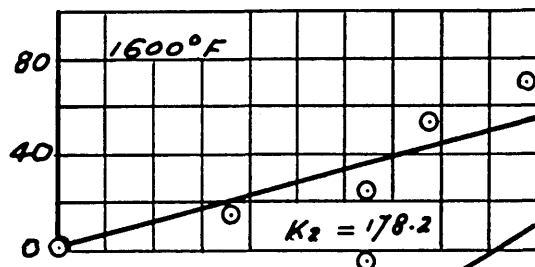
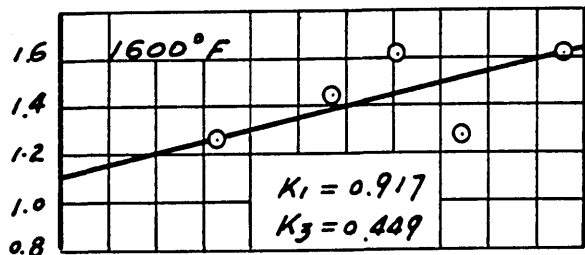
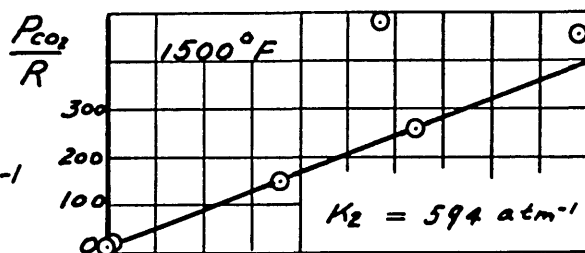
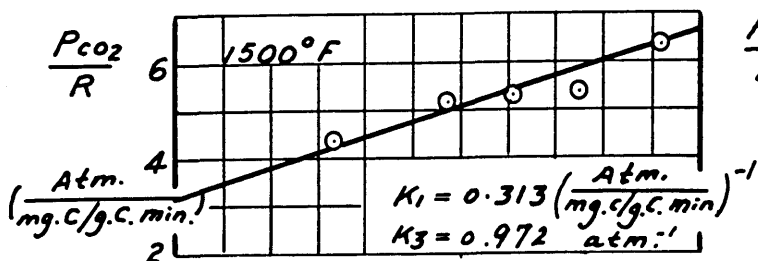
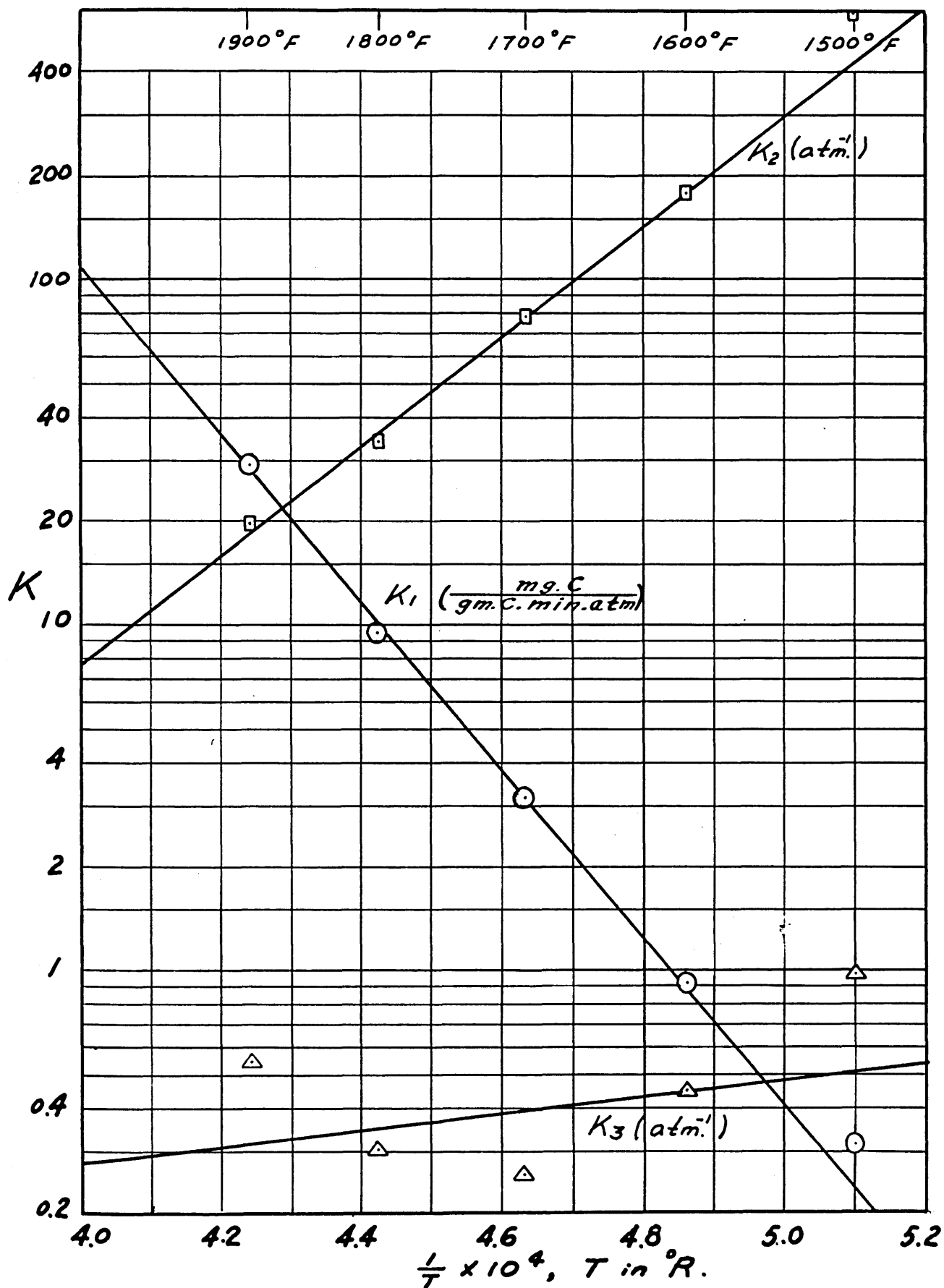


FIGURE (47) LANGMUIR EQUATION CONSTANTS

(New England Coke, 50-60 Mesh)



Repetition of the above calculation could be carried out if further refinement of constants is required. For the present purpose, these rate constants were considered sufficiently accurate.

Inspection of Figure 47 shows that K_1 and K_2 are simple functions of temperature, which can be expressed by the following Arrhenius-type equation:

$$K = K_0 e^{-E/RT} \quad (16)$$

The values of K_3 are not precise enough to draw any definite conclusion, but do not show contradiction to equation (16).

The constants K_0 and E were calculated for each of the constants K_1 , K_2 and K_3 . Their values are listed in Table 5.

TABLE 5 - Values of E and K_0 in $K = K_0 e^{-E/RT}$ (Coke)

E_1	+ 111,000 (Btu/lb.mole)	K_{10}	5.25×10^{11}	(mg.C./gm.C.min. atm.)
E_2	- 72,500	K_{20}	3.63×10^{-6}	(atm. ⁻¹)
E_3	- 11,000	K_{30}	3.02×10^{-2}	(atm. ⁻¹)

In Figure 48 the rates calculated from the Langmuir equation using the rate constants evaluated were plotted vs. the rates obtained experimentally. The average deviation is about 10%. The accuracies for high reaction rates are higher than for low ones.

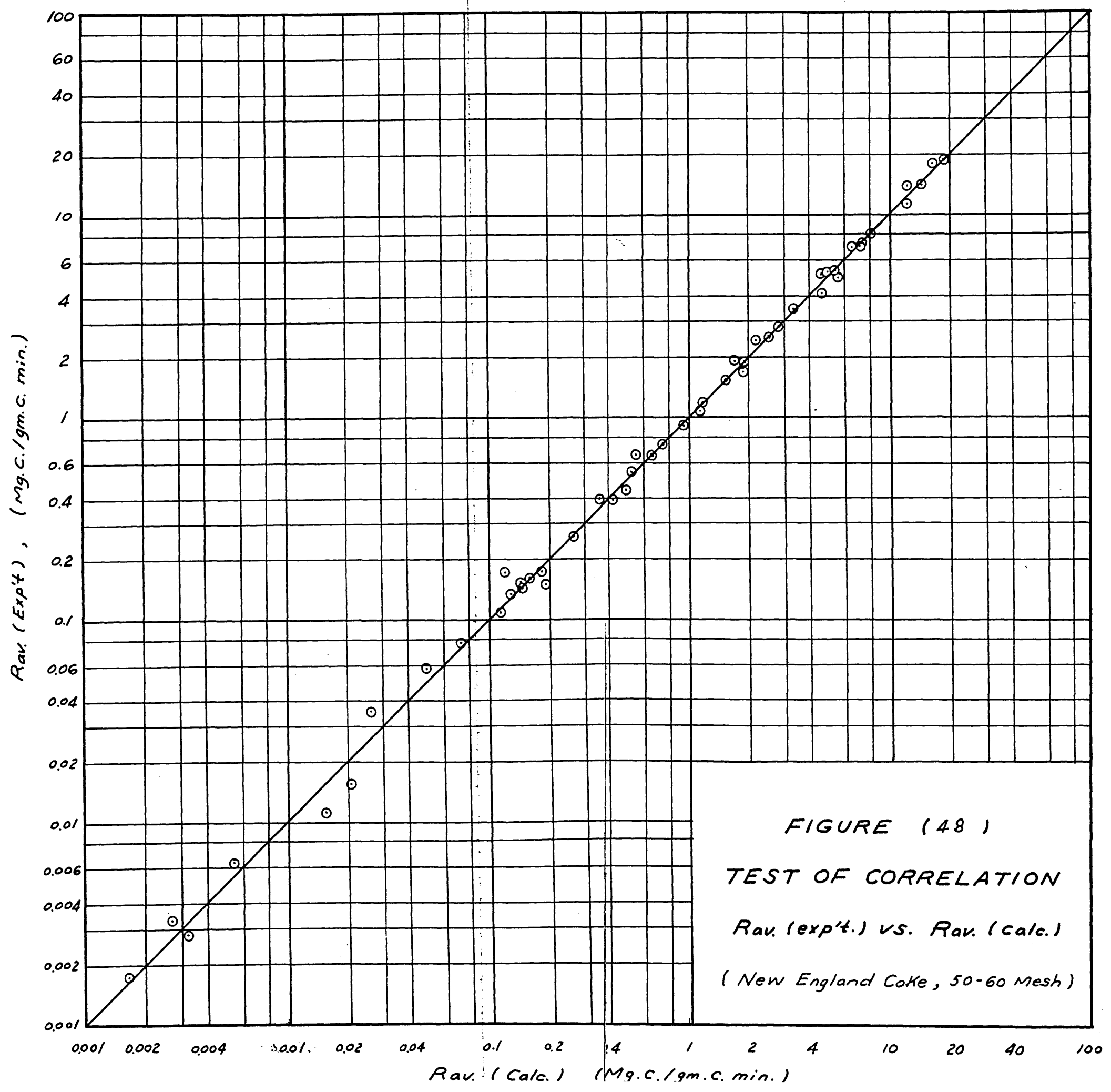


FIGURE (48)
TEST OF CORRELATION
 $R_{av} (exp't.)$ vs. $R_{av} (calc.)$
(New England Coke, 50-60 Mesh)

D. Comparison of the results of the present work on coke with those obtained in a fluidized bed by McBride

It was the original object of this work to find specific point reaction rate data under controlled reaction conditions, and by comparing the results obtained, determine the performance of a fluidized bed.

The fluidized bed technique was used by McBride to study the kinetics of the carbon-carbon dioxide reaction. In essence, his data were taken by passing metered inlet gas streams of various compositions through a batch bed of fluidized coal (20-200 mesh) in a vertical 1.78" I.D. x 7' 0" high tube maintained at the reaction temperature by external electric heat, the sum of the instrument readings, solid analyses, and the analysis of the corresponding exit gas constituting a data point. The data were correlated by McBride using the afore-mentioned Langmuir equation, which, when integrated across the bed assuming piston flow of the gas, gives this form:

$$K_1\pi W = \left[N_0 + (1+2K_2\pi)(2n_0+m_0) \right] \cdot \ln \frac{1}{1-f} - (1+2K_2\pi-K_3\pi)n_0f \quad (25)$$

while f = fractional decomposition of CO_2 in the bed

m_0 = flow rate of CO entering the bed, $\text{lb.mol.} \times 10^{-3}/\text{min.}$

n_0 = flow rate of CO_2 entering the bed, $\text{lb.mol.} \times 10^{-3}/\text{min.}$

N_0 = flow rate of N_2 entering the bed, $\text{lb.mol.} \times 10^{-3}/\text{min.}$

W = weight of carbon in bed, lb. atom.

π = total pressure, atm.

McBride determined the rate constants K_1 , K_2 and K_3 using these data points:

(a) 10 or 20% CO_2 in $\text{CO}_2\text{-N}_2$ mixture. This point has the greatest effect on the value of K_1 .

(b) 100% CO_2 . This point has the greatest effect on the value of K_3 .

(c) 40 or 60% CO_2 in $\text{CO}_2\text{-CO}$ mixture. This point determines the value of K_2 .

The constants determined by McBride are plotted vs. $1/T$ in Figure 49.

It can be seen that values of these constants differ greatly from those of the present work, shown in Figure 47.

McBride tested his correlation by plotting the fraction of CO_2 in the inlet gas decomposed at the exit, from experimental results, $f_{\text{exp't.}}$ vs. that calculated from the correlation, $f_{\text{calc.}}$. This plot is shown in Figure 50.

It is interesting to investigate the reasons why the two sets of constants obtained using coke from the same lot are different. If the assumption of piston flow is permissible in a fluidized bed, then it seems worthwhile to calculate f for McBride's experimental conditions using the Langmuir equation constants evaluated from the present work. The calculations were carried out and the results are shown in Figure 51.

Comparing Figures 50 and 51, it is apparent that slightly better correlation of McBride's data is obtained by using his own constants than the constants from the present

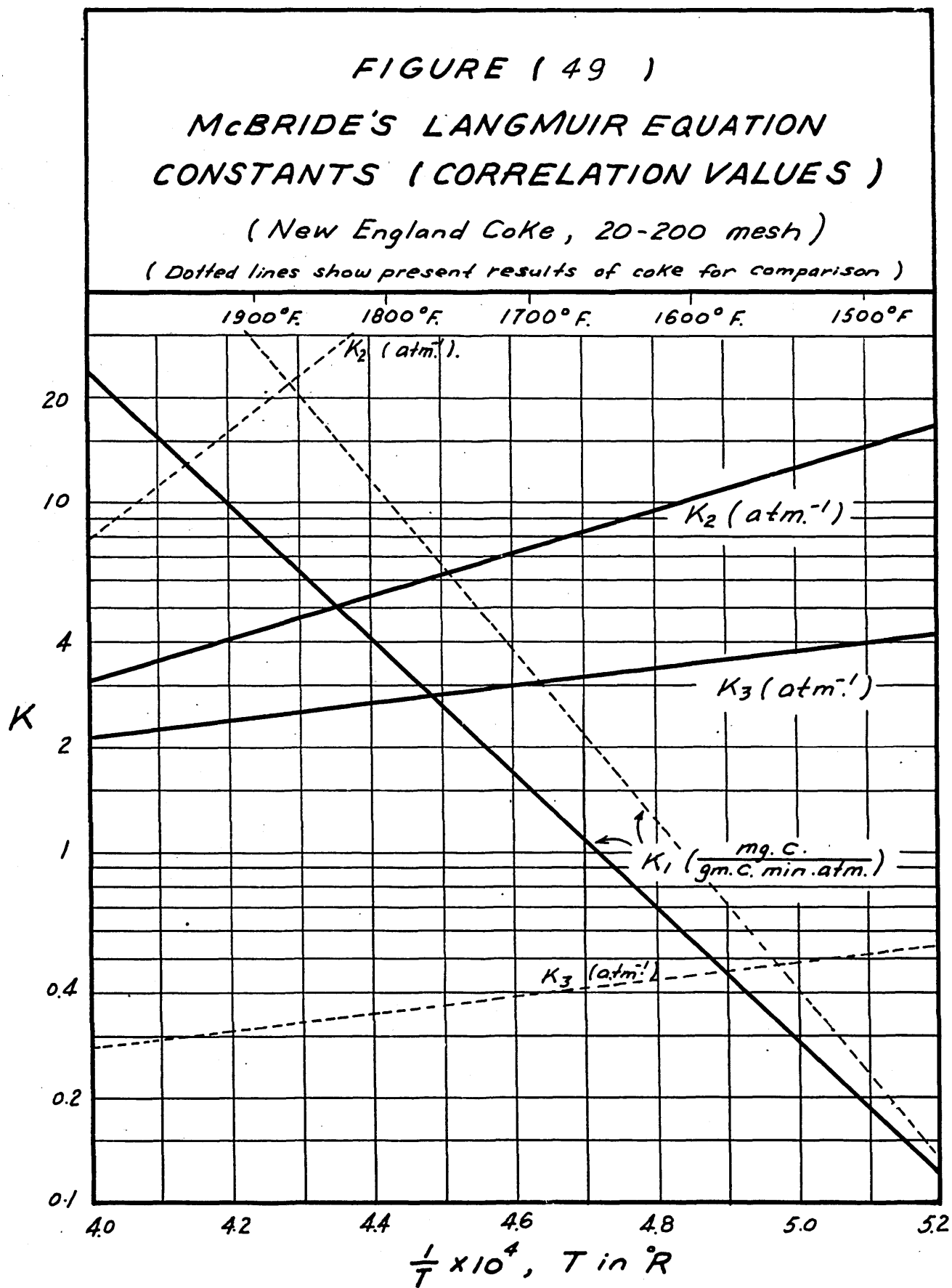


FIGURE (50)

PLOT OF $f_{exp't.}$ (FROM McBRIDE'S DATA)
 VS. $f_{calc.}$ (BY MEANS OF RATE CONSTANTS
 EVALUATED BY McBRIDE)

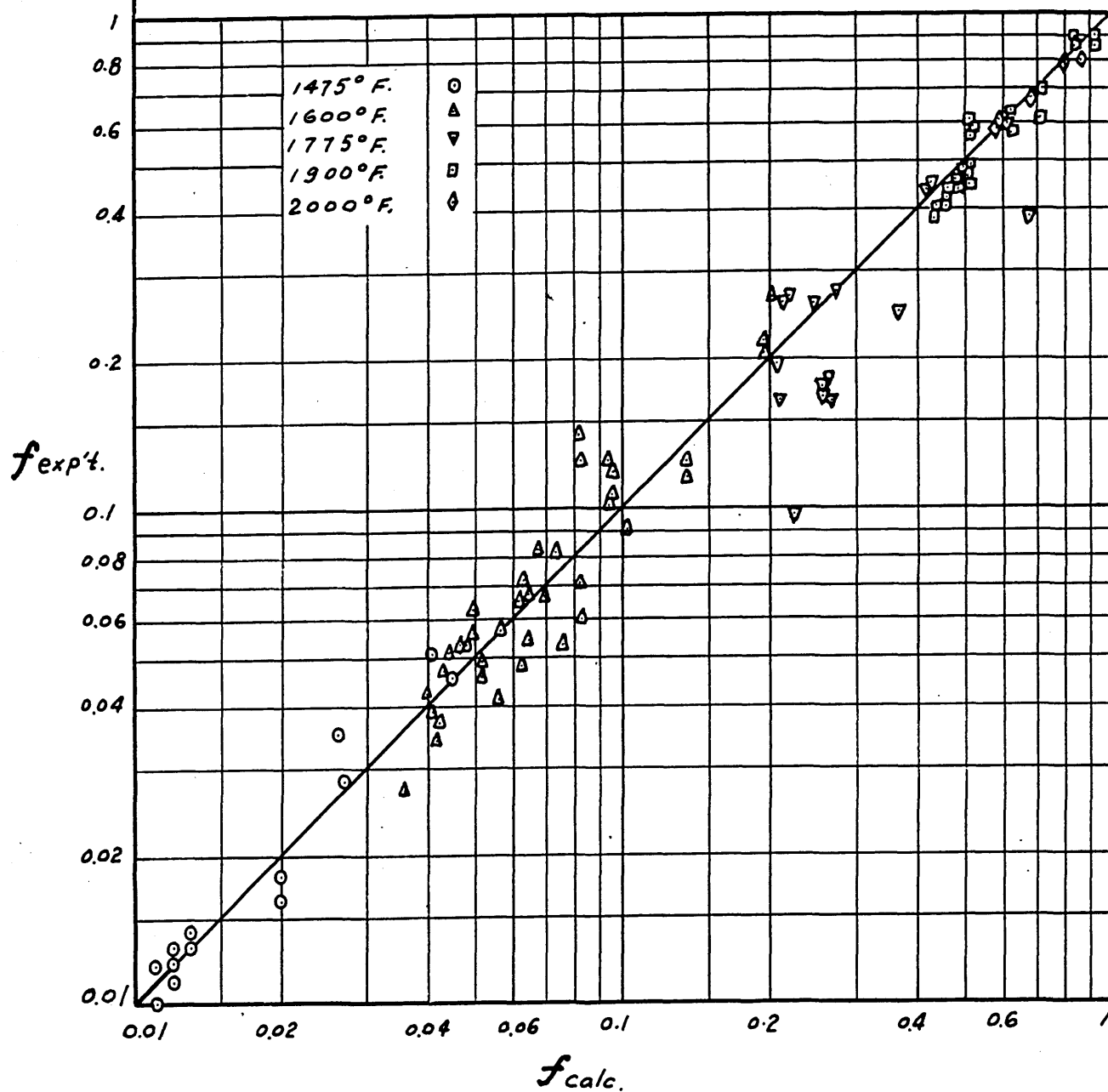
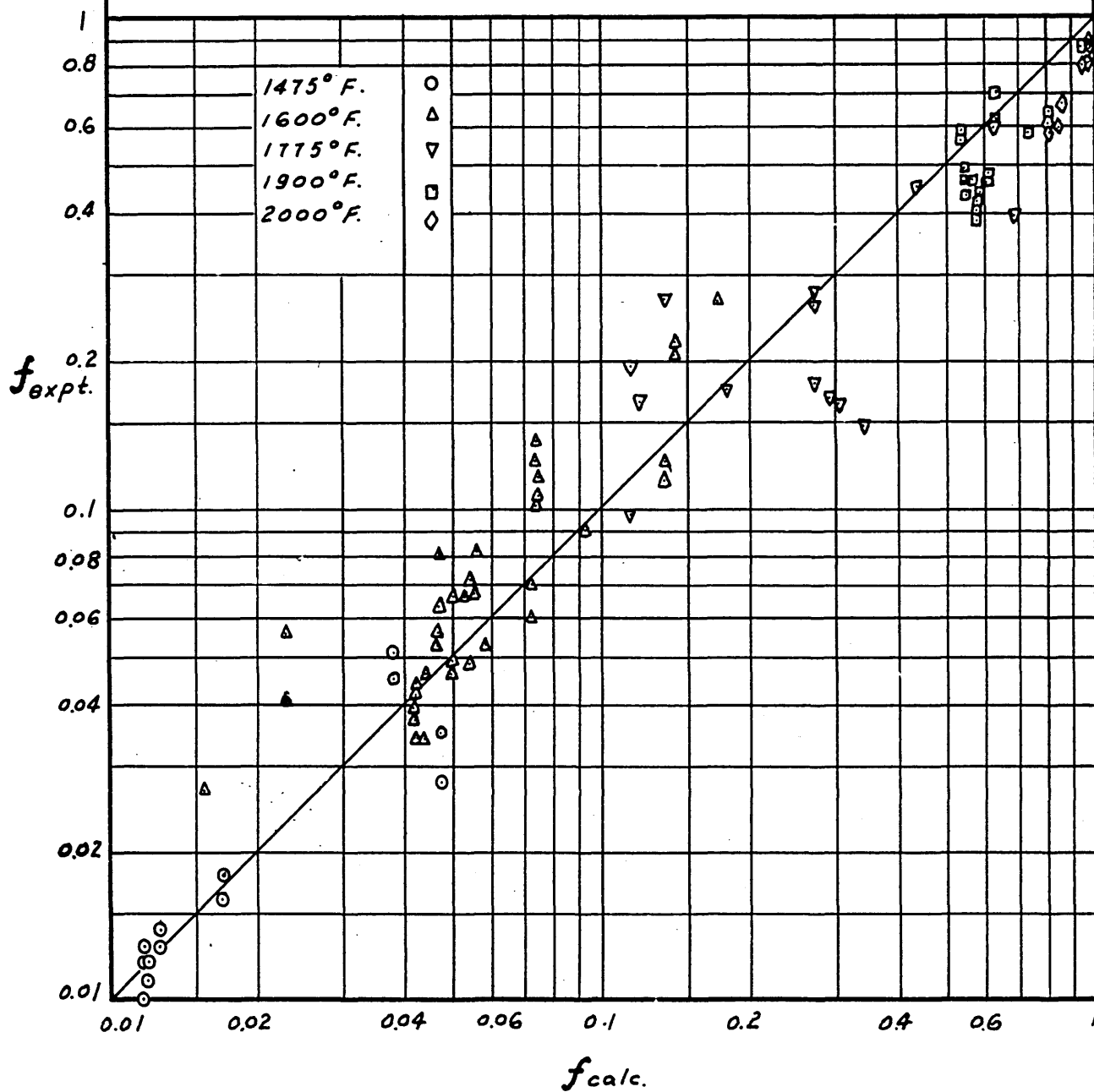


FIGURE (51)

PLOT OF $f_{\text{expt.}}$ [FROM McBRIDE'S DATA]
 VS. $f_{\text{calc.}}$ [BY MEANS OF RATE CONSTANTS
 FROM THE PRESENT WORK]



work. Nevertheless, the correlations using the constants from the present work can be said to be fair in view of the fact that the present work used an entirely different experimental technique.

The particle size used in McBride's work is 20-200 mesh, with an average value of 90 mesh, compared with 50-60 mesh in the present work. The particle size study at 1800°F. showed that a 90-mesh particle has a reactivity 1.5 times higher than one of 50-60 mesh. Granting this to be true for all cases, then in Figure 51, for most of the runs, the $f_{calc.}$ from the constants of the present work should shift to values 20% higher. By so doing, the points at 1775°F. or lower will be closer to the 45° line. A qualitative conclusion can be drawn that at temperatures up to 1775° F., the constants of the present work can be used to correlate the data from a fluidized bed, but at higher temperatures, the values of $f_{calc.}$ are always higher than the experimental values. This is possibly due to the assumption of "piston flow" being incorrect under these conditions.

It was observed by Göring under similar experimental conditions that the batch fluidized bed was characterized by bubblers of gas rising through the solid. The data of Mason (52) indicate that the mixing in a fluidized bed, due to the bubbling effect, is insufficient to eliminate partial pressure gradients at any given bed height. Göring obtained

a Langmuir equation correlation at 1600°F., but could not obtain a correlation at 1700° and 1800°F., when studying this reaction at high pressures. He stated that the Langmuir equation may be satisfactory, but the assumption of "piston flow" is vitiated at high conversions encountered at high temperatures.

Göring's explanation may well be applied in this connection indicating that the low $f_{\text{exp},t}$ at high temperatures as may be a consequence of low effectiveness of the fluidized bed at high temperatures where the conversions are high.

The results of Hinshelwood et al., using coconut charcoal, showed that the values of K_2 are high, indicating the severe retarding effect of CO. High values of K_2 were also obtained in the present work, but not by McBride. The reason for this is that in the fluidized system, a considerable amount of CO is always produced in the bed, which makes drawing exact conclusions from the overall results as to the true reaction mechanism very dubious.

An illustration of this point is given, using the data of McBride on his run U31 at 1600°F. The inlet gas being pure CO_2 , it was found that after passing through a bed with coke particles containing 0.206 lb. atom carbon, the CO_2 had reacted to the extent of 3.9%. Despite all the differences in the two experimental techniques and the assumptions made in evaluating the constants, the calculated fractional decomposition of CO_2 using the integrated Langmuir

equation and rate constants given first by McBride and then by the present work agree in both cases with the experimental results. But, if the progress of CO_2 decomposition is calculated as a function of the amount of carbon traversed by the gas, then the path of reaction is quite different, depending on whether McBride's or the present work's constants are used. This is demonstrated in Figure 52, which shows that the great retarding effect of CO shown clearly in this work may have been hidden in the study of the fluidized system.

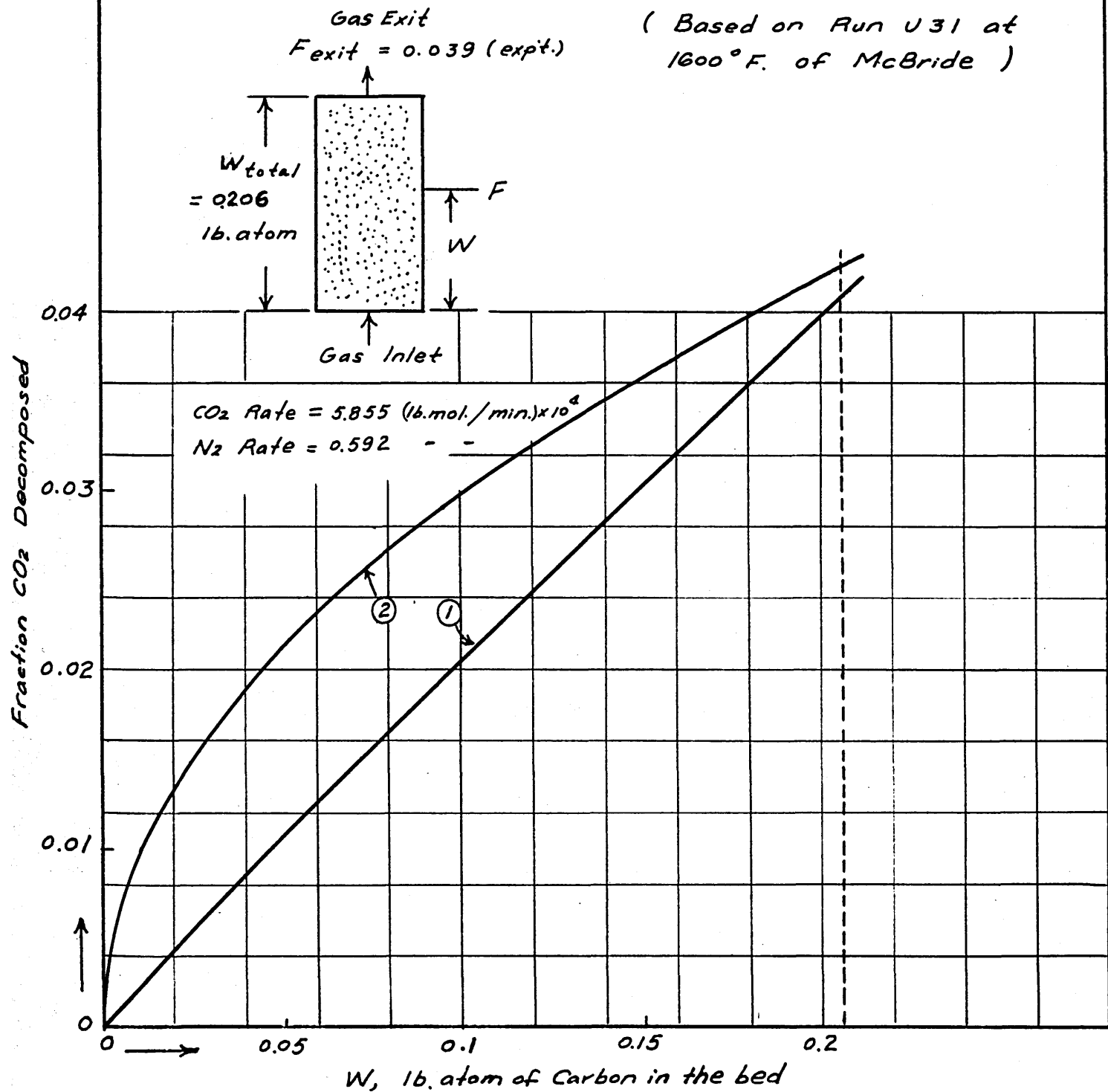
It is interesting to show the differences of the point reaction rates calculated using McBride's constants and the rates from the present work. To show this, Figure 53 was prepared in which two sets of curves are given. The curves for different $\text{CO}\%$, calculated from the Langmuir equation using McBride's constants, are closer to one another than the corresponding curves calculated using constants from the present work. This suggests that although McBride's constants may be used with fair success to interpret the overall results in a fluidized bed, yet they may fail to represent the point data and may be misleading in extrapolation to conditions not covered by experiment. The author believes the single-layer fixed bed to be a superior laboratory tool for elucidation of the reaction mechanism.

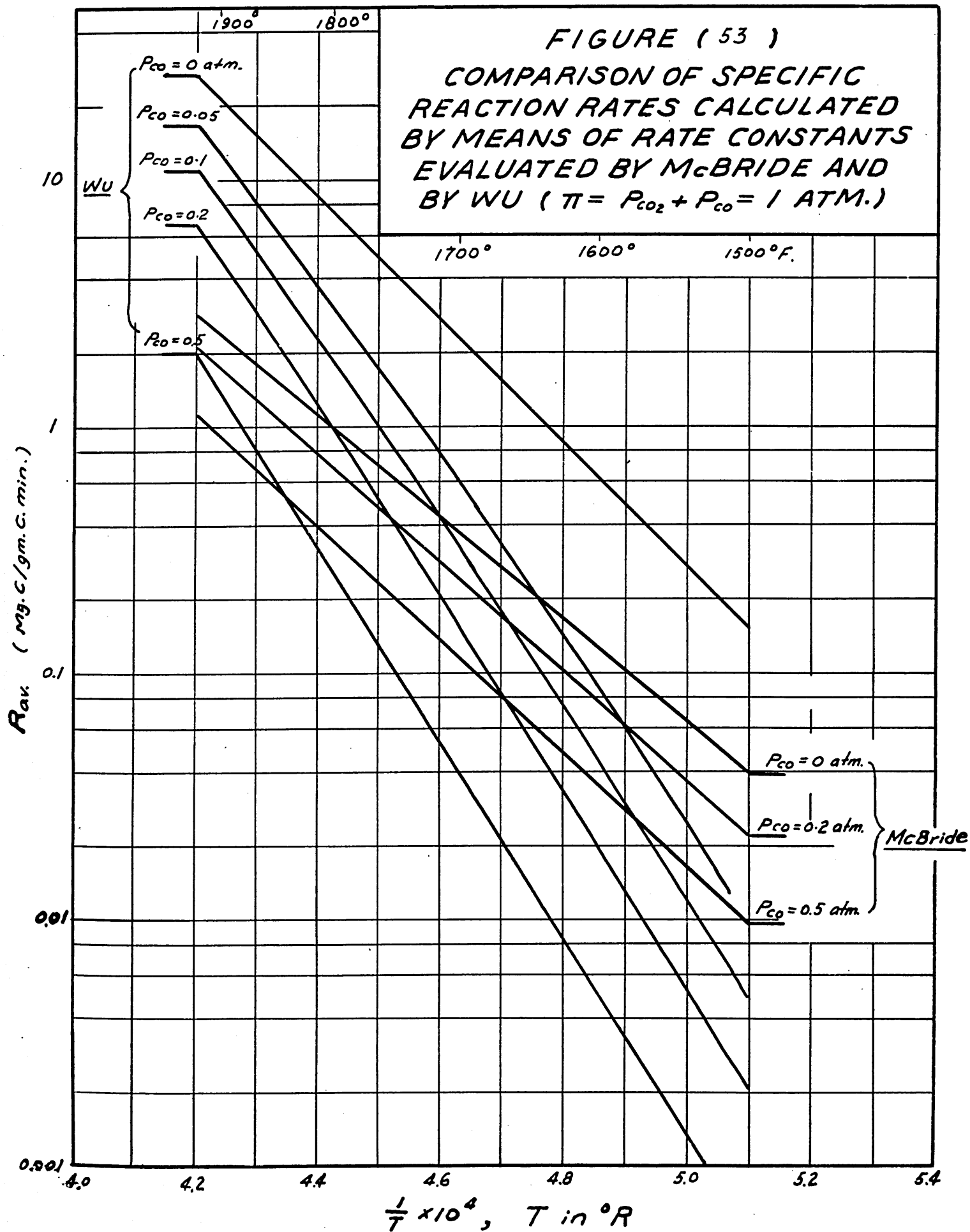
FIGURE (52)

FRACTION CO₂ DECOMPOSED VS. AMOUNT OF CARBON IN A FLUIDIZED BED

- ① Calculated based on integrated Langmuir equation using rate constants derived by McBride
- ② Calculated based on integrated Langmuir equation using rate constants evaluated in this present work

(Based on Run U 31 at 1600° F. of McBride)



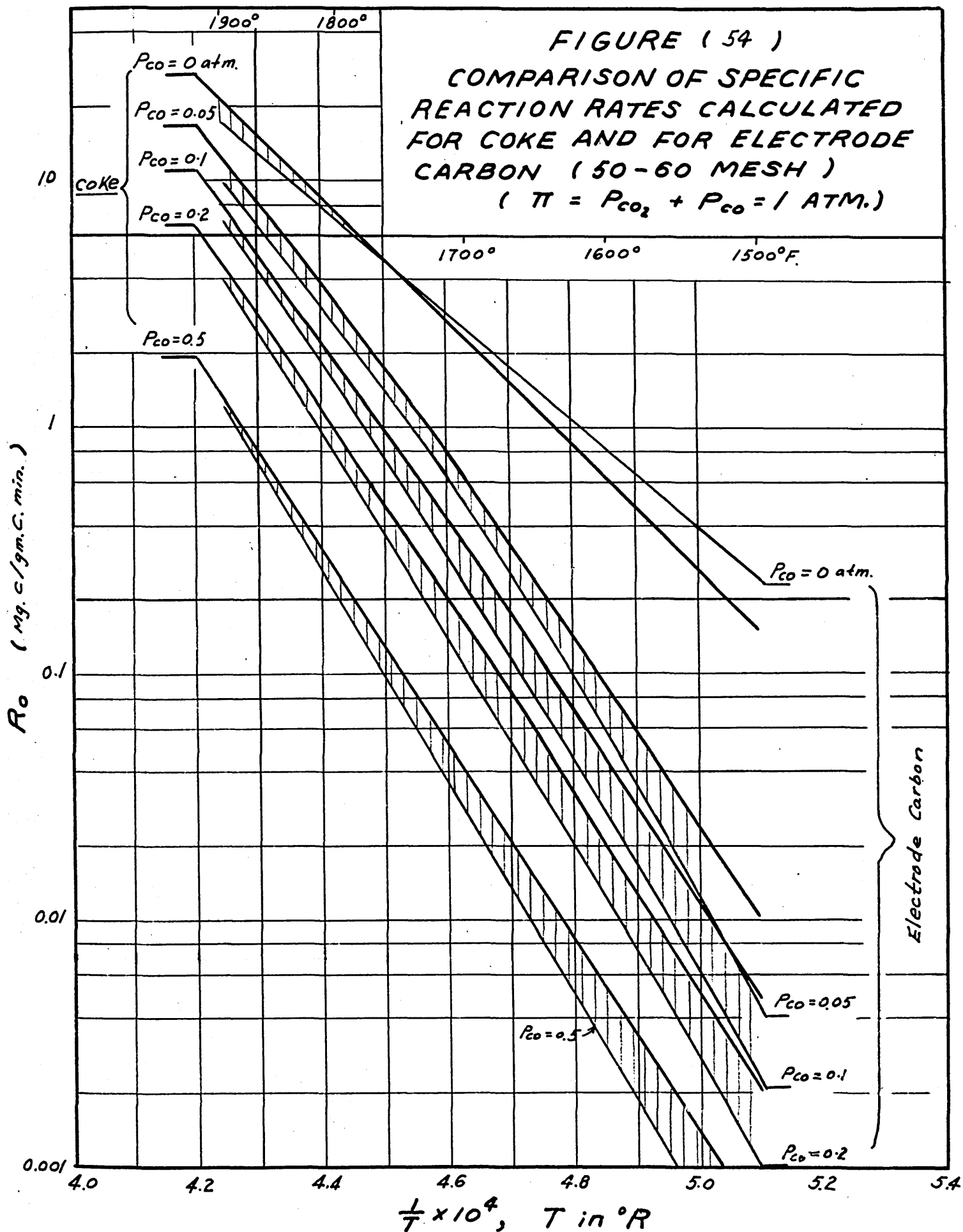


E. Comparison of the reactivity of coke with that of electrode carbon

The rate constants evaluated from the smoothed curves in Figures 35 and 47 for electrode carbon and for coke, respectively, are listed in Table 6. In Figure 54 two sets of curves for different CO% were calculated from the Langmuir equation using these smoothed rate constants for electrode carbon and for coke. It can be seen that in pure CO₂ the reactivity of electrode carbon at $F = 0$ is about the same as that of coke, but in CO₂-CO mixtures the reverse is generally true, due to the greater retarding effect of CO found in the case of electrode carbon.

Table 7 lists the energy values and basic constants required by equation (16), as evaluated by different authors. Except that obtained by McBride, the values of $E_1 - E_2$ evaluated by Hinshelwood et al. for coconut charcoal and obtained in this present work for coke and for electrode carbon are seen to be a constant of about 185,000 Btu./lb.mol. Although this cannot be explained on a theoretical basis, yet this may show eventually to be a basic property of carbon.

It is interesting to compare the value of the fictitious R_1 using coke particles of 50-60 mesh at 1800°F., with the value of R_1 found in the experiments using electrode carbon particles of the same size at the same temperature:



Coke:

$$R_{1(\text{fictitious, or ash-free})} = R_0 \left(1 + \frac{10(2 + \log_{10} D)F}{R_0} \right) = 5.1(1 + 3.05F) \quad (21b)$$

Electrode carbon:

$$R_1 = R_0(1 + 14F) = 6.705(1 + 14F) \quad (5c)$$

It is seen that the surface activation factor, m/R_0 , is about five times greater in the case of electrode carbon as in the case of coke. This difference may probably be attributed to the nature of the carbon structure, or its capacity to form active centers in the course of reaction.

TABLE 6 - Smoothed Langmuir Equation Constants

Constants	Reaction Temperature, °F.				
	1500	1600	1700	1800	1900
K_1 (mg.C/gm.C.min.atm.)					
Electrode carbon:	1.1	3.3	9.2	23	53
Coke:	0.234	0.90	3.18	10.2	29.0
K_2 (atm. ⁻¹)					
Electrode carbon:	4800	1200	370	113	40
Coke:	423	178.2	77.5	35.8	18.2
K_3 (atm. ⁻¹)					
Electrode carbon:	3.8	3.2	2.9	2.5	2.25
Coke:	0.505	0.449	0.388	0.35	0.32

TABLE 7 - Langmuir Equation Constants
from Different Authors

Author	Temp. Range Investigated, °F.	Carbon Sample	K_{10} mg.C/gm.C. min.atm.	E_1 Btu./lb. mol.	K_{20}^{-1} atm. ⁻¹	E_2 Btu./lb. mol.	K_{30}^{-1} atm. ⁻¹	E_3 Btu./lb. mol.
Hinshelwood et al.	1354-1524	Coconut shell charcoal (8-10 B.S.S.)	$10^{12.9}$	106,000	$10^{-7.9}$	-81,900	$10^{6.5}$	54,200
McBride	1475-2000	New England coke, 60-200 mesh	$10^{8.923}$	86,200	$10^{-1.94}$	-27,700	$10^{-0.586}$	-11,500
Wu	1500-1900	New England coke, 50-60 mesh	$10^{11.72}$	111,000	$10^{-5.44}$	-72,500	$10^{-1.52}$	-11,000
Wu	1600-1900	National Electrode Carbon, 50-60 mesh	$10^{10.086}$	90,100	$10^{-8.482}$	-109,000	$10^{-0.753}$	-11,920

Langmuir Equation:

$$\text{Rate} = \left(\begin{array}{l} \text{mg. Carbon reacted per} \\ \text{gm. of carbon in the} \\ \text{bed, per minute} \end{array} \right) = \frac{K_{10} e^{-E_1/RT} P_{CO_2}}{1 + K_{20} e^{-E_2/RT} P_{CO} + K_{30} e^{-E_3/RT} P_{CO_2}}$$

VII. CONCLUSIONS

From a study of the reaction of coke and electrode carbon particles in fixed-bed single layers with $\text{CO}_2\text{-N}_2$ and $\text{CO}_2\text{-CO}$ mixtures at 1500 to 1900°F. and atmospheric pressure, the following conclusions can be drawn:

(1) Over the range of temperatures and gas compositions investigated, the carbon-carbon dioxide reaction is controlled by chemical reaction, and not by a diffusional process.

(2) The reaction order with respect to the partial pressure of carbon dioxide approaches first order at low and zero order at high pressures of carbon dioxide.

(3) The retarding effect of carbon monoxide on the reaction is in general great. It is, however, much greater at low than at high temperatures.

(4) A Langmuir-type adsorption equation can be used to correlate the reaction rates with sufficient accuracy.

(5) The reactivity of electrode carbon in pure carbon dioxide is in general somewhat greater than that of coke, but the retarding effect of carbon monoxide is greater in the case of electrode carbon.

(6) Defining "effective" surface as a quantity to which the reaction rate is proportional in a heterogeneous system, the "effective" surface of electrode carbon per unit of mass is a unique and linear function of the fraction of carbon consumed, and is independent of temperature and gas

composition. The relation applies over the range of fraction carbon consumption of 0 to 0.3, over which range there is a five-fold increase in rate per unit mass of residual carbon. Whether the increase in "effective" surface is due to activation of existing surface or production of increased surface by burning in pores is not known.

(7) In the experiments using coke, the instantaneous reaction rate increases steadily during the course of the reaction, reaches a maximum and then declines. The maximum occurs at larger fractional consumption for smaller particles. These phenomena are consistent with the assumption of increase in "effective" surface (as in the case of electrode carbon) on which is superimposed an accumulation of ash which builds up a resistant layer tending to retard further reaction.

(8) The reaction rate of coke per unit mass decreases with increase in particle size, but the rate per unit superficial surface area (area of a sphere having mesh size of the particle) is not greatly influenced by particle size. However, the rate per unit of surface is slightly higher for large particles, indicating that in addition to the superficial area, the surface area of the large pores contributes to the reaction.

(9) The numerical constants of the Langmuir-form of rate equation applicable to the present data are

quite different from those obtained by McBride on the same coke using a method of comparing the integrated rate equation with the overall performance of a fluidized bed. When the rate equation is integrated over the carbon bed to predict change in gas composition in McBride's experiments, predictions based on the two sets of constants are found to be in fair agreement; but the paths predicted are markedly different. This suggests that the constants obtained from experiments on one fluidized bed may be unsafe for use in predicting performance of another.

VIII. RECOMMENDATIONS

The reaction rate determined in the present work represents that of a slice of carbon in a fixed or a fluidized bed. Fair agreement was obtained using the numerical constants of the Langmuir-form of rate equation applicable to the present data to predict the change in gas composition in McBride's experiments using a fluidized bed on the same coke. This suggests that results of the type obtained in the present work are of fundamental significance for the rigorous design of fluidized beds. For this purpose it is recommended that the following work be carried out:

(1) Experiments using fluidized beds of different sizes, operating under various entering gas compositions and various amounts of carbon in the bed;

(2) Experiments to study the gas flow pattern in fluidized beds, in order to obtain information on the assumptions being made in the integration of the Langmuir form of rate equation.

It is also recommended that in addition to the coke and electrode carbon used, various types of carbons be tested under similar reaction conditions, in order to compare the behavior of different types of carbons.

The change in reactivity of carbon accompanying progress of reaction is of so much greater significance than

anticipated as to make desirable a modification of apparatus which will make it possible to follow this change more effectively than the present apparatus permits. In addition, the equipment should be designed for use at high pressures. It is recommended that a continuous weighing equipment, either of the type developed by Oshima and Fukuda, or a setup using electric resistance strain gauges, be considered. An alternative is the use of a high precision gas analyzer. In this respect, the feasibility of using radioactive C_{14} or mass spectrometer might be investigated.

Also, photomicrographs and surface area measurements of the carbon particles used might be helpful means in further investigations.

APPENDIX

A. Details on Construction of Equipment

This equipment was used soon after it had been constructed by Blanc in his study of the effect of particle size on the $\text{CO}_2\text{-C}$ reaction. After Blanc's work, a number of modifications was made on the equipment. For those parts of the equipment which were still as originally constructed, the description as given by Blanc was used.

1. Furnace

The furnace used consisted of eight fire bricks put together and shaped so as to form a combustion area of the required form. Figure A1 is a sketch showing the cross section of the furnace.

To keep the bricks in the right position, a steel box was made into which the bricks fitted properly (see Figure A2).

The inside dimensions of the steel box were $8\text{-}\frac{7}{8}\text{"}$ x $8\text{-}\frac{7}{8}\text{"}$ x $12\text{-}\frac{1}{4}\text{"}$. It was constructed of $\frac{1}{8}\text{"}$ steel plate arc welded at all the seams with the exception of the front face which was supplied with a 1" flange around the four edges. This flange was drilled with equally spaced $\frac{1}{4}\text{"}$ holes to accommodate the bolts which were used to fasten the $\frac{1}{8}\text{"}$ steel cover in place after the bricks had been fitted into the furnace box. In the center of this front cover had been cut a horizontal slot $3\text{-}\frac{3}{4}\text{"}$ wide and $\frac{1}{2}\text{"}$ high, through which the nichrome pan with sample pan supporter supported on the alundum rods could be moved in. When the nichrome pan was in the required position in the

FIGURE (A I)
CROSS SECTION OF FURNACE

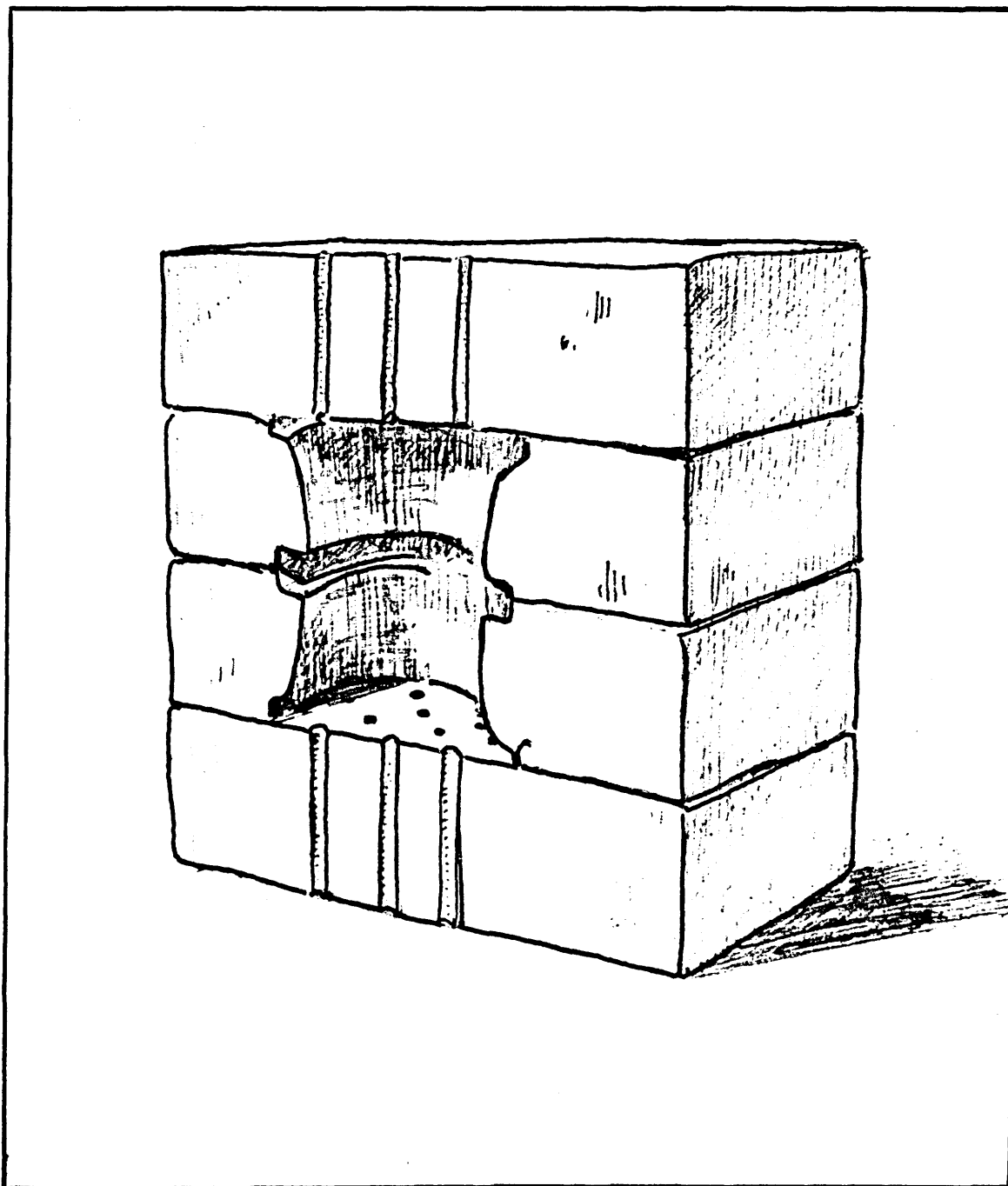


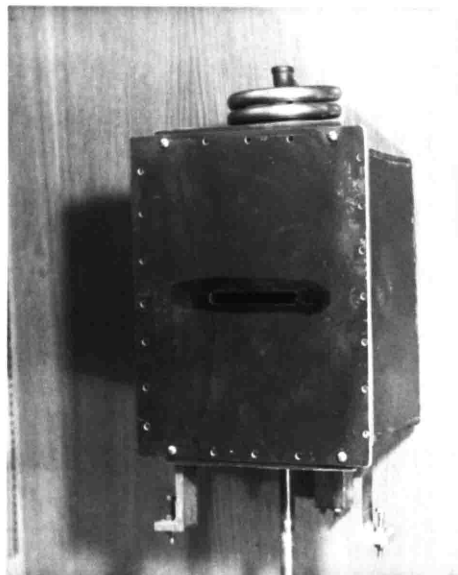


Figure A2

Photographs of Steel Box

(a) Steel Box without
Front Cover

(b) Steel Box with
Front Cover



combustion chamber, the slot was tightly sealed by the flat surface of a piece of insulation brick which was attached to the metal yoke into which the ends of the alundum rods were cemented.

The steel furnace box was equipped with three 4" legs the height of each of which was adjustable by means of bolts to maintain the box in a horizontal position after it had been placed inside of the cylindrical furnace container, and to insure that the slot in the front cover was at the proper height to allow the nichrome pan to be inserted into the combustion chamber.

The gas mixture entered the steel box through a 3/8" pipe fitted into the center of the base of the box, and after passing through the combustion chamber, left the top of the box through a 5-1/4" diameter coil of 3/8" steel tubing consisting of three turns which was connected to the box by means of a 3/8" 90° elbow, that was welded in the center of the top of the steel box. The purpose of this coil of steel tubing was to provide some degree of flexibility, so that after the steel box had been placed inside of the cylindrical furnace container, the cover of the container could be turned into the threaded pipe that was connected to the end of the coiled steel tubing by a 3/8" 90° elbow, without moving the furnace box out of position. When the top of the cylindrical container was turned on tightly, the steel coil was compressed slightly so that the furnace box was held rigidly in place inside of the

container.

There were six holes in the rear face of the furnace box. Two of these holes were for the lead wires to the two thermocouples, one of which was directly above, and the other directly below the nichrome pan in the combustion area. The other four holes were for the ends of the two heating elements.

On opposite sides of the floor of the steel box were placed two U-shaped steel braces 1" high. On top of these supports rested a 8-7/8" x 8-7/8" plate of 1/16" steel. This plate was drilled with twenty-five 3/16" holes in a symmetrical pattern. On top of this steel plate were placed two 8-3/4" x 4-1/4" x 2-1/2" bricks side by side that were also drilled with twenty-five 3/16" holes that coincided with those in the bottom steel plate. On top of these two bricks were placed two more that had been carved out to accommodate the lower heating unit, and a slideway for the nichrome pan supporter.

On top of this layer of two bricks were two more carved exactly as were the two described above.

The top layer of two bricks was drilled with twenty-five 3/16" holes just as was the bottom layer to provide an exit for the product gases.

On top of these two bricks is a 8-7/8" x 8-7/8" x 1/16" steel plate exactly the same as the bottom plate described above.

Into the 1" space which is left between this steel plate and the top of the steel box were fitted two 1" U-

shaped sheet steel braces that held all the bricks firmly in place.

2. Nichrome screen pan and sample pan supporter

The nichrome screen pan and sample pan supporter used to hold the carbon particles were made of 100 mesh nichrome screen (see Figures 4 to 8).

The screen of the pan supporter was tightly pressed between two concentric rings made of $3/16$ " x 0.064 " Chromel-A ribbon. The outside diameter of the larger ring was $3-3/16$ ", the inside diameter of the smaller one, $2-15/16$ ".

The outer ring was provided with two diametrically opposed supports which were turned in a tube form from Chromel-A ribbon so as to fit snugly around the two alundum rods upon which the pan was moved into and out of the furnace.

There were three different types of screen pans used in the experiments, as shown in Figures 4, 6 and 7. All the screen pans had an upturned edge to make handling the screen with carbon particles somewhat more convenient.

3. Flexure tube and yoke arrangement

The flexure tube and yoke arrangement was designed in the following manner in order to provide a simple, smoothly operating mechanism for inserting the nichrome screen pan and sample pan supporter with their carbon contents into the combustion area of the furnace, and for withdrawing it after the reaction between the carbon dioxide and the carbon particles has taken place.

The necessity of having a completely airtight

unit dictated this particular type of construction after it was demonstrated that the forward and backward motion of a smooth steel rod $3/8$ " in diameter through an airtight stuffing box was rendered so jerky that the carbon particles on the screen was caused to be moved or even lost.

To the steel face plate of the side arm of the cylindrical furnace container was welded a 3" square semi-flexible $1/16$ " brass sheet. A $1-1/4$ " hole was drilled through the brass sheet and a $1-1/2$ " hole through the $1/8$ " steel face plate. Into this hole was inserted a 39" length of $1-1/4$ " outside diameter brass tubing which was already equipped with the internal sliding mechanism. The brass tubing was welded securely to the brass sheet at a distance of one inch from one end. The other end of the brass tubing was plugged with a brass disc welded in place to render the entire unit airtight.

Because of the flexibility of the brass plate, the end of the brass tubing farthest from the furnace could be raised or lowered through an arc of approximately 1° without danger of rupturing the weld at the junction of the brass plate and the brass tubing, or causing permanent distortion of the brass plate.

In order to be able to regulate the raising and lowering of the end of the brass tubing precisely, a brass band was clamped tightly around the tubing and the lower portion of this band bolted to a knurled hand screw, each complete revolution of which raised or lowered the end of

the brass tubing $1/28$ of an inch. This screw attachment was securely held in place by a steel yoke which was welded to the steel beam extension from the side of the cylindrical furnace container.

In order that the brass tubing would normally rest in a horizontal position to facilitate the smooth sliding of the nichrome screen pan, a second iron yoke was welded to the steel extension beam directly behind the first adjustable support. The lower cross piece of this yoke which could be adjusted by turning the four set nuts up or down was raised to the proper level for supporting the brass flexure tube in a horizontal position. The upper horizontal cross bar served as a stop or upper limit for the motion of the end of the brass tube.

4. Cylindrical furnace container

The cylindrical furnace container was ordered from the A. F. Robinson Boiler Works of Cambridge, Mass. The shell of the container was constructed entirely out of $1/8$ " steel plate arc welded both inside and out at all the joints.

The main portion of the container was 15" inside diameter and 2' high. To the top edge of the cylinder was welded a $1-1/2$ " wide flange of $3/8$ " steel plate. Sixteen $1/2$ " drilled holes were equally spaced around this flange to accommodate the bolts for holding the circular $3/8$ " steel plate cover tightly in place. Between the top surface of the flange and the container cover was a circular rubber gasket made of $1/4$ " diameter rubber obtained from the White-

head Metal Products Co., of Cambridge, Mass. This gasket was used to provide an airtight junction between the cylinder and the cover so that the apparatus could be evacuated.

In the center of the top of the cylinder cover was drilled a 1/2" hole over which was brazed a reducing coupling to provide an exit port for the product gases.

To the side of the cylindrical shell midway between the top and the bottom was welded a side arm of 5" inside diameter, 12" long. To the end of this side arm was welded a flange of 1/4" steel 1" wide. This flange was drilled with eight equally spaced 1/4" holes to accommodate the bolts used to fasten the 1/4" steel face plate securely in place. Between the surface of the flange and the face plate was another rubber gasket 1/8" thick and cut to a width of 1-1/4". In the center of this face plate was welded a 3" square of semi-flexible brass sheet. Through the center of both the face plate and the brass sheet holes were drilled to accommodate the 1-1/4" flexure tube.

At a distance of one inch from the side of the cylindrical steel container the top of the side arm was cut out to accommodate another 5" inside diameter 2" high steel sleeve which was welded to the edges of the opening in a vertical position. To the top of this sleeve was welded a 1" wide x 1/4" thick flange, the top of which had been ground to provide a smooth surface upon which a 7" diameter x 1/2" thick Lucite plastic disc, serving as cover, was

clamped down. Between the flange and the Lucite disc was a circular rubber gasket, similar to the one used for the container cover. The device used to clamp down the Lucite disc, consisted of a 7" square x 1/4" thick flange, provided with a 5" diameter hole in the center. In the four corners of the flange were holes which accommodated four 1/4" bolts. The flange was put over the Lucite disc and pressed upon its surface by tightening the four bolts. These bolts were kept in position by two 1/4" thick steel straps, resting upon the lower surface of the flange welded to the sleeve.

The Lucite disc was removed at the end of each run, and was used as an observation post for watching the entry into and the withdrawal from the combustion area of the nichrome pan.

Through the 5" diameter sleeve opening the nichrome screen with its supporter was in each run put on and taken off the alundum supporting rods.

On a level with the center of this side arm in the side of the cylindrical shell was drilled a 1-1/2" hole into which was welded a 1-1/4" threaded fitting at the proper angle to provide an observation post for observing the entry and withdrawal of the nichrome pan into and from the combustion area. To render this apparatus airtight a hexagonal brass fitting with a plate glass face fitted between two rubber gaskets was screwed into this opening.

From the side of the cylindrical container 1-3/4"

directly below the side arm extended a U-shaped steel beam 51" long. It was attached to the container by two spot welds. At a distance of eight inches from the container it was welded securely to a yoke which supported a 1/16" thick 2-3/4" wide steel band which circled the side arm and was bolted securely in place on either side by two 1/4" bolts.

The cylindrical container was provided with three legs located at intervals of 120° around its lower circumference. The three legs were equipped with 5/8" bolts that could be adjusted to the desired height to maintain the cylindrical container in a horizontal position.

In the side of the cylindrical container directly opposite the extending side arm were three 1/2" holes into which were brazed three special 1-1/2" long brass nipples. Two of these nipples were made from a solid brass rod, and were provided with 1 mm. diameter holes drilled parallel to the body centerline of the rod. Through these holes the enameled thermocouple leads were led, and vacuum-proof insulated in place by means of Cenco Sealstix vacuum cement.

The third nipple was made of a 1/2" diameter brass tube, into the open end of which was fixed by means of Cenco Sealstix vacuum cement, a pear-shaped glass bulb, serving as insulator for four copper wires embedded in the glass. Two of these copper wires carried the current for the heating coils, the other two led to a 60-watt bulb located inside the cylindrical shell directly over the front of the furnace, to illuminate the interior of the container. Inside the container the copper wires were prevented from

touching any conducting surface by 1" lengths of double-holed alundum insulators.

The port for evacuating the system, and to which port also the McLeod gauge was connected, was located midway between the top and bottom of the container 90° distant from both the thermocouple ports and the 5" diameter side arm. This port was a 3/8" tube tee-welded into a slightly larger hole drilled in the side of the cylindrical container.

The gas mixture entered the bottom of the cylindrical container through a centrally located 1/4" diameter piece of pipe, brazed into the bottom, and protruding 3" on both sides of the bottom.

5. Calcium chloride drying tower

In order to remove the water vapor present in the gas stream (about 0.07%), the gas from the pressure cylinder, after passing through the 1/8" needle valve and rotameter was passed through a standard 4.5 cm. diameter x 30 cm. high glass drying tower, which was filled with calcium chloride pellets on top of which a 1" thick layer of Drierite had been put to serve as an indicator, in case any moisture slipped through the column of calcium chloride.

6. Oxygen removal apparatus

After flowing through the drying tower, the gas entered the top of the oxygen removal apparatus. This apparatus was constructed from 5.0 cm. diameter heavy walled Pyrex tube, 80 cm. high, and provided at both ends with 15 mm. diameter x 90 mm. long Pyrex tubing, to enable the slip-

ping on of rubber tubing. The apparatus was filled with a 3" layer of copper turnings, on top of which was poured seven pounds of chemically pure cupric oxide rods. This cupric oxide was reduced by means of hydrogen, re-oxidized with air, and again reduced with hydrogen, which rendered the copper more reactive with respect to oxygen. This treatment was originally used by Clifford (53) and Mullery, and was later improved by Smith. The height of the copper rod fillings was about two feet. On top of the copper rods was another layer of about 3" copper turnings.

The oxygen removal apparatus was heated by means of two heating coils wound around the outside of the Pyrex tube. Each coil extended over half the height of the tube, and got its power supplied from a Variac, Type 200-C, which was connected to the 115-volt power supply line.

To measure the temperature of the apparatus, two thermometers were located on the outside surface of the Pyrex tube, respectively at 1/4 and 3/4 of the height of the tube.

The Pyrex tube and thermometers were insulated by means of 1" Magnesia pipe insulation.

7. Temperature controller

A full description of the temperature controller used to maintain the required temperature in the reaction area was given by Port and Egbert, who designed and built the controller. A brief description is given under "Construction of Equipment".

8 Cooling coil

A cooling coil was constructed from copper tubing in the following manner: Two lengths of 1/2" copper tubing long enough to circle approximately one-third of the outside perimeter of the cylindrical furnace container were bent into shape and drilled with twenty-nine 1/4" holes equally spaced at 1/2" intervals. Into these holes were silver-soldered the ends of twenty-nine 19" lengths of 1/4" copper tubing, This unit was then attached to the outside of the cylindrical furnace container so that the straight copper tubes were in a vertical position by means of silver solder, and was also braced with a 3/4" band of stainless steel which circled the cylindrical container and was fastened with a metal buckle.

One end of the upper 1/2" copper tubing and the opposite end of the lower 1/2" tubing were closed with rubber stoppers. The other end of the bottom tubing was connected by rubber tubing to the tap and water was allowed to circulate through the tubes of the unit. The water left the coil through the end opening in the upper copper tube and flowed through a length of rubber tubing to a sink.

By allowing cold water to flow continuously through the tubes during the time the furnace was heated, a more comfortable situation was created for the operator, sitting next to the equipment.

9. Cenco Megavac vacuum pump

The vacuum pump used was a Cenco Megavac pump manufactured by the Central Scientific Company, Chicago, Ill.

B. Description and Calibration of Measuring Devices

1. Rotameter (Flowrator)

The meter used to measure the gas flow through the equipment was a conventional rotameter obtained from the Fischer and Porter Company, Hatboro, Pa., which rotameters are presently known under the name of Flowrators. It was the so-called Laboratory Type 03-B-150 with millimeter scale and hose connections. The float used was type FG 031. Calibration curves for CO₂, CO and N₂ were obtained by means of a wet test gas meter and are shown in Figure A3.

2. McLeod Gauge

During the evacuation period, the pressure in the equipment, when still above 2 mm. Hg., was measured by means of a U-tube filled with mercury. Below 2 mm. Hg. the pressure was determined by means of a conventional McLeod gauge.

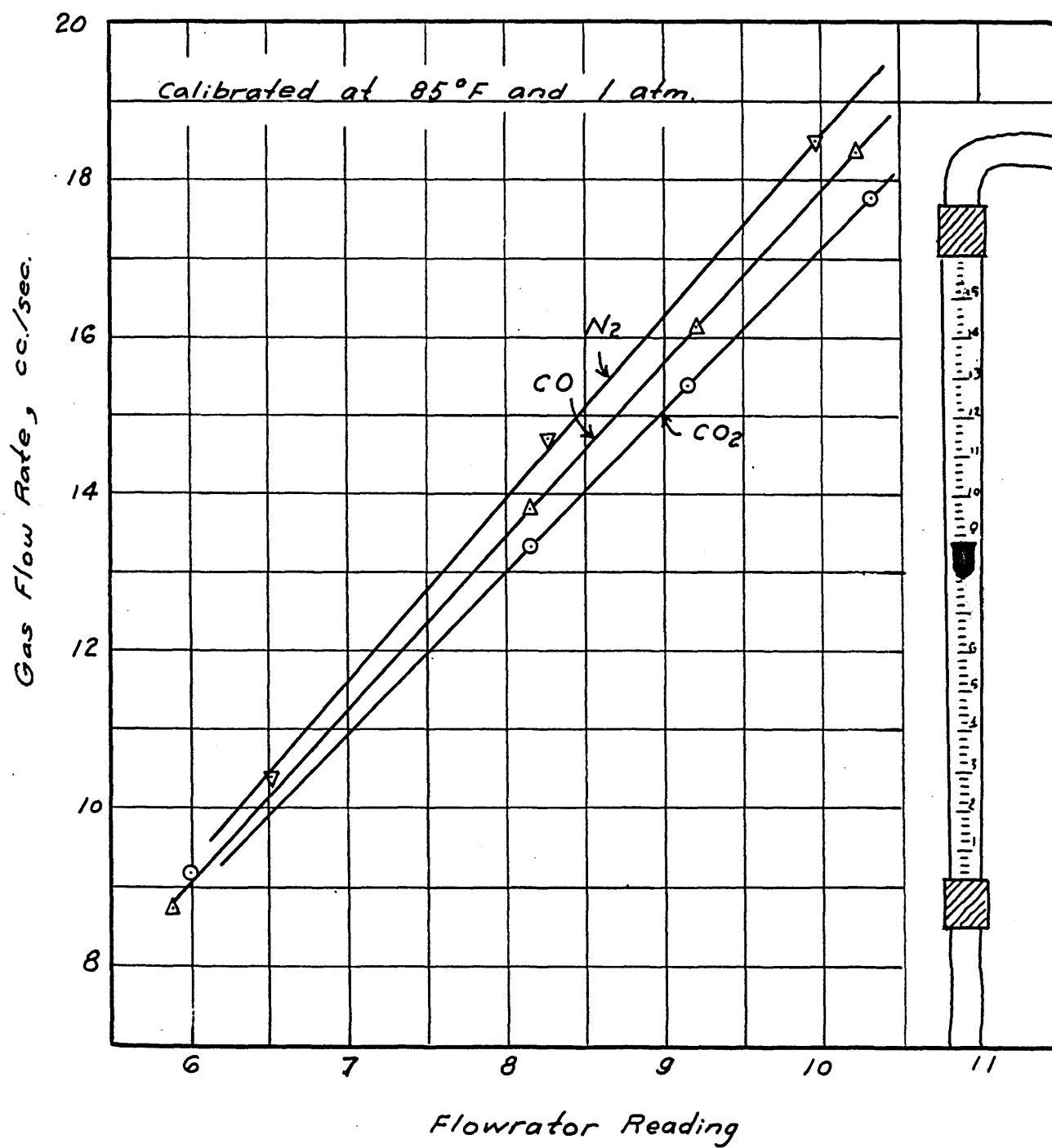
3. Potentiometer

The temperature in the reaction area was determined by readings from a potentiometer manufactured by the Brown Instrument Company, Philadelphia, Pa. The accuracy of this potentiometer was 1/50 of a millivolt.

4. Wet test gas meter

During the velocity runs, the higher gas flow rates applied were beyond the maximum capacity of the Flowrator. For these runs a wet test gas meter was installed at the outlet of the equipment, which enabled measuring the gas flow rate through the reaction area.

FIGURE (A3)
FLOWRATOR CALIBRATION



The wet test gas meter was manufactured by the Precision Scientific Company, Chicago, Ill.

5. Ammeters

Two A.C. ammeters were used, one of which was installed permanently in the furnace heating coil circuit. The other one was used to check periodically the current through the two oxygen removal apparatus heating coils. By means of a switch this ammeter could be put into either of the two circuits. The maximum capacity of both ammeters was 15 ampères.

6. Micro oxygen analyzer

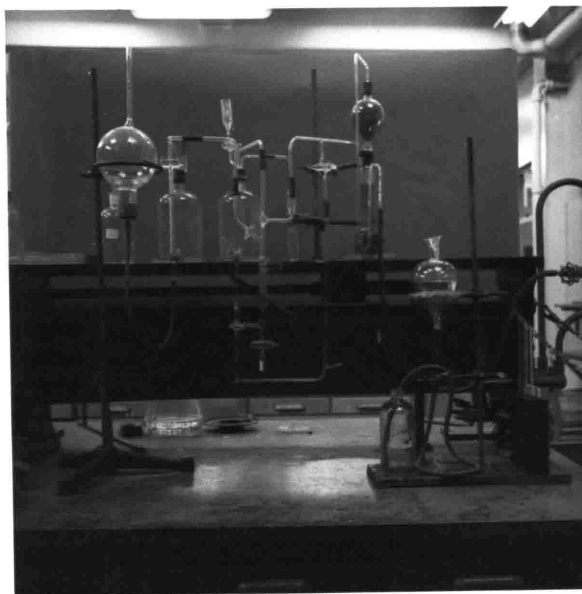
The micro oxygen analyzer used was constructed by R. J. Kallal, according to methods described in references (48) and (49). The accuracy obtainable with this analyzer amounted to a few parts per million. A picture of this equipment is shown in Figure A4.

7. Thermocouples

The two thermocouples used (one above, the other below the sample pan) were number 16 Chromel-Alumel wire, and were obtained from the Hoskins Manufacturing Company, Detroit, Mich. The thermocouples were calibrated with the aid of a standard Pt - Pt+13% Rh thermocouple in a special furnace, and showed over the temperature range of this investigation a constant positive deviation of 10 to 15° F. After installing the thermocouple in the reaction area, occasional check measurements were made by means of a new calibrated thermocouple which was inserted through the

Figure A4

Photograph of Oxygen Analyzer



slot opening in the furnace. After inserting this thermocouple, the opening was carefully insulated to prevent any heat loss. It was thus found that the originally measured positive deviation of 10 to 15° F. was maintained throughout all the experiments. As far as the deviation showed to be consistent, no correction was applied to the reaction temperature, as a 10 to 15° F. difference in the true values of the temperature was not considered to be important.

8. Balance

The balance used for weighing the sample pan and carbon particles was a standard analytical balance, manufactured by Voland and Sons, New Rochelle, N.Y., scaled to 1/10 of a milligram. The balance used for weighing the large coke particles was an assay balance which was scaled to 1/50 of a milligram.

C. Details on Materials Used

1. Carbon

Both coke and electrode carbon were used in the experiments. The coke used was from the New England Coke Company. The coke sample was crushed and graded by standard sieves and then heated in an oven at 110° C. overnight to remove moisture before use. The large spheres used were made from the coke by cutting a large piece carefully to the proper size. The proximate analysis of the coke as given by the Company was as follows:

Fixed carbon	92.5%
Volatile matter	0.9%
Ash	6.6%
Sulfur	0.65%
Moisture	2.6%
Initial fusion point, °F.	2165
Fusion point, °F.	2579
Flowing temperature, °F.	2732

From actual analysis, it was found that the ash content was 9.5%, and this figure was used throughout this work.

The electrode carbon was obtained from the National Carbon Company and was from the same lot as used by Smith et al. The carbon was crushed from the original 12" rod and sieved, and the fraction 50-60 mesh retained. To remove the moisture, the particles were heated at 110° C. overnight in an oven. After this the carbon was coked for 2 hours at 1800° F. in a vacuum of 0.4 mm. Hg. Mungen analyzed the carbon for ash, and determined the density of the carbon.

He reported:

Ash	0.4% by weight
Density	1.77 (average)

All the particles were stored in glass bottles with ground stopper, which bottle was kept in a desiccator. Only when preparing a sample for an experiment was the bottle taken out of the desiccator, and immediately put back into the desiccator after pouring the carbon particles on the screen.

2. Carbon dioxide

The carbon dioxide used was the purest available and was obtained from the Pure Carbonic, Inc., New York, N.Y. The analysis given by this Company was as follows:

CO ₂	99.50%
N ₂	0.342%
O ₂	0.086%
H ₂ O	0.072%

These figures agree with the check analyses, which were made before mixing up gases, as far as oxygen, carbon dioxide and nitrogen were concerned.

3. Carbon monoxide

The carbon monoxide used was obtained from the Matheson Company, Inc., East Rutherford, N.J. A recent analysis of half a dozen cylinders by the Company showed the following results:

CO	96.8%
CO ₂	0.36%
H ₂	0.97%
N ₂	1.0%
Saturated H.C.	0.8%
Fe	1.19 mg./liter
S	0.3202 mg./liter

4. Nitrogen

The nitrogen used was prepurified nitrogen obtained from the Air Reduction Sales Company, the specifi-

cations of which, as given by this Company were:

O ₂	< 0.001%
H ₂	< 0.001%
H ₂ O	0.000%

5. Cupric oxide

The cupric oxide used was chemically pure cupric oxide in wire form, and was purchased from the C. P. Baker Company.

6. Calcium chloride

Chemically pure calcium chloride was purchased from the Mallinckrodt Chemical Works. It was anhydrous, 8 mesh, containing not less than 96% calcium chloride.

7. Drierite

This indicating desiccant (8 mesh, anhydrous CaCO₄) was purchased from the W. A. Hammond Drierite Company, Xenia, Ohio.

8. Bricks and cement

The insulating fire bricks used in the furnace were manufactured by the Babcock and Wilcox Company, under the trade name of K-16 and had the lowest thermal conductivity and density of the available fire bricks.

The brick was very soft and porous and could easily be machined, cut and filed.

The cement used for coating the exposed surface of the brick was the 513A high temperature cement from the Norton Comapny, Mass.

9 . Chromel-A ribbon

The chromel-A ribbon used for making the frame

of the sample pan supporter was purchased from the Hoskins Manufacturing Company of Detroit. The size of this ribbon was $3/16$ " x 0.064 ".

10. Nichrome screen and nickel screen

The nichrome screen used was purchased from the Newark Wire Cloth Company, and was 100 mesh of 0.0031 " wire diameter.

The nickel screen used was purchased from the W. S. Tyler Company of Cleveland, Ohio. The screen was 200 mesh.

11. Alundum rods

The alundum rods used in the yoke arrangement were of the type generally used as thermocouple ceramic tubes. The size of this tube was $1/8$ " outside diameter, and $1/16$ " inside diameter.

The advantage of this tube was that it did not soften or lose its inert character at high temperatures.

12. Heating wires

The heating wire used in the furnace was Kanthal ribbon 0.197 " x 0.02 " with a specific resistance of 0.176 ohms per foot, and was purchased from the C. O. Jelliff Manufacturing Corporation.

Chromel-A ribbon of $1/16$ " x 0.0126 " with a specific resistance of 0.689 ohms per foot from the same Company was used as heating wire for the oxygen removal apparatus.

13. Thermocouple wires

The thermocouple wires used in the furnace were number 16 Chromel-Alumel wire.

14. Insulation for oxygen removal apparatus

Standard 1" magnesia pipe covering was used for thermal insulation of this apparatus.

15. Cenco-Sealstix vacuum cement

Cenco-Sealstix vacuum cement showed to be an excellent vacuum cement and insulator. It joins all kinds of dissimilar materials, and was successfully applied to obtain vacuum proof joints between glass and brass, enameled thermocouple wires and brass, etc. It was obtained from the Central Scientific Company, Chicago.

D. DATA SHEETS

TABLE (A1) DATA SHEET NO. ()

LIST OF GAS MIXTURES

GAS SYMBOL	% CO ₂	% CO	% N ₂
N ₂	00.00	0	100.00
N.A	82.50	0	17.50
N.B	69.20	0	30.80
N.C	55.60	0	44.40
N.D	32.10	0	67.90
N.E	79.30	0	20.70
N.F	69.90	0	30.10
N.G	54.90	0	45.10
N.H	41.60	0	58.40
N.I	9.94	0	90.06
N.J	21.80	0	78.20
CO ₂	99.45	0	0.55
CO.A	90.79	8.71	0.50
CO.B	85.82-80.62	13.7-18.9	0.48
CO.C	83.84	15.70	0.46
CO.D	75.78	23.80	0.42
CO.E	75.38	24.20	0.42
CO.F	61.66	38.00	0.34
CO.G	94.76	4.72	0.52
CO.H	94.95	4.53	0.52
CO.I	96.97	2.50	0.53
CO.J	92.85	6.64	0.51
CO.K	85.63	13.90	0.47
CO.L	98.54	0.92	0.54
CO.M	91.34	8.20	0.46

TABLE (A 2) DATA SHEET NO. ()
 N₂ BLANK RUNS (NEW ENGLAND COKE)

CARBON SAMPLE	New England Coke	COKING TEMPERATURE	1500° - 1900° F
ASH CONTENT	9.5 % by weight	COKING PRESSURE	1.026 atm.
PARTICLE SIZE	50-60 US mesh	COKING TIME	10 - 610 min.
GAS COMPOSITION	100% N ₂	GAS FLOW RATE	15 cc./sec. (85° F and 1 atm.)

Run No. CK-N-15.50.1 designates run No. 1 at 1500° F using pure N₂ and 50-60 mesh New England coke particles

Ø	Coking time, min.	ΔW	Loss of weight of sample during coking period, mg.
W _o	Weight of sample, gm.	F _{N2}	Fraction carbon weight loss in N ₂
0.905W _o	Weight of carbon in sample, gm.		

TEMP.	RUN NO.	Ø	W _o	0.905W _o	ΔW	F _{N2}
1500	CK-N-15.50.1	610	0.2395	0.2167	1.9	0.00877
	CK-N-15.50.2	463	0.2250	0.2036	1.6	0.00787
1600	CK-N-16.50.1	240	0.1821	0.1650	1.7	0.0103
	CK-N-16.50.2	100	0.1848	0.1673	1.35	0.00807
1700	CK-N-17.50.1	360	0.1708	0.1547	1.8	0.01164
	CK-N-17.50.2	120	0.1738	0.1572	2.35	0.01496
1800	CK-N-18.50.1	30	0.2010	0.1820	2.0	0.011
	CK-N-18.50.2	60	0.1824	0.1651	2.4	0.01453
1900	CK-N-19.50.1	10	0.1767	0.1600	1.1	0.0688

TABLE (A 3) DATA SHEET NO. ()

RESULTS OF CO₂-N₂ RUNS (NEW ENGLAND COKE)

CARBON SAMPLE	New England coke	REACTION TEMPERATURE	1500°- 1900° F
ASH CONTENT	9.5 % by weight	REACTION PRESSURE	1.026 atm.
PARTICLE SIZE	50-60 US mesh	REACTION TIME	10 - 650 min.
GAS COMPOSITION	CO ₂ -N ₂ mixtures	GAS FLOW RATE	15 cc./ sec. (85° F & 1 atm.)

Run No. CK-N.A-15.50.1 designates run No. 1 at 1500° F using gas mixture N.A. and 50-60 mesh New England coke particles

θ	Reaction time, min.	ΔW	Loss of weight of sample during reaction, mg.
π	Total pressure, atm.	F_{CO_2}	Fraction carbon weight loss in CO ₂ -N ₂
P_{CO_2}	Partial pressure of CO ₂ , atm.	F_{N_2}	Fraction carbon weight loss in N ₂
P_{N_2}	Partial pressure of N ₂ , atm.	F	Corrected fraction carbon weight loss, $F_{CO_2} - F_{N_2}$
W_0	Weight of sample, gm.	$R_{av.}$	Average specific reaction rate, $(-\ln(1-F))/\theta \times 1000$
$0.905W_0$	Weight of carbon in sample, gm.		mg.C./gm. C. min.

RUN NO.	θ	π	P_{CO_2}	P_{N_2}	W_0	$0.905W_0$	ΔW	F_{CO_2}	F_{N_2}	F	$R_{av.}^*$	$R_{av.}^{**}$ corrected	$R_{av.}^{***}$ calc.
TEMPERATURE 1500° F													
CK-CO ₂ -15.50.1	650	1.025	1.019	0.008	0.1888	0.1708	17.2	0.1006	0.00895	0.0916	0.148	0.160	0.160
CK-N.A-15.50.1	600	1.028	0.848	0.180	0.1541	0.1395	12.8	0.0918	0.00868	0.0831	0.146	0.157	0.146
CK-N.B-15.50.1	600	1.026	0.710	0.316	0.1544	0.1398	11.3	0.0808	0.00868	0.0721	0.125	0.134	0.131
CK-N.C-15.50.1	600	1.026	0.570	0.456	0.1543	0.1397	9.6	0.0688	0.00868	0.0601	0.103	0.110	0.115
CK-N.D-15.50.1	600	1.026	0.329	0.697	0.1581	0.1432	7.3	0.0510	0.00868	0.0423	0.072	0.076	0.078
TEMPERATURE 1600° F													
CK-CO ₂ -16.50.1	120	1.068	1.062	0.006	0.1610	0.1457	10.5	0.0722	0.00854	0.0637	0.548	0.658	0.659
CK-N.A-16.50.1	180	1.026	0.846	0.180	0.1450	0.1312	13.7	0.1043	0.00960	0.0947	0.553	0.662	0.562
CK-N.B-16.50.1	180	1.026	0.710	0.316	0.1579	0.1428	10.8	0.0756	0.00960	0.0660	0.380	0.439	0.493
CK-N.C-16.50.1	180	1.026	0.570	0.456	0.1512	0.1368	9.6	0.0702	0.00960	0.0606	0.347	0.398	0.417
CK-N.D-16.50.1	180	1.026	0.329	0.697	0.1543	0.1397	7.1	0.0508	0.00960	0.0412	0.234	0.261	0.263
TEMPERATURE 1700° F													
CK-CO ₂ -17.50.1	120	1.025	1.019	0.006	0.1083	0.0981	21.7	0.2210	0.01496	0.2060	1.925	2.550	2.550
CK-N.A-17.50.1	60	1.026	0.846	0.180	0.1517	0.1372	14.8	0.1078	0.01164	0.0962	1.688	2.450	2.190
CK-N.B-17.50.1	60	1.024	0.708	0.316	0.1496	0.1353	11.4	0.0843	0.01164	0.0727	1.258	1.708	1.895
CK-N.C-17.50.1	60	1.026	0.570	0.456	0.1498	0.1355	10.7	0.0789	0.01164	0.0673	1.162	1.563	1.572
CK-N.D-17.50.1	60	1.026	0.329	0.697	0.1612	0.1460	7.9	0.0541	0.01164	0.0425	0.724	0.902	0.958
TEMPERATURE 1800° F													
CK-CO ₂ -18.50.1	30	1.026	1.020	0.006	0.1560	0.1412	22.3	0.1578	0.01100	0.1468	5.30	7.34	7.37
CK-N.A-18.50.1	30	1.026	0.846	0.180	0.1510	0.1366	20.8	0.1524	0.01100	0.1414	5.08	7.04	6.37
CK-N.B-18.50.1	30	1.025	0.709	0.316	0.1496	0.1353	17.2	0.1271	0.01100	0.1161	4.11	5.46	5.50
CK-N.C-18.50.1	30	1.026	0.570	0.456	0.1530	0.1384	14.1	0.1079	0.01100	0.0909	3.18	4.08	4.60
CK-N.C-18.50.1	30	1.026	0.329	0.697	0.1502	0.1360	10.5	0.0772	0.01100	0.0662	2.28	2.83	2.83
TEMPERATURE 1900° F													
CK-CO ₂ -19.50.1	10	1.026	1.020	0.006	0.1513	0.1370	19.1	0.1394	0.00688	0.1325	14.24	19.00	19.00
CK-N.A-19.50.1	10	1.026	0.846	0.180	0.1529	0.1383	18.3	0.1323	0.00688	0.1254	13.40	18.40	16.75
CK-N.B-19.50.1	10	1.026	0.710	0.316	0.1534	0.1389	15.2	0.1093	0.00688	0.1024	10.83	14.46	14.86
CK-N.C-19.50.1	10	1.026	0.570	0.456	0.1532	0.1387	12.5	0.0902	0.00688	0.0833	8.72	11.28	12.60
CK-N.D-19.50.1	10	1.026	0.329	0.697	0.1568	0.1418	9.7	0.0684	0.00688	0.0615	6.34	8.09	8.09

- * Average specific reaction rate corrected only for V.C.M. based on N₂ blank runs
 ** Average specific reaction rate corrected for both V.C.M. and gas composition
 *** Average specific reaction rate calculated from rate expression

TABLE (A4) DATA SHEET NO. ()

RESULTS OF CO₂-CO RUNS (NEW ENGLAND COKE)

CARBON SAMPLE	New England coke	REACTION TEMPERATURE	1500° - 1900° F
ASH CONTENT	9.5 % by weight	REACTION PRESSURE	1.026 atm.
PARTICLE SIZE	50-60 US mesh	REACTION TIME	10 - 700 min.
GAS COMPOSITION	CO ₂ -CO mixtures	GAS FLOW RATE	15 cc./ sec. (85° F & 1 atm.)

Run No. CK-CO.A-15.50.1 designates run No. 1 at 1500° F using gas mixture CO.A and 50-60 mesh New England coke particles

θ	Reaction time, min.	ΔW	Loss of weight of sample during reaction, mg.
π	Total pressure, atm.	F _{CO₂}	Fraction carbon weight loss in CO ₂ -CO mixtures
P _{CO}	Partial pressure of CO, atm.	F _{N₂}	Fraction carbon weight loss in N ₂ , not listed
P _{CO₂}	Partial pressure of CO ₂ , atm.	F	Corrected fraction carbon weight loss, F _{CO₂} - F _{N₂}
P _{N₂}	Partial pressure of N ₂ , = π - P _{CO} - P _{CO₂} , not listed, atm.	R _{av.}	Average specific reaction rate, (-ln(1-F)/θ) x 1000, mg.C./gm.C. min.
W ₀	Weight of sample, gm.		
0.905W ₀	Weight of carbon in sample, gm.		

RUN NO.	θ	π	P _{CO₂}	P _{CO}	W ₀	0.905W ₀	ΔW	F _{CO₂}	F	R _{av.} *	P _{CO₂} ** corrected	P _{CO} **	R _{av.} *** calc.
TEMPERATURE 1500° F													
CK-CO ₂ -15.50.1	650	1.025	1.019	0.0000	0.1888	0.1708	17.20	0.1006	0.0916	0.1476	1.019	0.0003	0.1470
CK-CO.A-15.50.1	380	1.025	0.931	0.0892	0.1612	0.1458	1.40	0.0096	0.0024	0.0063	0.931	0.0892	0.0053
CK-CO.B-15.50.1	540	1.030	0.884	0.1410	0.1545	0.1398	1.30	0.0093	0.0010	0.0019	0.884	0.1410	0.0032
CK-CO.C-15.50.1	700	1.011	0.847	0.1590	0.1724	0.1560	1.75	0.0112	0.0021	0.0033	0.847	0.1590	0.0028
CK-CO.D-15.50.1	605	1.026	0.778	0.2440	0.3743	0.3390	3.30	0.0097	0.0010	0.0017	0.778	0.2440	0.0017
TEMPERATURE 1600° F													
CK-CO ₂ -16.50.1	120	1.068	1.062	0.0000	0.1610	0.1457	10.50	0.0723	0.0637	0.5480	1.060	0.0020	0.5300
CK-CO.A-16.50.1	100	1.025	0.931	0.0892	0.1579	0.1428	2.00	0.0140	0.0059	0.0593	0.931	0.0894	0.0493
CK-CO.B-16.50.1	210	1.025	0.826	0.1940	0.1579	0.1428	1.90	0.0133	0.0033	0.0157	0.826	0.1940	0.0210
CK-CO.C-16.50.1	240	1.025	0.859	0.1610	0.1819	0.1646	3.10	0.0188	0.0085	0.0358	0.859	0.1610	0.0261
CK-CO.D-16.50.1	240	1.025	0.779	0.2440	0.1447	0.1308	1.70	0.0130	0.0027	0.0113	0.779	0.2440	0.0160
TEMPERATURE 1700° F													
CK-CO ₂ -17.50.1	120	1.025	1.019	0.0000	0.1083	0.0981	21.70	0.2210	0.0206	1.9250	1.011	0.0076	1.7280
CK-CO.A-17.50.1	30	1.027	0.933	0.0894	0.1677	0.1517	2.95	0.0195	0.0119	0.4000	0.930	0.0921	0.3500
CK-CO.B-17.50.1	60	1.027	0.853	0.1690	0.1689	0.1528	3.40	0.0222	0.0106	0.1768	0.852	0.1700	0.1860
CK-CO.C-17.50.1	60	1.025	0.859	0.1610	0.1669	0.1510	3.10	0.0205	0.0089	0.1483	0.858	0.1620	0.1964
CK-CO.E-17.50.1	120	1.025	0.775	0.2480	0.2177	0.1970	6.95	0.0353	0.0203	0.1716	0.774	0.2490	0.1188
TEMPERATURE 1800° F													
CK-CO ₂ -18.50.1	30	1.026	1.020	0.0000	0.1560	0.1412	22.30	0.1578	0.1468	5.30	1.000	0.0200	4.770
CK-CO.A-18.50.1	30	1.031	0.936	0.0897	0.1516	0.1372	9.30	0.0678	0.0568	1.95	0.928	0.0973	1.920
CK-CO.B-18.50.1	20	1.030	0.857	0.1680	0.1405	0.1272	3.70	0.0291	0.0213	1.08	0.853	0.1720	1.138
CK-CO.C-18.50.1	30	1.025	0.859	0.1610	0.2109	0.1910	8.70	0.0456	0.0346	1.17	0.853	0.1670	1.165
CK-CO.D-18.50.1	40	1.025	0.779	0.2440	0.1552	0.1404	5.90	0.0420	0.0295	0.75	0.776	0.2470	0.764
TEMPERATURE 1900° F													
CK-CO ₂ -19.50.1	10	1.026	1.020	0.0000	0.1513	0.1370	19.10	0.1394	0.1325	14.24	0.982	0.0375	12.54
CK-CO.A-19.50.1	10	1.022	0.928	0.0891	0.1626	0.1471	11.10	0.0756	0.0687	7.12	0.907	0.1099	7.20
CK-CO.B-19.50.1	10	1.030	0.884	0.1410	0.1476	0.1335	7.40	0.0554	0.0485	4.98	0.871	0.1540	5.62
CK-CO.C-19.50.1	10	1.028	0.861	0.1615	0.1480	0.1340	7.80	0.0582	0.0513	5.28	0.847	0.1757	4.98
CK-CO.D-19.50.1	10	1.021	0.774	0.2430	0.2411	0.2180	8.90	0.0408	0.0339	3.45	0.759	0.2580	3.39

* Average specific reaction rate corrected for V.C.M. based on N₂ blank runs
 ** Pressures corresponding to corrected gas compositions
 *** Average specific reaction rate calculated from rate expression

TABLE (A5) DATA SHEET NO. ()

INFLUENCE OF GAS FLOW RATE ON REACTION RATE (NEW ENGLAND COKE)

CARBON SAMPLE	New England coke	REACTION TEMPERATURE	1600° - 1900° F
ASH CONTENT	9.5 % by weight	REACTION PRESSURE	1.026 atm.
PARTICLE SIZE	50-60 US mesh	REACTION TIME	10 - 120 min.
GAS COMPOSITION	100% CO ₂	GAS FLOW RATE	15 - 100 cc./ sec. (85° F & 1 atm.)

Run No. CK-V-CO₂-16.50.1 designates run No. 1 at 1600° F using pure CO₂ and 50-60 mesh New England coke particles; V indicates that the variable for the series of runs is the gas velocity

θ	Reaction time, min.	ΔW	Loss of weight of sample during reaction, mg.
V	Gas flow rate, cc./sec. measured at 85° F and 1 atm.	F _{CO₂}	Fraction carbon weight loss in CO ₂
W ₀	Weight of sample, gm.	F _{N₂}	Fraction carbon weight loss in N ₂
0.905W ₀	Weight of carbon in sample, gm.	F	Corrected fraction carbon weight loss, $\frac{F_{CO_2} - F_{N_2}}{0.001}$
R _{av.}	Average specific reaction rate, $\frac{-\ln(1-F)/\theta}{0.001}$		mg.C./gm.C.min.

RUN NO.	θ	V	W ₀	0.905W ₀	ΔW	F _{CO₂}	F _{N₂}	F	R _{av.}	1/V
TEMPERATURE 1600° F										
CK-V-CO ₂ -16.50.1	120	15.32	0.0898	0.0813	6.2	0.0762	0.00854	0.00677	0.567	0.0653
CK-V-CO ₂ -16.50.2	120	32.30	0.0893	0.0808	6.3	0.0779	0.00854	0.00694	0.582	0.03095
CK-V-CO ₂ -16.50.3	120	83.20	0.0898	0.0813	6.65	0.0818	0.00854	0.00733	0.614	0.01202
TEMPERATURE 1700° F										
CK-V-CO ₂ -17.50.1	60	15.10	0.0904	0.0819	11.2	0.1368	0.0116	0.1252	2.23	0.0662
CK-V-CO ₂ -17.50.2	60	25.90	0.0907	0.0820	11.9	0.1452	0.0116	0.1336	2.39	0.0386
CK-V-CO ₂ -17.50.3	60	55.00	0.0898	0.0813	12.0	0.1475	0.0116	0.1359	2.43	0.0182
CK-V-CO ₂ -17.50.4	60	104.80	0.0903	0.0818	12.5	0.1528	0.0116	0.1412	2.54	0.00953
TEMPERATURE 1800° F										
CK-V-CO ₂ -18.50.1	30	15.00	0.0889	0.0805	15.5	0.1925	0.011	0.1815	6.67	0.0667
CK-V-CO ₂ -18.50.2	30	15.40	0.0898	0.0813	15.7	0.1930	0.011	0.1820	6.69	0.0649
CK-V-CO ₂ -18.50.3	30	22.50	0.0889	0.0805	16.2	0.2010	0.011	0.1900	7.02	0.0444
CK-V-CO ₂ -18.50.4	30	26.80	0.0891	0.0806	15.4	0.1912	0.011	0.1802	6.62	0.0373
CK-V-CO ₂ -18.50.5	30	37.10	0.0891	0.0806	16.1	0.1998	0.011	0.1888	6.97	0.0269
CK-V-CO ₂ -18.50.6	30	62.30	0.0902	0.0817	16.9	0.2070	0.011	0.1960	7.27	0.0161
CK-V-CO ₂ -18.50.7	30	94.30	0.0889	0.0805	16.5	0.2050	0.011	0.1940	7.19	0.0106
TEMPERATURE 1900° F										
CK-V-CO ₂ -19.50.1	10	14.65	0.0905	0.0819	14.1	0.1722	0.0069	0.1653	18.07	0.0683
CK-V-CO ₂ -19.50.2	10	15.30	0.0897	0.0811	13.9	0.1714	0.0069	0.1645	17.97	0.0653
CK-V-CO ₂ -19.50.3	10	20.60	0.0907	0.0820	14.4	0.1756	0.0069	0.1687	18.46	0.0486
CK-V-CO ₂ -19.50.4	10	27.50	0.0905	0.0819	14.1	0.1722	0.0069	0.1653	18.07	0.0363
CK-V-CO ₂ -19.50.5	10	27.50	0.0884	0.0800	14.0	0.1750	0.0069	0.1681	18.40	0.0363
CK-V-CO ₂ -19.50.6	10	50.00	0.0888	0.0804	14.2	0.1764	0.0069	0.1695	18.57	0.0200
CK-V-CO ₂ -19.50.7	10	85.10	0.0895	0.0810	14.5	0.1790	0.0069	0.1721	18.88	0.0118
CK-V-CO ₂ -19.50.8	10	93.00	0.0905	0.0819	14.5	0.1770	0.0069	0.1701	18.64	0.0108

TABLE (A6) DATA SHEET NO. ()

NITROGEN BLANK RUNS

CARBON SAMPLE	New England coke	COKING TEMPERATURE	1800° F
ASH CONTENT	9.5 % by weight	COKING PRESSURE	1.026 atm.
PARTICLE SIZE	as indicated	COKING TIME	15 - 90 min.
GAS COMPOSITION	100% N ₂	GAS FLOW RATE	15 cc./sec. (85° F & 1 atm.)

Run No. CK-N-18.50.3 designates run No. 3 at 1800° F using pure N₂ and 50-60 mesh New England coke particles

θ Coking time, min.

ΔW Loss of weight of sample during coking period, mg.

W. Weight of sample, gm.

F_{N₂} Fraction carbon weight loss in N₂

0.905W Weight of carbon in sample, gm.

RUN NO.	θ	W.	0.905W _c	ΔW	F _{N₂} × 10 ²
8 - 12 mesh		Diameter = 2.03 mm.			
CK-N-18.08.1	90	0.1023	0.0927	1.3	1.40
CK-N-18.08.2	45	0.1068	0.0966	1.1	1.04
50-60 mesh		Diameter = 0.274 mm.			
CK-N-18.50.3	90	0.1036	0.0938	1.8	1.92
CK-N-18.50.4	90	0.1013	0.0918	1.8	1.96
CK-N-18.50.5	60	0.0990	0.0895	1.3	1.45
CK-N-18.50.6	60	0.0981	0.0887	1.3	1.46
CK-N-18.50.7	30	0.0997	0.0902	1.2	1.33
CK-N-18.50.8	15	0.1025	0.0927	0.8	0.863
80-100 mesh		Diameter = 0.163 mm.			
CK-N-18.80.1	90	0.0997	0.0902	2.8	3.11
CK-N-18.80.2	45	0.0991	0.0897	2.0	2.23

TABLE (A7) DATA SHEET NO. ()
 INFLUENCE OF D ON R (NEW ENGLAND COKE)

CARBON SAMPLE New England coke REACTION TEMPERATURE 1800° F
 ASH CONTENT 9.5 % by weight REACTION PRESSURE 1.026 atm.
 PARTICLE SIZE 0.163-9.18 mm. REACTION TIME 10-90 min.
 GAS COMPOSITION 100% CO₂ GAS FLOW RATE 15 cc./ sec.
 (85° F and 1 atm.)

Run No. CK-CO₂-18.08.1 designates run No. 1 at 1800° F
 using pure CO₂ and 8-12 mesh New England coke particles

- θ Reaction time, min.
- W₀ Weight of sample, gm.
- 0.905W₀ Weight of carbon in sample, gm.
- ΔW Loss of weight of sample during reaction, mg.
- F_{CO2} Fraction carbon weight loss in CO₂
- F_{N2} Fraction carbon weight loss in N₂
- F Corrected fraction carbon weight loss, $F_{CO2} - F_{N2}$
- R_{av.} Average specific reaction rate, $1000(-\ln(1-F)/\theta)$, mg.C/gm.C.min.

RUN NO.	θ	W ₀	0.905W ₀	ΔW	F _{CO2}	F _{N2}	F	R _{av.}
D.1 Diameter = 9.18 mm.								
CK-CO ₂ -18.D.1.1	30	0.38242	0.34612	5.90	0.0170	0.0062	0.0108	0.353
	2 60			13.93	0.0402	0.0102	0.0300	0.508
	3 90			22.86	0.0660	0.0128	0.0532	0.608
D.2 Diameter = 7.9 mm.								
CK-CO ₂ -18.D.2.1	30	0.26916	0.24356	5.88	0.0241	0.0062	0.0179	0.603
	2 60			13.45	0.0552	0.0102	0.0450	0.769
	3 90			22.50	0.0923	0.0128	0.0795	0.921
D.3 Diameter = 7.23 mm.								
CK-CO ₂ -18.D.3.1	30	0.19312	0.17482	4.33	0.0248	0.0062	0.0186	0.627
	2 60			10.45	0.0598	0.0102	0.0496	0.849
	3 90			17.62	0.1008	0.0129	0.0879	1.021
D.4 Diameter = 7.08 mm.								
CK-CO ₂ -18.D.4.1	30	0.12200	0.11041	3.44	0.0311	0.0062	0.0249	0.840
	2 60			7.28	0.0659	0.0102	0.0557	0.956
	3 90			11.91	0.1079	0.0129	0.0950	1.110

TABLE (A7) Cont.

RUN NO.	θ	W.	0.905W.	ΔW	F _{CO2}	F _{N2}	F	R _{av.}
D.5 Diameter = 5.29 mm.								
CK-CO ₂ -18.D.5.1	30	0.07896	0.07146	2.50	0.035	0.0063	0.0287	0.970
2	60			4.54	0.0636	0.0103	0.0533	0.914
3	90			8.99	0.126	0.0131	0.1129	1.33
D.6 Diameter = 4.82 mm.								
CK-CO ₂ -18.D.6.1	30	0.06068	0.05491	2.10	0.0383	0.0064	0.0319	1.08
2	60			4.57	0.0832	0.0104	0.0728	1.26
3	90			7.12	0.1298	0.0131	0.1167	1.38
D.7 Diameter = 4.23 mm.								
CK-CO ₂ -18.D.7.1	30	0.04023	0.03641	1.15	0.0316	0.0065	0.0251	0.847
2	60			2.91	0.0798	0.0105	0.0693	1.200
3	90			4.71	0.1292	0.0133	0.1159	1.370
D.8 Diameter = 3.71 mm.								
CK-CO ₂ -18.D.8.1	30	0.02818	0.02550	1.40	0.0548	0.0066	0.0482	1.648
2	60			3.09	0.1212	0.0106	0.1106	1.958
3	90			4.80	0.1883	0.0134	0.1749	2.140
D.9 Diameter = 2.63 mm.								
CK-CO ₂ -18.D.9.1	30	0.01358	0.01230	1.07	0.0868	0.0067	0.0801	2.785
2	60			2.31	0.1880	0.0106	0.1774	3.260
3	90			3.48	0.2830	0.0135	0.2695	3.490
D.10 Diameter = 2.49 mm.								
CK-CO ₂ -18.D.10.1	30	0.01082	0.00979	0.88	0.0898	0.00685	0.0829	2.85
2	60			1.94	0.198	0.0107	0.187	3.45
3	90			3.04	0.310	0.0136	0.296	3.90
D.11 Diameter = 2.35 mm.								
CK-CO ₂ -18.D.11.1	30	0.00826	0.00747	0.66	0.0883	0.00695	0.0813	2.83
2	60			1.46	0.1954	0.0108	0.1846	3.40
3	90			2.14	0.287	0.0137	0.273	3.545

TABLE (A7) Cont.

RUN NO.	θ	W_0	$0.905W_0$	ΔW	F_{CO_2}	F_{N_2}	F	$R_{av.}$
8 - 12 mesh Diameter = 2.03 mm.								
CK-CO ₂ -18.08.1	10	0.1094	0.0991	3.60	0.0363	0.0033	0.033	3.36
	20	0.1022	0.0924	6.40	0.0692	0.0055	0.0637	3.30
	30	0.1031	0.0932	11.00	0.1181	0.0072	0.1109	3.92
	40	0.1020	0.0922	17.6	0.1910	0.0100	0.1810	3.98
	50	0.1008	0.0912	26.9	0.2950	0.0140	0.281	3.67
16-20 mesh Diameter = 1.02 mm.								
CK-CO ₂ -18.16.1	10	0.1047	0.0947	4.5	0.0476	0.0040	0.0436	4.50
	20	0.1051	0.0951	8.2	0.0862	0.0063	0.0800	4.17
	30	0.1040	0.0942	13.3	0.1413	0.0080	0.1330	4.76
	40	0.1023	0.0925	22.7	0.245	0.0107	0.2340	5.33
	50	0.1033	0.0936	35.0	0.374	0.0151	0.3590	4.94
30-40 mesh Diameter = 0.51 mm.								
CK-CO ₂ -18.30.1	10	0.1006	0.0910	4.10	0.0451	0.0051	0.0400	4.10
	20	0.0993	0.0898	8.8	0.0980	0.0076	0.0904	4.75
	30	0.1008	0.0912	8.6	0.0943	0.0076	0.0867	4.52
	40	0.1006	0.0910	13.7	0.1505	0.0094	0.1411	5.07
	50	0.0999	0.0904	23.8	0.263	0.0123	0.2510	5.78
	60	0.1026	0.0928	39.0	0.420	0.0168	0.4030	5.73
50-60 mesh Diameter = 0.274 mm.								
CK-CO ₂ -18.50.2	10	0.1063	0.0963	6.6	0.0685	0.0066	0.0619	6.40
	20	0.1009	0.0913	11.5	0.1258	0.00995	0.1158	6.16
	30	0.1022	0.0924	18.5	0.2000	0.0121	0.188	6.93
	40	0.1027	0.0928	28.8	0.3100	0.0153	0.295	7.00
	50	0.1017	0.0919	47.0	0.511	0.0198	0.491	7.50
70-80 mesh Diameter = 0.194 mm.								
CK-CO ₂ -18.70.1	10	0.1014	0.0918	9.0	0.0979	0.00818	0.0897	9.40
	20	0.1004	0.0908	14.5	0.1596	0.0124	0.1472	7.97
	30	0.1025	0.0927	22.1	0.2390	0.0152	0.224	8.45
	40	0.0992	0.0898	34.0	0.3790	0.0192	0.360	8.93
	50	0.1010	0.0913	47.8	0.5230	0.0225	0.500	9.25
	60	0.0986	0.0892	51.9	0.582	0.0242	0.558	9.07
80-100 mesh Diameter = 0.163 mm.								
CK-CO ₂ -18.80.1	10	0.1014	0.0917	10.0	0.109	0.00906	0.100	10.54
	20	0.1021	0.0923	18.2	0.197	0.0142	0.183	10.10
	30	0.1008	0.0913	25.3	0.277	0.0176	0.259	10.00
	40	0.1041	0.0942	41.0	0.436	0.0234	0.413	10.68
	50	0.1060	0.0959	64.6	0.673	0.0310	0.642	11.40

TABLE (A 8) DATA SHEET NO. ()

WEIGHT PER COKE PARTICLE

<u>Particle Size</u>	<u>Particle Diameter</u> D, (mm.)	<u>Number of Particles</u> <u>Counted</u>	<u>Total Weight</u> (gm.)	<u>Weight per Particle</u> (mg.)
D1	9.18	1	0.38242	382.42
D2	7.9	1	0.26916	269.16
D3-7	5.73	5	0.49499	99.00
D8	3.71	1	0.02818	28.18
D9-11	2.49	3	0.03266	10.89
8-12	2.03	15	0.1020	6.8
16-20	1.02	233	0.20814	0.894
30-40	0.51	437	0.06215	0.1422
50-60	0.274	463	0.01273	0.0275
70-80	0.194	641	0.00645	0.01005
80-100 mesh	0.163	1154	0.00745	0.00645

TABLE (A9) DATA SHEET NO. ()

COKING RUN AND N₂ BLANK RUNS (NATIONAL ELECTRODE CARBON)

CARBON SAMPLE	National electrode carbon	TEMPERATURE	1600° - 1900° F
ASH CONTENT	0.4 % by weight	PRESSURE	as indicated
PARTICLE SIZE	50-60 US-mesh	TIME	as indicated
GAS COMPOSITION	as indicated	GAS FLOW RATE	as indicated

Run No. EC-N-16.50.1 designates run No. 1 at 1600° F using pure N₂ and 50-60 mesh National electrode carbon particles

T	Temperature, °F	W ₀	Weight of sample, gm.
π	Total pressure, atm.	0.996W	Weight of carbon in sample, gm.
θ	Time of run, min.	ΔW	Loss of weight of sample, mg.
V	Gas flow rate, cc./sec. (85° F & 1 atm.)	F	Weight fraction carbon lost

RUN NO.	DESCRIPTION	T	π	θ	GAS	W ₀	0.996W ₀	ΔW	F
EC-C-18.50.1	Coking sample in vacuum	1800	0.4 mm. Hg.	120	Vacuum	15.0969	15.0366	128.3	0.0085
EC-N-16.50.1	N ₂ blank runs	1600	1.026	90	N ₂	0.1026	0.1022	0.1	
EC-N-17.50.1		1700	1.026	30	N ₂	0.1045	0.1041	0.0	
EC-N-18.50.1		1800	1.026	10	N ₂	0.1197	0.1192	0.1	
EC-N-19.50.1		1900	1.026	5	N ₂	0.1046	0.1042	0.1	

TABLE (A10) DATA SHEET NO. ()

RESULTS OF CO₂-N₂ GAS MIXTURES (NATIONAL ELECTRODE CARBON)

CARBON SAMPLE National electrode carbon REACTION TEMPERATURE 1600°- 1900° F
 ASH CONTENT 0.4 % by weight REACTION PRESSURE 1.026 atm.
 PARTICLE SIZE 50-60 US mesh REACTION TIME 5 - 90 min.
 GAS COMPOSITION CO₂-N₂ mixtures GAS FLOW RATE 15 cc./sec. (85° F & 1 atm.)

Run No. EC-N.A-16.50.1 designates run No. 1 at 1600° F using gas mixture N.A and 50-60 mesh National electrode carbon particles

θ Reaction time, min. F Weight fraction carbon lost
 P_{CO2} Partial pressure of CO₂, atm. R₀ Instantaneous specific reaction rate at F = 0,
 P_{N2} Partial pressure of N₂, atm. -1000 ln[1-F/(1+14F)]/15θ, mg.C./gm.C.min.
 W₀ Weight of sample, gm. R_{av.} Average specific reaction rate, -1000 ln (1-F)/θ,
 0.996W Weight of carbon in sample, gm. mg.C./gm.C.min.
 ΔW Loss of weight of sample during reaction, mg.

RUN NO.	P _{CO2}	P _{N2}	W ₀	0.996W ₀	Δ W	F	R ₀	R _{av.}	R _{av.} calc.
TEMPERATURE 1600° F θ = 90 min.									
EC-CO ₂ -16.50.2	1.020	0.006	0.1151	0.1147	14.2	0.1237	0.842	1.467	1.39
EC-CO ₂ -16.50.3	1.020	0.006	0.1013	0.1009	12.3	0.1218	0.833	1.443	1.36
EC-N.E-16.50.1	0.814	0.212	0.1020	0.1016	10.0	0.0985	0.718	1.152	1.21
EC-N.F-16.50.1	0.717	0.309	0.1010	0.1006	9.3	0.0924	0.687	1.077	1.14
EC-N.G-16.50.1	0.563	0.463	0.1025	0.1021	9.6	0.0940	0.695	1.097	1.06
EC-N.H-16.50.1	0.426	0.599	0.1047	0.1043	7.5	0.0719	0.571	0.829	0.87
EC-N.J-16.50.1	0.224	0.802	0.1036	0.1032	5.0	0.0485	0.421	0.552	0.556
EC-N.I-16.50.1	0.102	0.924	0.1096	0.1092	3.2	0.0293	0.277	0.330	0.305
TEMPERATURE 1700° F θ = 30 min.									
EC-CO ₂ -17.50.1	1.020	0.006	0.1078	0.1074	11.8	0.1098	2.325	3.878	4.025
EC-CO ₂ -17.50.2	1.020	0.006	0.1035	0.1031	13.1	0.1270	2.57	4.525	4.270
EC-N.E-17.50.1	0.814	0.212	0.1082	0.1078	11.0	0.1020	2.21	3.586	3.70
EC-N.F-17.50.1	0.717	0.309	0.1023	0.1019	10.3	0.1010	2.19	3.549	3.54
EC-N.G-17.50.1	0.563	0.463	0.1037	0.1034	9.0	0.0870	1.974	3.034	3.09
EC-N.H-17.50.1	0.426	0.599	0.1010	0.1006	8.2	0.0815	1.88	2.834	2.72
EC-N.J-17.50.1	0.224	0.802	0.1007	0.1003	4.9	0.0488	1.27	1.668	1.685
EC-N.I-17.50.1	0.102	0.924	0.1055	0.1051	2.8	0.0266	0.762	0.899	0.875
TEMPERATURE 1800° F θ = 10 min.									
EC-CO ₂ -18.50.1	1.020	0.006	0.1003	0.0999	9.7	0.0971	6.40	10.215	10.72
EC-CO ₂ -18.50.3	1.020	0.006	0.1050	0.1046	11.6	0.1110	7.035	11.766	11.25
EC-N.E-18.50.1	0.814	0.212	0.1081	0.1077	10.0	0.0928	6.20	9.740	9.82
EC-N.F-18.50.1	0.717	0.309	0.1030	0.1026	9.1	0.0887	5.99	9.289	9.27
EC-N.G-18.50.1	0.563	0.463	0.1028	0.1024	8.7	0.0849	5.81	8.873	8.34
EC-N.H-18.50.1	0.426	0.599	0.1047	0.1043	6.1	0.0585	4.39	6.028	6.58
EC-N.J-18.50.1	0.224	0.802	0.1040	0.1036	3.8	0.0367	3.02	3.740	4.10
EC-N.I-18.50.1	0.102	0.924	0.1064	0.1060	2.4	0.0226	1.98	2.286	2.17
TEMPERATURE 1900° F θ = 5 min.									
EC-CO ₂ -19.50.1	1.020	0.006	0.1180	0.1176	19.3	0.1641	18.30	35.862	33.00
EC-CO ₂ -19.50.2	1.020	0.006	0.1015	0.1011	15.7	0.1553	17.63	33.756	32.10
EC-CO ₂ -19.50.3	1.020	0.006	0.1014	0.1010	15.4	0.1525	17.44	33.094	31.80
EC-N.E-19.50.1	0.814	0.212	0.1080	0.1076	14.2	0.1320	15.84	28.314	27.80
EC-N.E-19.50.2	0.814	0.212	0.1056	0.1052	13.1	0.1245	15.23	26.592	27.10
EC-N.F-19.50.1	0.717	0.309	0.1056	0.1052	12.4	0.1179	14.67	25.092	25.30
EC-N.G-19.50.1	0.563	0.463	0.1040	0.1036	10.4	0.1004	13.12	21.162	21.60
EC-N.H-19.50.1	0.426	0.599	0.1010	0.1006	8.9	0.0885	11.98	18.534	18.20
EC-N.J-19.50.1	0.224	0.802	0.1024	0.1020	5.1	0.0500	7.76	10.260	10.60
EC-N.I-19.50.1	0.102	0.924	0.1021	0.1017	2.8	0.0275	4.71	5.578	5.32

TABLE (A11) DATA SHEET NO. ()

RESULTS OF CO₂-CO MIXTURES (NATIONAL ELECTRODE CARBON)

CARBON SAMPLE National electrode carbon REACTION TEMPERATURE 1600° - 1900° F
 ASH CONTENT 0.4 % by weight REACTION PRESSURE 1.026 atm.
 PARTICLE SIZE 50-60 US mesh REACTION TIME 5 - 90 min.
 GAS COMPOSITION CO₂-CO mixtures GAS FLOW RATE 15 cc./sec.(85° F & 1 atm.)

Run No. EC-CO.A-16.50.1 designates run No. 1 at 1600° F using gas mixture CO.A and 50-60 mesh National electrode carbon particles

θ Reaction time, min. ΔW Loss of weight of sample during reaction, mg.
 P_{CO₂} Partial pressure of CO₂, atm. F Weight fraction carbon lost during reaction
 P_{CO} Partial pressure of CO, atm. R₀ Instantaneous specific reaction rate at F = 0,
 P_{N₂} Partial pressure of N₂, atm. -1000 ln[1-F/(1+14F)]/150, mg.C./gm.C.min.
 W₀ Weight of sample, gm. R_{av.} Average specific reaction rate, -1000 ln(1-F)/θ,
 0.996W Weight of carbon in sample, gm. mg.C./gm.C.min.

RUN NO.	P _{CO₂}	P _{CO}	P _{N₂}	W ₀	0.996W ₀	ΔW	F	R ₀	R _{av.}	R _{av.} calc.
TEMPERATURE 1600° F θ = 90 min.										
EC-CO ₂ -16.50.2	1.020	0.000	0.006	0.1151	0.1147	14.2	0.1237	0.842	1.467	1.390
EC-CO ₂ -16.50.3	1.020	0.000	0.006	0.1013	0.1009	12.3	0.1218	0.833	1.443	1.360
EC-CO.L-16.50.1	1.010	0.010	0.006	0.1026	0.1022	2.5	0.0244	0.236	0.274	0.250
EC-CO.L-16.50.1	0.995	0.025	0.006	0.1047	0.1043	1.0	0.0096	0.101	0.107	0.108
EC-CO.G-16.50.1	0.972	0.048	0.006	0.1120	0.1116	0.6	0.00538	0.058	0.060	0.057
EC-CO.J-16.50.1	0.953	0.068	0.005	0.1015	0.1011	0.4	0.00395	0.043	0.044	0.041
EC-CO.K-16.50.1	0.878	0.143	0.005	0.1045	0.1041	0.7	0.00671	0.036	0.038	0.018(θ=180 min.)
TEMPERATURE 1700° F θ = 30 min.										
EC-CO ₂ -17.50.1	1.020	0.000	0.006	0.1078	0.1074	11.8	0.1098	2.325	3.88	4.03
EC-CO ₂ -17.50.2	1.020	0.000	0.006	0.1035	0.1031	13.1	0.1270	2.570	4.53	4.27
EC-CO.L-17.50.1	1.010	0.010	0.006	0.1074	0.1070	5.8	0.0542	1.377	1.86	1.69
EC-CO.L-17.50.2	1.010	0.010	0.006	0.1026	0.1022	5.8	0.0567	1.427	1.95	1.72
EC-CO.I-17.50.1	0.995	0.025	0.006	0.1076	0.1072	2.6	0.0242	0.703	0.82	0.84
EC-CO.G-17.50.1	0.972	0.048	0.006	0.1032	0.1028	1.4	0.0136	0.418	0.46	0.47
EC-CO.J-17.50.1	0.953	0.068	0.005	0.1031	0.1027	1.1	0.0107	0.333	0.36	0.34
EC-CO.M-17.50.1	0.937	0.084	0.005	0.1033	0.1029	1.1	0.0107	0.334	0.36	0.26
EC-CO.K-17.50.1	0.878	0.143	0.005	0.1051	0.1047	0.7	0.0067	0.215	0.22	0.16
TEMPERATURE 1800° F θ = 10 min.										
EC-CO ₂ -18.50.1	1.020	0.000	0.006	0.1003	0.0999	9.7	0.0971	6.40	10.22	10.72
EC-CO ₂ -18.50.2	1.020	0.000	0.006	0.1050	0.1046	11.6	0.1110	7.04	11.77	11.25
EC-CO.L-18.50.1	1.010	0.010	0.006	0.1031	0.1027	6.7	0.0653	4.76	6.76	7.09
EC-CO.L-18.50.2	1.010	0.010	0.006	0.1064	0.1060	8.1	0.0764	5.37	7.95	7.45
EC-CO.I-18.50.1	0.995	0.025	0.006	0.1007	0.1003	4.7	0.0468	3.68	4.79	4.77
EC-CO.H-18.50.1	0.975	0.046	0.005	0.1048	0.1044	4.4	0.0421	3.38	4.30	3.33
EC-CO.G-18.50.1	0.972	0.048	0.006	0.1038	0.1034	3.1	0.0299	2.53	3.04	3.05
EC-CO.J-18.50.1	0.953	0.068	0.005	0.1018	0.1014	2.4	0.0236	2.07	2.40	2.31
EC-CO.M-18.50.1	0.937	0.084	0.005	0.1036	0.1032	2.2	0.0216	1.90	2.18	1.84
EC-CO.K-18.50.1	0.878	0.143	0.005	0.1008	0.1004	1.2	0.01194	1.11	1.20	1.13
TEMPERATURE 1900° F θ = 5 min.										
EC-CO ₂ -19.50.1	1.020	0.000	0.006	0.1180	0.1176	19.3	0.1641	18.30	35.86	33.00
EC-CO ₂ -19.50.2	1.020	0.000	0.006	0.1015	0.1011	15.7	0.1553	17.63	33.76	32.10
EC-CO ₂ -19.50.3	1.020	0.000	0.006	0.1014	0.1010	15.4	0.1525	17.44	33.09	31.80
EC-CO.L-19.50.1	1.010	0.010	0.006	0.1052	0.1048	13.7	0.1307	15.73	27.99	27.50
EC-CO.I-19.50.1	0.995	0.025	0.006	0.1031	0.1027	10.5	0.1022	13.27	21.56	20.60
EC-CO.G-19.50.1	0.972	0.048	0.006	0.1121	0.1117	9.4	0.0841	11.53	17.57	15.70
EC-CO.G-19.50.2	0.972	0.048	0.006	0.1100	0.1096	11.8	0.1077	14.14	22.79	16.60
EC-CO.J-19.50.1	0.953	0.068	0.005	0.1043	0.1039	6.4	0.0615	9.13	12.69	12.30
EC-CO.K-19.50.1	0.878	0.143	0.005	0.1014	0.1010	3.6	0.0356	5.86	7.25	7.21

TABLE (A12) DATA SHEET NO. ()

INFLUENCE OF GAS FLOW RATE ON REACTION RATE (NATIONAL ELECTRODE CARBON)

CARBON SAMPLE National electrode carbon REACTION TEMPERATURE 1600°- 1900° F
 ASH CONTENT 0.4 % by weight REACTION PRESSURE 1.026 atm.
 PARTICLE SIZE 50-60 US mesh REACTION TIME 5 - 90 min.
 GAS COMPOSITION 100% CO₂ (Trace of N₂) GAS FLOW RATE 15 - 109.4 (85° F & 1 atm.)
 cc./sec.

Run No. EC-V-CO₂-16.50.1 designates run No. 1 at 1600° F using pure CO₂ and 50-60 mesh National electrode carbon particles; V indicates that the variable for the series of runs is the gas velocity

θ Reaction time, min. ΔW Loss of weight of sample during reaction, mg.
 V Gas flow rate, cc./sec., measured at 85° F and 1 atm. F Weight fraction carbon lost during reaction
 W_o Weight of sample, gm. P_{CO₂} Partial pressure of CO₂, atm.
 0.996W_o Weight of carbon in sample, gm. P_{N₂} Partial pressure of N₂, atm.
 R_{av.} Average specific reaction rate, -1000 ln(1-F)/θ, mg.C./gm.C.min.

RUN NO.	V	P _{CO₂}	P _{N₂}	W _o	0.996W _o	ΔW	F	R _{av.}	1/V
TEMPERATURE 1600° F θ = 90 min.									
EC-CO ₂ -16.50.2	15.0	1.020	0.006	0.1151	0.1147	14.2	0.1237	1.467	0.0666
EC-CO ₂ -16.50.3	15.0	1.020	0.006	0.1013	0.1009	12.3	0.1218	1.443	0.0666
EC-V-CO ₂ -16.50.1	23.1	1.020	0.006	0.1021	0.1019	11.90	0.1169	1.381	0.0433
EC-V-CO ₂ -16.50.2	36.3	1.021	0.005	0.1079	0.1075	12.6	0.1171	1.384	0.0273
EC-V-CO ₂ -16.50.3	83.0	1.021	0.005	0.1030	0.1026	13.2	0.1286	1.527	0.0121
TEMPERATURE 1700° F θ = 30 min.									
EC-CO ₂ -17.50.1	15.0	1.020	0.006	0.1078	0.1074	11.8	0.1098	3.878	0.0666
EC-CO ₂ -17.50.2	15.0	1.020	0.006	0.1035	0.1031	13.1	0.1270	4.525	0.0666
EC-V-CO ₂ -17.50.1	23.1	1.020	0.006	0.1054	0.1050	13.0	0.1238	4.405	0.0433
EC-V-CO ₂ -17.50.2	34.4	1.021	0.005	0.1025	0.1021	14.2	0.1390	4.989	0.0291
EC-V-CO ₂ -17.50.3	81.6	1.021	0.005	0.1030	0.1026	14.6	0.1423	5.117	0.0123
TEMPERATURE 1800° F θ = 10 min.									
EC-CO ₂ -18.50.1	15.0	1.020	0.006	0.1003	0.0999	9.7	0.0971	10.215	0.0666
EC-CO ₂ -18.50.2	15.0	1.020	0.006	0.1050	0.1046	11.6	0.1110	11.766	0.0666
EC-V-CO ₂ -18.50.1	23.1	1.020	0.006	0.1019	0.1015	11.5	0.1133	12.026	0.0433
EC-V-CO ₂ -18.50.2	35.3	1.021	0.005	0.1032	0.1028	11.7	0.1138	12.082	0.0283
EC-V-CO ₂ -18.50.3	84.0	1.021	0.005	0.1021	0.1017	12.7	0.1249	13.342	0.0119
EC-V-CO ₂ -18.50.4	85.3	1.021	0.005	0.1087	0.1083	13.4	0.1237	13.205	0.0117
TEMPERATURE 1900° F θ = 5 min.									
EC-CO ₂ -19.50.1	15.0	1.020	0.006	0.1180	0.1176	19.3	0.1641	35.862	0.0666
EC-CO ₂ -19.50.2	15.0	1.020	0.006	0.1015	0.1011	15.7	0.1553	33.756	0.0666
EC-CO ₂ -19.50.3	15.0	1.020	0.006	0.1014	0.1010	15.4	0.1525	33.094	0.0666
EC-V-CO ₂ -19.50.1	23.1	1.020	0.006	0.1012	0.1008	15.3	0.1515	32.858	0.0433
EC-V-CO ₂ -19.50.2	35.3	1.020	0.006	0.1087	0.1083	16.7	0.1540	33.448	0.0283
EC-V-CO ₂ -19.50.3	80.7	1.021	0.005	0.1013	0.1009	17.5	0.1734	38.088	0.0124
EC-V-CO ₂ -19.50.4	85.3	1.021	0.005	0.1019	0.1015	18.7	0.1841	40.694	0.0117
EC-V-CO ₂ -19.50.5	109.4	1.021	0.005	0.1006	0.1002	20.6	0.2055	46.010	0.0091

TABLE (A13) DATA SHEET NO. ()

INFLUENCE OF REACTION TIME ON REACTION RATE (NATIONAL ELECTRODE CARBON)

CARBON SAMPLE National electrode carbon REACTION TEMPERATURE 1600° - 1900° F
 ASH CONTENT 0.4 % by weight REACTION PRESSURE 1.026 atm.
 PARTICLE SIZE 50-60 US mesh REACTION TIME 4 - 90 min.
 GAS COMPOSITION as indicated GAS FLOW RATE 15 cc./sec. (85° F & 1 atm.)

Run No. EC-T-CO₂-16.50.1 designates run No. 1 at 1600° F using pure CO₂ and 50-60 mesh National electrode carbon particles; T indicates that the variable for the series of runs is time of reaction

T Reaction temperature, °F
 θ Reaction time, min.
 P_{CO2} Partial pressure of CO₂, atm.
 P_{CO} Partial pressure of CO, atm.
 P_{N2} Partial pressure of N₂, atm.
 W₀ Weight of sample, gm.
 0.996W₀ Weight of carbon in sample, gm.
 ΔW Loss of weight of sample during reaction, mg.
 F Weight fraction carbon lost during reaction
 R₀ Instantaneous specific reaction rate at F = 0, -1000 ln(1-F)/(14F) / 15θ, mg.C./gm.C/min.
 R_{av.} Average specific reaction rate, -1000 ln(1-F)/θ, mg.C./gm.C.min.

RUN NO.	T	θ	P _{CO2}	P _{CO}	P _{N2}	W ₀	0.996W ₀	ΔW	F	R ₀	R _{av.}	R _{av. calc.}
EC-CO ₂ -16.50.2	1600	90	1.020	0	0.006	0.1151	0.1147	14.2	0.1237	0.842	1.467	1.39
EC-CO ₂ -16.50.3	1600	90	1.020	0	0.006	0.1013	0.1009	12.3	0.1218	0.833	1.442	1.36
EC-T-CO ₂ -16.50.1	1600	60	1.020	0	0.006	0.1020	0.1016	7.4	0.0729	0.867	1.262	1.17
EC-T-CO ₂ -16.50.2	1600	45	1.021	0	0.005	0.1072	0.1068	5.7	0.0534	0.909	1.219	1.07
EC-T-CO ₂ -16.50.3	1600	30	1.020	0	0.006	0.1048	0.1044	3.2	0.0309	0.870	1.047	0.96
EC-CO ₂ -17.50.1	1700	30	1.020	0	0.006	0.1074	0.1073	11.8	0.1098	2.325	3.878	4.03
EC-CO ₂ -17.50.2	1700	30	1.020	0	0.006	0.1031	0.1027	13.1	0.1270	2.570	4.525	4.27
EC-T-CO ₂ -17.50.1	1700	20	1.020	0	0.006	0.1012	0.1008	7.0	0.0694	2.500	3.596	3.48
EC-T-CO ₂ -17.50.2	1700	10	1.020	0	0.006	0.1009	0.1005	3.1	0.0307	2.590	3.119	2.91
EC-T-CO ₂ -18.50.1	1800	20	1.021	0	0.005	0.1011	0.1007	29.5	0.2929	6.59	17.33	17.70
EC-T-CO₂-18.50.2	1800	15	1.021	0	0.005	0.1037	0.1033	20.3	0.1963	6.84	14.57	14.35
EC-CO ₂ -18.50.1	1800	10	1.020	0	0.006	0.1003	0.0999	9.7	0.0971	6.40	10.22	10.72
EC-CO ₂ -18.50.2	1800	10	1.020	0	0.006	0.1050	0.1046	11.6	0.1110	7.04	11.77	11.25
EC-T-CO ₂ -18.50.3	1800	5	1.020	0	0.006	0.1063	0.1059	4.4	0.0415	6.66	8.48	8.55
EC-T-CO ₂ -19.50.1	1900	10	1.020	0	0.006	0.1062	0.1058	38.2	0.3610	15.00	44.79	49.80
EC-T-CO ₂ -19.50.2	1900	8	1.021	0	0.005	0.1009	0.1005	37.1	0.3690	19.00	57.57	50.60
EC-T-CO ₂ -19.50.3	1900	7	1.021	0	0.005	0.1054	0.1050	31.3	0.2980	19.04	50.55	44.40
EC-CO ₂ -19.50.1	1900	5	1.020	0	0.006	0.1180	0.1176	19.3	0.1641	18.30	35.86	33.00
EC-CO ₂ -19.50.3	1900	5	1.020	0	0.006	0.1014	0.1010	15.4	0.1525	17.44	33.09	31.80
EC-CO ₂ -19.50.2	1900	5	1.020	0	0.006	0.1015	0.1011	15.7	0.1553	17.63	33.78	32.10
EC-T-CO ₂ -19.50.4	1900	4	1.021	0	0.005	0.1015	0.1011	12.6	0.1245	19.60	33.19	28.30
EC-T-CO.M-17.50.1	1700	90	0.937	0.084	0.005	0.1048	0.1044	5.5	0.0527	0.45	0.602	0.326
EC-T-CO.M-17.50.2	1700	60	0.937	0.084	0.005	0.1027	0.1023	2.9	0.0283	0.40	0.478	0.290
EC-CO.M-17.50.1	1700	30	0.937	0.084	0.005	0.1033	0.1029	1.1	0.0107	0.33	0.359	0.263
EC-T-CO.L-18.50.1	1800	20	1.010	0.010	0.006	0.1071	0.1067	21.5	0.2015	5.22	11.25	10.85
EC-CO.L-18.50.1	1800	10	1.010	0.010	0.006	0.1031	0.1027	6.7	0.0653	4.78	6.75	7.10
EC-CO.L-18.50.2	1800	10	1.010	0.010	0.006	0.1064	0.1060	8.1	0.0764	5.37	7.95	7.45
EC-T-CO.H-18.50.1	1800	30	0.975	0.046	0.005	0.1038	0.1034	16.8	0.1623	3.02	5.90	5.10
EC-T-CO.H-18.50.2	1800	20	0.975	0.046	0.005	0.1041	0.1037	9.5	0.0917	3.07	4.81	4.08
EC-CO.H-18.50.1	1800	10	0.975	0.046	0.005	0.1048	0.1044	4.4	0.0421	3.38	4.30	3.32
EC-T-CO.M-18.50.1	1800	30	0.937	0.084	0.005	0.1044	0.1040	12.1	0.1163	2.42	4.12	2.88
EC-T-CO.M-18.50.2	1800	25	0.937	0.084	0.005	0.1022	0.1018	8.9	0.0875	2.38	3.66	2.60
EC-T-CO.M-18.50.3	1800	25	0.937	0.084	0.005	0.1005	0.1001	8.7	0.0869	2.37	3.64	2.58
EC-T-CO.M-18.50.4	1800	20	0.937	0.084	0.005	0.1014	0.1011	6.5	0.0642	2.36	3.32	2.37
EC-CO.M-18.50.1	1800	10	0.937	0.084	0.005	0.1036	0.1032	2.2	0.0216	1.90	2.18	1.94
EC-T-N.J-18.50.1	1800	30	0.224	0	0.802	0.1029	0.1025	19.7	0.1921	3.37	7.11	7.01
EC-T-N.J-18.50.2	1800	25	0.224	0	0.802	0.1028	0.1024	15.5	0.1512	3.46	6.56	6.32
EC-T-N.J-18.50.3	1800	20	0.224	0	0.802	0.1037	0.1033	12.2	0.1180	3.67	6.28	5.70
EC-T-N.J-18.50.4	1800	15	0.224	0	0.802	0.1018	0.1014	7.4	0.0730	3.46	5.05	4.87
EC-N.J-18.50.1	1800	10	0.224	0	0.802	0.1040	0.1036	3.8	0.0367	3.02	3.74	4.12

E. Calculations for Experiments Using Electrode Carbon Particles of 50-60 mesh

1. Sample calculations

For the sample calculations, the experimental data as supplied by Run EC-CO.L-18.50.2 will be used.

a. General information

Run No.	EC-CO.L-18.50.2
Carbon sample	National electrode carbon
Ash content	0.4% by weight
Particle size	50-60 US mesh
Gas composition	98.54% CO ₂ , 0.92% CO and 0.54% N ₂
Reaction temperature	1800° F.
Reaction pressure	1.026 atm.
Time of reaction	10 minutes
Gas flow rate	15 cc./sec. (measured at 85° F. and 1 atm.)

b. Initial weight of sample 0.1068 gm.

Initial weight of carbon (corrected for ash)

$$0.1068 \times (1 - 0.004) = 0.1064 \text{ gm.}$$

c. Decrease in weight of sample during reaction

$$0.0081 \text{ gm.}$$

d. Fractional decrease in weight of carbon due to reaction

$$F = 0.0081/0.1064 = 0.0764$$

e. Average specific reaction rate, R_{av} .

$$\begin{aligned} R_{av} &= - \ln (1-F)/\theta = - \ln (1-0.0764)/10 \\ &= 0.007948 \text{ gm. C./gm. C. min.} \\ &\text{or } 7.948 \text{ mg. C./gm. C. min.} \end{aligned}$$

f. Initial instantaneous specific reaction rate, R_0 ,

$$\begin{aligned} R_0 &= \frac{1}{15\theta} (\ln (1+14F) - \ln (1-F)) \\ &= \frac{1}{15\theta} (\ln 2.07 - \ln 0.9236) \\ &= 0.00537 \text{ gm. C./gm. C. min.} \\ &\text{or } 5.37 \text{ mg. C./gm. C. min.} \end{aligned}$$

g. R_{av} . calculated from correlation,

$$\begin{aligned}
 R_{av} &= \left\{ \frac{15 \ln (1-F)}{\ln \left(\frac{1-F}{1+14F} \right)} \right\} \left\{ \frac{K_1 P_{CO_2}}{1 + K_2 P_{CO} + K_3 P_{CO_2}} \right\} \\
 &= \left\{ \frac{15 \ln 0.9236}{\ln \left(\frac{0.9236}{2.07} \right)} \right\} \left\{ \frac{23.0 \times 1.010}{1 + 113 \times 0.010 + 2.45 \times 1.010} \right\} \\
 &= 7.45 \text{ mg. C./gm. C. min.}
 \end{aligned}$$

2. Integration of instantaneous specific reaction rate equation

The equation obtained when expressing the instantaneous specific reaction rate as a linear function of the fraction of carbon reacted is as follows:

$$R_1 = - \frac{dW}{Wd\theta} = mF + R_0 \quad (5)$$

in which

W is the weight of the carbon in the bed at any time θ

m is a constant

F is the fraction of carbon reacted

R_0 is the instantaneous specific reaction rate at $F = 0$

When putting $W = (1-F)W_0$, in which W_0 is the initial weight of the carbon, then $dW = -W_0dF$, which substituted in equation (5) gives:

$$R_1 = \frac{W_0 dF}{(1-F)W_0 d\theta} = \frac{dF}{(1-F)d\theta} = mF + R_0$$

Rearranged and integrating:

$$\int_0^F \frac{dF}{(1-F)(mF+R_0)} = \int_0^\theta d\theta$$

or

$$\int_0^F \frac{dF}{R_0 + (m-R_0)F - mF^2} = \theta$$

or

$$\theta = \frac{1}{R_0 \left(\frac{m}{R_0} + 1\right)} \ln \frac{1 + \left(\frac{m}{R_0}\right)F}{1 - F} \quad (11)$$

When substituting in equation (11) $\frac{m}{R_0} = 14$, then the following results:

$$\theta = \frac{1}{15R_0} \ln \frac{1 + 14F}{1 - F}$$

or

$$R_0 = \frac{1}{15\theta} \ln \frac{1 + 14F}{1 - F} \quad (11b)$$

Equation (11b) can also be rearranged to give an expression for F as follows:

$$F = \frac{e^{15R_0\theta} - 1}{e^{15R_0\theta} + 14} \quad (11c)$$

3. Calculation of (m/R_0) values

The average value of (m/R_0) for each series of time runs was obtained by a series of trial and error solutions from equation (11a) (see Discussion and Interpretation of Results), which looks as follows:

$$\frac{\theta_1}{\theta_2} = \frac{\ln [1 + (m/R_0)F_1] - \ln (1-F_1)}{\ln [1 + (m/R_0)F_2] - \ln (1-F_2)} \quad (11a)$$

In the evaluation of the average (m/R_0) value, runs as far apart as possible in the values of θ were chosen. The results are shown in Table (A14).

It is seen that in general the values of (m/R_0) calculated, range from 11 to 18.5. An exception is formed by the EC-T-CO.M-17.50 series of runs (in which series the accuracy is low) giving high values of (m/R_0) . An average value of 14 was used in the correlation of data for all runs.

TABLE (A14) Calculation of (m/R_0)

Run No.	θ	F	(m/R_0)
(1) EC-CO ₂ -16.50.2	90	0.1237	12.0
(2) EC-T-CO ₂ -16.50.3	30	0.0309	
(1) EC-T-CO ₂ -16.50.1	60	0.0729	13.0
(2) EC-T-CO ₂ -16.50.3	30	0.0309	
(1) EC-CO ₂ -17.50.2	30	0.1270	13.8
(2) EC-T-CO ₂ -17.50.2	10	0.0307	
(1) EC-T-CO ₂ -17.50.1	20	0.0694	11.0
(2) EC-T-CO ₂ -17.50.2	10	0.0307	
(1) EC-T-CO ₂ -18.50.1	20	0.2929	13.5
(2) EC-T-CO ₂ -18.50.3	5	0.0415	
(1) EC-T-CO ₂ -18.50.1	20	0.2929	16.0
(2) EC-CO ₂ -18.50.1	10	0.0971	
(1) EC-T-CO ₂ -19.50.2	8	0.3690	18.0
(2) EC-CO ₂ -19.50.1	5	0.1641	
(1) EC-T-N.J-18.50.2	25	0.1512	14.4
(2) EC-T-N.J-18.50.4	15	0.0730	
(1) EC-T-N.J-18.50.1	30	0.1921	12.0
(2) EC-T-N.J-18.50.4	15	0.0730	
(1) EC-T-CO.L-18.50.1	20	0.2015	11.0
(2) EC-CO.L-18.50.2	10	0.0764	
(1) EC-T-CO.H-18.50.1	30	0.1623	11.8
(2) EC-T-CO.H-18.50.2	20	0.0917	
(1) EC-T-CO.M-18.50.1	30	0.1163	17.5
(2) EC-T-CO.M-18.50.4	20	0.0642	
(1) EC-T-CO.M-18.50.2	25	0.0875	17.5
(2) EC-T-CO.M-18.50.4	20	0.0642	
(1) EC-T-CO.M-17.50.1	90	0.0527	53
(2) EC-CO.M-17.50.1	30	0.0107	
(1) EC-T-CO.M-17.50.2	60	0.0283	60
(2) EC-CO.M-17.50.1	30	0.0107	

4. Effective surface area ratio calculations

The effective surface area ratios were calculated from equation (10a) (see Discussion and Interpretation of Results) by substituting a value of 14 for (m/R_0) . The equation was hence used in the following form:

$$\frac{A}{A_0} = (1-F)x(1+14F) \quad (10b)$$

The values calculated for $\frac{A}{A_0}$ were listed in Table (A15).

The maximum value of $\frac{A}{A_0}$ was found by putting the derivative of $\frac{A}{A_0}$ with respect to F equal to zero, and then solving for F.

$$\frac{d(\frac{A}{A_0})}{dF} = 14(1-F) - (1+14F) = 0$$

Solved: $F = 0.465$

The calculated values were plotted in Figure 26.

TABLE (A15) Effective Surface Area Ratios

F	1 - F	1 + 14F	A/A ₀
0.0	1.0	1.0	1.0
0.1	0.9	2.4	2.16
0.2	0.8	3.8	3.04
0.3	0.7	5.2	3.64
0.4	0.6	6.6	3.96
0.465	0.535	7.51	4.02 max.
0.5	0.5	8.0	4.00
0.6	0.4	9.4	3.76
0.7	0.3	10.8	3.24
0.8	0.2	12.2	2.44
0.9	0.1	13.6	1.36
1.0	0.0	15.0	0.00

5. Testing the validity of equation (11)

The extent to which equation (11) (see Discussion and Interpretation of Results) fitted the experimental data was investigated by substituting the average value of R_0 calculated for each series of runs into the equation, and then solving for θ at fixed values of F .

The results, according to which the curves in Figure 24 were drawn are listed in Table (A16).

TABLE (A16) Calculation of F and θ

Series of Runs	R_0 average	$\theta = \left(\frac{1}{15 R_0} \right) \ln \left(\frac{1 + 14F}{1 - F} \right)$						
		$F =$ 0.02	$F =$ 0.05	$F =$ 0.07	$F =$ 0.10	$F =$ 0.15	$F =$ 0.20	$F =$ 0.30
EC-T-CO ₂ -16.50	0.864	20.6	44.9	58.5	75.9	99.7	—	—
EC-T-CO ₂ -17.50	2.496	7.1	15.6	20.3	26.3	34.6	41.6	53.6
EC-T-CO ₂ -18.50	6.705	2.7	5.8	7.5	9.8	12.9	15.5	19.9
EC-T-CO ₂ -19.50	18.00	1.0	2.2	2.8	3.6	4.8	5.8	7.43
EC-T-CO.M-17.50	0.396	45.0	98.0	—	—	—	—	—
EC-T-CO.L-18.50	5.12	3.5	7.6	9.9	12.8	16.9	20.3	26.1
EC-T-CO.H-18.50	3.16	5.6	12.3	16.0	20.7	27.8	32.9	42.3
EC-T-CO.M-18.50	2.25	7.9	17.3	22.5	29.1	38.4	46.2	59.4
EC-T-N.J-18.50	3.40	5.2	11.4	14.9	19.3	25.4	30.6	39.4

F. Calculations for Experiments Using Coke Particles of Different Sizes

1. Sample calculations

For the sample calculations, the experimental data as supplied by Run CK-CO₂-18.50.6 will be used.

a. General information

Run No.	CK-CO ₂ -18.50.6
Carbon sample	New England coke
Ash content	9.5% by weight
Particle size	50-60 US mesh
Gas composition	100% CO ₂
Reaction temperature	1800° F.
Reaction pressure	1.026 atm.
Time of reaction	90 minutes
Gas flow rate	15 cc./sec. (measured at 85° F. and 1 atm.)

b. Before reaction:

Weight of pan + sample	0.9041 gm.
Weight of pan	0.8024
Weight of sample	0.1017

After reaction:

Weight of pan + sample	0.8575
Weight of pan	0.8028
Weight of sample	0.0547

Decrease in weight 0.0470

c. Calculation of the average specific reaction

rate

Weight of sample before reaction on ash free basis, gm. $0.905 W_0 = 0.905 \times 0.1017 = 0.0919$

$$F_{CO_2} = W/W_0 = 0.0470/0.0919 = 0.511$$

$$F_{N_2} = 0.0198 \text{ (from correction chart)}$$

$$F = 0.511 - 0.0198 = 0.491$$

$$\ln (1-F) = -0.67531$$

$$R_{av.} = -\ln(1-F)/\theta = 0.67531/90 = 7.50 \times 10^{-3}$$

gm.C./gm.C.min. or 7.50 mg.C./gm.C.min.

2. Calculation of R_1 values

R_1 , the instantaneous specific reaction rate, is defined by the following equation:

$$R_1 = \frac{-dW}{Wd\theta} = \frac{-d(1-F)}{(1-F)d\theta} = \frac{-d \ln(1-F)}{d\theta} \quad (1)$$

Figure 15 (the $1-F$ vs. θ plot) was used in the evaluation of R_1 , which was found as the slope at a particular point divided by $1-F$. The values of R_1 calculated by this method are listed in Table (A17).

R_1 calculated from the following empirical equation, which were checked for the particle sizes 8-100 mesh, are also listed in Table (A20) for comparison with the experimental values.

$$R_1 = R_0 \left(1 + \frac{10(2+\log_{10}D)F}{R_0} \right) e^{-5.5DF^{1.85}} \quad (24)$$

TABLE (17) VALUES OF R_1 (exp't. and calc.)

Size	D	R_0		F = 0.01	0.02	0.03	0.05
D1	9.18	0.55		0.25	0.66	0.72	1.05
D2	7.9	0.64		0.65	0.77	1.03	1.15
D3-7	5.73	0.88	exp't	1.11	1.12	1.11	1.37
D8	3.71	1.4		1.41	1.58	1.90	2.21
D9-11	2.49	2.0		2.27	2.55	2.70	2.90

Size	D	R_0		F=0.05	0.10	0.15	0.20	0.25	0.30	0.35	0.40	0.45	0.50	0.55
8-12 mesh	2.03	2.85	exp't calc.	3.73	4.55	4.56	3.95	3.07	2.42					
				3.83	4.42	4.52	4.22	3.65	2.95					
16-20	1.02	3.6	exp't calc.	4.23	5.40	6.14	6.45	5.56	4.40					
				4.50	5.18	5.58	5.71	5.59	5.25					
30-40	0.51	4.15	exp't calc.	4.80	5.65	6.50	6.90	6.75	6.15	5.20	4.83			
				4.96	5.64	6.17	6.56	6.78	6.87	6.76	6.57			
50-60	0.274	5.1	exp't calc.	6.00	6.80	7.10	7.23	7.65	7.87	8.30	8.10	8.10		
				5.79	6.40	6.93	7.38	7.75	8.00	8.17	8.22	8.24		
70-80	0.194	7.05	exp't calc.	8.15	8.53	8.50	8.76	8.82	9.24	9.80	9.58	9.80	9.75	8.63
				7.65	8.22	8.70	9.12	9.46	9.73	9.81	10.00	10.10	10.10	10.00
80-100	0.163	8.5	exp't calc.	9.65	9.85	10.00	10.20	9.94	10.80	11.20	11.90	11.80	12.20	12.00
				9.07	9.59	10.00	10.45	10.75	10.85	11.20	11.30	11.40	11.35	11.30

000

3. List of values of R_0 , $R_1(\text{max.})$ and $R_{av.}$ at $F = 0.1$

The values of R_0 , $R_1(\text{max.})$ and $R_{av.}$ at $F = 0.1$ calculated are listed in Table (A18).

TABLE (A18)

Particle Size	D (mm.)	R_0	$R_1(\text{max.})$ (mg.C./gm.C.min.)	$R_{av.}$ at $F=0.1$
D1	9.18	0.55	1.03	--
D2	7.9	0.64	1.13	--
D3-7	5.7	0.88	1.60	1.20
D8	3.7	1.40	2.39	1.95
D9-11	2.49	2.00	3.95	2.96
8-12	2.03	2.85	4.55	3.76
16-20	1.02	3.60	5.96	4.48
30-40	0.51	4.15	6.70	4.72
50-60	0.274	5.10	8.10	6.59
70-80	0.194	7.05	9.70	8.42
80-100 mesh	0.163	8.50	12.60	10.70

4. Calculation of the density and the specific reaction rate based on superficial surface area at $F = 0$

R_0 is the specific reaction rate based on unit weight of carbon at $F = 0$. It could be transformed to the specific reaction rate based on unit superficial surface area at $F = 0$. The superficial surface area of coke particles was determined by assuming spheres of diameter equal to the mesh opening. The specific reaction rate based on unit superficial surface area is equal to the following expression:

$(R_0) \times (\text{weight per particle}) / \pi D^2, \text{ mg. C. reacted per unit superficial surface area in mm.}^2 \text{ per minute.}$

The calculated values, together with the density of particles, are listed in Table (A19).

TABLE (A19)

THE DENSITY OF COKE AND THE REACTION RATE BASED ON SUPERFICIAL SURFACE AREA

Particle Size	Particle Diameter D (mm.)	Density (Gm./cc.)	R_0	$R_0 \times \left(\frac{\text{Wt. per particle}}{\pi D^2} \right)$
			(Mg.C./gm.C.min.)	(Mg.C./mm. ² min.)
D1	9.18	0.945	0.55	0.000793
D2	7.9	1.04	0.64	0.000877
D3-7	5.73	1.00	0.88	0.000840
D8	3.71	1.05	1.4	0.000909
D9-11	2.49	1.35	2.0	0.00112
8-12	2.03	1.55	2.85	0.0015
16-20	1.02	1.61	3.6	0.000988
30-40	0.51	2.05	4.15	0.000723
50-60	0.274	2.55	5.1	0.000594
70-80	0.194	2.62	7.05	0.000598
80-100 mesh	0.163	2.84	8.5	0.000656

G. Calculations for Experiments Using Coke Particles of 50-60 Mesh

1. Sample calculations

For the sample calculations, the experimental data as supplied by Run CK-CO₂-18.50.1 will be used.

a. General information

Run No.	CK-CO ₂ -18.50.1
Carbon sample	New England coke
Ash content	9.5% by weight
Particle size	50-60 US mesh
Gas composition	99.45% CO ₂ - 0.55% N ₂
Reaction temperature	1800° F.
Reaction pressure	1.026 atm.
Time of reaction	30 minutes
Gas flow rate	15 cc./sec. (measured at 85° F. and 1 atm.)

- b. Initial weight of sample 0.1560 gm.
Initial weight of carbon (corrected for ash)

$$0.1560 \times (1-0.095) = 0.1412 \text{ gm.}$$

- c. Decrease in weight of sample during reaction

$$0.0223 \text{ gm.}$$

- d. Fractional decrease in weight of sample in CO₂

$$F_{\text{CO}_2} = 0.0223/0.1412 = 0.1578$$

- e. Fractional decrease in weight of sample in N₂

$$F_{\text{N}_2} = 0.011$$

- f. Fractional decrease in weight of carbon due to reaction

$$F = 0.1578 - 0.011 = 0.1468$$

- g. Average specific reaction rate, corrected for ash and V.C.M.

$$R_{\text{av.}} = -\ln (1-F)/\theta = -\ln (1-0.1468)/30$$

$$= 0.0053 \text{ gm. C./gm. C.min.}$$

$$\text{or } 5.3 \text{ mg.C./gm.C.min.}$$

2. Correction of gas composition of CO₂-CO runs for CO generated

In the reaction area, the effective CO concentration is somewhat higher than the CO concentration of the entering gas stream due to the CO generated during the reaction. As this difference is usually small, it can be regarded as proportional to the rate of CO generation, or the rate of decrease in the weight of carbon for various runs at the same temperature, provided that the gas flow pattern remains the same in these runs. The relation can be expressed as follows:

$$\Delta P_{CO} = kW_0F/\theta \quad (G-1)$$

where ΔP_{CO} is the difference between the effective CO partial pressure and the CO partial pressure of the entering gas; k is a proportionality constant.

To evaluate ΔP_{CO} for the run using pure CO₂ as the entering gas at a certain temperature, velocity runs were made. From the results obtained, R_v , the average specific reaction rate at infinite velocity, was found by extrapolating the R_{av} . vs. $1/V$ curve shown in Figure 13 to $1/V = 0$. It is apparent that R_v should be the reaction rate corresponding to $\Delta P_{CO} = 0$.

The value of R_{av} ., obtained from the pure CO₂ run using the double screen pan setup as shown in Figure 4, is less than the value of R_v at the same temperature, because of the fact that the CO retarding effect being eliminated at $1/V = 0$. These reaction rates can be expressed by the Langmuir equation:

$$R_v = \frac{K_1 P_{CO_2}}{1 + K_3 P_{CO_2}} \quad (G-2)$$

and

$$R_{av.} = \frac{K_1 (P_{CO_2} - \Delta P_{CO})}{1 + K_2 \Delta P_{CO} + K_3 (P_{CO_2} - \Delta P_{CO})} \quad (G-3)$$

Dividing equation (G-2.) by (G-3):

$$\frac{R_v}{R_{av.}} = \left(\frac{1 + K_2 \Delta P_{CO} + K_3 (P_{CO_2} - \Delta P_{CO})}{1 + K_3 P_{CO_2}} \right) \left(\frac{P_{CO_2}}{P_{CO_2} - \Delta P_{CO}} \right) \quad (G-4)$$

For illustration, from the pure CO₂ run using the double screen pan setup at 1800° F., the value of R_{av.} was found to be 5.3 mg. C. per gm. C. per min., which can be expressed by the Langmuir equation with approximate constants:

$$R_{av.} = 5.3 = \frac{8.23 (P_{CO_2} - \Delta P_{CO})}{1 + 28.7 \Delta P_{CO} + 0.589 (P_{CO_2} - \Delta P_{CO})} \quad (G-5)$$

The corresponding R_v obtained from the velocity runs was found to be 7.23 mg. C. per gm. C. per min., which can be shown to be:

$$R_v = 7.23 = \frac{8.23 P_{CO_2}}{1 + 0.589 P_{CO_2}} \quad (G-6)$$

Dividing equation (G-6) by (G-5):

$$\frac{R_v}{R_{av.}} = \left(\frac{1 + 28.7 \Delta P_{CO} + 0.589 (P_{CO_2} - \Delta P_{CO})}{1 + 0.589 P_{CO_2}} \right) \cdot \left(\frac{P_{CO_2}}{P_{CO_2} - \Delta P_{CO}} \right) \quad (G-7)$$

Putting P_{CO₂} = 1.020 atm., ΔP_{CO} was found to be 0.02 atm., which is the effective CO partial pressure.

Let this pure CO₂ run be run 1. In the calculation

of ΔP_{CO} of Run 2, representing any of the CO_2 -CO runs at $1800^\circ F.$, equation (G-1) can be applied:

$$(\Delta P_{CO})_1 = k(W_{OF}/\theta)_1 \quad (G-8)$$

and $(\Delta P_{CO})_2 = k(W_{OF}/\theta)_2 \quad (G-9)$

therefore

$$\frac{(\Delta P_{CO})_1}{(\Delta P_{CO})_2} = \frac{(W_{OF}/\theta)_1}{(W_{OF}/\theta)_2} \quad (G-10)$$

or $(\Delta P_{CO})_2 = \frac{0.02 (W_{OF}/\theta)_2}{0.1412 \times 0.1468/30} \quad (G-11)$

By this method, ΔP_{CO} for each of the CO_2 -CO runs was calculated, using the approximate values of K_2 and K_3 evaluated from the experimental data.

The amount of ΔP_{CO} , added to the value of P_{CO} of the entering gas represents the effective CO partial pressure for a particular run, as shown in Table (A4).

The corrected Langmuir equation constants were evaluated using these corrected gas compositions. This procedure can be used again if refinement of the constants is necessary. For this investigation, these corrected constants are considered to be final.

3. Correction of $R_{av.}$ for CO_2-N_2 runs due to CO generated

For the CO_2-N_2 runs, ΔP_{CO} was calculated from equation (G-1) using ΔP_{CO} evaluated for pure CO_2 runs at a certain temperature. To find the average specific reaction rate corresponding to the entering gas composition, the Langmuir equation with approximate constants was used.

For illustration, Run CK-N.C-18.50.1 was used.

ΔP_{CO} for this run was evaluated as follows:

$$\begin{aligned} \Delta P_{CO} &= (W_{OF}/\theta) \times \frac{0.02}{0.1412 \times 0.1468/30} \\ &= \frac{0.02 \times 0.1384 \times 0.0909/30}{0.1412 \times 0.1468/30} = 0.01235 \text{ atm.} \quad (G-12) \end{aligned}$$

$R_{av.}$ corrected to correspond to the entering gas composition (CO free) can be found from the Langmuir equation:

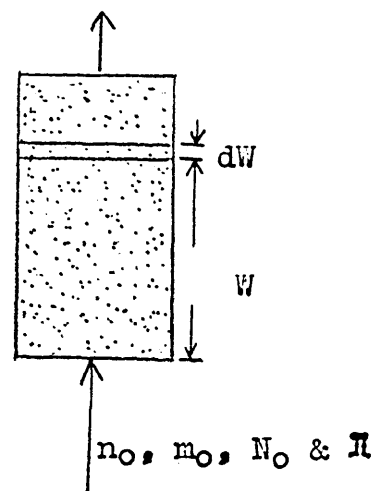
$$\begin{aligned} \frac{R_{av.} \text{ corrected}}{R_{av.}} &= \frac{R_{av.} \text{ corrected}}{3.18} \\ &= \left(\frac{0.570}{0.57 - 0.1235} \right) \left(\frac{1 + 28.7 \times 0.01235 + 0.589 \times (0.57 - 0.01235)}{1 + 0.589 \times 0.57} \right) \\ &= 4.08 \text{ mg.C./gm.C.min.} \quad (G-13) \end{aligned}$$

The corrected Langmuir equation constants were evaluated from these corrected reaction rates.

4. Integration of the Langmuir equation

Nomenclature:

- f Fractional decomposition of CO_2
- m_o Flow rate of CO entering the bed, $\text{lb.mol.} \times 10^{-3}/\text{min.}$
- n_o Flow rate of CO_2 entering the bed, $\text{lb.mol.} \times 10^{-3}/\text{min.}$
- N_o Flow rate of N_2 entering the bed, $\text{lb.mol.} \times 10^{-3}/\text{min.}$
- n Flow rate of CO_2 passing any point in the bed, $\text{lb.mol.} \times 10^{-3}/\text{min.}$
- W Weight of carbon in bed, lb.atom.



When applying the Langmuir equation to a differential section of a fluidized bed, the following results:

$$\frac{-dn_{\text{CO}_2}}{dW} = \frac{K_1 P_{\text{CO}_2}}{1 + K_2 P_{\text{CO}} + K_3 P_{\text{CO}_2}} \quad (\text{G-14})$$

The total molar flow rate at any section in the bed is:

$$(N_o + 2n_o + m_o - n)$$

then:

$$P_{\text{CO}_2} = \left(\frac{n}{N_o + 2n_o + m_o - n} \right) \pi$$

$$P_{\text{CO}} = \left(\frac{2(n_o - n) + m_o}{N_o + 2n_o + m_o - n} \right) \pi$$

$$-\frac{dn}{dW} = \frac{K_1 \pi n}{(N_0 + 2n_0 + m_0 - n) + \{2(n_0 - n) + m_0\} K_2 \pi + n K_3 \pi} \quad (G-15)$$

$$-\int_0^W K_1 \pi dW = \int_{n_0}^n \left(\frac{N_0 + 2n_0 + m_0 - n}{n} + \{2(n_0 - n) + m_0\} K_2 \pi + n K_3 \pi \right) dn \quad (G-16)$$

Integrating equation (G-16), assuming piston-like flow:

$$1 = \frac{N_0 + (1 + K_2 \pi)(2n_0 + m_0)}{K_1 \pi W} \ln \frac{1}{1-f} - \frac{(1 + 2K_2 \pi - K_3 \pi) n_0 f}{K_1 \pi W} \quad (G-17)$$

in which $f = n/n_0$

$$\text{Putting:} \quad A = \frac{N_0 + (1 + K_2 \pi)(2n_0 + m_0)}{K_1 \pi W} \quad (G-18)$$

$$\text{and} \quad B = \frac{(1 + 2K_2 \pi - K_3 \pi) n_0}{K_1 \pi W} \quad (G-19)$$

then equation (G-17) becomes:

$$A \ln \left(\frac{1}{1-f} \right) - Bf = 1 \quad (G-20)$$

When f is small, equation (G-20) becomes:

$$\frac{Af^2}{2} + (A-B)f - 1 = 0 \quad (G-21)$$

5. Calculation of the fraction of CO₂ decomposed in a fluidized bed

From the experimental results of McBride, the fraction of CO₂ decomposed, f , of each run was calculated by means of equation (G-20), using the rate constants evaluated in this work for coke. The results are listed in Table (A20). In this Table are also listed the experimental values of f of McBride and the values of f calculated by McBride using McBride's rate constants.

TABLE (A20)

FRACTION OF CARBON DIOXIDE DECOMPOSED IN A FLUIDIZED BED

(Excluding runs with $f < 0.01$)

<u>RUN R — 1475° F.</u>													
Run No.	R11C	R12C	R13	R14	R21C	R22C	R23	R24C	R25C	R26C	R33	R37C	R88C
$f_{\text{exp't}}$	0.012	0.012	0.051	0.045	0.035	0.028	0.013	0.011	0.018	0.016	0.014	0.01	0.012
f_{McBride}	0.012	0.012	0.044	0.045	0.026	0.027	0.012	0.012	0.020	0.020	0.013	0.011	0.011
f_{Wu}	0.012	0.012	0.038	0.038	0.047	0.047	0.012	0.012	0.017	0.017	0.013	0.012	0.012
<u>RUN N — 1600° F.</u>													
Run No.	N3C	N4C	N5C	N6C	N7C	N8C	N9	N10	N14C	N15C	N19C	N20C	N21C
$f_{\text{exp't}}$	0.071	0.067	0.066	0.081	0.118	0.107	0.205	0.218	0.063	0.056	0.048	0.065	0.041
f_{McBride}	0.063	0.065	0.070	0.073	0.096	0.096	0.198	0.198	0.050	0.050	0.063	0.062	0.056
f_{Wu}	0.054	0.055	0.050	0.047	0.075	0.075	0.142	0.142	0.047	0.047	0.054	0.054	0.023
Run No.	N22C	N23C	N24C	N27C	N28C	N31							
$f_{\text{exp't}}$	0.056	0.082	0.083	0.126	0.101	0.269							
f_{McBride}	0.056	0.067	0.066	0.094	0.095	0.202							
f_{Wu}	0.023	0.056	0.055	0.074	0.075	0.172							

TABLE (A 20) - cont.

RUN U -- 1600° F.

Run No.	U16C	U17C	U18C	U19C	U25C	U26C	U27	U30C	U31C	U32C	U33	U38C	U39
$f_{\text{exp't}}$	0.034	0.034	0.125	0.116	0.090	0.070	0.060	0.037	0.039	0.053	0.054	0.046	0.049
f_{McBride}	0.042	0.041	0.136	0.136	0.103	0.082	0.083	0.042	0.041	0.075	0.064	0.052	0.052
f_{Wu}	0.044	0.042	0.136	0.136	0.093	0.073	0.073	0.042	0.042	0.059	0.059	0.050	0.050

Run No.	U40C	U41C	U44C	U45C	U46C	U47C	U48C	U49C	U1
$f_{\text{exp't}}$	0.053	0.052	0.027	0.027	0.046	0.046	0.042	0.044	0.140
f_{McBride}	0.048	0.047	0.036	0.036	0.043	0.043	0.040	0.040	0.082
f_{Wu}	0.047	0.047	0.015	0.015	0.044	0.044	0.042	0.042	0.074

RUN O -- 1775° F.

Run No.	03C	04C	05	06C	08C	09C	010
$f_{\text{exp't}}$	0.168	0.181	0.166	0.248	0.177	0.097	0.386
f_{McBride}	0.259	0.264	0.268	0.369	0.260	0.225	0.683
f_{Wu}	0.290	0.270	0.300	0.340	0.180	0.115	0.69

TABLE (A20) - cont.

RUN U -- 1775° F.

Run No.	U7C	U8C	U9C	U10C	U11C	U12C	U13	U14C	U15C
$f_{\text{exp't}}$	0.195	0.166	0.268	0.262	0.452	0.448	0.598	0.273	0.258
f_{McBride}	0.209	0.210	0.220	0.218	0.431	0.428	0.610	0.273	0.248
f_{Wu}	0.115	0.120	0.135	0.135	0.440	0.430	0.640	0.270	0.270

RUN Z -- 1900° F.

Run No.	Z1C	Z2C	Z5	Z6	Z11	Z12	Z27	Z28	Z7C	Z8C	Z21C	Z22C
$f_{\text{exp't}}$	0.460	0.460	0.699	0.611	0.870	0.891	0.465	0.455	0.434	0.431	0.492	0.484
f_{McBride}	0.482	0.480	0.721	0.715	0.851	0.847	0.492	0.490	0.489	0.489	0.515	0.515
f_{Wu}	0.610	0.610	0.630	0.630	0.950	0.950	0.570	0.570	0.550	0.550	0.550	0.550

Run No.	Z3C	Z4C	Z13C	Z14C	Z15C	Z16	Z17	Z18	Z19	Z20	Z23C	Z24
$f_{\text{exp't}}$	0.471	0.456	0.580	0.580	0.906	0.862	0.642	0.604	0.590	0.567	0.467	0.449
f_{McBride}	0.499	0.495	0.627	0.626	0.932	0.931	0.519	0.508	0.521	0.521	0.508	0.508
f_{Wu}	0.610	0.620	0.740	0.740	0.990	0.990	0.810	0.810	0.540	0.540	0.560	0.560

TABLE (A20) - cont.

		<u>RUN Z -- 1900° F.</u>										
Run No.		Z25C	Z26C	Z29C	Z30C	Z31C	Z32C	Z33C	Z34C			
$f_{\text{exp't}}$		0.469	0.449	0.440	0.460	0.422	0.403	0.401	0.387			
f_{McBride}		0.489	0.487	0.475	0.474	0.458	0.458	0.440	0.436			
f_{Wu}		0.620	0.620	0.590	0.590	0.580	0.580	0.580	0.580			
		<u>RUN AD -- 2000° F.</u>										
Run No.		AD1C	AD2C	AD4C	AD5C	AD6C	AD7	AD8	AD9	AD10	AD11	AD12
$f_{\text{exp't}}$		0.675	0.682	0.592	0.600	0.585	0.807	0.796	0.891	0.902	0.797	0.799
f_{McBride}		0.685	0.685	0.594	0.604	0.598	0.870	0.870	0.929	0.929	0.803	0.803
f_{Wu}		0.870	0.870	0.810	0.860	0.850	0.980	0.980	0.990	0.990	0.960	0.960
$f_{\text{exp't}}$		The fraction of CO ₂ decomposed in the fluidized bed obtained experimentally by McBride										
f_{McBride}		The fraction of CO ₂ decomposed in the fluidized bed calculated by means of the rate constants evaluated by McBride										
f_{Wu}		The fraction of CO ₂ decomposed in the fluidized bed calculated by means of the rate constants evaluated in the present work										

H. Equilibrium of the Carbon-Carbon Dioxide Reaction

The equilibrium constant for the carbon-carbon dioxide reaction is shown as a function of temperature in Figure A5 , using the data of Austin and Day (54) and Rossini et al. (55).

The percent of CO₂ in an equilibrium mixture was calculated and listed in Table (A21). It can be seen that at the temperatures used in this investigation, the equilibrium mixture is always much higher in CO content than the gas mixture used, and hence the reverse reaction can be neglected.

TABLE (A21)

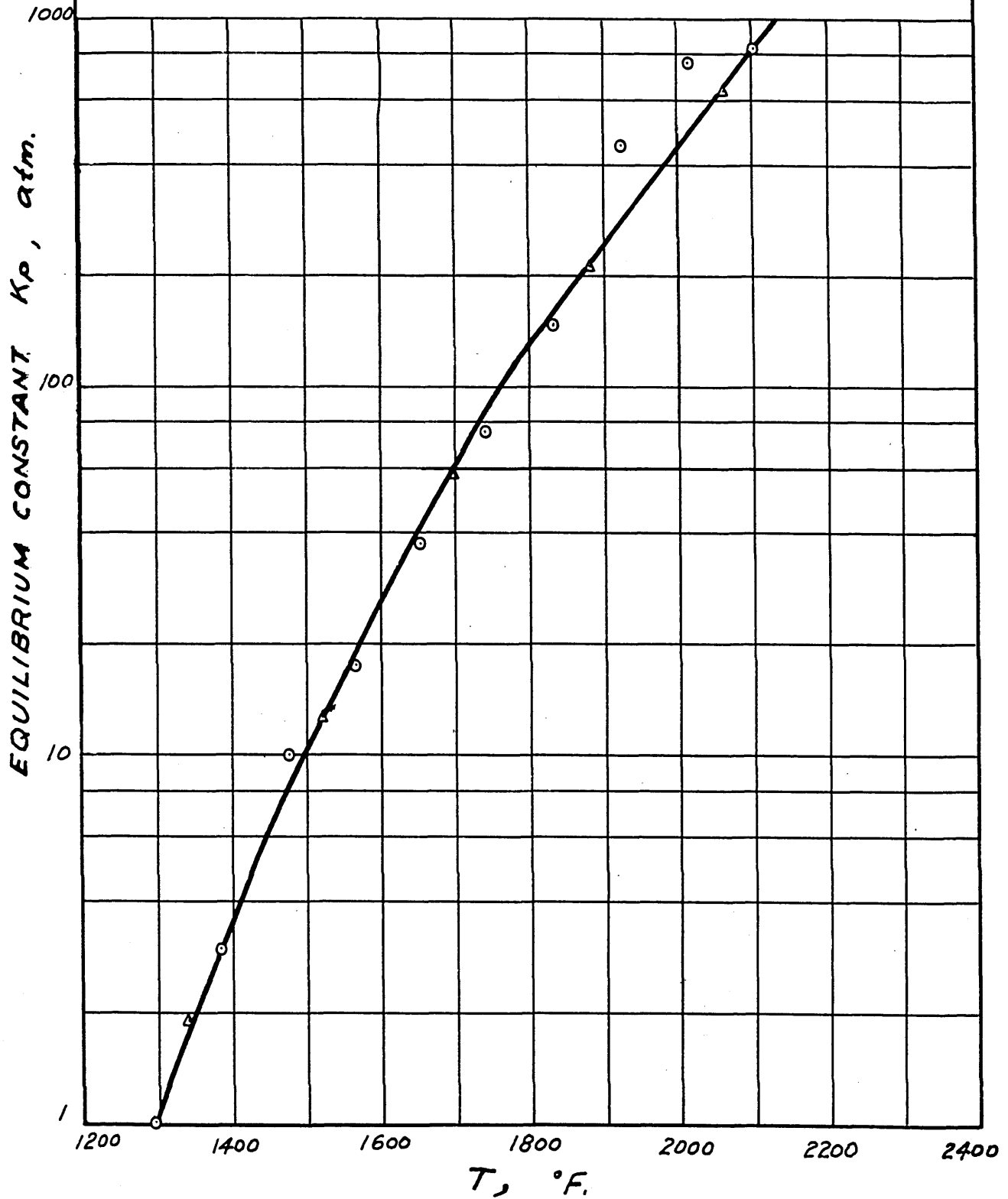
Equilibrium Mixture Composition
of CO₂, CO & Carbon System

<u>Temp. °F.</u>	<u>% CO₂</u>
1200	86.5
1300	34.2
1400	17.2
1500	8.7
1600	4.0
1700	1.7
1800	0.84
1900	0.4

FIGURE (A 5) EQUILIBRIUM CONSTANT
 $K_p = P_{CO}^2 / P_{CO_2}$ FOR THE REACTION CO_2
 $+ C = 2CO$ VS. TEMPERATURE

○ Austin & Day

△ Rossini et al.



I. Discussion of Errors

Reference is also made to Blanc's discussion of errors.

1. The oxygen effect

Since Blanc performed his experiments using this equipment, the possibility of oxygen being present in the system during reaction has practically been eliminated. This was achieved by improving the vacuum tightness of the system, and by replacing all steel pipe connections by rubber and glass tubing. Periodically, oxygen analyses were made of the gas mixture in the equipment by means of a micro oxygen analyzer (see Figure A4). It was found that the oxygen content was always below 50 parts per million. A simple calculation will show that even quantitative conversion of this amount of oxygen to CO or CO₂ has very little influence on the reaction rate. Furthermore, experiments showed that the catalytic effect of small amount of oxygen to the carbon-carbon dioxide reaction was not existing. The oxygen effect very probably can be assumed to be not important.

2. Reaction between gases or carbon and nichrome screen

As reported by Blanc, it was found that the nichrome screen used for the pan and sample pan supporter reacted with the gas mixtures used. When using a new screen, a green layer was formed on the metal, which served as a protective coating against further attack. After the first two or three runs a slight increase in weight of the

screen pan was observed, due to the formation of this layer. After this first increase the weight remained practically constant. The screen pans were weighed before and after each run, which eliminated possible unknown changes in weight.

Carbon particles sticking to the screen after reaction were not observed during these experiments. It was found that after about 30 runs the screen became somewhat brittle, and had a tendency to crack when trying to bend it. This bending was necessary every now and then because the screen of the big pan supporter, due to stretching, became slightly buckled, resulting in touching the brick of the furnace when moving the pan in and out. To avoid any possible trouble due to this behavior, the screen was replaced every 30 runs by a new one. It can be said that no significant errors were due at any time of the experiments to the use of the nichrome screen.

3. The effect of volatile combustible matter present in carbon

The coke sample used contained about 2% of V.C.M. During the reaction run, part of the loss of weight was due to the liberation of V.C.M. This was corrected from the data on the basis that same amount of V.C.M. would be given off in N_2 as in any reacting gas mixture for same period of time at the same temperature. This correction, for runs at high temperatures, was as small as 5% of the reaction rate, but it was considerably large for runs at low temperatures, especially for a gas mixture containing high

percent of CO. Consequently, the results of these last mentioned runs were considered not dependable.

The electrode carbon sample used contained negligible amount of V.C.M. Correction was not applied in this case.

4. The effect of gas composition

Due to the carbon monoxide formed in the reaction, the composition of the reacting gas as supplied will differ from the effective gas composition around the particle. An exact picture of the flow pattern of the gas along the particle and its influence on the gas composition at a specific point on the surface of the particle is not easily visualized. However, the results of the velocity runs show that the extrapolated reaction rates attained at infinite gas velocity (at which condition the composition of the entering and leaving gases are identical) are practically the same as when applying the normally used velocity of 15 cc./sec., in the case using the single screen pan setup. But when the double screen pan setup was used in the runs of coke particles of 50-60 mesh, the differences in reaction rates were noticeable. Corrections were made to the gas compositions for the CO₂-CO runs and to the reaction rates for the CO₂-N₂ runs.

(Note: The increased reaction rates observed at 1800 and 1900° F., when applying gas velocities greater than 35 cc./sec. in the experiments using electrode carbon particles of 50-60 mesh, have been explained earlier).

5. The effect of oxygen and moisture adsorbed on the surface of the carbon

The carbon particles were dried in an oven at 110° C. for overnight. After this procedure, the carbon particles were stored in a stoppered bottle placed in a desiccator, and were only exposed to the atmosphere when a sample had to be prepared. It is clear that the adsorption of oxygen on the carbon surface could not be avoided, the influence of which is hence included in the reaction rates reported. Presumably, the error thus caused is far from significant.

The adsorption of moisture on the carbon surface was tested by exposing a sample to the atmosphere for one hour. No significant change in weight was observed. The influence of adsorbed moisture on the reaction rates reported can hence probably be neglected.

6. The effect of change in particle size of the carbon due to reaction

The percentage change in weight of the carbon particles before and after reaction was in general below 15%. However, microscopic examination of particles which had lost nearly 40% in weight showed that even in those extreme cases the particle size of either coke or electrode carbon was still practically the same as before reaction. The only visible difference was formed by the appearance of the surface which had changed from rather smooth to more porous like.

Assuming the particle size to be constant during reaction was hence probably permissible.

7. The temperature control of the furnace

The temperature controller used maintained the temperature steady within 1° F. The reaction temperature was taken as the average of the temperature readings of the thermocouples above and below the pan, the difference between which two amounted to maximum 40° F., which was later reduced to 10° F. in the experiments using electrode carbon of 50-60 mesh and coke of different sizes by putting alundum rods in between the ribbon.

Calibration of the two thermocouples showed, - (see Description and Calibration of Measuring Devices) - that over the temperature range of the investigation, both indicated from 10 to 15° F. high. Check calibrations periodically made during the experiments showed a consistent performance of the thermocouples.

It can hence be said that the reaction temperatures reported are probably from 10 to 15° F., on the high side.

8. The weighing

The accuracy of the analytical balance used was ± 0.0001 grams. For a 10% decrease in the weight of carbon, this may result in an error of 1%. In the runs with low fractional decrease in weight of carbon, the errors may be as high as 30%. It is for this reason that the data obtained in the last mentioned runs must be considered to be far less reliable than the ones obtained in the runs first mentioned.

9. Sample losses due to jerking of the pan

As already reported, the continuous heating re-

sulted in stretching and buckling of the screen of the pan. This may in some runs have caused the touching of the brick by the bottom of the screen, when moving the sample into and out of the furnace. However, the operation of the pan by means of the magnet arrangement was very smooth and can never have resulted in the loss of carbon particles, as touching the brick does not affect the carbon sample on the screen.

In a few runs it was observed that some particles after the reaction period were lying outside the sample screen pan on the supporter. The results of these runs were discarded, and the runs were repeated. The dislocation of the particles must probably be ascribed to "jumping" during heating or cooling of the stretched screen.

10. Particles blown off the sample supporter

The velocity required for the fluidization of the carbon particles (obtained by comparison with the fluidization velocity required for coke) is far higher than the velocity applied in the experiments. A check was obtained by making a picture of the carbon pattern on the sample supporter before and after a normal reaction run, as shown in Figure 9. The patterns were so identical that any motion of the particles during normal reaction runs can be considered to be out of the question. However, as reported, sloughing off of minute carbon particles must have occurred during the velocity runs made with velocities greater than about 35 cc./sec., at 1800 and 1900° F., reaction temperatures, using electrode carbon particles. The results of these runs,

however, were discarded.

11. Particles fallen through the screen

As already reported, microscopic examination of the particles before and after reaction showed that the particle size remained practically constant during reaction. Hence, it is very unlikely that particles as such can have fallen through the 100 mesh screen. As to possible disintegration of the particles, it can be said that the electrode carbon particles reacted at 1800 and 1900° F., could often partly be rubbed out to a graphite like dust. During the experiments, the impression was, however, obtained that only a much higher gas velocity or rough treatment of the particles might result in a loss due to this possible dust formation. The gas velocity required to do this was apparently obtained at the aforementioned velocity runs, whereas the rough treatment necessary to achieve this only was applied when pouring the reacted sample into a sample bottle after all weighing procedures, etc., were over. It is needless to say that the treatment of the sample supporter with carbon sample during the weighing was an extremely careful procedure, so that losses due to this reason probably did not occur.

12. Brick particles falling on the sample supporter

When starting these series of experiments, the furnace had been in rather continuous operation for almost several months, during which many preliminary runs were made. The bricks and brick coating could hence be assumed to be thoroughly heat-treated, and during not one of the

runs made were brick particles found on the pan. This source of possible errors is definitely out of the question.

13. Preparation and analysis of gas mixtures

The gas mixtures used were prepared by mixing the components in a gas cylinder reserved for this purpose. After mixing, the cylinder was put overnight in a hot water bath in order to insure a homogeneous mixture. The composition of each gas mixture was checked several times during the experiments by means of an Orsat gas analyzer. The results of these analyses always checked within the precision of the apparatus. The accuracy obtainable with the Orsat gas analyzer used, was ± 0.05 cc.

As mentioned under "Oxygen effect", periodical oxygen analyses were made by means of a micro oxygen analyzer. The accuracy of this apparatus amounted to a few parts per million.

J. Derivations of Rate Equation for Reaction of Carbon with Carbon Dioxide

In the present work concerning the reaction of carbon with carbon dioxide, satisfactory correlations of reaction rates were obtained using an equation of the following form:

$$\text{Rate} = \frac{K_1 P_{\text{CO}_2}}{1 + K_2 P_{\text{CO}} + K_3 P_{\text{CO}_2}} \quad (12)$$

This form of equation has been used to correlate data by Semechkova and Frank-Kamenetzky on sugar charcoal, Hinshelwood et al. on cocoanut charcoal, and McBride on coke. Since several (at least three) different schemes of reaction mechanism will lead to this equation, the problem of deciding upon the details of the mechanism is not solved simply by proving that equation (12) correlates data.

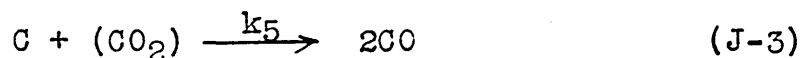
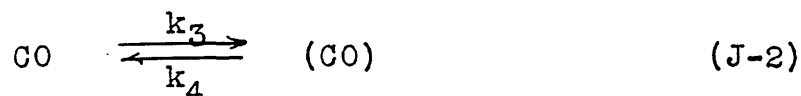
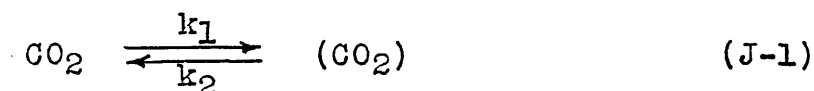
A derivation based on each of three mechanisms follows.

1. Langmuir-Hinshelwood derivation

Hinshelwood et al. (34) presented the following derivation as representative of the simplest application of the early ideas of Langmuir (56) on the effect of surface adsorption on heterogeneous reactions. It is to be noted that Langmuir himself has not presented the following derivation, and in fact stated when writing in 1915 about the reaction of carbon with carbon dioxide (37) that he did not believe carbon dioxide was adsorbed. He gave

instead equation (J-12), which is given later in the section of Derivation of Semechkova and Frank-Kamenetzky, as representing the reaction mechanism.

Hinshelwood et al. made the assumption that both the reactant, CO_2 , and the retarding product, CO , are adsorbed as such on the carbon surface, and that the rate of reaction is proportional to the fraction of the surface covered by the reactant. The mechanism can then be expressed by the following equations:



in which equations, (...) represents gas in the adsorbed state, k_1 , k_2 , k_3 , k_4 and k_5 are reaction rate constants,

The surface consists of equivalent and independent reaction sites, each of which can be occupied by one CO_2 or one CO molecule. When a steady state on the surface is attained, the following relations hold:

$$k_1 P_{\text{CO}_2} (1 - s_1 - s_2) = (k_2 + k_5) s_1 \quad (\text{J-4})$$

$$k_3 P_{\text{CO}} (1 - s_1 - s_2) = k_4 s_2 \quad (\text{J-5})$$

in which s_1 and s_2 are the fractions of the active surface occupied by carbon dioxide and carbon monoxide respectively.

The rate of reaction per unit surface is given by:

$$\text{Rate} = k_5 s_1 = \frac{k_5 k_1 P_{CO_2}}{k_2 + k_5} (1 - s_1 - s_2) \quad (\text{J-6})$$

Rearranging equations (J-4) and (J-5) gives:

$$s_1 = \frac{k_1 P_{CO_2}}{k_2 + k_5} (1 - s_1 - s_2) \quad (\text{J-7})$$

$$s_2 = \frac{k_3 P_{CO}}{k_4} (1 - s_1 - s_2) \quad (\text{J-8})$$

Adding (J-7) and (J-8) results in:

$$s_1 + s_2 = \left(\frac{k_3 P_{CO}}{k_4} + \frac{k_1 P_{CO_2}}{k_2 + k_5} \right) (1 - s_1 - s_2) \quad (\text{J-9})$$

or:

$$(1 - s_1 - s_2) = \frac{1}{1 + \left(\frac{k_3}{k_4} P_{CO} + \left(\frac{k_1}{k_2 + k_5} \right) P_{CO_2} \right)} \quad (\text{J-10})$$

substituting this in equation (J-6) gives:

$$\text{Rate} = k_5 s_1 = \frac{\left(\frac{k_5 k_1}{k_2 + k_5} \right) P_{CO_2}}{1 + \left(\frac{k_3}{k_4} \right) P_{CO} + \left(\frac{k_1}{k_2 + k_5} \right) P_{CO_2}} \quad (\text{J-11})$$

which is seen to be of the same form as equation (12).

According to this derivation, the constants in equation (12) can be expressed as:

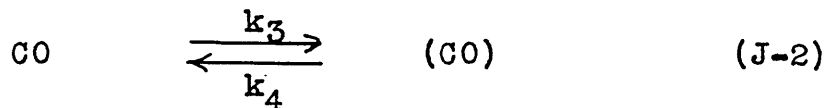
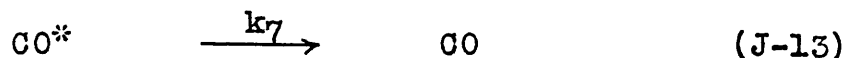
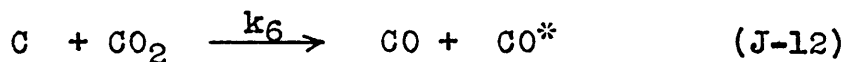
$$K_1 = \frac{k_5 k_1}{k_2 + k_5} = k_5 K_3$$

$$K_2 = \frac{k_3}{k_4} = \text{CO adsorption equilibrium constant}$$

$$K_3 = \frac{k_1}{k_2 + k_5}$$

2. Derivation of Semechkova and Frank-Kamenetzky

Although Hinshelwood et al. presented the above derivation as an example, he referred in addition to the following derivation due to Semechkova and Frank-Kamenetzky. The assumptions made are that carbon dioxide is not adsorbed as such, but reacts with the carbon to give an atom of oxygen which remains on the surface, and a molecule of carbon monoxide which passes into the gas phase. The adsorbed oxygen atom, taking up an atom of carbon from the surface forms gaseous carbon monoxide at a steady rate. Carbon monoxide present in the gas phase is always in equilibrium with carbon monoxide in the adsorbed state on the surface (this is the sole part of the reaction scheme which is identical with the previous derivation). There is a distinction between the adsorbed oxygen and the adsorbed carbon monoxide. The following equations express the mechanism:



in which CO^* represents an O atom adsorbed on carbon, and (CO) represents CO in the adsorbed state. k_6 , k_7 , k_3 and k_4 are reaction rate constants.

When a steady state on the surface is attained, the following relations hold:

$$\begin{aligned} \text{Rate of consumption of carbon} &= k_6 P_{CO_2} (1 - s_3 - s_2) \\ &= k_7 s_3 \quad (\text{J-14}) \end{aligned}$$

Equilibrium between gaseous and adsorbed CO gives:

$$k_4 s_2 = k_3 P_{CO} (1 - s_3 - s_2) \quad (\text{J-15})$$

in which s_3 and s_2 are the fractions of the active surface occupied by CO^* and (CO) respectively.

Division of (J-15) by (J-14) gives the following:

$$\frac{k_4 s_2}{k_7 s_3} = \frac{k_3 P_{CO}}{k_6 P_{CO_2}} \quad (\text{J-16})$$

When solving from (J-16) for s_2 and substituting in (J-14), the result is:

$$k_1 P_{CO_2} \left\{ 1 - s_3 \left(1 + \frac{k_7 k_3 P_{CO}}{k_4 k_6 P_{CO_2}} \right) \right\} = k_7 s_3 \quad (\text{J-17})$$

or

$$s_3 = \frac{k_6 P_{CO_2}}{k_7 + \frac{k_7 k_3}{k_4} P_{CO} + k_6 P_{CO_2}} \quad (\text{J-18})$$

from which the rate is found to be:

$$\text{Rate} = k_7 s_3 = \frac{k_6 P_{CO_2}}{1 + \frac{k_3}{k_4} P_{CO} + \frac{k_6}{k_7} P_{CO_2}} \quad (\text{J-19})$$

It is seen that also this expression is of the same form as equation (12).

In this case the constants in equation (12) are:

$$K_1 = k_6$$

$$K_2 = k_3/k_4 = \text{CO adsorption equilibrium constant}$$

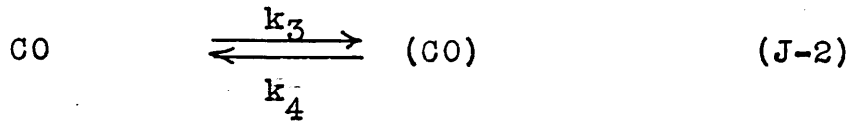
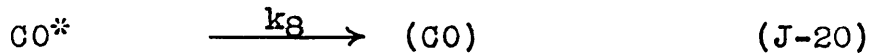
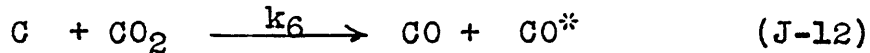
$$K_3 = k_6/k_7 = K_1/k_7$$

3. Modified Semechkova and Frank-Kamenetzky Derivation

This derivation, presented here by the present author, is based on a reaction mechanism which is an alternative of the above-mentioned one.

In this derivation the assumption is also made that carbon dioxide is not adsorbed as such, but reacts with the carbon to form a gaseous carbon monoxide molecule, and an adsorbed oxygen atom, which is next transformed at a steady rate, not to gaseous CO, but to (CO), the adsorbed CO, the concentration of which on the surface is in equilibrium with the CO in the gas phase.

The following equations represent this mechanism:



When a steady state is attained on the surface, the following relations hold:

$$Rate = k_8 s_3 = k_6 P_{CO_2} (1 - s_3 - s_2) \quad (J-21)$$

$$k_4 s_2 = k_8 s_3 + k_3 P_{CO} (1 - s_3 - s_2) \quad (J-22)$$

Division of (J-22) by (J-21) results in

$$\frac{k_4 s_2 = k_8 s_3}{k_8 s_3} = \frac{k_3 P_{CO}}{k_6 P_{CO_2}} \quad (J-23)$$

or

$$s_2 = s_3 \left(\frac{k_8}{k_4} \right) \left(1 + \frac{k_3 P_{CO}}{k_6 P_{CO_2}} \right) \quad (J-24)$$

Substitution of (J-24) into (J-21) results in

$$k_8 s_3 = k_6 P_{CO_2} \left(1 - s_3 - s_3 \left(\frac{k_8}{k_4} \right) \left(1 + \frac{k_3 P_{CO}}{k_6 P_{CO_2}} \right) \right) \quad (J-25)$$

from which

$$s_3 = \frac{k_6 P_{CO_2}}{k_6 P_{CO_2} + k_6 P_{CO_2} \left(\frac{k_8}{k_4} \right) \left(1 + \frac{k_3 P_{CO}}{k_6 P_{CO_2}} \right) + k_8} \quad (J-26)$$

The rate is then found to be:

$$\text{Rate} = k_8 s_3 = \frac{k_6 P_{CO_2}}{1 + \left(\frac{k_3}{k_4} \right) P_{CO} + k_6 \left(\frac{1}{k_8} + \frac{1}{k_4} \right) P_{CO_2}} \quad (J-27)$$

which equation is seen to be of the same form as equation (12).

In this case the constants in equation (12) are:

$$K_1 = k_6$$

$$K_2 = k_3/k_4 = \text{CO adsorption equilibrium constant}$$

$$K_3 = k_1 \left(\frac{1}{k_8} + \frac{1}{k_4} \right) = K_1 \left(\frac{1}{k_8} + \frac{1}{k_4} \right)$$

The rate constants are usually expressed on the basis of unit weight of carbon (called the specific reaction rate), instead of unit surface of carbon, which was used in these derivations. When the rate equation is used on a weight basis, it is to be noted that an assumption is made that the weight is a measure of the surface area.

K. NOMENCLATURE

A	Effective surface area per carbon particle, at $F = F$
A_0	Effective surface area per carbon particle, at $F = 0$
C	Proportionality constant defined by equation (7)
C_0	Proportionality constant defined by equation (6)
D	Particle diameter, mm.
E	Energy value, Btu./lb.mole
e	Base of natural logarithms
F	Fractional decrease in weight of carbon sample
f	Fractional decomposition of CO_2 in a fluidized bed
K_0	Basic constant in Arrhenius equation
K_1	Langmuir equation constant, mg.C./gm.C.min.atm.
K_2	Carbon monoxide adsorption constant, atm. ⁻¹
K_3	Carbon dioxide adsorption constant, atm. ⁻¹
K_r	Reaction rate constant, mg.C./effective surface area.min.
k	Rate constant
m	Rate of change of R_1 with respect to F
m_0	Flow rate of CO entering the fluidized bed, lb.mol.x10 ⁻³ per minute
m/R_0	Surface activation factor
N_0	Flow rate of N_2 entering the fluidized bed, lb.mol.x10 ⁻³ per minute
n_0	Flow rate of CO_2 entering the fluidized bed, lb.mol.x10 ⁻³ per minute
n	Flow rate of CO_2 passing any point in fluidized bed, lb.mol.x10 ⁻³ per minute
P_{CO_2}	Partial pressure of CO_2 , atm.
P_{CO}	Partial pressure of CO, atm.

P_{N_2}	Partial pressure of N_2
R	Gas law constant, 1.987 Btu./lb.mole/°R.
R_0	Instantaneous specific reaction rate at $F = 0$, mg.C./gm.C.min.
$R_{av.}$	Average specific reaction rate, mg.C./gm.C.min.
R_i	Instantaneous specific reaction rate at $F = F$, mg.C./gm.C.min.
s	Fractional surface covered
T	Reaction temperature, °R.
V	Gas flow rate measured at 85° F., and 1 atm., cc./sec.
W	Weight of carbon sample at $F = F$, gm.
W_0	Weight of carbon sample at $F = 0$, gm.
$W_{av.}$	Average weight of carbon sample, gm.
ΔW	Decrease in weight of carbon sample during reaction, mg.
θ	Time of reaction, min.
π	Total pressure, atm.

L. Literature Cited

- (1) Graham, H.S., "Gasification of Carbon by Steam and Carbon Dioxide in a Fluidized Powder Bed" Sc.D. Thesis, Chem. Eng., M.I.T. (1947)
- (2) McBride, G.T., "Gasification of Carbon by Carbon Dioxide in a Fluidized Bed", Sc.D. Thesis, Chem. Eng., M.I.T. (1947)
- (3) Goring, G.E., "Effect of Pressure on the Rate of CO₂ Reduction by High Temperature Coke in a Fluidized Bed", Sc.D. Thesis, Chem. Eng., M.I.T. (1949)
- (4) Paxton, R.R., "Low-Temperature Oxidation of Carbon" Sc.D. Thesis, Chem. Eng., M.I.T. (1949)
- (5) Guerin, H., "Le Probleme de la Reactivite des Combustibles Solides", (1945)
- (6) Wu, P.C., "Literature Survey on Kinetics of the Steam-Carbon and Carbon Dioxide-Carbon Reactions", 2 Vols. (1947)
- (7) Henri Sainte-Claire Deville, H., C.R. de l'Ac. des Sc. 59, 873-876 (1864); C.R. de l'Ac. des Sc. 60, 317-325 (1865)
- (8) Boudouard, O., C.R. de l'Ac. des Sc., 128, 98 (1898); 128, 307, 822, 1524 (1898); 128, 824, 1524 (1899); 130, 132-134 (1900)
- (9) Kassler, R., XVI Congres de Chimie Industrielle, 314-327 (1933)
- (10) Pire, L., Anales de la Societat espanola de Fisica y Quimica, 33, 474-491 (1935)
- (11) Müller, W. and Jandl, E., Brenn. Chem., 19, 45-48 (1938)
- (12) Hoehn, K., Glückauf, 79, 166-170 (1943)
- (13) Hollings, H., and Siderfin, N., J. Soc. Chem. Ind., 46, 76T-84T (1927)
- (14) Rhead, T.F.E., and Wheeler, R.V., J. Chem. Soc., 101, 831-845 (1912)
- (15) Wheeler, R.V., and Stopes, M., Fuel, 2, 29-41 (1923)

- (16) Oshima, Y., and Fukuda, Y., Fuel in Sc. and Pract. Vol. XI, 4, 135 (1932)
- (17) Tu, C.M., Davis, H., and Hottel, H.C., Ind. Eng. Chem., 26, 749-757 (1934)
- (18) Parker, A.S., and Hottel, H.C., Ind. Eng. Chem., 28, 1334-1341 (1936)
- (19) Clement, J., Adams, L., and Haskins, C., Bureau of Mines Bull., 7, (1911)
- (20) Branson, W.R., and Cobb, J.W., Gas J., 178, 901-905 (1927)
- (21) Key, A., and Cobb, J.W., J.S.C.I., 49, 439-444T (1930)
- (22) Bolland, C., and Cobb, J.W., J.S.C.I., 52, 180, and 153T-159T (1933)
- (23) Blakeley, T.H., and Cobb, J.W., Gas J., 208, 351-353, 526-527, 748-749 (1934)
- (24) Drakeley, T.J., J.S.C.I., 50, 319-330T (1931)
- (25) Mayers, M.A., J. Amer. Chem. Soc., 56, 70-76 (1934); 61, 2053-2058 (1939)
- (26) Perrott, G., and Fieldner, A., Proc. Testing Mat., Techn. Papers, 23, II, 475 (1923)
- (27) Fischer, F., Brener, P.K., and Broche, H., Brenn. Chemie, 4, 33-39 (1923)
- (28) Arend, G.P., and Wagner, J., Fuel in Sc. and Pract., 5, 106-116 (1926)
- (29) Bodmer, G., Bull. Suisse Gas., 6, 181-186, 198-212, 239-245 (1926)
- (30) Rieffel, M. Chimie et Industrie, 26, 280-288, 531-540 (1931)
- (31) Gevers-Orban, E., Rev. Univ. Mines, 10, 313-320, 347-352, 376-386 (1934)
- (32) Cassan, H., Chal. Ind., 18, 355-364, and 406-412 (1937); C.R., 206, 1296-1299 (1938)
- (33) Semchikova, A.F. and Frank-Kamenetzky, D.A., Acta Physicochim, U.R.S.S., 12, 879 (1940)

- (34) Gadsby, J., Hinshelwood, C.N., and Sykes, K.W., Proc. Roy. Soc., No. 1009, Vol. 187, 129-151 (1946)
- (35) Gadsby, J., Long, F.J., Sleightholm, P., and Sykes, K.W., Proc. Roy. Soc., No. 1034, Vol. 193, 357-376 (1948)
- (36) Long, F.J., and Sykes, K.W., Proc. Roy. Soc., No. 1034, Vol. 193, 376-399 (1948)
- (37) Langmuir, J., J. Amer. Chem. Soc., 37, 1154-1156 (1915)
- (38) Meyer, L., and Martin, H., Z. Elektrochem., 41, 136-146 (1935)
- (39) Meyer, L., Trans. Fara., 34, 1056-1061 (1938)
- (40) Sihvonen, V., Brenn. Chem., 17, 281-285 (1936)
- (41) Eucken, A., Z. angew. chem., 43, 986-992 (1930)
- (42) Mungen, R., "The Combustion of Carbon in Carbon Dioxide", S.M. Thesis, Chem. Eng., M.I.T. (1947)
- (43) Mullery, E.A., and Hottel, H.C., "The Combustion of Carbon in Carbon Dioxide", S.B. Thesis, Chem. Eng., M.I.T. (1948)
- (44) Smith, F.W., "The Influence of Gas Flow on the Heterogeneous Reactions of Carbon", Sc.D. Thesis, Chem. Eng., M.I.T. (1949)
- (45) Port, Jr., F.J., "Heat Transmission by Radiation from Gases", Sc.D. Thesis, Chem. Eng., M.I.T. (1942)
- (46) Egbert, R.B., "Heat Transmission by Radiation from Gases", Sc.D. Thesis, Chem. Eng., M.I.T. (1942)
- (47) Kallal, R.J., "Reactions of Ethylene with Alcohols" Sc.D. Thesis, Chem. Eng., M.I.T. (1949)
- (48) Uhrig, K., Roberts, F.M., and Levin, H., Anal. Ed., Ind. Eng. Chem., 17, 31-34 (1945)
- (49) Powell, J.S., and Joy, P.C., Anal. Ed., Ind. Eng. Chem., 21, 296-297 (1949)
- (50) Blanc, L.F., "The Influence of Particle Size of Coke on the Rate of its Reaction with Carbon Dioxide", S.B. Thesis, Chem. Eng., M.I.T. (1948)

- (51) Duffy, Jr., B.J., and Leinroth, Jr., J.P., "The Rate of Gasification of Anthracite Coke by Carbon Dioxide in a Fluidized Bed", S.M. Thesis, Chem. Eng., M.I.T., (1947)
- (52) Mason, E.A., and Gilliland, E.R., Ind. Eng. Chem., 41, 1191-1196 (1949)
- (53) Clifford, Jr., G.F., "The Combustion of Carbon in Mixtures of Carbon Dioxide and Nitrogen", S.B. Thesis, Chem. Eng., M.I.T. (1948)
- (54) Austin, J.B., and Day, M.J., Ind. Eng. Chem., 33, 23-31 (1941)
- (55) Rossini et al., J. Res. Nat. Bur. Stds. R.P., 1634, 34, 143-161 (1945)
- (56) Langmuir, I., J. Amer. Chem. Soc., 38, 2221 (1916)

M. Biographical Note

The author was born July 23, 1920 in Taiyuan, Shansi, China, where he lived and schooled until the age of 17. When the Sino-Japanese war broke out in 1937, he with his family moved south and settled at Chungking, then the war-time capital of China.

At Chungking, he entered the National Central University in 1939, majored in Chemical Engineering, and received the degree of Bachelor of Science in 1943. He then worked one year at the Research Laboratory of the Tung-Li Oil Works at Chungking.

In 1945, he came to the United States and entered the University of Michigan, where he received his Master of Science degree in Chemical Engineering in 1946. He then transferred to the Massachusetts Institute of Technology, received the degree of Doctor of Science in Chemical Engineering in 1949.